

DO NOT REMOVE FROM THE
RESEARCH OFFICE

Urban Interstate Portland Cement Concrete Rehabilitation Alternatives for Washington State

WA-RD 202.1

Final Report
April 1991



Washington State Department of Transportation
Planning, Research and Public Transportation Division

in cooperation with the
United States Department of Transportation
Federal Highway Administration

TECHNICAL REPORT STANDARD TITLE PAGE

1. REPORT NO. WA-RD 202.1	2. GOVERNMENT ACCESSION NO.	3. RECIPIENT'S CATALOG NO.
4. TITLE AND SUBTITLE URBAN INTERSTATE PORTLAND CEMENT CONCRETE PAVEMENT REHABILITATION ALTERNATIVES FOR WASHINGTON STATE	5. REPORT DATE April 1991	6. PERFORMING ORGANIZATION CODE
	8. PERFORMING ORGANIZATION REPORT NO.	
7. AUTHOR(S) J. Mahoney, Jo A. Lary, Linda M. Pierce, Newton C. Jackson, Ernest I. Barenberg	10. WORK UNIT NO.	
9. PERFORMING ORGANIZATION NAME AND ADDRESS Washington State Transportation Center (TRAC) University of Washington, JE-10 The Corbet Building, Suite 204; 4507 University Way N.E. Seattle, Washington 98105	11. CONTRACT OR GRANT NO. Y3399, Task 12	
12. SPONSORING AGENCY NAME AND ADDRESS Washington State Department of Transportation Transportation Building, KF-01 Olympia, Washington 98504	13. TYPE OF REPORT AND PERIOD COVERED Final Report	
14. SPONSORING AGENCY CODE		
15. SUPPLEMENTARY NOTES This study was conducted in cooperation with the U.S. Department of Transportation, Federal Highway Administration. FHWA Headquarters Technical Contact was Mr. Roger Larson.		
16. ABSTRACT Two urban Interstate portland cement concrete (PCC) pavements (SR 5 in Seattle and SR 90 in Spokane) were studied in order to (1) determine the mechanisms causing their deterioration, (2) estimate when the pavement condition would become unacceptable and the best time for rehabilitation, and (3) determine suitable rehabilitation alternatives. The rehabilitation alternatives were examined on a life-cycle cost basis. The research done in this study was a combination of efforts at the University of Washington through the Washington State Transportation Center (TRAC), University of Illinois, and the Washington State Department of Transportation.		
17. KEY WORDS Portland cement concrete, pavement, rehabilitation	18. DISTRIBUTION STATEMENT No restrictions. This document is available to the public through the National Technical Information Service, Springfield, VA 22616	
19. SECURITY CLASSIF. (of this report) None	20. SECURITY CLASSIF. (of this page) None	21. NO. OF PAGES 350
		22. PRICE

Final Report

**Research Project Y 3399, Task 12
PCC Pavement Performance**

**URBAN INTERSTATE PORTLAND CEMENT
CONCRETE REHABILITATION ALTERNATIVES
FOR WASHINGTON STATE**

by

**Joe P. Mahoney
Professor of Civil Engineering
University of Washington**

**Jo A. Lary
Research Assistant
University of Illinois**

**Linda M. Pierce
Research Engineer II
Washington State Department of Transportation**

**Newton C. Jackson
Pavement and Soils Engineer
Washington State Department of Transportation**

**Ernest J. Barenberg
Professor of Civil Engineering
University of Illinois**

**Washington State Transportation Center (TRAC)
University of Washington, JE-10
The Corbet Building, Suite 204
4507 University Way N.E.
Seattle, Washington 98105**

**Washington State Department of Transportation
Technical Monitor
Newton C. Jackson
Pavement and Soils Engineer**

Prepared for

**Washington State Transportation Commission
Department of Transportation
and in cooperation with
U.S. Department of Transportation
Federal Highway Administration**

March 1990

Revised April 1991

DISCLAIMER

The contents of this report reflect the views of the authors, who are responsible for the facts and the accuracy of the data presented herein. The contents do not necessarily reflect the official views or policies of the Washington State Transportation Commission, Department of Transportation, or the Federal Highway Administration. This report does not constitute a standard, specification, or regulation.

ACKNOWLEDGMENTS

The authors express their appreciation for the information provided by WSDOT Districts 1 (Seattle) and 6 (Spokane). Further, Mr. Roger Larson of the FHWA provided extensive information to the authors during the conduct of this study.

TABLE OF CONTENTS

Chapter	Page
1.0 Introduction.....	1-1
1.1 The Problem.....	1-1
1.2 Background.....	1-3
1.3 Objectives.....	1-5
1.4 Report Organization.....	1-6
2.0 Site Selection and Data Collection.....	2-1
2.1 Site Selection.....	2-1
2.1.1 SR 5.....	2-2
2.1.2 SR 90.....	2-2
2.2 Data Collection.....	2-4
2.2.1 Coring.....	2-4
2.2.1.1 SR 5.....	2-4
2.2.1.2 SR 90.....	2-7
2.2.2 Crack Survey.....	2-7
2.2.2.1 SR 5.....	2-7
2.2.2.2 SR 90.....	2-12
2.2.3 Faulting Survey.....	2-14
2.2.3.1 SR 5.....	2-14
2.2.3.2 SR 90.....	2-15
2.2.4 Nondestructive Deflection Testing.....	2-15
2.2.5 Climatological Data.....	2-18
2.2.6 Traffic Data.....	2-23
2.2.7 Bridge Clearances.....	2-23
3.0. Data Analysis.....	3-1
3.1 Coring and Laboratory Testing.....	3-1
3.1.1 SR 5.....	3-1
3.1.2 SR 90.....	3-4
3.2 Cracking and Faulting Survey.....	3-5
3.2.1 Cracking.....	3-5
3.2.2 Faulting.....	3-14
3.3 Nondestructive Deflection Testing.....	3-15
3.3.1 Load Transfer Efficiency.....	3-15
3.3.1.1 SR 5.....	3-16
3.3.1.2 SR 90.....	3-19
3.3.2 Relative Movement at Joints and Cracks.....	3-21
3.3.3 Voids.....	3-25
3.3.3.1 SR 5.....	3-30
3.3.3.2 SR 90.....	3-33

TABLE OF CONTENTS (Continued)

<u>Chapter</u>	<u>Page</u>
3.3.4 Material Strength Predictions.....	3-34
3.3.4.1 Pavement Layer Material Strengths	3-34
3.3.4.2 SR 5.....	3-43
3.3.4.3 SR 90.....	3-46
3.3.4.4 Schmidt Hammer.....	3-48
3.4 Climatological Data.....	3-49
3.4.1 Thermal Gradients.....	3-49
3.4.2 Thermal Stresses	3-50
3.5 Traffic.....	3-56
4.0 Portland Cement Concrete Pavement Performance Evaluation.....	4-1
4.1 Failure Mechanisms	4-1
4.1.1 SR 90	4-2
4.1.1.1 Transverse Cracking.....	4-2
4.1.1.2 Faulting.....	4-11
4.1.2 SR 5 — Longitudinal Cracking.....	4-18
4.2 Distress Propagation Rates — Cracking.....	4-36
5.0 Portland Cement Concrete Rehabilitation Alternatives	5-1
5.1 Portland Cement Concrete Overlays.....	5-1
5.1.1 Bonded Overlays	5-3
5.1.2 Partially Bonded Overlays	5-5
5.1.3 Unbonded Overlays.....	5-5
5.2 Asphalt Concrete Overlays.....	5-8
5.2.1 Pre-Overlay Repair.....	5-10
5.2.1.1 Pressure Grouting.....	5-10
5.2.1.2 Crack and Seat.....	5-11
5.2.1.3 Load Transfer Devices	5-12
5.2.2 Stress-Relieving Interlayers	5-12
5.2.3 Crack-Arresting Interlayers.....	5-13
5.2.4 Fabrics	5-13
5.2.5 Performance of Asphalt Concrete Projects in Washington State.....	5-14
5.3 Reconstruction.....	5-20
5.3.1 Subbase Type	5-21
5.3.2 Shoulder Type	5-23
5.3.3 Joint Design.....	5-25
5.3.4 Recycling.....	5-25
5.4 Feasible Rehabilitation Alternatives	5-26
5.4.1 Bridge Clearances	5-26
5.4.2 Life-Cycle Cost Analysis of Rehabilitation Strategies	5-27
5.4.3 SR 5	5-34
5.4.4 SR 90	5-35

TABLE OF CONTENTS (Continued)

<u>Chapter</u>	<u>Page</u>
6.0 Conclusions and Recommendations.....	6-1
6.1 Conclusions.....	6-1
6.2 Recommendations.....	6-3
References.....	References-1

LIST OF APPENDICES

<u>Appendix</u>	<u>Page</u>
A. Literature Review.....	A-1
B. Bridge Clearances.....	B-1
C. Core Thicknesses, Load Transfer Efficiencies, Plays, Voids.....	C-1
D. Backcalculation Procedure Description.....	D-1
E. Backcalculated Material Properties and Concrete Thicknesses.....	E-1
F. CMS Input Files, Temperature Differentials, and Thermal Gradients.	F-1
G. Economic Tables.....	G-1
H. Cost Calculations.....	H-1
I. Review of Caltrans PCC Pavement Design, Performance, and Rehabilitation.....	I-1

LIST OF FIGURES

Figure		Page
1.1	Pavement Age for WSDOT PCC Interstate Pavements — Districts 1, 3 and 4 (Westside).....	1-2
1.2	Pavement Age for WSDOT PCC Interstate Pavements — Districts 5 and 6 (Eastside).....	1-2
2.1	Basic Site Information — SR 5 Seattle (milepost 176.35-176.43)...	2-3
2.2	Basic Site Information — SR 90 Spokane (milepost 278.60-278.75)	2-5
2.3	PCC Cores — Plan View, SR 5 Seattle (Northbound)	2-6
2.4	PCC Cores — Plan View, SR 90 Spokane (Westbound).....	2-8
2.5	Values for Portland Cement Concrete Pavements Developed for PMS [after Reference 2.2].....	2-9
2.6	Crack Survey — Plan View, SR 5 Seattle (Northbound)	2-11
2.7	Crack Survey — SR 90 Spokane (Westbound)	2-13
2.8	Faulting Survey — SR 5 Seattle (Northbound)	2-16
2.9	Faulting Survey — SR 90 Spokane (Westbound).....	2-17
2.10	Arrangement of Deflection Sensors for Determining Load Transfer Efficiency at Approach and Leave Sides of a Joint or Crack	2-19
2.11	FWD Plate Locations — Plan View, SR 5 Seattle (Northbound).....	2-20
2.12	FWD Plate Locations — Plan View, SR 90 Spokane (Westbound).	2-21
3.1	Performance Curves for SR 5 and SR 90.....	3-8
3.2	Performance Curves Using Adjusted Fatigue Equations	3-10
3.3	Fatigue Results of 140 Beam Tests (Reference 3.13)	3-11
3.4	“Generic” Performance Curves.....	3-13
3.5	The Concept of Joint Load Transfer Efficiency (LTE).....	3-17
3.6	The Concept of Play.....	3-22
3.7	Joint or Crack Faulting versus Play (both I-5 and I-90 Data Points)	3-26
3.8	Joint or Crack Faulting versus Play (SR 5 Data Points)	3-27
3.9	Joint or Crack Faulting versus Play (SR 90 Data Points)	3-28
3.10	Steps in Void Formation (after Reference 3.14)	3-29
3.11	Indicated Void Locations for Transverse Joints — SR 5 Seattle.....	3-32
3.12	Indicated Void Locations for Transverse Joints and Cracks — SR 90 Spokane	3-32
3.13	Concept and Calculation of Deflection Basin Area	3-36
3.14	Area versus Radius of Relative Stiffness	3-37
3.15	Normalized Deflections versus Radius of Relative Stiffness.....	3-39
3.16	Prediction of k from Center Deflection.....	3-40
3.17	Prediction of k from Deflection at 36 inches	3-41
3.18	Temperature Change through 9-inch PCC Slab, July 15 — SR 5.....	3-51
3.19	Temperature Change through 7/8-inch PCC Slab, July 15 — SR 90	3-52
3.20	Curl Stress along the Transverse Joint —SR 5	3-57
3.21	Curl Stress along the Pavement Edge — SR 5.....	3-58
3.22	Curl Stress along the Transverse Joint — SR 90	3-59
3.23	Curl Stress along the Pavement Edge — SR 90.....	3-60

LIST OF FIGURES (Continued)

Figure		Page
4.1	Critical Fatigue Damage Location and Tensile Stress Direction for Mid-Slab Loading	4-3
4.2	Deflected Slab Shape Under Temperature Gradient	4-5
4.3	Curl Stress along the Pavement Edge — SR 90.....	4-6
4.4	Computed Tensile Stresses Across Bottom of PCC Slab at Midpoint between Transverse Joints for Various Transverse Positions of Axle Load [from Reference 4.12]	4-7
4.5	Illustration of the Mean Distance from Slab Edge to Outside of Dual Tires	4-8
4.6	Lateral Traffic Distribution for a Single Axle.....	4-10
4.7	Joint Load Effectiveness for Gravel and Cement Treated Subbase for Various Joint Openings [from Reference 4.18].....	4-13
4.8	Joint Load Effectiveness [from Reference 4.18].....	4-14
4.9	Influence of Slab Thickness and Foundation Support on Corner Deflection (computed with F.E. program) [from Reference 4.12]	4-16
4.10	Influence of Mechanical Load Transfer Device on Joint Effectiveness after 12 Years of Service [Reference 4.20]	4-17
4.11	Transverse Joint Deflection to Center Slab Deflection Ratio — SR 5	4-21
4.12	Transverse Joint Deflection to Center Slab Deflection Ratio — SR 90	4-22
4.13	Transverse Joint Deflection to Center Slab Deflection Ratio — All Data from SR 5 and 90.....	4-23
4.14	Temperature Gradient through 9-inch PCC Slab — SR 5	4-25
4.15	Percent Traffic in Each 6-inch Increment	4-27
4.16	Load Stresses for Different Load Locations along the Transverse Joint	4-28
4.17	Curl Stress Along the Transverse Joint — SR 5	4-30
4.18	Load, Curl, and Total Stress Along the Transverse Joint — SR 5....	4-31
4.19	Lateral Distribution of Fatigue Damage (18,000 Pound Single Axle) “Generic” Performance Curve”	4-33
4.20	Percent Slabs Cracked versus Cumulative ESALs	4-37
4.21	Crack Propagation Rate Example	4-38
4.22	Summary of Concrete Overlay on Existing Pavements [from Reference 5.2]	4-39
5.1	The Effectiveness of Mismatched Joints in Inhibiting the Development of Faulting and Pumping [from Reference 5.3]	5-2
5.2	Design Curve Comparing Present IDOT Thicknesses with the Mechanistic Based Procedure for Various Shoulder Types [from Reference 5.22]	5-7
5.3		5-24

LIST OF TABLES

Table		Page
2.1	SR 5 — WSDOT PMS System Distress Survey (Control Section 1728, Approximate MP 176.4).....	2-10
2.2	SR 90 — WSDOT PMS System Distress Survey (Control Section 3203, Approximate MP 278.6).....	2-14
2.3	Climatological Data for Seattle, Washington.....	2-22
2.4	Climatological Data for Spokane, Washington.....	2-22
3.1	Core Strength Data, SR 5	3-2
3.2	Core Strength Data, SR 90	3-4
3.3	Fatigue Data for Developing Performance Curves	3-7
3.4	Fatigue Data for Developing Adjusted Performance Curves.....	3-12
3.5	Summary of Load Transfer Efficiencies — SR 5	3-18
3.6	Summary of Load Transfer Efficiencies — SR 90	3-20
3.7	Load Transfer Efficiencies for Varying Levels of Aggregate Interlock	3-23
3.8	Summary of Play — SR 5	3-24
3.9	Summary of Play — SR 90.....	3-24
3.10	Summary of Voids — SR 5.....	3-31
3.11	Summary of Voids — SR 90.....	3-33
3.12	Summary of Backcalculated E and k, SR 5	3-44
3.13	Summary of Backcalculated E and k, SR 90	3-47
3.14	Temperature Differentials and Thermal Gradients — SR 5	3-55
3.15	Temperature Differentials and Thermal Gradients — SR 90	3-55
3.16	Equivalent Axle Load Estimate — SR 5, NE 175th (MP 176.35)....	3-61
3.17	Equivalent Axle Load Estimate — SR 90, MP 279.26.....	3-62
4.1	Ratio of Transverse Joint Deflection to Slab Center Deflection — SR 5	4-19
4.2	Ratio of Transverse Joint Deflection to Slab Center Deflection — SR 90.....	4-20
4.3	Void Evaluation at Slab Centers — SR 5	4-24
4.4	Pass-to-Coverage Ratios Along the Transverse Joint	4-34
5.1a	Performance of AC Overlays on District 4 PCCP — SR 5 Northbound.....	5-15
5.1b	Performance of AC Overlays on District 4 PCCP — SR 5 Southbound.....	5-17
5.2	Present Worth Cost Summary.....	5-31
5.3	Results of Total User Cost Calculations	5-32
6.1	Summary of Total Rehabilitation Costs	6-2

CHAPTER 1.0 INTRODUCTION

1.1 THE PROBLEM

The portland cement concrete (PCC) pavement used on the Interstate highway system in the urban areas of Washington have exceeded their original design lives (which were about 20 years). On SR 5, sections of PCC pavement in Vancouver, Olympia, Tacoma, Seattle, and Bellingham are all over 20 years old. On SR 90 the section of PCC pavement in Spokane is over 20 years old, as is SR 405 in Renton. Not only have these pavements begun to exceed their design lives, but in many cases, they have also experienced traffic loads over twice that to which they were originally designed. The distribution of all Interstate PCC pavement ages is shown in Figure 1.1 (western Washington) and Figure 1.2 (eastern Washington). This information shows that over 50 percent of the Interstate PCC pavement in western Washington and about 25 percent of the PCC pavement in eastern Washington is 20 or more years old.

In general, pavement conditions range from good to poor in these areas, with pavement distress such as longitudinal and transverse cracking, joint faulting, and wheelpath wear becoming rapidly more apparent. In high traffic volume areas of western Washington such as SR 5 in Vancouver and Seattle and SR 405 in Renton, the predominant distress is longitudinal cracking in the wheel path. No other state with similar pavement has experienced as high an incidence of this type of distress. The progression of this defect with time gives it the appearance of fatigue failure; however, at the time this study was started, there was disagreement among pavement specialists as to whether PCC pavement fatigue may be manifested in this manner.

With the large amount of PCC pavement at or just over 20 years in service, obviously WSDOT is nearing a time when it will need to rehabilitate or rebuild many of these pavements. WSDOT is planning now (1989) how best to rehabilitate these

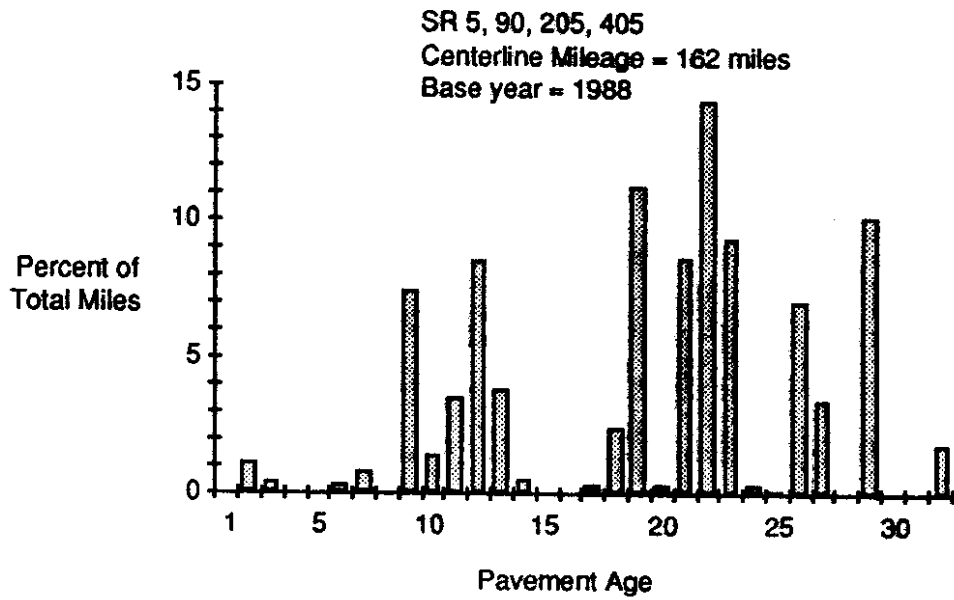


Figure 1.1. Pavement Age for WSDOT PCC Interstate Pavements - Districts 1, 3 and 4 (Westside)

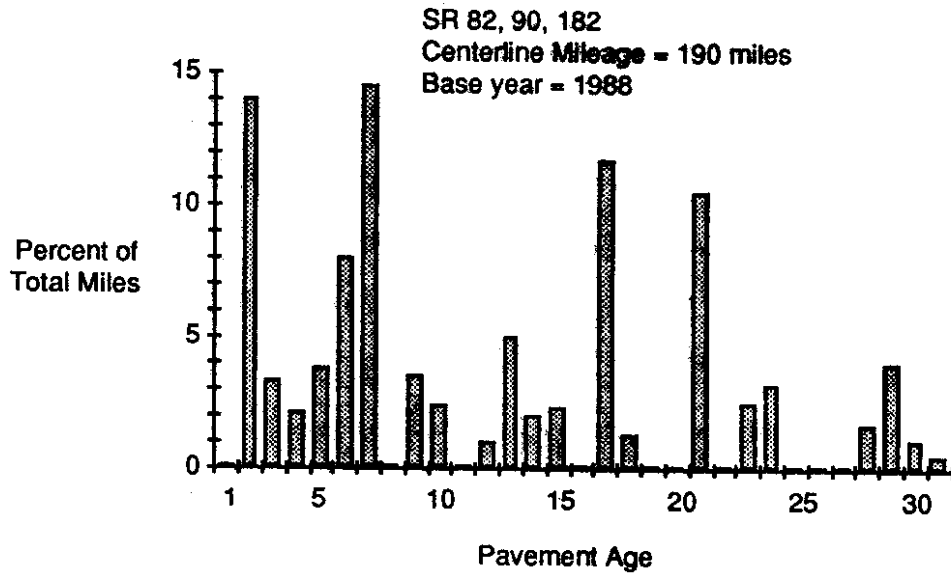


Figure 1.2. Pavement Age for WSDOT PCC Interstate Pavements - Districts 5 and 6 (Eastside)

pavements in an orderly manner so as to make the optimum use of the limited funds available, as well as to minimize the impact on the urban areas and traveling public.

At the time this study was started, WSDOT had few tools available to accomplish this task. Limited information was available for predicting pavement deterioration from faulting and transverse cracking, and none was available for predicting longitudinal cracking. The rate at which the individual segments of Interstate PCC pavement deteriorate must be known to determine both when to fund the individual projects, as well as what type of project to fund. Both the timing and the type of rehabilitation are dependent upon each other.

1.2 BACKGROUND

The major issue associated with the rehabilitation of the urban Interstate PCC pavement in Washington is timing. Almost all of the urban Interstate PCC pavements were constructed between 1961 and 1965. They have required almost no maintenance or rehabilitation over the intervening 25 years. Even after 25 years of service, some sections show almost no signs of cracking or faulting. This unusually good performance is probably due to well drained subgrade, mild climate, high quality aggregate, and high strength PCC pavement. These qualities also probably explain why Washington is also experiencing so much cracking distress (such as longitudinal cracking) as opposed to joint related distress (such as faulting).

To illustrate that these pavement structures have served well, the 1973 "AASHTO Interim Guides for Design of Pavement Structures" was used as a guideline to evaluate project-specific data that will be explained in subsequent chapters of this report (mostly Chapter 3.0 — Data Analysis).

For SR 5 in Seattle, the pavement slab should have been 9.5 inches thick to accommodate the traffic it withstood in its first 20 years (about 11,300,000 ESALs). (This assumes a $k \approx 150$ psi, working stress = $0.75 \times$ modulus of rupture (≈ 775 psi) = 580 psi,

and a terminal serviceability index ($p_t = 2.5$.) The actual pavement thickness was 9.0 inches, which, according to the AASHTO Design Guide, should have accommodated only 10,000,000 ESALs. As of December 1989, the pavement had accommodated about 15,000,000 ESALs and still had not decreased in serviceability to a $p_t = 2.5$. Thus, it had carried 50 percent more traffic than planned and was still functioning at an adequate serviceability level.

For SR 90 in Spokane, the pavement slab should have been 8.25 inches thick to accommodate the traffic it withstood in its first 20 years (about 5,000,000 ESALs). (This assumes a $k \approx 200$ psi, working stress = $0.75 \times$ modulus of rupture (≈ 700 psi) = 525 psi, and $p_t = 2.5$.) The actual pavement thickness was 7.8 inches, which, according to the AASHTO Design Guide, should have accommodated only 3,500,000 ESALs to $p_t = 2.5$ (which was reached in 1987 (age = 22 years)). Thus, it had carried 60 percent more traffic than could have been reasonably expected.

All of these factors contribute to the difficulty in planning the rehabilitation of these pavements. Because a large portion of the urban Interstate was built at about the same time, many of these pavement sections will likely need rehabilitation at the same time. The performance patterns experienced to date (a high incidence of longitudinal cracking and joint faulting) indicate that performance curves or models developed for other states, individually or in combination, may not be reasonable to apply in the state of Washington.

To plan and program for the rehabilitation of the existing PCC pavement on the urban Interstate system, WSDOT must confirm the mechanism of failure, determine some rate of deterioration for each individual project, and obtain a valid assessment of rehabilitation alternatives that apply in the urban environment. Clearly, the same issues apply to rural Interstate pavements, but the options are generally not as restricted because of traffic considerations and bridge overpasses and clearances.

Part of the problem in rehabilitating high-volume urban PCC pavement (or any type of pavement structure) is basically the level of traffic. For example, a slightly dated report

to Congress on the status of U.S. highways [1.1] revealed the following average ADT levels for U.S. Interstate highways:

- a. Rural Interstate ADT: 12,000
- b. Urban Interstate ADT: 51,000

Typical recent ADT values for urban sections of I-5 and I-90 are as follows:

- a. Seattle area I-5 ADT: 214,000
- b. Spokane area I-90 ADT: 52,000

Thus, ADT for I-90 in Spokane is about at the national average for urban Interstate highways; however, the corresponding value for I-5 in Seattle is about four times greater than the national average. These kinds of traffic levels not only complicate rehabilitation considerations but also the selection of the rehabilitation strategy type because of traffic flow (interruption) problems.

Traffic consideration, as well as initial rehabilitation construction costs, associated pavement performance, and user costs, will require the use of life-cycle costs. Life-cycle costing of viable rehabilitation alternatives will aid WSDOT decision-makers in selecting a reasonable rehabilitation strategy (keeping in mind that numerous site/project specific factors influence the final decision).

1.3 OBJECTIVES

The original study objectives were to model existing PCC pavements to

- 1. define the failure mode(s),
- 2. estimate deterioration rates, and
- 3. develop optimum rehabilitation alternatives and associated timing.

This was done, as will be described in this report, for two urban pavement sections, SR 5 in Seattle and SR 90 in Spokane.

1.4 REPORT ORGANIZATION

This report contains five other chapters. Chapter 2.0 discusses the sites selected for this study and the data collected. Chapter 3.0 contains the data analyses, Chapter 4.0 a performance evaluation of PCC pavement, Chapter 5.0 rehabilitation alternatives, and finally, Chapter 6.0 the conclusions and recommendations. Also included in this report are several appendices that provide supporting details.

CHAPTER 2.0

SITE SELECTION AND DATA COLLECTION

To evaluate PCC pavement performance in Washington, it was necessary to study pavements that exhibited typical behavior and that contained the common distress types observed throughout the state. To complete the evaluations, pavement sections fulfilling the above criteria first had to be identified, and then those most conducive to study had to be selected. This chapter discusses the site selection process and provides pertinent information about each site.

Once study sites were selected, several activities were undertaken to collect information pertinent to pavement performance. These activities are also described in this chapter.

2.1 SITE SELECTION

The study objectives included selecting two pavement sites for evaluation. [2.1] One site was to be located in eastern Washington and was to contain transverse (mid-panel) cracking and joint faulting. The other site was to be located in western Washington, where longitudinal cracking is commonly observed. (However, there are several areas along the SR 5 route that currently exhibit faulting.) An additional criterion for site selection was that the pavement section must have adequate site distance so that during field work the lanes being evaluated could be blocked off safely. The availability of a complete performance history based on Washington State Department of Transportation (WSDOT) condition surveys for the two sites was also a consideration in selection.

After possible pavement sections were evaluated, two sites were selected. One site was located north of Seattle in the northbound lanes of SR 5 (at approximately 175th N.E.), and the other site was located west of Spokane in the westbound lanes of SR 90 (near the Abbott Road overpass).

2.1.1 SR 5

The portion of SR 5 containing the selected test section was built under Federal Aid Interstate Project No. SR-5-3(200)170, and construction was completed in December 1964. Four 12-foot wide PCC lanes were constructed in each direction, bounded by asphalt concrete surfaced shoulders. The transverse joints were sawed at 15-foot intervals. This pavement and others built at the same time, in contrast to current construction, have transverse joints that are perpendicular to the pavement centerline rather than skewed.

The pavement design for this Federal Aid project was 0.75 foot (9 inches) of plain-jointed PCC, over 0.17 foot (2 inches) of crushed surfacing top course, over 0.42 foot (5 inches) of special ballast, over a silty sand subgrade.

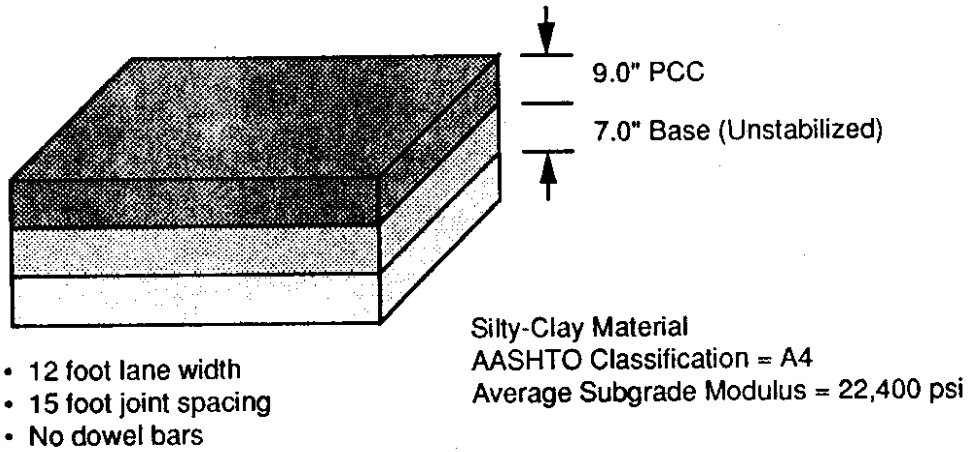
The section selected for evaluation was 420 feet long, with the southern end beginning at approximately Milepost 176.35. The test section included the two outer northbound lanes. To provide a representative sample of the 56 PCC slabs in the section, 24 were evaluated. The pavement cross-section and other basic site information are shown as Figure 2.1.

2.1.2 SR 90

The length of SR 90 containing the selected test section was constructed under Federal Aid Interstate Project Numbers SR-90-5(16)270 and SR-90-6(32)271. Construction was completed in April 1964. SR 90 in this location has six lanes, three in each direction, bounded on the inside by an asphalt concrete shoulder and on the outside by a 3-foot wide curb and gutter section adjacent to an asphalt concrete shoulder. The curb and gutter section was built after the traffic lanes were placed and was constructed without any ties to these lanes. The traffic lanes are 12 feet wide, with transverse joints sawed at 15-foot intervals. The transverse joints were sawed normal to the pavement centerline.

The pavement design for these Federal Aid projects was 0.65 foot (7.8 inches) of plain-jointed portland cement concrete, over 0.20 foot (2.4 inches) of crushed surfacing

Pavement Cross-Section



Climate

Climate Zone	= Wet non-freeze
Average Annual Temperature	= 53 F°
Average Annual Temperature Range	= 39 F°
Mean Annual Precipitation	= 39 inches
Corps of Engineers Mean Freezing Index	= 25 °F-days

Traffic

Estimated two-way ADT	= 145,900
% Commercial Trucks	= 4

Figure 2.1. Basic Site Information - SR 5 Seattle
(milepost 176.35 - 176.43)

top course, over 0.25 foot (3 inches) of special gravel base, over a sandy subgrade with some silt.

The section evaluated during this study was 840 feet long. The test site included the two outer westbound lanes. To provide a representative sample, 24 of the 112 slabs in this section were evaluated. The pavement cross-section and other basic site information are shown as Figure 2.2.

2.2 DATA COLLECTION

Site visits were made to the SR 5 test section in September 1986 and to the SR 90 test section in July 1986 and July 1987. During the 1986 visits several data collection activities were completed, including PCC coring, a crack survey, a faulting survey, and nondestructive deflection testing. Deflection data were also collected during the 1987 SR 90 site visit. In addition to field data collection activities, climatological data and traffic data for the two sites were collected, as were bridge clearance data along SR 5 and SR 90.

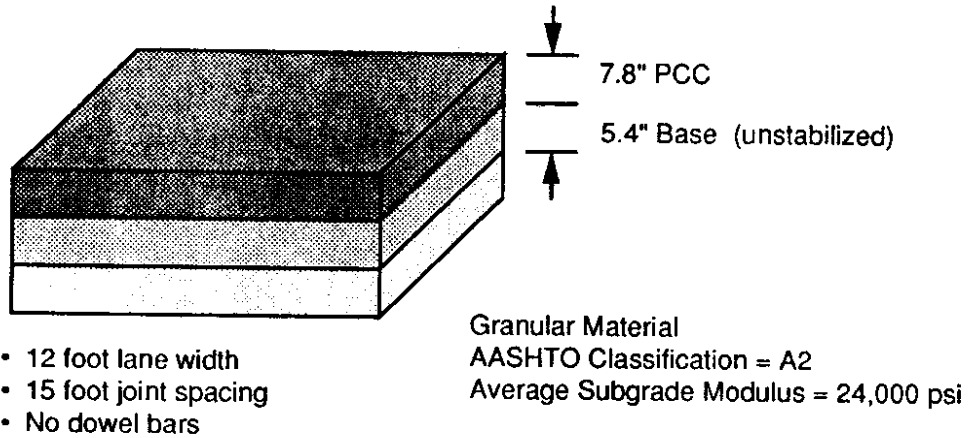
2.2.1 Coring

WSDOT crews conducted an extensive coring program at both the SR 5 and SR 90 test sections. The WSDOT crews used a 4-inch diameter drill and a wet drilling process to core the concrete. Each core was tagged and packed for shipment to the University of Washington Department of Civil Engineering materials laboratory for subsequent evaluation.

2.2.1.1 SR 5. At the SR 5 site, 40 cores were drilled. Cores were obtained at intact slab centers, at transverse joints, at the longitudinal joint, in intact areas between joints and cracks, and at longitudinal cracks. Each core location is shown in Figure 2.3.

This pavement section contained one slab with a longitudinal crack just beginning to propagate from the transverse joint towards the slab center (Lane 2, Slab 26). Three cores (cores 36, 37 and 38) were drilled along this crack until the crack tip was contained in a

Pavement Cross-Section



Climate

Climate Zone	= Wet-dry freeze
Average Annual Temperature	= 47 F°
Average Annual Temperature Range	= 65 F°
Mean Annual Precipitation	= 17 inches
Corps of Engineers Mean Freezing Index	= 667 °F-days

Traffic

Estimated two-way ADT	= 38,300
% Commercial Trucks	= 13

Figure 2.2. Basic Site Information - SR 90 Spokane (milepost 278.60 - 278.75)

Plotted 9/3/86
Revised 9/30/86

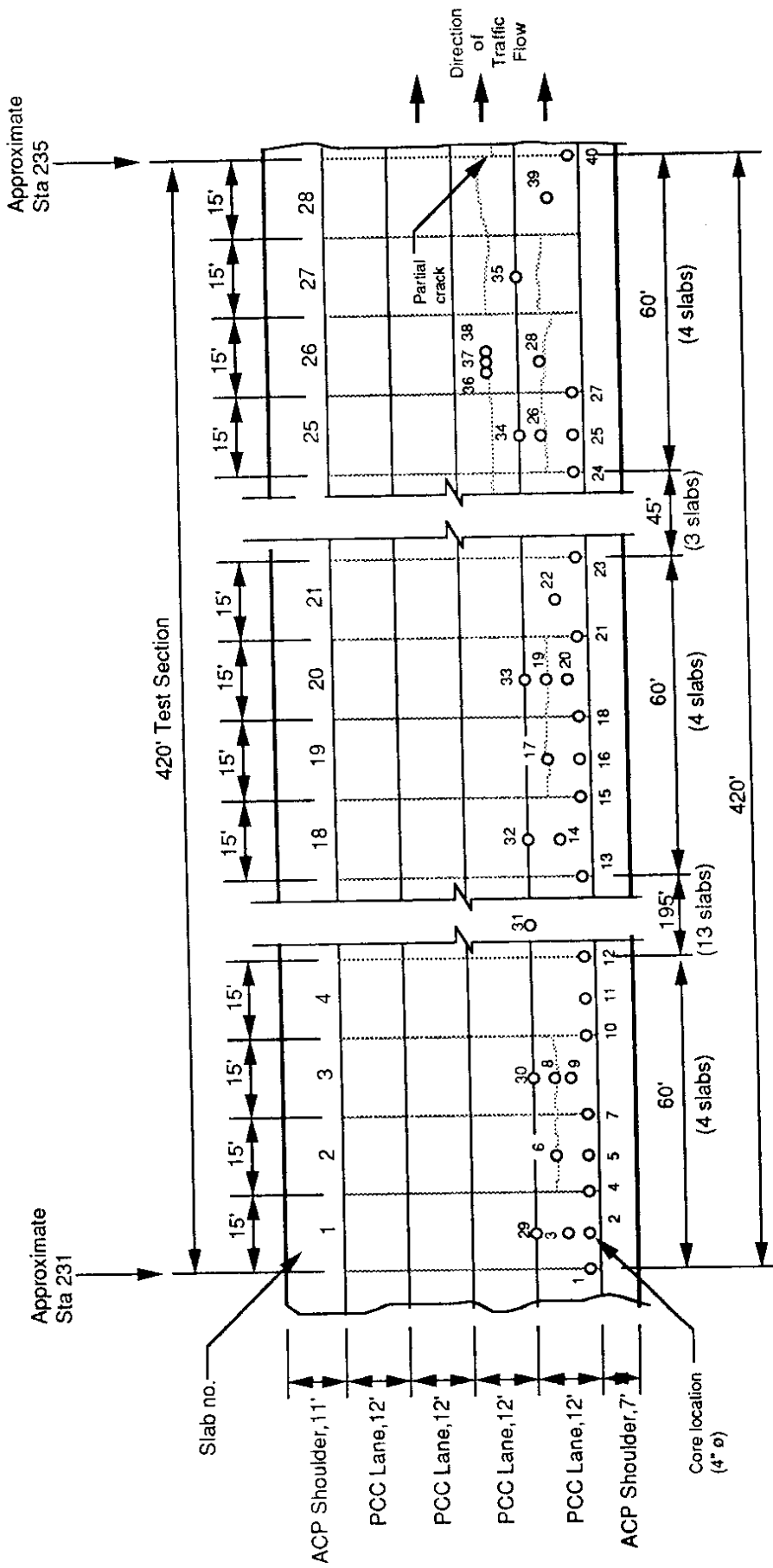


Figure 2.3. PCC Cores - Plan View, SR 5 Seattle (Northbound)

core. An examination of the core revealed that the crack initially developed at the bottom of the slab because the crack was wider at the bottom than at the top. This crack initiation location indicated a fatigue type of failure.

2.2.1.2 SR 90. Cores were drilled at 51 locations in the SR 90 site. Intact slab centers, transverse joints, the longitudinal joint, intact areas between cracks and joints, and transverse cracks were cored. Figure 2.4 shows each core location.

Two observations made during the coring process at this site warrant mention. First, at several joints the concrete at the bottom of the slab appeared to have "eroded." Second, substantial wear appeared in both the cement paste and the aggregate along crack and joint faces at this site, in contrast to the SR 5 site, where little wear was apparent.

2.2.2 Crack Survey

Each crack location and its condition were recorded at both the SR 5 and 90 test sections during the 1986 site visits by University of Washington and WSDOT personnel. In addition, previously collected pavement condition data that documented pavement condition were reviewed.

WSDOT has conducted visual surveys for several years. When these surveys are conducted, information about pavement condition is recorded. The data collected are used in the Washington State Pavement Management System to prioritize rehabilitation needs statewide. The distress types, measurement criteria, and associated deduct points used in the WSDOT Pavement Management System for PCC are shown in Figure 2.5. [2.2]

2.2.1.1 SR 5. The major distress type observed at this site during the September 1986 survey was longitudinal cracking. Longitudinal cracks were present in 11 of the 24 slabs evaluated (46 percent). All cracks were spalled, with spalled widths varying from about 1.0 to 3.5 inches. The mean spall width was about 2.0 inches. The spall depths varied from slightly less than 1.0 inch to 3.0 inches, with a mean depth of

Plotted 6/26/86
 Revised 6/27/86
 Revised 7/03/86
 Revised 7/18/86 (Coring completed 7/09/86)

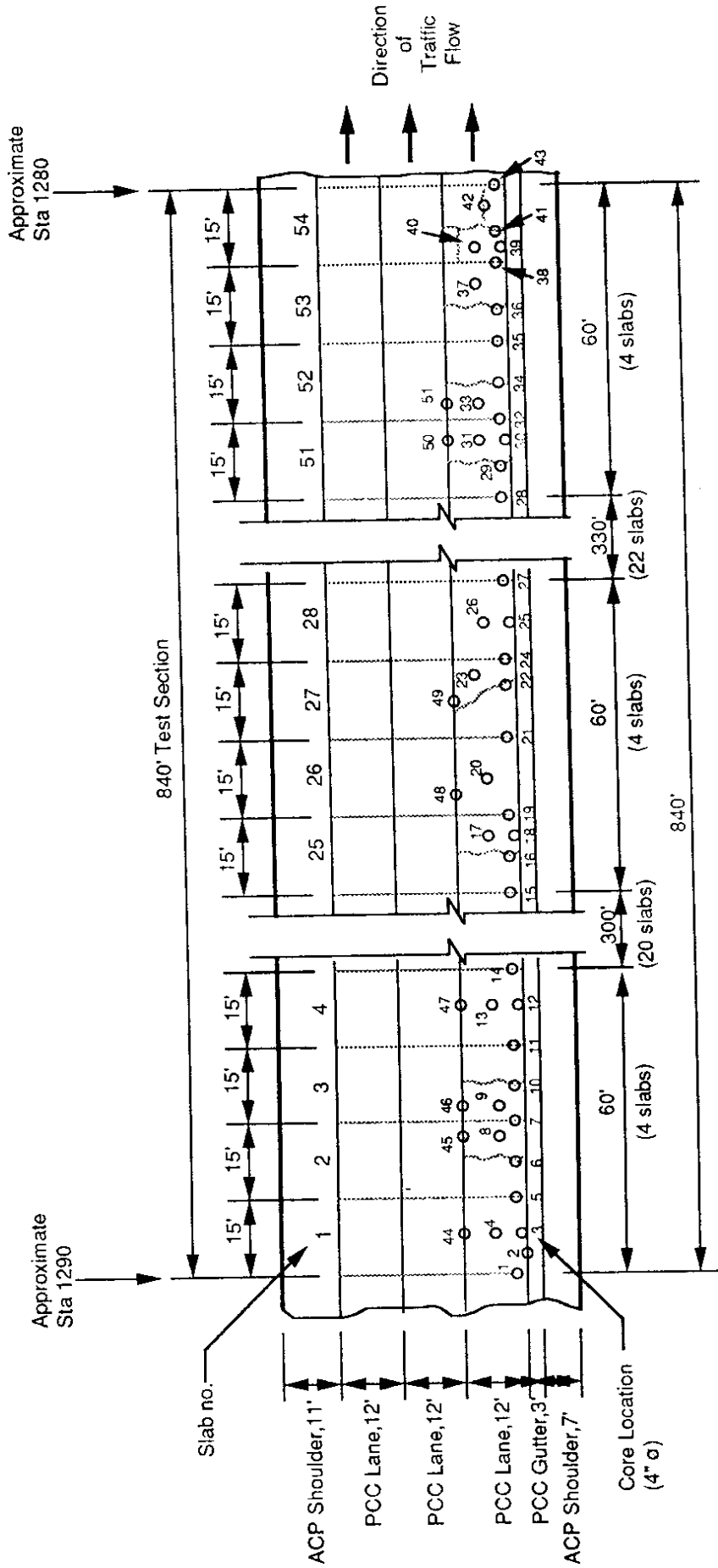


Figure 2.4. PCC Cores - Plan View, SR 90 Spokane (Westbound)

Distress Type	Distress Severity			Distress Extent		
Cracking Averaging 1/8+	Units per Panel Length	(1) (2) (3)	1-2 3-4 4+	Percent of Panels		
				1-25	26-50	51+
				5	10	20
				10	20	35
Raveling Disintegration Popouts Scaling		(1) (2) (3)	Slight Moderate Severe	Percent of Area		
				1-25	26-75	76+
				0	0	0
				0	0	0
Spalling at Joints and Cracks	Average Width in Inches	(1) (2) (3)	1/4-1 1-3 3+	Percent of Joints		
				1-15	16-50	51+
				5	10	15
				10	20	30
Pumping Blowing	Percent of Panel Length	(1) (2) (3)	1-9 10-50 51+	Percent of Joints		
				1-15	16-35	36+
				0	0	0
				0	0	0
Blowups	Number per Mile	(1) (2) (3)	1 2-3 4+	Blowups per Mile		
				1	2-3	4+
				0	0	0
				0	0	0
Faulting Curling Warping Settlement	Average Displacement in Inches	(1) (2) (3)	1/8-1/4 1/4-1/2 1/2+	Percent of Panels		
				1-15	16-35	36+
				5	10	20
				10	20	30
Patching	Percent of Panels	(1) (2) (3)	1-5 6-20 21+	Percent of Area per Panel		
				1-5	6-25	26+
				0	0	0
				0	0	0
Rutting Pavement Wear	Average Depth in Inches	(1) (2) (3)	1/4-1/2" 1/2-3/4" Over 3/4"	Percent of Joints		
				1/4-1/2	1/2-3/4	3/4+
				0	0	0
				0	0	0

Pavement Condition Rating = $100 - \Sigma$ (Defect Values)

Figure 2.5 Values for Portland Cement Concrete Pavements Developed for PMS [after Reference 2.2]

slightly more than 1.5 inches. Figure 2.6 documents the location and condition of all cracks observed during the survey.

The visual survey data collected by WSDOT indicated that longitudinal cracks were first observed in the control section containing this test site in 1975, or 11 years after construction. The cracking at this point must have been relatively minor because it was not observed during the 1979 survey.

Table 2.1 summarizes the distress survey data collected for the control section between 1975 and 1988. The data collected indicated that the amount (extent) of longitudinal cracking and its severity have remained in the same rating category (1-25 percent cracked and 1-2 cracks per slab) since 1975, although the amount of cracking was probably at the low end of the 1-25 percent category in 1975 and was at the higher end of that range during this study. The spall severity observed did not change during this period; however, between the 1986 and 1988 surveys the spalling extent increased to the highest recording level (51+ percent).

**Table 2.1 SR 5 — WSDOT PMS System Distress Survey
(Control Section 1728, Approximate MP 176.4)**

Survey Year ¹	Cracking ²		Joint and Crack Spalling	
	Extent (% Panels Cracked)	Severity (Cracks per Panel Length)	Extent (% Spalled)	Severity (Average Width in Inches)
1975	1-25	1-2	1-15	1/4-1
1979	None	None	None	None
1983	1-25	1-2	16-50	1/4-1
1984	1-25	1-2	16-50	1/4-1
1986	1-25	1-2	16-50	1/4-1
1988	1-25	1-2	51+	1/4-1

¹ No distress was observed prior to 1975

² Longitudinal cracks

Plotted 9/3/86
Revised 9/30/86

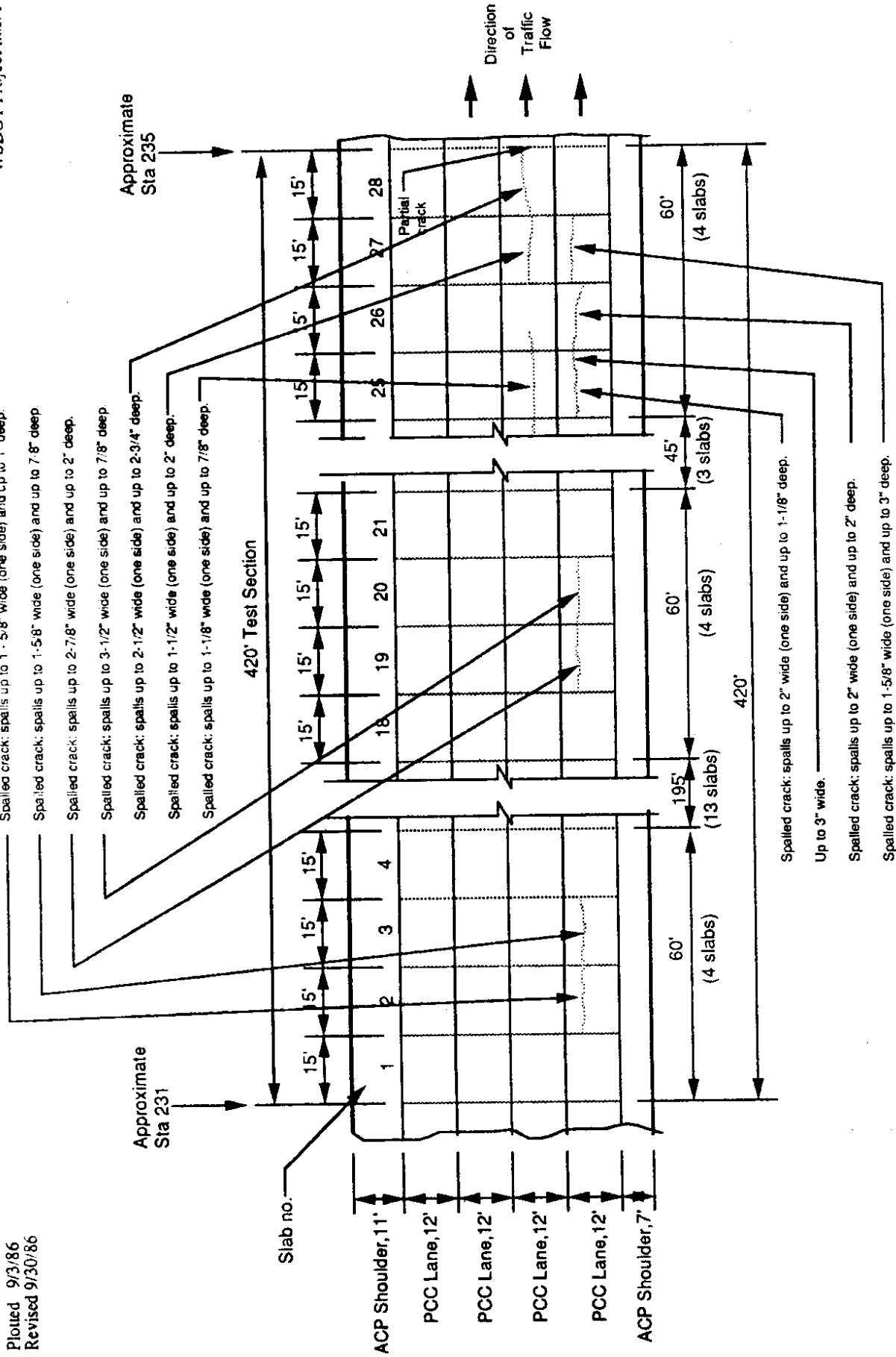


Figure 2.6. Crack Survey - Plan View, SR 5 Seattle (Northbound)

Discrepancies did exist among the survey data WSDOT collected and those measured during the September 1986 site survey. A discrepancy existed for cracking extent, which the WSDOT survey data indicated was between 1 and 25 percent and the site survey indicated was approximately 50 percent. This discrepancy resulted from the differences in methodologies used to conduct the condition surveys. The survey results are recorded for each mile and are completed by a rating team driving along the pavement at relatively slow speeds. It is possible that the control section containing the test site had, on the average, a 1 to 25 percent incidence rate of cracked slabs, whereas the test site had substantially more cracked slabs.

In addition to the longitudinal cracking observed, significant wheelpath wear was present in SR 5 north of Seattle (likely due to studded tires). While pavement wear is a category in the WSDOT pavement management system, this wear was not recorded during the WSDOT visual condition surveys.

2.2.2.2 SR 90. Transverse cracking was observed during the July 1986 SR 90 site visit. Of the 24 slabs evaluated, nine were cracked (37.5 percent). The cracks observed were spalled, with spall widths ranging from 0.75 inch to 2.0 inches. The mean spall width was slightly more than 1.5 inches. Spall depths ranged from 0.75 inch to 2.0 inches, with a mean depth of slightly more than 1.0 inch. Figure 2.7 illustrates each crack condition and location in June 1986. A subsequent examination of the slabs in December 1989 revealed only one additional crack occurring during the intervening 2.5-year period (the longitudinal cracks in Lane 2, Slabs 50 and 51).

The visual survey data collected by WSDOT at the control section containing the test site are presented in Table 2.2. They indicated that transverse cracking was first observed in this section in 1969, just four to five years after construction. This cracking was not observed in the 1971 survey but was again observed in the 1973 survey.

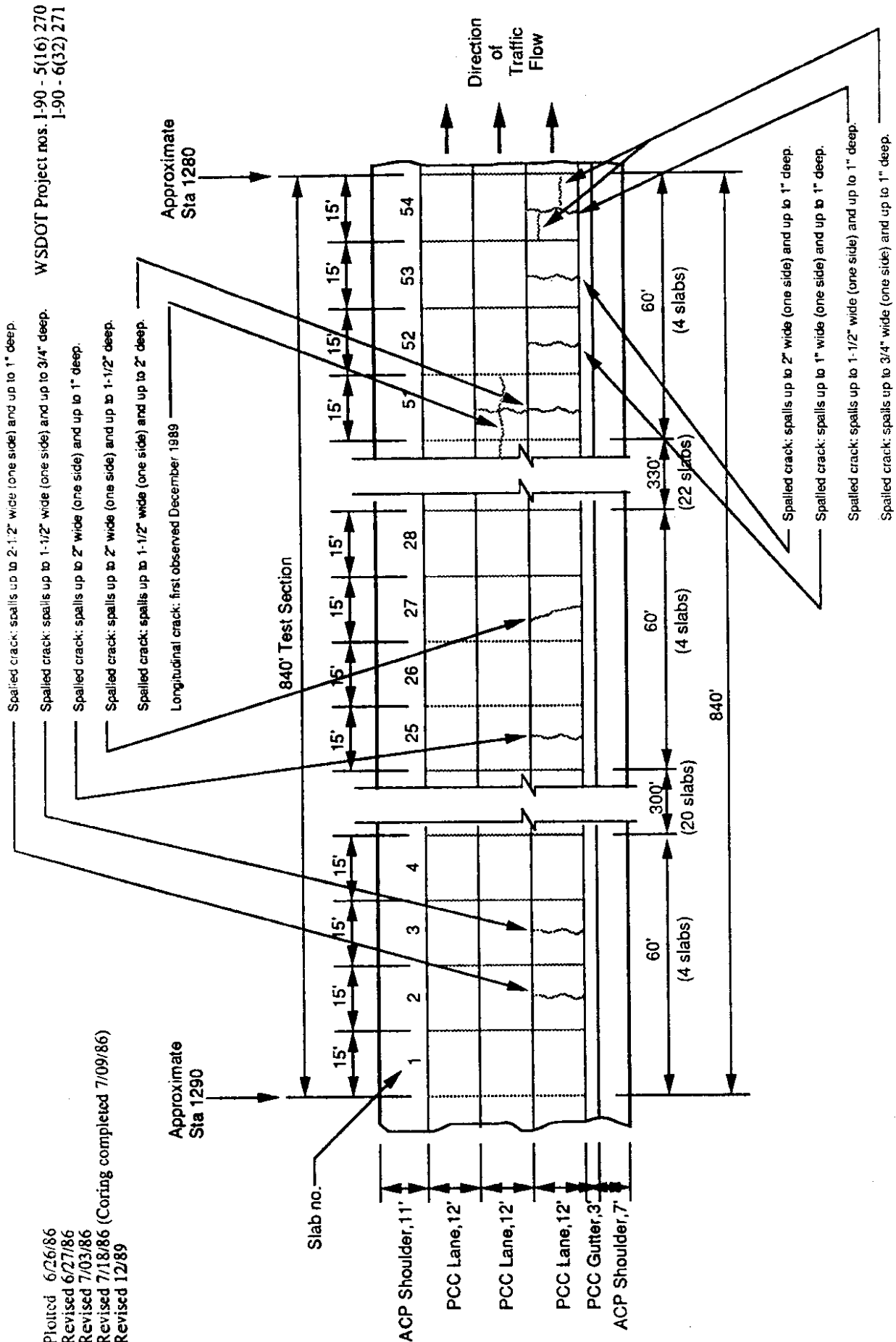


Figure 2.7. Crack Survey, SR 90 Spokane (Westbound)

**Table 2.2 SR 90 — WSDOT PMS System Distress Survey
(Control Section 3203, Approximate MP 278.6)**

Survey Year ¹	Cracking ²		Joint and Crack Spalling		Faulting	
	Extent (% Panels Cracked)	Severity (Cracks per Panel Length)	Extent (% Spalled)	Severity (Average Width in Inches)	Extent (% Slabs)	Severity (Average Depth in Inches)
1969	1-25	1-2	None	None	None	None
1971	None	None	1-15	1/4-1	1-15	1/8-1/4
1973	1-25	1-2	1-15	1/4-1	36+	1/8-1/4
1975	1-25	1-2	16-50	1/4-1	36+	1/8-1/4
1977	1-25	1-2	16-50	1/4-1	36+	1/8-1/4
1983	1-25	1-2	16-50	1/4-1	36+	1/8-1/4
1984	1-25	3-4	51+	1/4-1	36+	1/8-1/4
1986	26-50	1-2	51+	1/4-1	36+	1/4-1/2

¹ No distress was observed prior to 1969

² Transverse cracks

The data contained in Table 2.2 indicated that cracking extent had increased since 1984, while the severity had remained constant. In addition, the percentage of cracks/joints that were spalled increased to the highest category in 1984 (51+ percent), while the severity remained constant (1/4-1 inch width).

2.2.3 Faulting Survey

Faulting measurements were made for transverse and longitudinal joints at the SR 5 site and for transverse joints and cracks at the SR 90 site. Faulting was measured to the nearest 1/16 inch.

2.2.3.1 SR 5. The transverse joint faulting measurements were made at the slab edges because the significant wheelpath wear may have invalidated faulting measurements made in the wheelpaths. In addition, longitudinal joint faulting was measured. No faulting was noted across the longitudinal cracks.

The transverse joint faulting ranged from 0.0625 inch (1/16 inch) to 0.1875 inch (3/16 inch). The mean transverse joint faulting was 0.082 inch, with an associated

standard deviation of 0.047 inch. No measurable faulting was found along the longitudinal joint, except at the south corner of Slab 18 and at the north corner of Slab 28, where the faulting was measured to be 0.125 inch (1/8 inch). The faulting survey results are presented in Figure 2.8.

No faulting was recorded by WSDOT for the PMS files along this section of SR 5 because the minimum faulting level at which distress is recorded is 1/8 inch or greater. The faulting at SR 5 was for the most part less than this level.

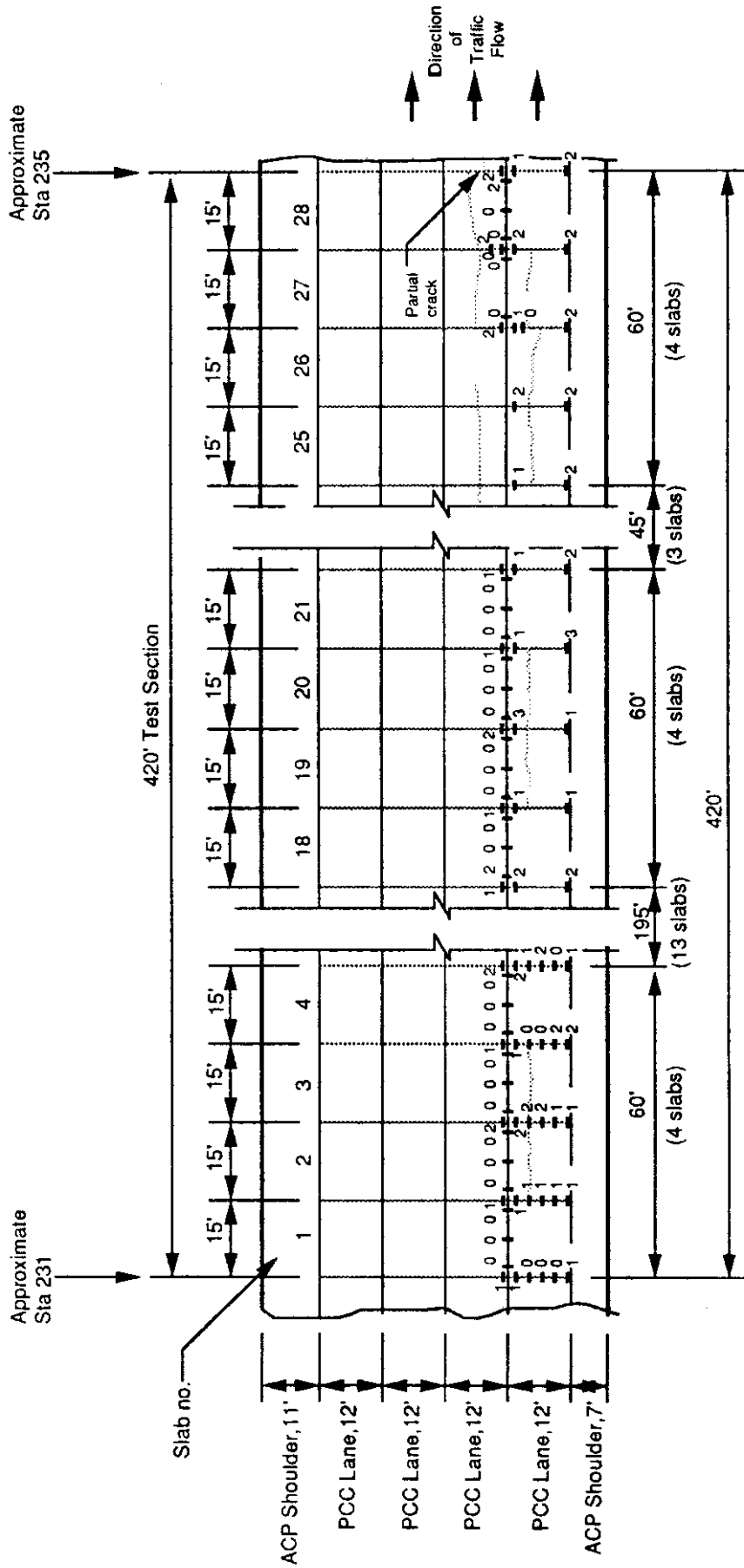
2.2.3.2 SR 90. Faulting measurements were made along the transverse joints and cracks at this test section. Each transverse joint was faulted, with faults ranging from 0.125 inch (1/8 inch) to 0.375 inch (3/8 inch), with a mean value of 0.22 inch and an associated standard deviation of 0.05 inch.

Transverse crack faulting was less severe than that measured at the transverse joints and ranged from no faulting to 0.25 inch (1/4 inch). The mean faulting at the transverse cracks was 0.10 inch, with a standard deviation of 0.09 inch. The faulting survey results for SR 90 are presented in Figure 2.9.

Faulting along this stretch of SR 90 was first observed during the 1971 visual condition survey (see Table 2.2). An increased amount of faulting was noted during the 1973 survey. The percentage of slabs with faulting had been in the highest rating category (36+ percent) since 1973. In 1986, the severity increased from the 1/8 to 1/4-inch category to the 1/4 to 1/2-inch category.

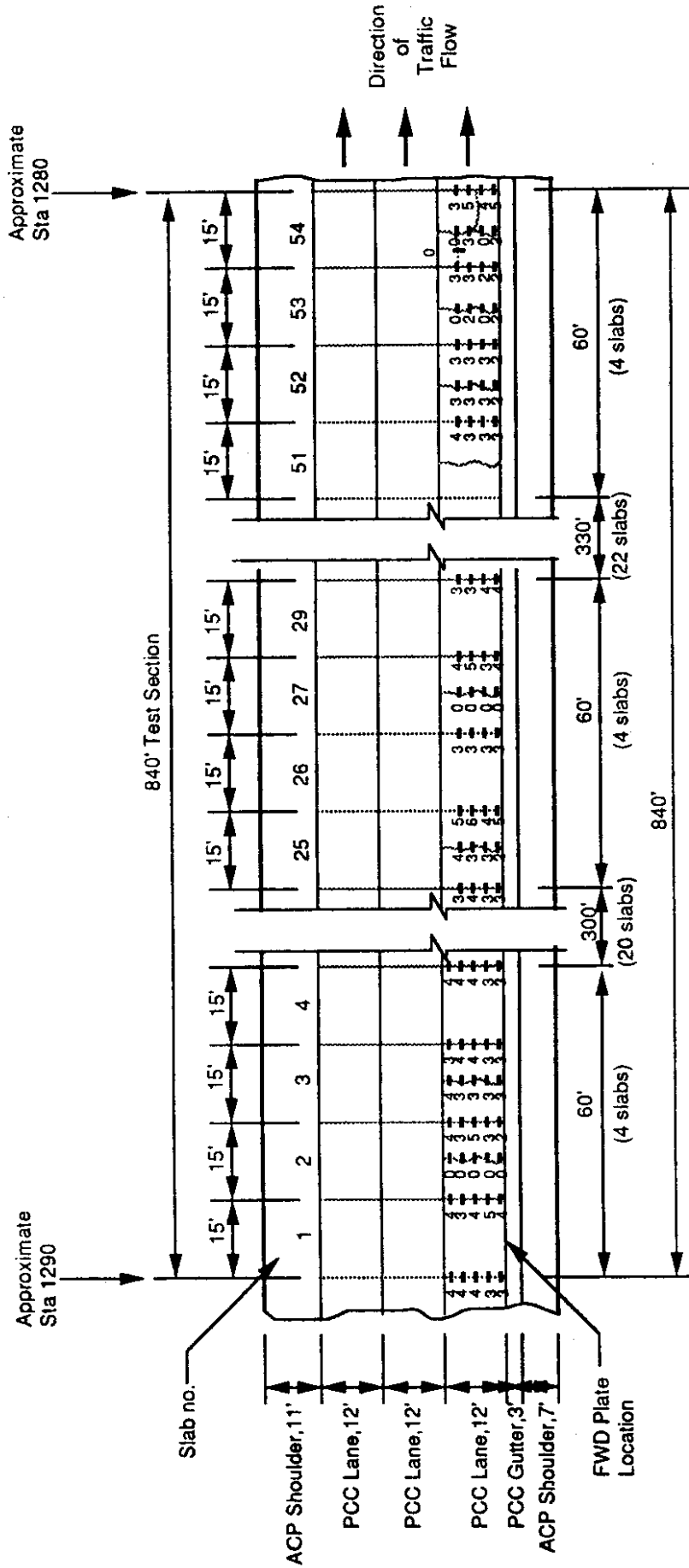
2.2.4 Nondestructive Deflection Testing

Nondestructive deflection testing was conducted with the WSDOT Falling Weight Deflectometer (FWD). Testing was conducted at the SR 5 test section during September 1986 and at the SR 90 test section during July 1986 and July 1987. The deflection data collected at SR 90 in 1987 were not used in this study because inconsistencies in the data



Note: Faulting survey conducted 9/3/86 and 9/4/86. Measurements at the slab edges provide the best estimate of true faulting since the wheelpaths have experienced significant wear. Measurements as shown in 1/16's of an inch.

Figure 2.8. Faulting Survey, SR 5 Seattle (Northbound)



Note: Faulting measurements were taken near the slab edges, both wheel paths and the center of the slab at contraction joints and cracks in the direction of traffic flow. Measurements in 1/16's of an inch.

Figure 2.9. Faulting Survey, SR 90 Spokane (Westbound)

indicated the center (directly under the load) velocity transducer was not recording properly.

Load levels of approximately 6,000, 9,000, 12,000 and 15,000 pounds of force were applied to the pavement during this study. At each test point, eight drops were performed, two at each load level. The air temperature during testing was also recorded.

FWD testing was conducted for both sites at the following locations: slab center, transverse joints, and slab corners. The transverse joint testing was conducted on both the approach and leave sides. To test the approach side of the joint, the loading plate was placed in front of the joint, with the other velocity transducers located across the joint. The leave side of the joint was tested by placing the loading plate at the joint edge on the leave slab with an extra velocity transducer mounted behind the loading plate across the joint. The concepts of slab approach and leave sides and of transverse joint testing are illustrated in Figure 2.10. The slab corners were also tested on both sides of each joint.

In addition, at the SR 5 site, testing was conducted along the longitudinal joint and two longitudinal cracks. At the SR 90 site, additional testing was conducted on both the approach and leave sides of all transverse cracks. The FWD test point locations for the SR 5 and SR 90 test sections are shown in Figures 2.11 and 2.12, respectively.

2.2.5 Climatological Data

Several types of climatological data were collected during this study for each test section. The information collected comprised mean daily maximum and minimum temperature for each month, mean monthly temperature, mean normal heating and cooling degree days, and mean daily solar radiation. [2.3] In addition, mean monthly wind velocity, mean monthly percentage of possible sunshine, and mean monthly percentage of sky cover data were collected. [2.4] These data are presented in Table 2.3 for Seattle (SR 5) and in Table 2.4 for Spokane (SR 90).

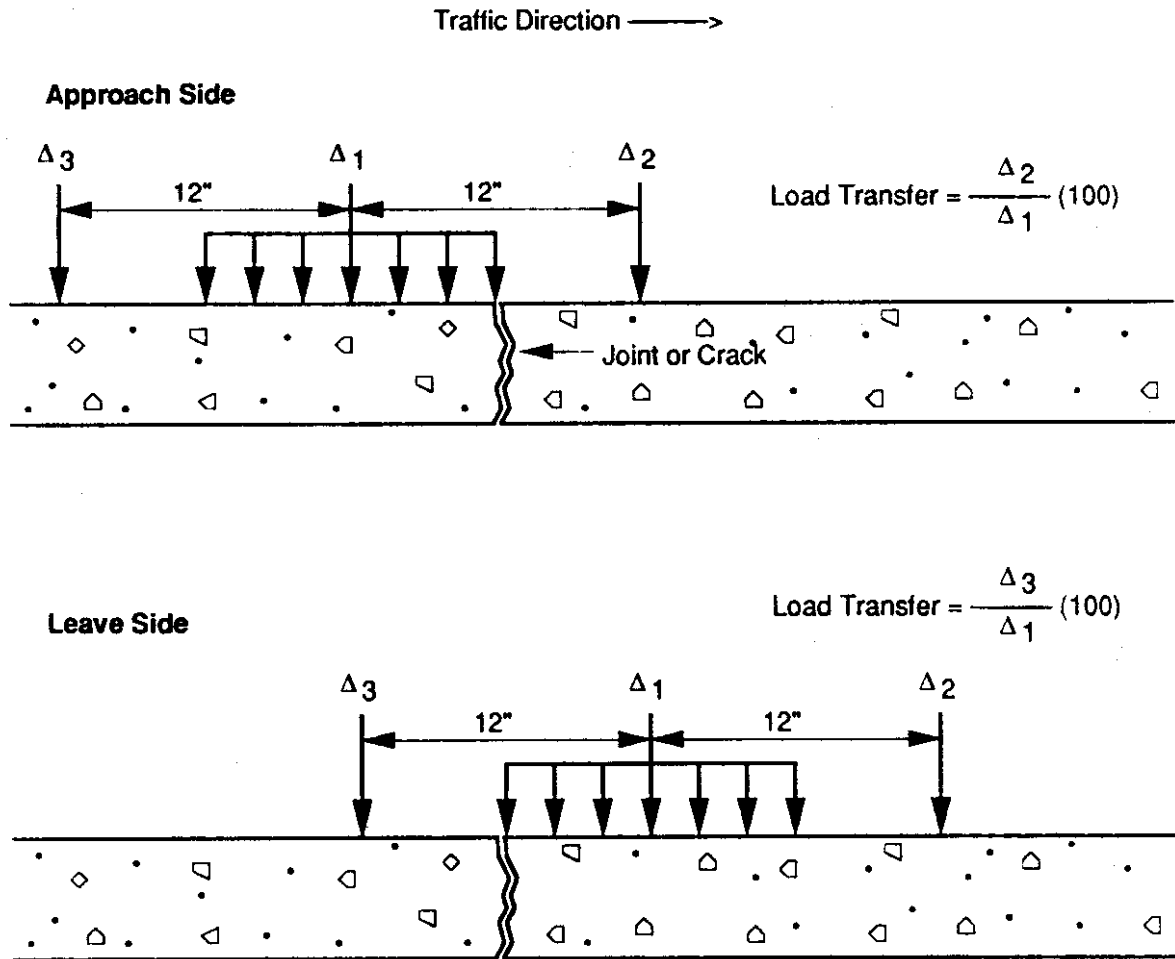


Figure 2.10. Arrangement of Deflection Sensors for Determining Load Transfer Efficiency at Approach and Leave Sides of a Joint or Crack

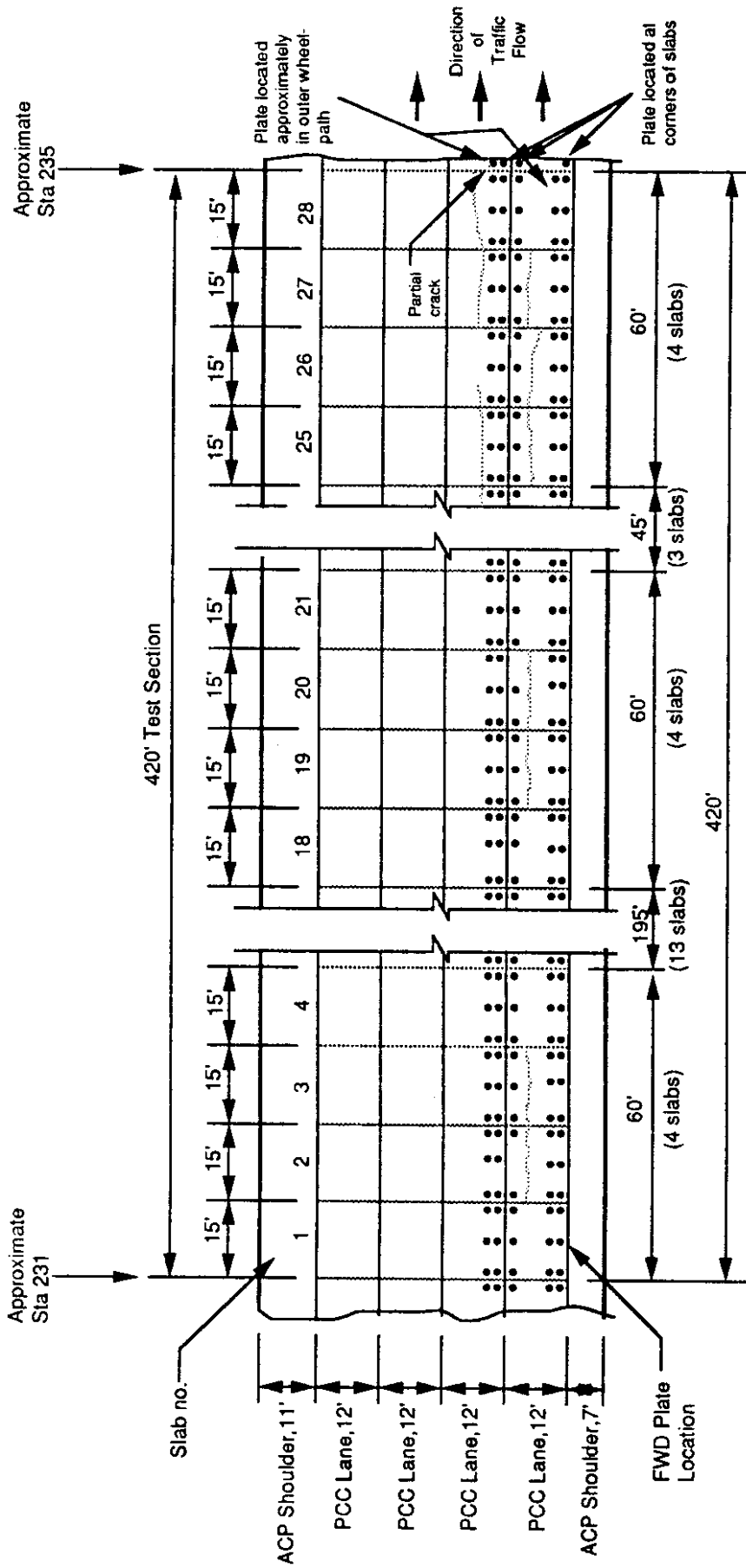


Figure 2.11. FWD Plate Locations - Plan View, SR 5 Seattle (Northbound)

Plotted 6/26/86
Revised 6/27/86
Revised 7/03/86
Revised 8/11/86

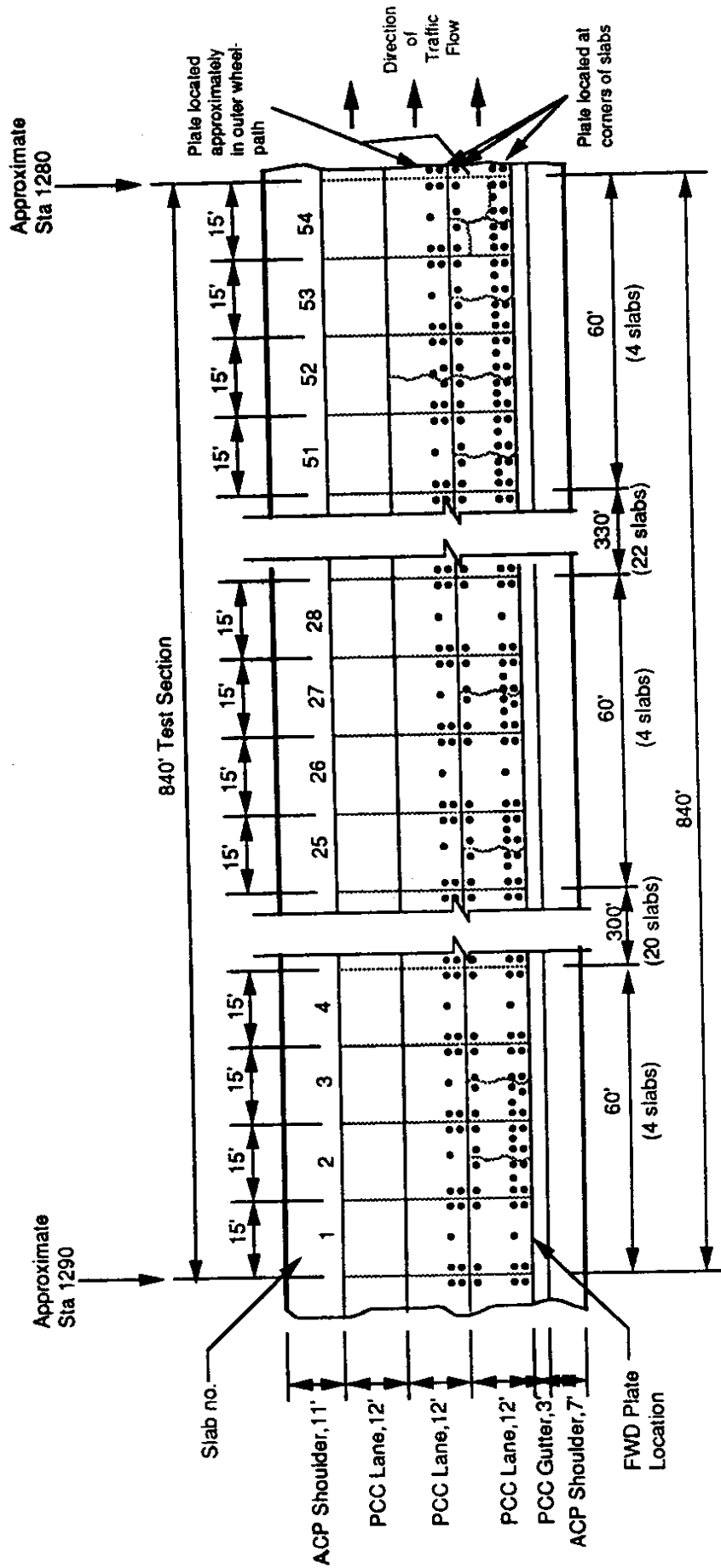


Figure 2.12. FWD Plate Locations - Plan View, SR 90 Spokane (Westbound)

Table 2.3 Climatological Data for Seattle, Washington

Month	Normal Temperature (°F)			Normal Degree Days		Total Hemispheric Mean Daily Solar Radiation		Wind and Sunshine		
	Daily Max	Daily Min	Monthly	Base 65°F		BTU/Ft ²	Langleys	Wind Velocity	% Possible Sunshine	% Sky Cover
				Heating	Cooling					
Jan	43.4	33.0	38.2	831	0	261.7	71.0	9.9	24	8.5
Feb	48.5	36.0	42.3	636	0	495.0	134.3	9.7	38	8.2
Mar	51.5	36.6	44.1	648	0	849.4	230.4	9.9	50	7.9
Apr	57.0	40.3	48.7	489	0	1293.5	350.9	9.6	53	7.7
May	64.1	45.6	54.9	313	0	1713.9	464.9	9.0	56	7.1
Jun	69.0	50.6	59.8	167	11	1801.8	488.7	8.8	54	7.1
Jul	75.1	53.8	64.5	80	65	2248.2	609.8	8.3	64	5.3
Aug	73.8	53.7	63.8	82	45	1616.3	438.4	7.9	63	5.8
Sep	68.7	50.4	59.6	170	8	1147.7	311.3	8.1	59	6.2
Oct	59.4	44.9	52.2	397	0	656.2	178.0	8.6	44	7.5
Nov	50.4	38.8	44.6	612	0	337.2	91.5	9.2	30	8.3
Dec	45.4	35.5	40.5	760	0	211.1	57.3	9.8	20	8.7
Ann	58.8	43.3	51.1	5185	129	1052.7	285.5	9.1	46	7.4

Latitude: 47°27'N
 Longitude: 122°18'W
 Elevation: 122

Table 2.4 Climatological Data for Spokane, Washington

Month	Normal Temperature (°F)			Normal Degree Days		Total Hemispheric Mean Daily Solar Radiation		Wind and Sunshine		
	Daily Max	Daily Min	Monthly	Base 65°F		BTU/Ft ²	Langleys	Wind Velocity	% Possible Sunshine	% Sky Cover
				Heating	Cooling					
Jan	31.1	19.6	25.4	1228	0	315.0	85.4	8.7	26	8.3
Feb	39.0	25.3	32.2	918	0	605.9	164.3	9.2	38	8.0
Mar	46.2	28.8	37.5	853	0	1040.6	282.3	9.6	53	7.4
Apr	57.0	35.2	46.1	567	0	1494.9	405.5	9.8	60	7.1
May	66.5	42.8	54.7	327	8	1918.0	520.2	8.9	63	6.6
Jun	73.6	49.4	61.5	144	39	2082.8	565.0	8.9	65	6.1
Jul	84.3	55.1	69.7	21	167	2357.4	639.4	8.3	80	3.7
Aug	81.9	54.0	68.0	47	140	1942.0	526.8	8.1	77	4.1
Sep	72.5	46.7	59.6	196	34	1435.3	389.3	8.1	70	4.9
Oct	58.1	37.5	47.8	533	0	840.9	228.1	8.0	53	6.4
Nov	41.8	29.2	35.5	885	0	397.7	107.9	8.3	28	8.0
Dec	33.9	24.0	29.0	1116	0	255.2	69.2	8.7	21	8.5
Ann	57.2	37.3	47.3	6835	388	1223.8	332.0	8.7	53	6.6

Latitude: 47°38'N
 Longitude: 117°32'W
 Elevation: 721

2.2.6 Traffic Data

The number of 18,000 lb. equivalent axle loads applied to each test pavement were estimated from the yearly ADT, percentage of trucks and equivalency factors for single and combination trucks. These equivalency factors were developed from W-4 tables for Washington state. The specific data are shown in Chapter 3.0.

2.2.7 Bridge Clearances

To evaluate feasible rehabilitation alternatives, bridge clearances in the project area must be evaluated. WSDOT has established the following minimum bridge clearance requirements: 14.5 feet for Interstate resurfacing projects, and 16.0 feet for Interstate safety improvement projects. [2.5] Bridge clearance data throughout the state were examined to determine the maximum additional pavement thickness that could be constructed over the existing pavement structures near the test sections. These data were located in the WSDOT 1987 Bridge List. The data collected for SR 5 from Tacoma to Bellingham, and for SR 90 from SR 902 (west of Spokane) to SR 27 (east of Spokane), are presented in Appendix B.

CHAPTER 3.0

DATA ANALYSES

The data collected during this study, descriptions of which are provided in Chapter 2.0, were analyzed to provide insight into what causes the distress observed in PCC pavements in Washington state. The data analysis techniques used and the results obtained are presented in this chapter.

3.1 CORING AND LABORATORY TESTING

The cores obtained from the two test sections were transported to the University of Washington laboratory for evaluation. The evaluations included thickness measurements, compressive strength tests, and splitting tensile strength tests. The compressive strength tests were conducted in accordance with ASTM C42 and the splitting tensile strength tests in accordance with ASTM C496.

Concrete core lengths were measured to obtain the concrete layer thickness. This thickness is a necessary input parameter for pavement layer strength back calculation techniques. Pavement layer thicknesses have a significant influence on back calculated material stiffnesses and, therefore, the more accurately pavement layer thicknesses are known, the better are the estimated values. [3.1] The compressive strength test results were used to estimate the concrete elastic modulus (modulus of elasticity), and the resulting modulus was used as a check on the back calculated concrete moduli. Use of fatigue equations to predict distress requires concrete flexural strength. Concrete flexural strength was estimated from the splitting tensile strength test results, as well as from the compressive strength test results.

3.1.1 SR 5

Of the 40 cores obtained at this site, thickness measurements were made on 28. The measured concrete thicknesses were compared to the 9.0-inch PCC slab thickness for

this site. The mean core thickness was 9.06 inches, with a standard deviation of 0.41 inch and a coefficient of variation (COV) of 4.6 percent. This mean thickness was approximately 0.7 percent greater than the design thickness and for all intents and purposes could be considered the design thickness. The minimum thickness measured was 8.25 inches, and the maximum was 9.625 inches, a significant thickness variation (1.375 inches) in just 420 feet. Thicknesses for each core measured are presented in Appendix C, Table C.1.

Compressive strength tests were conducted on four cores obtained from the site. The results are presented in Table 3.1. The mean compressive strength was 11,406 pounds per square inch (psi), with a standard deviation of 176 psi and a COV of 1.5 percent. Five cores were tested for splitting tensile strength. These test results are also presented in Table 3.1. The mean splitting tensile strength was 923 psi, with a standard deviation of 78 psi and a COV of 8.5 percent.

The results from the compressive strength tests were used to estimate the concrete elastic modulus. The concrete elastic modulus was calculated to be 6,088,000 psi based on the following relationship proposed by the American Concrete Institute [3.2]:

Table 3.1. Core Strength Data, SR 5

Test Type	Core No.	Height (in.)	Diameter (in.)	Failure Load (lbs.)	Correction Factor	Compressive Strength (psi)	Splitting Tensile Strength (psi)
Compressive	2	7 13/16	4.0	140,000	1.00	11,141	----
Compressive	9	7 28/32	4.0	144,450	1.00	11,495	----
Compressive	25	7 13/16	4.0	144,400	1.00	11,491	----
Compressive	39	7 29/32	4.0	144,450	1.00	11,495	----
Tensile	3	7 17/32	4.0	39,200		----	828
Tensile	5	7 19/32	4.0	43,000		----	901
Tensile	14	7 17/32	4.0	47,850		----	1,011
Tensile	16	7 19/32	4.0	47,500		----	996
Tensile	22	7 9/16	4.0	41,700		----	878
					Mean	11,406	923
					Std. Dev.	176	78
					Coeff. of Var.	1.5	8.5

$$E_{PCC} = 57,000 (f'_c)^{1/2} \quad \text{Equation 3.1}$$

where: E = the concrete elastic modulus, psi
 f'_c = the compressive strength, psi.

The results from the splitting tensile strength tests were used to estimate concrete flexural strength. A flexural strength of 1,151 psi was calculated from the splitting tensile strength test results with the following relationship [3.3]:

$$FS = 1.02 (ST) + 210 \quad \text{Equation 3.2}$$

where: FS = flexural strength, psi
 ST = splitting tensile strength, psi.

In addition, the modulus of rupture (flexural strength) was calculated from the compressive strength test results with the following equation [3.4]:

$$MR = 10 (CS)^{1/2} \quad \text{Equation 3.3}$$

where: MR = modulus of rupture, psi
 CS = compressive strength, psi

In comparison to the 1,151 psi from the splitting tensile strength results, the modulus of rupture was calculated to be 1,068 psi, a 7 percent difference.

Engineers know that concrete gains flexural strength over time. [3.5] For design and evaluation purposes, the 28th day and 90th day flexural strengths (moduli of rupture) are useful to know. An equation does exist to estimate 28th day flexural strength from current concrete flexural strength measurements. The 28th day strength can be converted to 90th day flexural strength for use in concrete fatigue equations. To obtain the 28th day modulus of rupture, the following equation was used [3.6]:

$$F_A = 1.22 + 0.17 \log_{10} T - 0.05 (\log_{10} T)^2 \quad \text{Equation 3.4}$$

where: F_A = ratio of modulus of rupture at time T to modulus of rupture at 28 days
 T = time since slab construction, years.

The modulus of rupture at 28 days was calculated by dividing the currently measured modulus of rupture by F_A . This calculation resulted in a 28th day flexural strength of 776 psi. The 90th day flexural strength was approximately 10 percent higher, or 854 psi. [6]

3.1.2 SR 90

Fifty-one cores were obtained at this site, of which 46 were used for thickness measurements. The mean core thickness was 7.72 inches, with a standard deviation of 0.33 inch and a COV of 4.3 percent. The minimum thickness measured was 6.75 inches and the maximum was 8.50 inches. The design thickness for this pavement section was 7.8 inches, so the average core thickness was less, by approximately 1 percent, than the design thickness. As at the SR 5 site, the concrete thickness varied significantly (1.75 inches) over the 840-foot test site length. Table C.2 in Appendix C contains the thicknesses for each core measured.

Four cores from the site were selected for compressive strength tests. The results are presented in Table 3.2. The mean compressive strength was 8,984 psi, with a standard

Table 3.2. Core Strength Data, SR 90

Test Type	Core No.	Height (in.)	Diameter (in.)	Failure Load (lbs.)	Correction Factor	Compressive Strength (psi)	Splitting Tensile Strength (psi)
Compressive	17	7 11/32	4.0	122,500	0.99	9,651	----
Compressive	23	7 1/2	4.0	111,500	1.00	8,873	----
Compressive	25	7 8/32	4.0	114,500	0.99	9,021	----
Compressive	39	7 9/32	4.0	106,500	0.99	8,390	----
Tensile	3	7 1/2	4.0	36,250		----	769
Tensile	9	7 9/16	4.0	35,450		----	746
Tensile	13	7 29/32	4.0	34,750		----	700
Tensile	20	7 3/32	4.0	35,350		----	793
					Mean	8,984	752
					Std. Dev.	520	40
					Coeff. of Var.	5.8	5.3

deviation of 520 psi and a COV of 5.8 percent. Splitting tensile strength tests were conducted on four cores. The test results are also presented in Table 3.2. The mean splitting tensile strength was 752 psi, with a standard deviation of 40 psi and a COV of 5.3 percent.

The results from the compressive strength and splitting tensile strength tests were used to estimate concrete elastic modulus and flexural strength. On the basis of the compressive strength tests, the concrete elastic modulus was calculated to be 5,403,000 psi, and the flexural strength was estimated to be 948 psi. The flexural strength, estimated from the splitting tensile strength tests, was calculated to be 977 psi, or about 3 percent higher than that predicted from the compressive strength tests.

The calculated modulus of rupture at 28 days was found to be 697 psi. The 90th day flexural strength was estimated to be 767 psi.

3.2 CRACKING AND FAULTING SURVEY

3.2.1 Cracking

Cracks occur in a pavement when the concrete fatigues after a number of stress cycles, or when the stress induced in the slab (by load, temperature, shrinkage or a combination of these) exceeds the concrete flexural strength. The fatigue rate is related to the number of stress applications and their magnitudes. The closer the induced stresses are to the concrete flexural strength, the more rapid the fatigue failure. [3.5]

The number of stress cycles a pavement can withstand before fracture (cracking) can be estimated with a fatigue equation that predicts allowable load repetitions and that incorporates a stress ratio (applied stress/flexural strength). Generally, the rate at which cracking occurs in a pavement is relatively low until a given number of stress cycles have occurred, and then crack occurrence increases rapidly. The crack survey data collected during this study were used to develop a performance curve for Washington state PCC

pavements. A performance curve provides a means to evaluate crack propagation rates, as discussed in Chapter 4.0.

The visual condition survey data WSDOT collected provided general information about crack extent and severity, but did not provide the actual percentage of slabs cracked at a given point in time. Only general information was provided because the WSDOT survey rating categories span a cracking extent range rather than documenting an exact cracking level. Therefore, these survey data could not be used to provide reference points for creating a performance curve.

The cracking data collected during the site visits, and the core thickness data, were used to develop a performance curve. Thickness ranges were developed from the core data (1/4-inch increments were used). The percentage of slabs cracked in each thickness range was determined, and the average core thickness was calculated. This evaluation was done for both the SR 5 and 90 pavements. The ranges used, the number of data points in each range, and the percentage of slabs cracked are shown in Table 3.3.

To develop a performance curve, the fatigue damage associated with the mean thickness in each thickness range was calculated. Fatigue damage was also calculated for the mid-range thickness. The fatigue data for this case are also presented in Table 3.3. To compute fatigue damage, the following fatigue equation was used [3.6]:

$$\log N_f = 16.61 - 17.61 * (\text{stress}/\text{MR}) \quad \text{Equation 3.5}$$

where: stress = load + thermal stress. The load stress was calculated using Westergaard's edge stress equation for SR 90 and using the ILLI-SLAB finite element program for SR 5. The thermal stress used for SR 5 was 99 psi and for SR 90 was 142 psi. The curl stress development is described later in this chapter.

MR = modulus of rupture, assumed to 750 psi.

Table 3.3. Fatigue Data for Developing Performance Curves

Thickness Range (inches)	n	% Slabs Cracked	Average Thickness (inches)	Fatigue Damage Ratio	Middle of Thickness Range (in.)	Fatigue Damage Ratio
SR 5						
8.25-8.49	2	100.0	8.438	0.031	8.375	0.034
8.75-8.99	4	50.0	8.883	0.014	8.875	0.014
9.00-9.24	1	0.0	9.000	0.012	9.125	0.010
9.25-9.49	3	33.3	9.427	0.007	9.375	0.007
9.50-9.74	3	66.6	9.541	0.006	9.625	0.005
SR 90						
7.25-7.49	2	100.0	7.355	8.110	7.375	11.853
7.50-7.74	7	71.4	7.567	3.365	7.625	4.151
7.75-7.79	7	42.9	7.881	1.107	7.875	1.578
8.00-8.24	5	20.0	8.05	0.560	8.125	0.646
8.25-8.50	3	0.0	8.36	0.203	8.375	0.283

Note: Modulus of Rupture = 750 psi
 Fatigue Equation: $\log N_f = 16.61 - 17.61 (\text{stress}/\text{MR})$
 Stress: thermal stress + load stress

These limited data helped to develop the performance curves presented in Figure 3.1. Regression analyses were used to develop a best-fit curve for the data. As can be seen from Figure 3.1, the performance curves for SR 5 and 90 had the same shape, but the curve for SR 5 was offset about two log cycles from that for SR 90. Because the data from SR 5 and 90 were clearly in different groups, a separate curve was developed for each site. The differences between the two curves could have been caused by several factors, including the following:

1. inappropriate fatigue equations, which could have been possible because the failure mode for the two test sections was different (longitudinal cracking for SR 5 and transverse cracking for SR 90);
2. errors in traffic estimates or early trafficking by construction traffic when concrete flexural strength was low; early trafficking would have used up significant fatigue life;

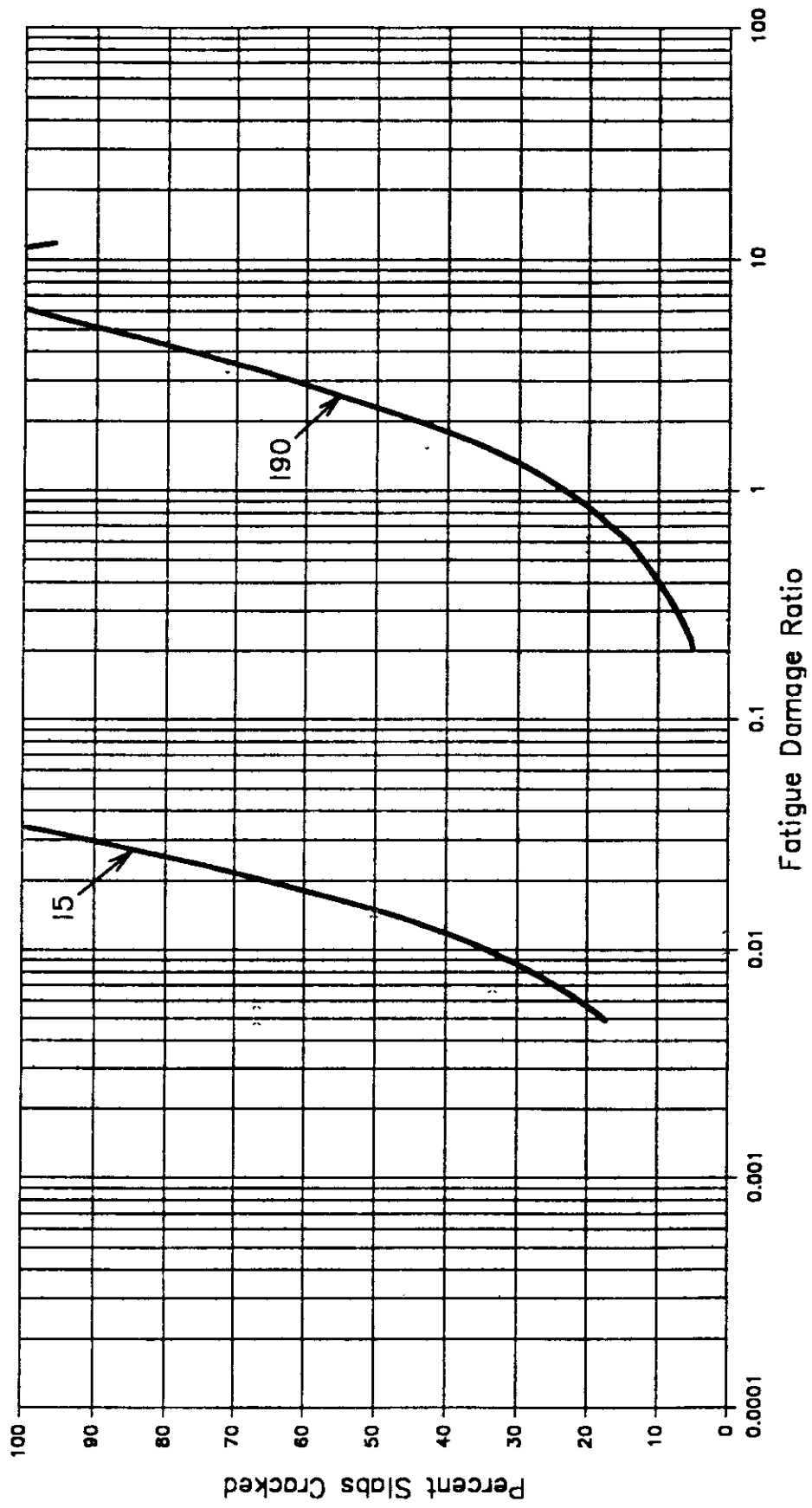


Figure 3.1 Performance Curves for SR 5 and SR 90

3. a different flexural strength than the 750 psi assumed;
4. inaccuracies in the thicknesses used in the calculations (and hence errors in the stress calculations); and/or
5. insufficient data.

Fatigue equations are usually developed from laboratory test data. These equations generally represent a 50 percent failure probability, or in other words, 50 percent of the pavement slabs should be cracked when the fatigue damage reaches 1.0. The fatigue equation used to develop the performance curves was developed during the Zero-Maintenance Design study [3.6] and corresponded to a failure probability of 24 percent (or 24 percent of the slabs cracked at a fatigue damage of 1.0). The curve for SR 90 indicated approximately 24 percent of the slabs cracked at a fatigue damage of 1.0, so this fatigue equation appeared valid for that site.

The curve for SR 5, on the other hand, indicated that 50 percent of the slabs cracked at a fatigue damage of about 0.01. To bring the data points from the two sites into the same range, fatigue equations having the same slope as that used initially (17.61) were developed. These equations were developed for a 50 percent failure probability and are as follows:

$$\text{SR 5: } \log N_f = 14.70 - 17.61 (\text{stress/MR}) \quad \text{Equation 3.6}$$

$$\text{SR 90: } \log N_f = 16.85 - 17.61 (\text{stress/MR}) \quad \text{Equation 3.7}$$

The performance curves resulting from these equations are shown in Figure 3.2. The data used to develop the curves are presented in Table 3.4. The relationship between these curves is illustrated in Figure 3.3, which shows the laboratory fatigue test results for 140 beams. To bring the SR 5 curve to the same location (the same intercept) on the figure as the SR 90 curve, a 135 psi change in flexural strength was required. This change in flexural strength was about a 1 standard deviation decrease, considering that a typical flexural strength coefficient of variation is 15 percent.

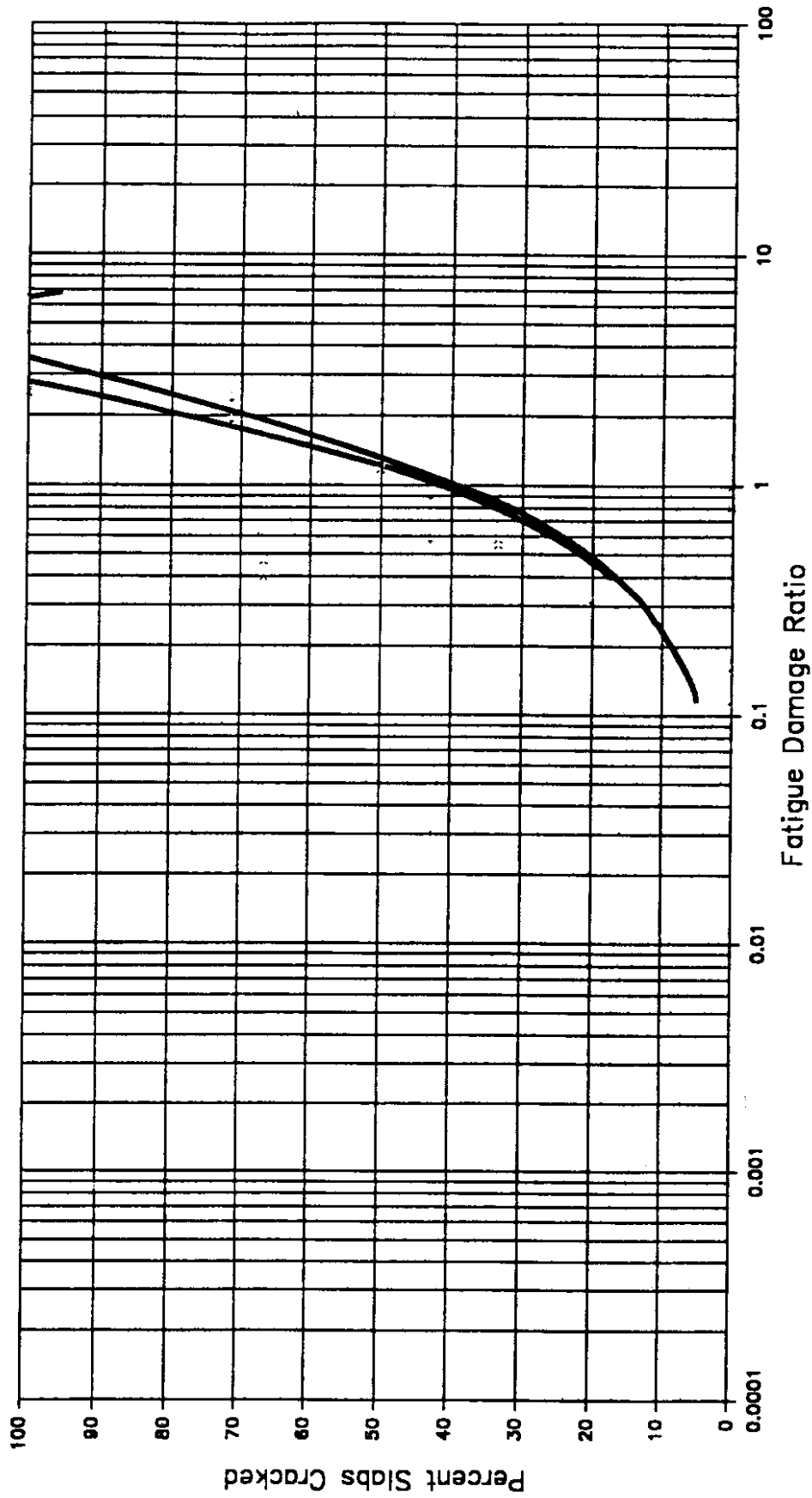


Figure 3.2 Performance Curves Using Adjusted Fatigue Equations

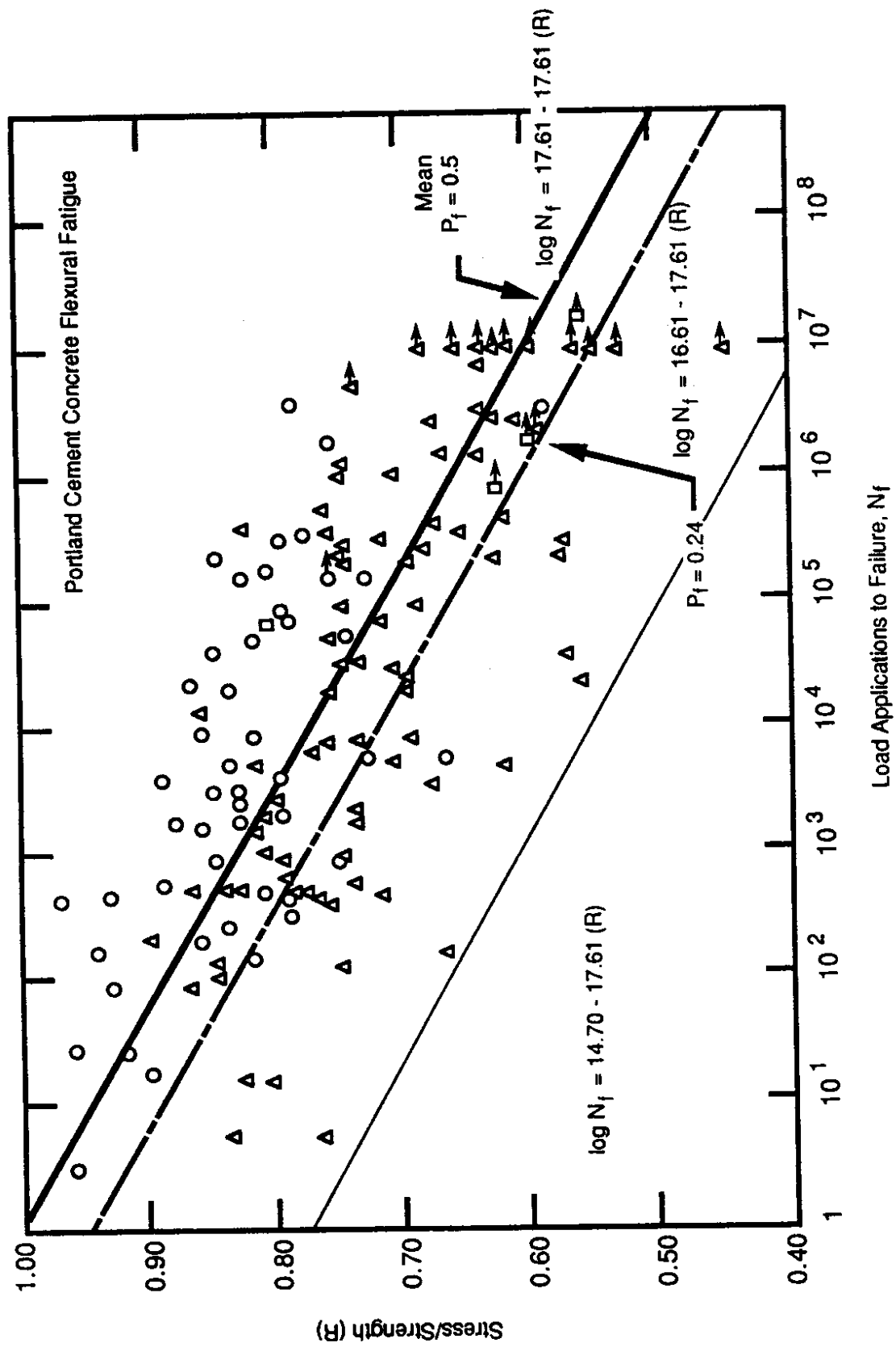


Figure 3.3. Fatigue Results of 140 Beam Tests (Reference 3.13)

Table 3.4. Fatigue Data for Developing Adjusted Performance Curves

Thickness Range (inches)	n	% Slabs Cracked	Average Thickness (inches)	Fatigue Damage Ratio	Middle of Thickness Range (in.)	Fatigue Damage Ratio
SR 5						
8.25-8.49	2	100.0	8.438	2.519	8.375	2.807
8.75-8.99	4	50.0	8.883	1.182	8.875	1.182
9.00-9.24	1	0.0	9.000	1.005	9.125	0.810
9.25-9.49	3	33.3	9.427	0.554	9.375	0.585
9.50-9.74	3	66.6	9.541	0.471	9.625	0.401
SR 90						
7.25-7.49	2	100.0	7.355	4.667	7.375	6.821
7.50-7.74	7	71.4	7.567	1.936	7.625	2.388
7.75-7.79	7	42.9	7.881	0.585	7.875	0.908
8.00-8.24	5	20.0	8.05	0.322	8.125	0.372
8.25-8.50	3	0.0	8.36	0.117	8.375	0.162

Note: Modulus of Rupture = 750 psi

Fatigue Equation: $\log N_f = 16.85 - 17.61 (\text{stress}/\text{MR})$ for SR 90 and
 $\log N_f = 14.70 - 17.61 (\text{stress}/\text{MR})$ for SR 5

Stress: thermal stress + load stress

Importantly, both the SR 5 and 90 curves had the same slope (17.61). The equal slopes indicated that the percentage of cracking was a function of the stress/flexural strength ratio, or of the factors influencing this ratio (load, concrete flexural strength, curl stress, subgrade support, concrete elastic modulus). This observation lends credence to the argument that the longitudinal cracking observed at SR 5 was fatigue-related.

A "generic" curve developed using both the SR 5 and 90 data is provided in Figure 3.4. A description of how this generic curve can be used to predict crack propagation rates is provided in Chapter 4.0. As more data become available, additional points should be developed and the curve(s) refined.

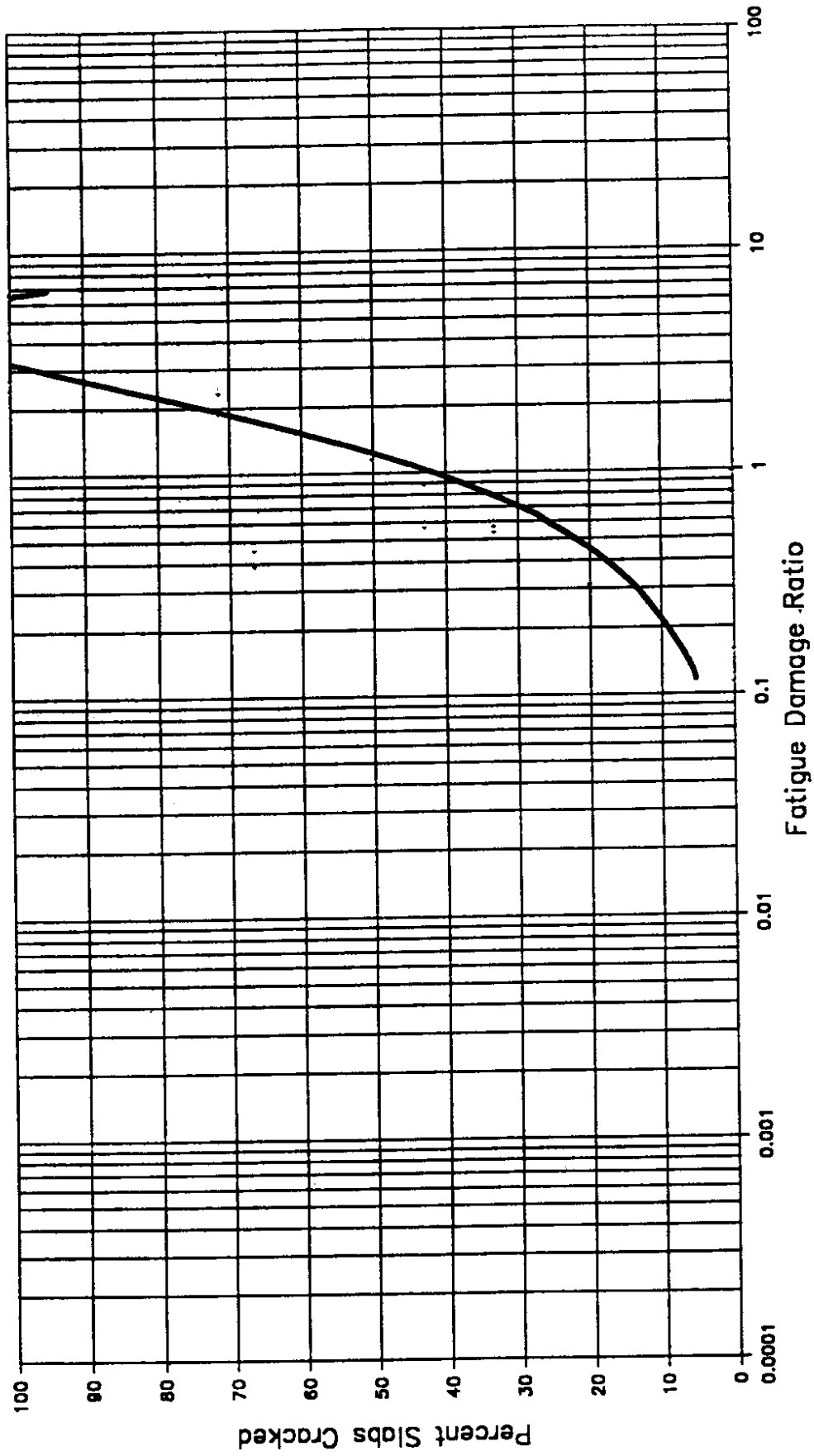


Figure 3.4 "Generic" Performance Curve

3.2.2 Faulting

The mechanisms causing faulting have been well-documented and are described in Chapter 4.0. The presence of faulting is an important consideration when a rehabilitation alternative is selected because if faulting has occurred, the joint and/or crack faces are moving relative to one another. This relative joint movement indicates that rapid joint reflection cracking could occur if an asphalt concrete overlay is applied. Thus, a faulting evaluation provides guidance in selecting a potential rehabilitation alternative.

According to engineers interviewed during development of the Zero-Maintenance Design Procedure, faulting is considered to be the most serious distress occurring in PCC pavements. [3.6] Joint or crack faulting causes a rough pavement ride, and when faulting reaches a critical level, maintenance is required to improve ride quality to a level satisfactory to users. According to results presented in the Zero-Maintenance Design study, this critical faulting level is 0.20 inch.

Interestingly, the WSDOT visual condition survey method indicated that faulting between 1/8 inch and 1/4 inch is low severity. The Pavement Condition Index (PCI) visual condition survey method, developed at the Army Corps of Engineers Construction Engineering Research Laboratory, indicates that faulting between 1/8 inch and 3/8 inch is low severity.[3.8] However, in fairness, the PCI procedure was developed for roadways and parking lots, where higher faulting levels are tolerable because traffic moves at lower speeds than on the highway. The faulting levels assigned a low severity rating appeared to include the faulting level considered critical (0.20-inch) by engineers interviewed during the Zero-Maintenance Design study.

The SR 90 test section had an average faulting level of 0.22 inch. The SR 5 site had virtually no faulting.

3.3 NONDESTRUCTIVE DEFLECTION TESTING

The nondestructive deflection testing data were evaluated in several ways. The data were used to evaluate load transfer efficiency at joints and cracks and to evaluate whether voids existed under the concrete slab corners. Additionally, the measured deflections were used to evaluate pavement layer material strengths.

3.3.1 Load Transfer Efficiency

When a wheel load is applied at a joint or crack, both the loaded slab and the adjacent unloaded slab deflect. The amount the unloaded slab deflects is directly related to joint performance. If a joint is performing perfectly, both the loaded and unloaded slabs deflect equally. The amount the pavement deflects is important because when deflection occurs, tensile stresses are induced in the slab. The magnitude of these tensile stresses has a direct impact on pavement performance, i.e., the lower the stress, the longer the fatigue life. [3.5]

If joint performance is perfect and both slabs deflect equally, both slabs experience the same deflection and the same stress. The stresses induced in the loaded slab are thus reduced by 50 percent over what they would have been if there had been no load transfer between adjacent slabs. Besides affecting the magnitude of stress induced in the pavement, joint performance also affects faulting. If joint performance is poor, it is likely that joint faulting will occur.

Because stresses induced by wheel loads are difficult to measure in the field, a model is necessary that can predict stresses under various loading conditions. Such a model is the ILLI-SLAB finite element computer program developed at the University of Illinois. [3.9] A detailed description of ILLI-SLAB can be found in Reference 3.10. The results produced by the program have been validated by extensive comparisons to theory and field data. To properly predict pavement response under load, appropriate joint

behavior must be modeled. The FWD deflection data collected at the sites were used to evaluate joint performance.

Joint performance can be evaluated by calculating load transfer efficiency (LTE) across a joint or crack using the deflection data measured. The concept of joint load transfer efficiency is illustrated in Figure 3.5. Load transfer efficiency can be calculated using the following equation [3.6]:

$$\text{LTE} = (\Delta_u / \Delta_l) * 100 \quad \text{Equation 3.8}$$

where:

- LTE = load transfer efficiency, percent
- Δ_u = the deflection of the unloaded slab, mils
- Δ_l = the loaded slab deflection, mils.

Joint efficiency depends on several factors, including temperature (which affects joint opening), number and magnitude of load applications, foundation support, aggregate particle angularity, and the presence of mechanical load transfer devices. [3.6] No mechanical load transfer devices were installed in the SR 5 or SR 90 pavements, so load transfer was provided solely by aggregate interlock across the joint or crack.

As mentioned, temperature plays a major role in determining joint effectiveness. In general, the lower the temperature, the lower the load transfer efficiency. Load transfer efficiency is reduced because joints open during cooler weather, reducing contact between faces. [3.11] Joint load transfer efficiency has also been shown, in both laboratory and field studies, to decrease with increasing load applications. [3.12, 3.13] However, this impact is lessened for harder and more angular aggregates. The aggregate characteristics play a more significant role after many load applications. [3.12, 3.13]

3.3.1.1 SR 5. Deflections were measured across transverse joints, with the load applied on both the approach and leave slabs, across the longitudinal joint, and across two longitudinal cracks. The air temperature during testing was approximately 60 degrees Fahrenheit, and the testing was conducted between 11 p.m. and 4 a.m. The measured deflections were used to calculate load transfer efficiencies at each location. The load

Joint Load Transfer

- Aggregate Interlock
- Keyways
- Dowel Bars

$$\text{Load Transfer Efficiency (\%)} = \frac{\Delta_u}{\Delta_l} \times 100$$

Where Δ_u = unloaded slab deflection
 Δ_l = loaded slab deflection

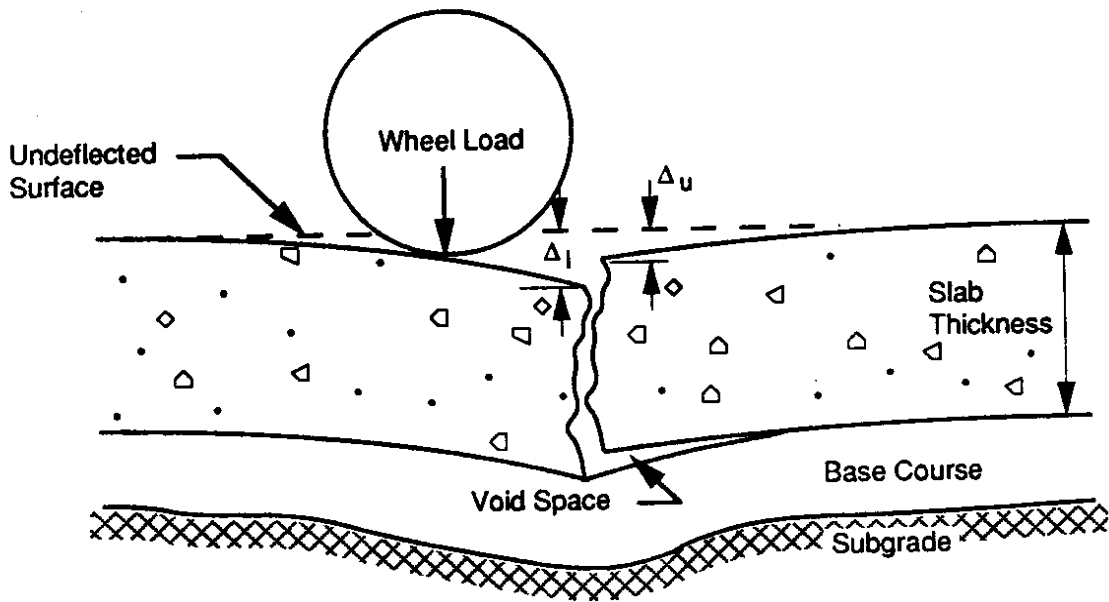


Figure 3.5. The Concept of Joint Load Transfer Efficiency (LTE)

transfer efficiencies are summarized in Table 3.5. The average load transfer efficiency (over all four applied load levels) for each joint and crack evaluated is provided in Appendix C, Table C.3.

The results presented in Table 3.5 show that the average load transfer efficiency for the approach side of the transverse joints was 91.2 percent and for the leave side was 92.1 percent. These load transfers efficiencies were high for the temperature at which the joints were tested, as well as for the pavement age (22 years) and number of load applications (approximately 13,000,000 ESALs). The load transfer efficiencies at the site showed very little variation, as evidenced by the low standard deviations and coefficients of variation.

Table 3.5. Summary of Load Transfer Efficiencies — SR 5

Row	Location	Mean LTE (%)	Standard Deviation	COV (%)	Maximum LTE (%)	Minimum LTE (%)
1 (outer lane)	TJ - A	90.7	11.4	12.6	100.0	52.8
	TJ - L	91.4	8.6	9.4	98.8	63.5
2 (outer lane)	TJ - A	92.8	5.8	6.2	100.0	81.2
	TJ - L	91.2	4.1	4.5	97.0	84.2
3 (outer lane)	TJ - A	92.0	3.0	3.3	96.6	87.2
	TJ - L	94.4	2.9	3.1	99.2	89.4
4 (inner lane)	TJ - A	88.9	12.3	13.7	100.0	49.0
	TJ - L	91.8	7.7	8.4	100.0	69.9
5 (inner lane)	TJ - A	91.5	4.8	5.2	97.7	80.8
	TJ - L	91.8	2.9	3.2	95.4	85.8
	LJ - A	63.3	28.6	45.2	97.7	21.5
	LJ - L	69.3	19.2	27.7	91.5	39.0
	LC - A	74.7	20.4	27.3	95.2	51.2
	LC - L	59.2	29.6	50.1	92.3	13.5

Notes: TJ = transverse joint
LJ = longitudinal joint
LC = longitudinal crack
A = approach
L = leave

The load transfer efficiencies across the longitudinal joint and longitudinal cracks were much lower and more variable than those for the transverse joints. The average load transfer efficiency for the longitudinal joint, when the load was applied on Lane 2, was 65.7 percent and for the load applied on Lane 1, was 68.7 percent. There was significant variation between the maximum and minimum load transfer efficiencies measured (21.5 to 97.7 percent).

The mean load transfer efficiencies measured on either side of the longitudinal crack were 76.8 percent and 59.6 percent. One explanation for the difference in load transfers may be that the crack faces were not vertical. If this were the case, when loaded on one side, the loaded slab would have been supported by the unloaded slab, which would have resulted in a lower measured load transfer efficiency.

Even though several longitudinal joint and crack locations showed low load transfer efficiency, these joints and cracks were not faulted. They experienced little, if any, stress reversal because wheel loads moved parallel to the cracks rather than across them.

3.3.1.2 SR 90. Deflections were measured across each transverse joint and crack, with the FWD load applied to both the approach and leave slabs. The air temperature during testing ranged from 55 degrees Fahrenheit for Row 3 to 72 degrees Fahrenheit for Row 5. Testing was conducted between 4 a.m. and 10 a.m. With the FWD data, load transfer efficiencies for each joint and crack were calculated. Table 3.6 summarizes the load transfer efficiencies measured at this site. The load transfer efficiencies measured for each joint and crack are provided in Appendix C, Table C.4.

The results in Table 3.6 show that the average transverse joint approach side load transfer efficiency was 59.7 percent, and that of the joint leave side was 74.0 percent. The average load transfer efficiency for the transverse crack approach side was 72.8 percent, and that for the crack leave side was 76.6 percent. There was also a large variation in the load transfer efficiencies in each row, as evidenced by the high coefficients of variation.

Table 3.6. Summary of Load Transfer Efficiencies — SR 90

Row	Location	Mean LTE (%)	Standard Deviation	COV (%)	Maximum LTE (%)	Minimum LTE (%)
1 (inner lane)	TJ - A	73.3	15.2	20.7	90.6	46.1
	TJ - L	84.3	5.6	6.6	91.2	72.1
	TC - A	87.5	1.3	1.5	-	-
	TC - L	94.5	0.8	0.9	-	-
2 (inner lane)	TJ - A	69.5	24.0	34.6	93.7	29.8
	TJ - L	84.5	10.5	12.5	95.7	65.7
	TC - A	89.9	0.7	0.8	-	-
	TC - L	93.7	1.5	1.6	-	-
3 (outer lane)	TJ - A	53.7	32.1	59.8	93.8	11.4
	TJ - L	75.9	20.0	26.3	94.2	38.0
	TC - A	70.5	17.6	25.0	89.2	38.3
	TC - L	72.2	20.6	28.5	92.9	37.5
4 (outer lane)	TJ - A	55.2	21.1	38.2	82.5	21.3
	TJ - L	67.7	16.3	24.1	84.5	32.5
	TC - A	56.0	22.1	39.6	84.0	21.4
	TC - L	62.2	16.4	26.4	89.1	41.0
5 (outer lane)	TJ - A	46.9	17.3	36.8	75.0	24.6
	TJ - L	57.7	14.5	25.2	78.5	33.8
	TC - A	60.2	16.7	27.7	79.3	28.8
	TC - L	60.6	17.1	28.2	84.5	36.9

Notes: TJ = transverse joint
 TC = transverse crack
 A = approach
 L = leave

These load transfer efficiencies were, on the average, much lower than those measured at the SR 5 site. The lowest load transfer efficiencies measured in each row at the SR 90 test site were about 25 percent. Some researchers have suggested that a load transfer efficiency between 15 and 25 percent will be measured across a joint even if the joint faces are not in contact because the subgrade provides some shear resistance.

3.3.2 Relative Movement at Joints and Cracks

In several cases, and in particular at the SR 90 test section, the load transfer efficiency increased when the applied load was increased. This observation was inconsistent with previous research efforts, which indicated that load transfer efficiency was constant over a given loading range, and led to an investigation of why this phenomenon was observed. [3.11]

This increase in load transfer efficiency with load was hypothesized to result from movement of the joint or crack faces relative to one another, and only at higher loads did the two faces come into full contact. This concept is illustrated in Figure 3.6. In essence, the amount one slab could move vertically before it contacted the adjacent slab was the phenomenon being measured.

The ability to evaluate the magnitude of the relative joint movement would be beneficial in two ways. First, joints exhibiting "play" or relative movement are likely to fault. Having the ability to predict which joints or cracks are at risk would be helpful in preventing faulting. Second, joints or cracks exhibiting play are likely to rapidly reflect through an asphalt concrete overlay applied to the concrete pavement. Thus, insight into feasible rehabilitation alternatives would be provided.

To determine whether the hypothesis was correct, and to see whether relative joint movement could be evaluated, the following procedure was followed. First, the deflection under the load and the deflection 12 inches from the load and across the joint/crack (the same deflections used to calculate load transfer efficiency) were added together. This sum was divided by 2 to give the expected deflection on the unloaded slab if load transfer was 100 percent. If the load transfer efficiency was 100 percent, the loaded and unloaded slab deflections would be approximately equal, hence the division by 2. The justification for this calculation was that the loaded slab deflection plus the unloaded slab deflection would give the free-edge deflection, which is a constant for a given load and loaded area. The

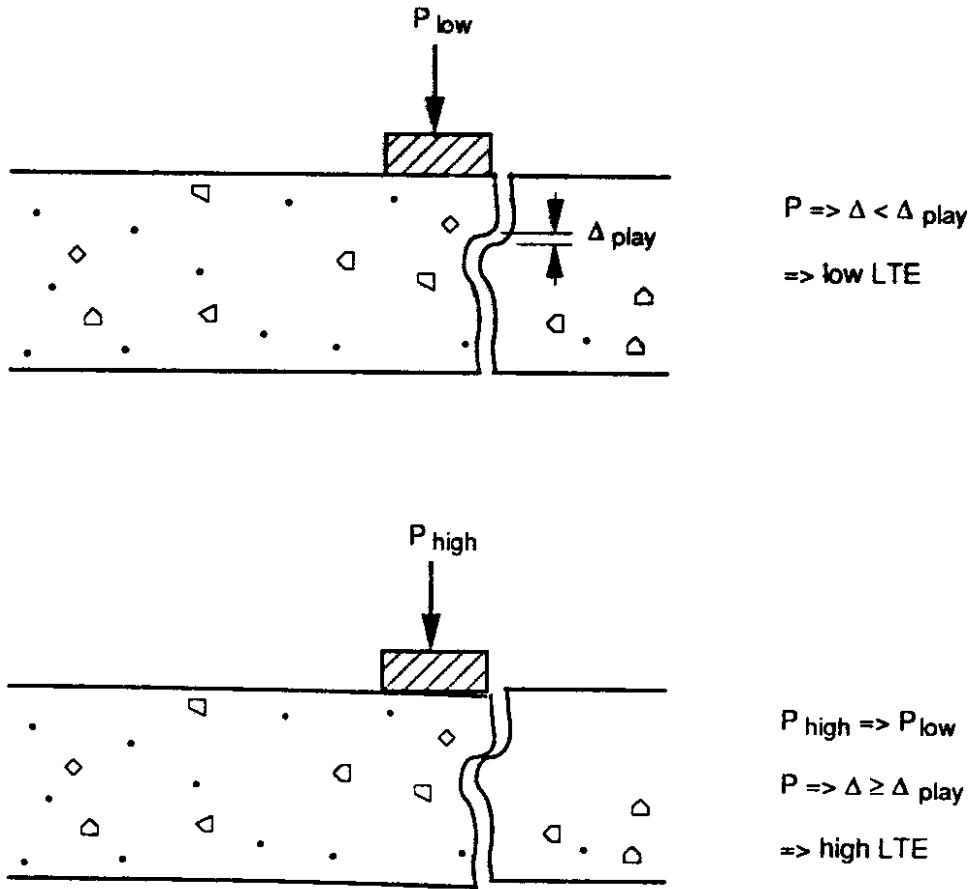


Figure 3.6. The Concept of Play

actual measured deflections were used to calculate the free-edge deflection, rather than a theoretically calculated value, because the actual subgrade support under the joints or cracks was unknown and might have varied across the joint.

Even with very high aggregate interlock (perfect load transfer), the deflection on the unloaded slab is slightly less than that on the loaded slab. Even at the slab center, the measured deflection at 12 inches is less than the deflection under the load. To evaluate what percentage of the loaded slab deflection the unloaded slab deflection should have been, the ILLI-SLAB finite element program was run for several levels of aggregate interlock. This evaluation was completed for both PCC pavement thicknesses under study (9.0 and 7.8 inches). The results are presented in Table 3.7 and show that load transfer efficiency tended to become asymptotic at about 95 to 96 percent. For this analysis, a value of 95 percent was chosen.

The next step was to multiply the average deflection (the loaded plus unloaded slab deflection divided by 2) by this 0.95 factor to estimate the expected unloaded slab deflection. The deflection measured by the FWD on the unloaded slab was then subtracted from this value to estimate the play in the joint or crack. The play data for SR 5 are summarized in Table 3.8, and those for SR 90 are summarized in Table 3.9.

Table 3.7. Load Transfer Efficiencies for Varying Levels of Aggregate Interlock

Slab Thickness (inches)	Aggregate Interlock Factor	Deflection Under Load (mils)	Deflection Across Joint (mils)	Load Transfer Efficiency (%)
7.8	10 ⁴	43.76	28.42	64.9
7.8	10 ⁵	37.85	34.32	90.7
7.8	10 ⁶	36.95	35.22	95.3
7.8	10 ⁸	36.83	35.34	95.9
9.0	10 ⁴	37.80	23.73	62.8
9.0	10 ⁵	32.29	29.24	90.6
9.0	10 ⁶	31.40	30.12	95.9
9.0	10 ⁸	31.29	30.24	96.6

k = 100 pci
Joint spacing = 20 feet

Table 3.8. Summary of Play - SR 5

Row	Location	Mean Play (mils)	Standard Deviation	Maximum Play (mils)	Minimum Play (mils)
1 (outer lane)	TJ - A	0.002	0.830	2.72	-0.74
	TJ - L	-0.012	0.588	2.00	-0.58
3 (outer lane)	TJ - A	-0.096	0.193	0.21	-0.45
	TJ - L	-0.194	0.233	0.01	-0.53
4 (inner lane)	TJ - A	0.208	1.108	3.89	-0.61
	TJ - L	-0.012	0.588	1.70	-0.74
	LJ - A	1.639	2.019	4.98	-0.25
	LJ - L	1.006	1.068	2.70	-0.01
	LC - A	0.203	0.796	1.48	-0.56
	LC - L	2.670	3.577	9.35	-0.03

Notes: TJ = transverse joint
 LJ = longitudinal joint
 LC = longitudinal crack
 A = approach
 L = leave

Table 3.9. Summary of Play - SR 90

Row	Location	Mean Play (mils)	Standard Deviation	Maximum Play (mils)	Minimum Play (mils)
2 (inner lane)	TJ - A	2.013	2.633	7.82	-0.18
	TJ - L	-0.132	0.923	1.48	-0.90
	TC - A	0.040	-	-	-
	TC - L	-0.730	-	-	-
3 (outer lane)	TJ - A	3.821	3.356	9.72	0.18
	TJ - L	1.516	1.793	4.78	-0.30
	TC - A	2.150	3.099	9.12	-0.23
	TC - L	1.813	2.609	6.81	0.00
5 (outer lane)	TJ - A	2.577	1.493	4.87	0.58
	TJ - L	1.817	1.012	3.47	0.53
	TC - A	1.595	1.133	3.49	0.57
	TC - L	1.554	1.013	3.12	0.39

Notes: TJ = transverse joint
 TC = transverse crack
 A = approach
 L = leave

To evaluate whether measured play could be used to predict faulting, the faulting measured at each joint or crack was plotted against the average play calculated for that joint or crack. The results are presented in Figure 3.7 for all data points from both SR 5 and 90, in Figure 3.8 for SR 5, and in Figure 3.9 for SR 90. The trend in the data was that faulting increased as play increased.

Note that not all joints with faulting showed play, and negative values of play were calculated for some joints and cracks. These observations could have been due to two factors: the multiplication factor assumed (0.95) and the time of year the joints were tested.

The joints and cracks were tested in the summer, when they would have been likely to exhibit minimum play (temperatures were high, meaning the joints and cracks were more tightly closed than if testing had been accomplished at lower temperatures). At present, a justification for selecting a limiting value for play does not exist, but on the basis of the data, a value of 1/1000-inch (1 mil) seems reasonable. A final minimum value will have to be developed on the basis of tests conducted at varying temperatures and levels of joint opening and on pavements with varying faulting levels.

3.3.3 Voids

Voids under concrete slab edges and corners result when material is pumped from under the leave slab to under the approach slab. Voids initially form under the leave slab; however, as pumping continues, voids can form under both the approach and leave slabs. A diagram showing void formation is provided in Figure 3.10. Voids are most commonly found in the outer traffic lane along the outer pavement edge. Voids occur at this location because most heavy truck traffic uses this lane and also because material pumps more easily along the shoulder-traffic lane joint.

Voids were evaluated to help identify potential rehabilitation alternatives and to locate areas where loss of support was occurring that would eventually result in joint or crack faulting. Generally, if voids are present, joints and cracks are working (because the

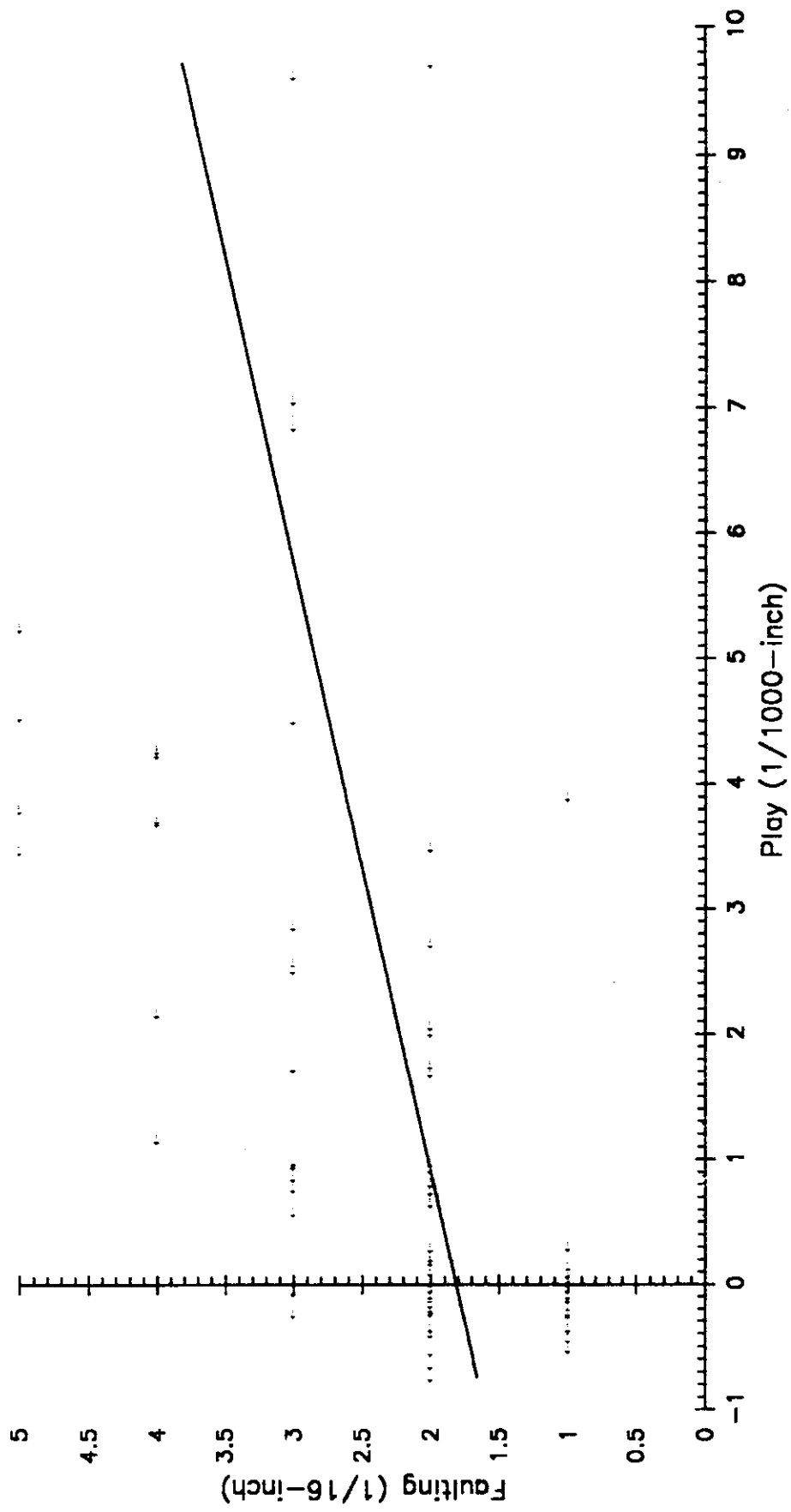


Figure 3.7 Joint or Crack Faulting versus Play (Both SR 5 and SR 90 Data Points)

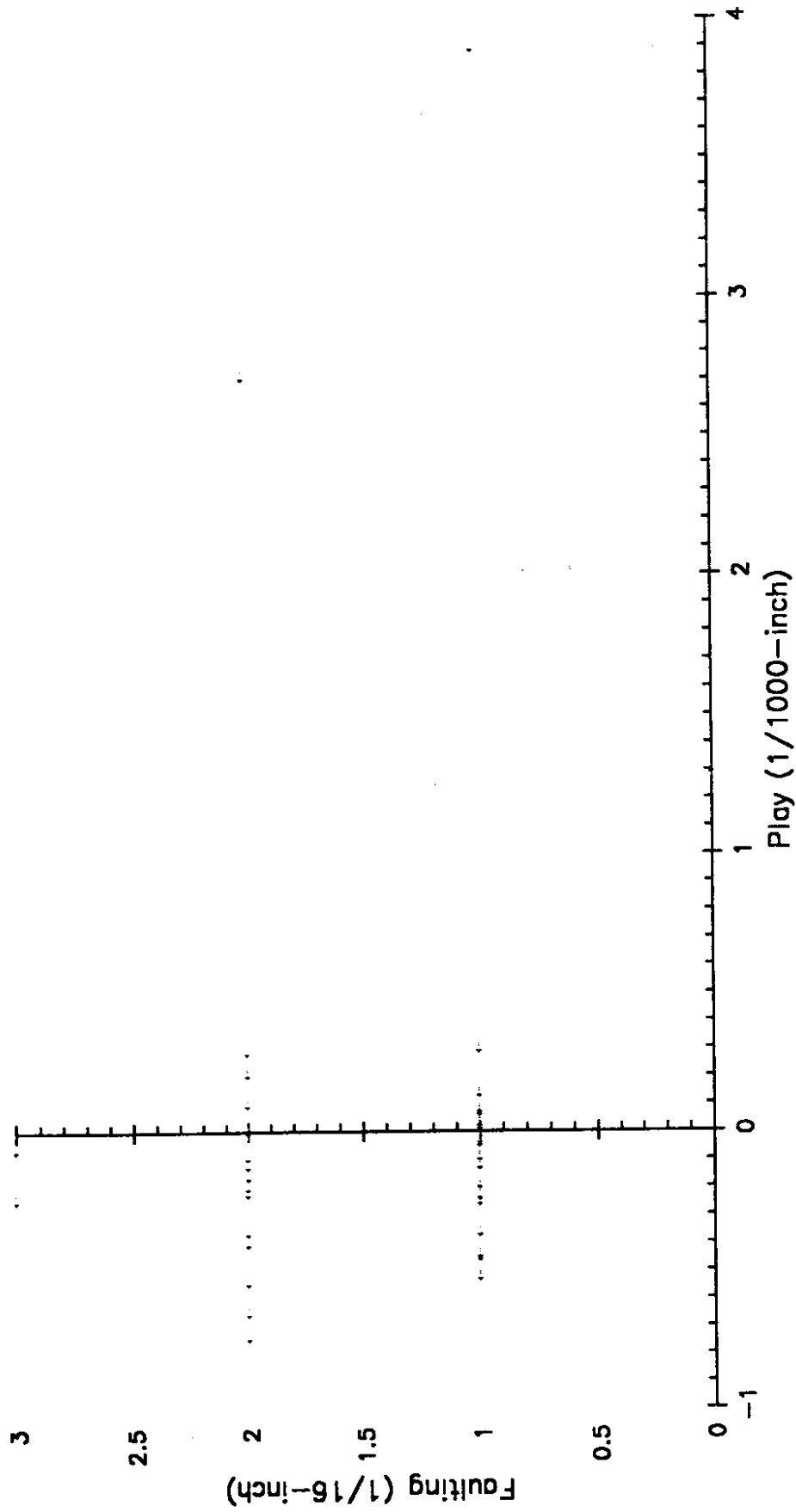


Figure 3.8 Joint or Crack Faulting versus Play (SR 5 Data Points)

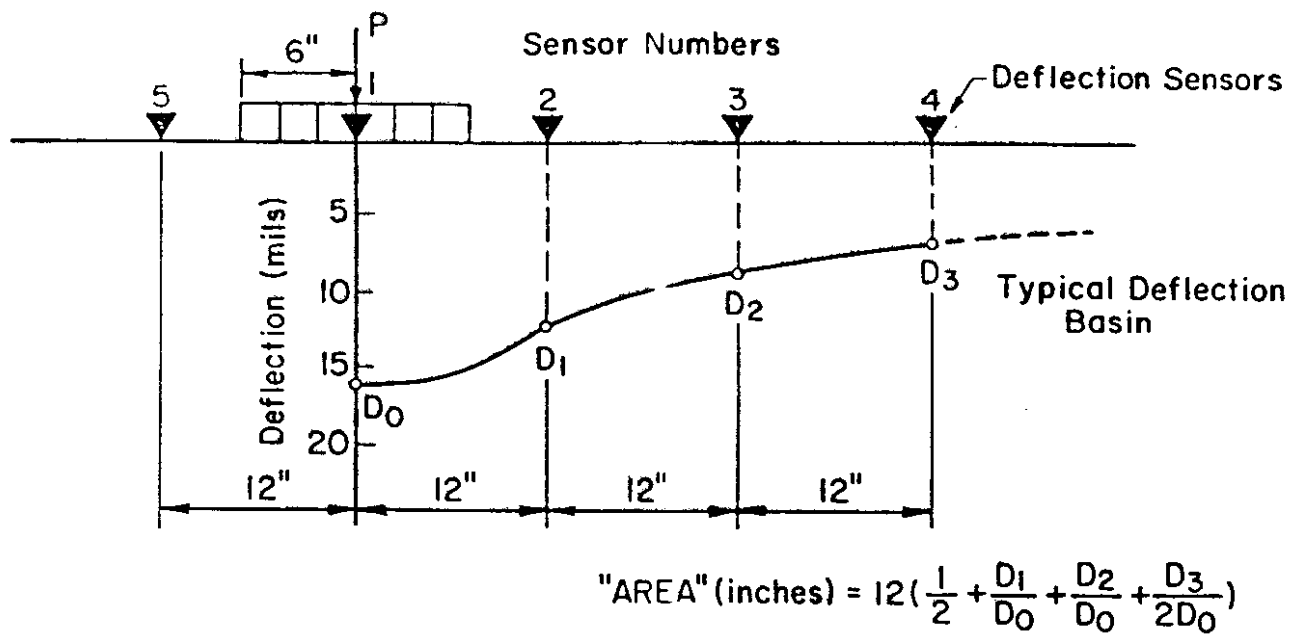


Figure 3.13. Concept and Calculation of Deflection Basin Area

Area versus I-k

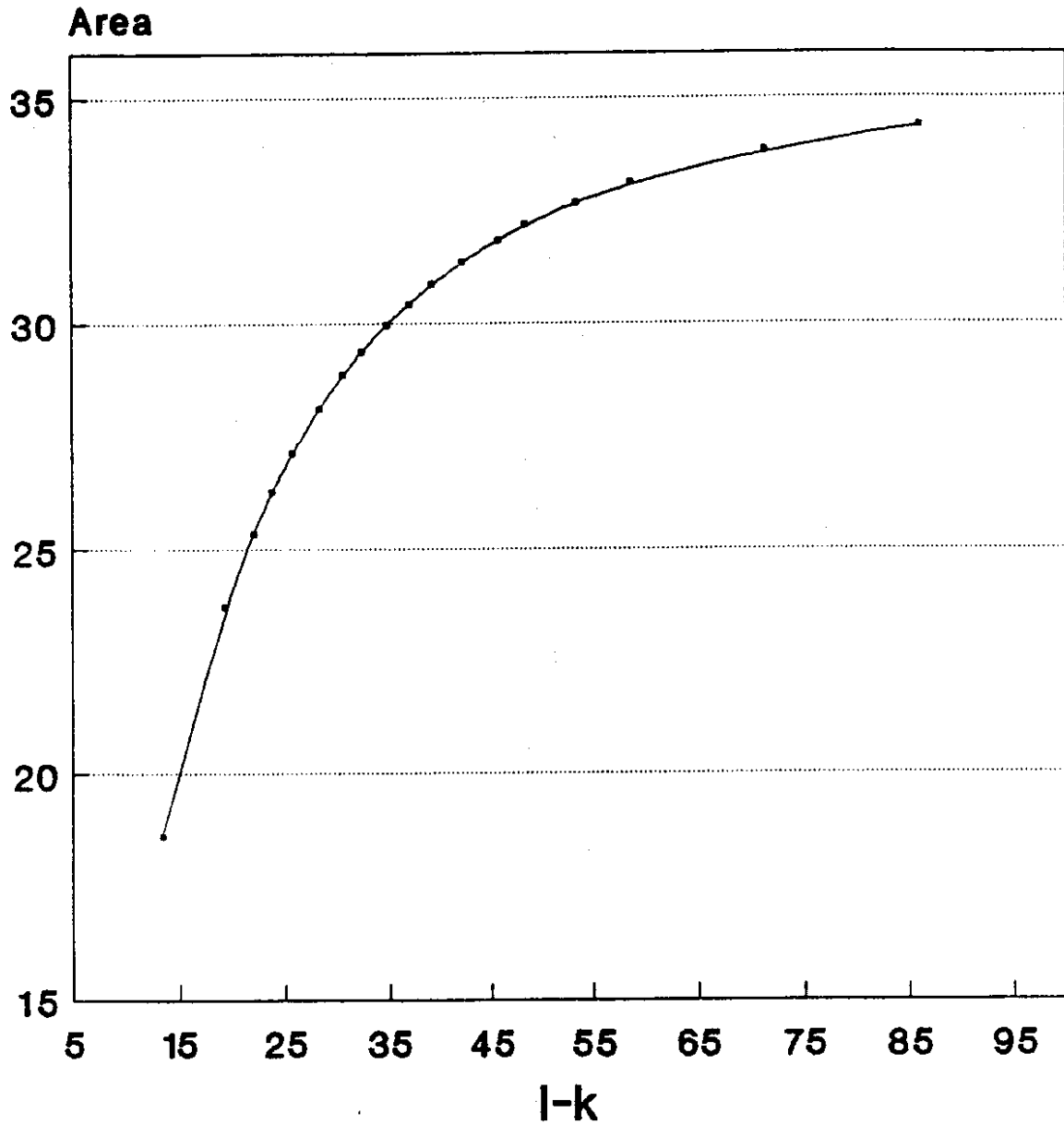


Figure 3.14. Area vs Radius of Relative Stiffness

$$l = [Eh^3/12(1-u^2)k]^{1/4} \quad \text{Equation 3.10}$$

where: E = slab elastic modulus, psi
h = slab thickness, inches
u = Poisson's ratio
k = modulus of subgrade reaction, pci.

4. Back calculate the subgrade support value, k, in pounds per square inch per inch (pci), as follows:

$$k = (d_i/D_i)(P/l^2) \quad \text{Equation 3.11}$$

where: d_i = the normalized sensor deflection (from Figure 3.15) corresponding to the measured sensor deflection, D_i
 D_i = the measured deflection, with i ranging from 0 (the sensor directly under the load) to 3 (the sensor at 36 inches from the load), mils
P = the applied load, pounds
l = the radius of relative stiffness, inches.

The normalized deflections obtained from Figure 3.15 are only valid for an applied load radius of 5.91 inches (that of the FWD load plate).

The subgrade support value, k, can also be estimated from Figures 3.16 and 3.17, which provide graphical solutions to the above equation. To use these figures, however, the measured deflections must be normalized to a 9,000-pound load. Figure 3.16 applies to the center deflection, D_0 , and Figure 3.17 applies to the deflection measured at 36 inches, D_3 . The subgrade support value is interpolated between the curves presented at the intersection of the deflection and l values.

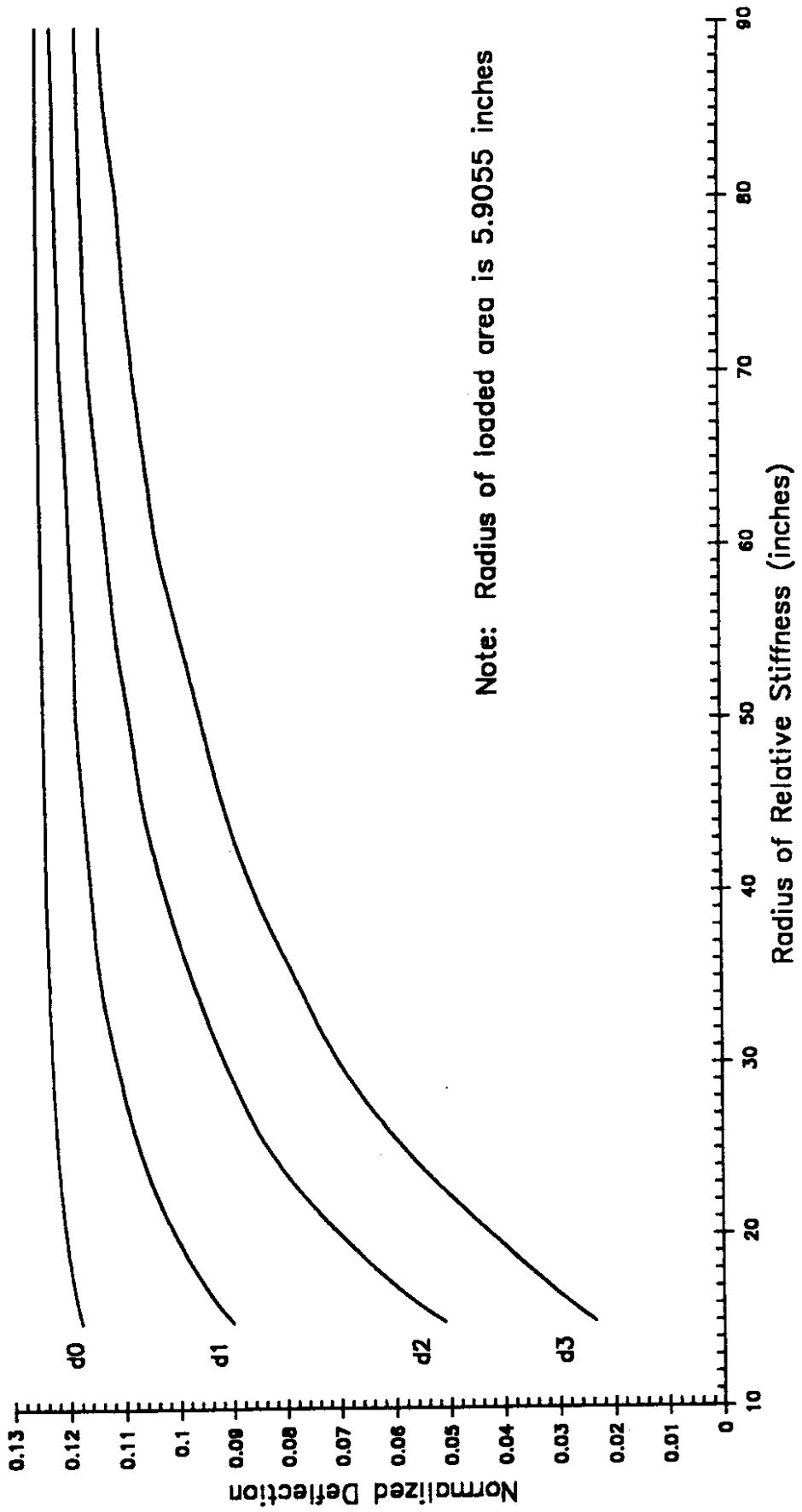


Figure 3.15 Normalized Deflections versus Radius of Relative Stiffness

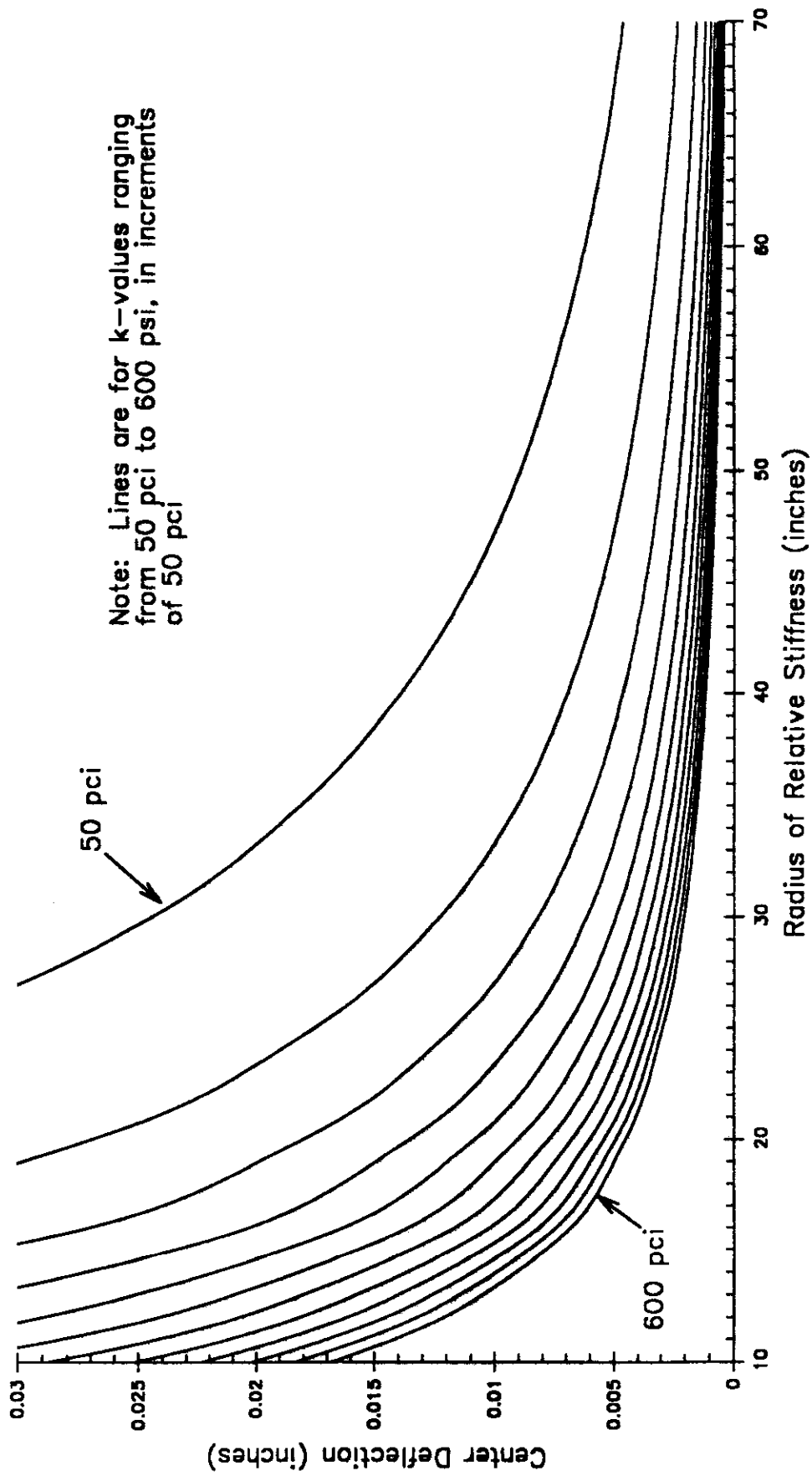


Figure 3.16 Prediction of k from Center Deflection

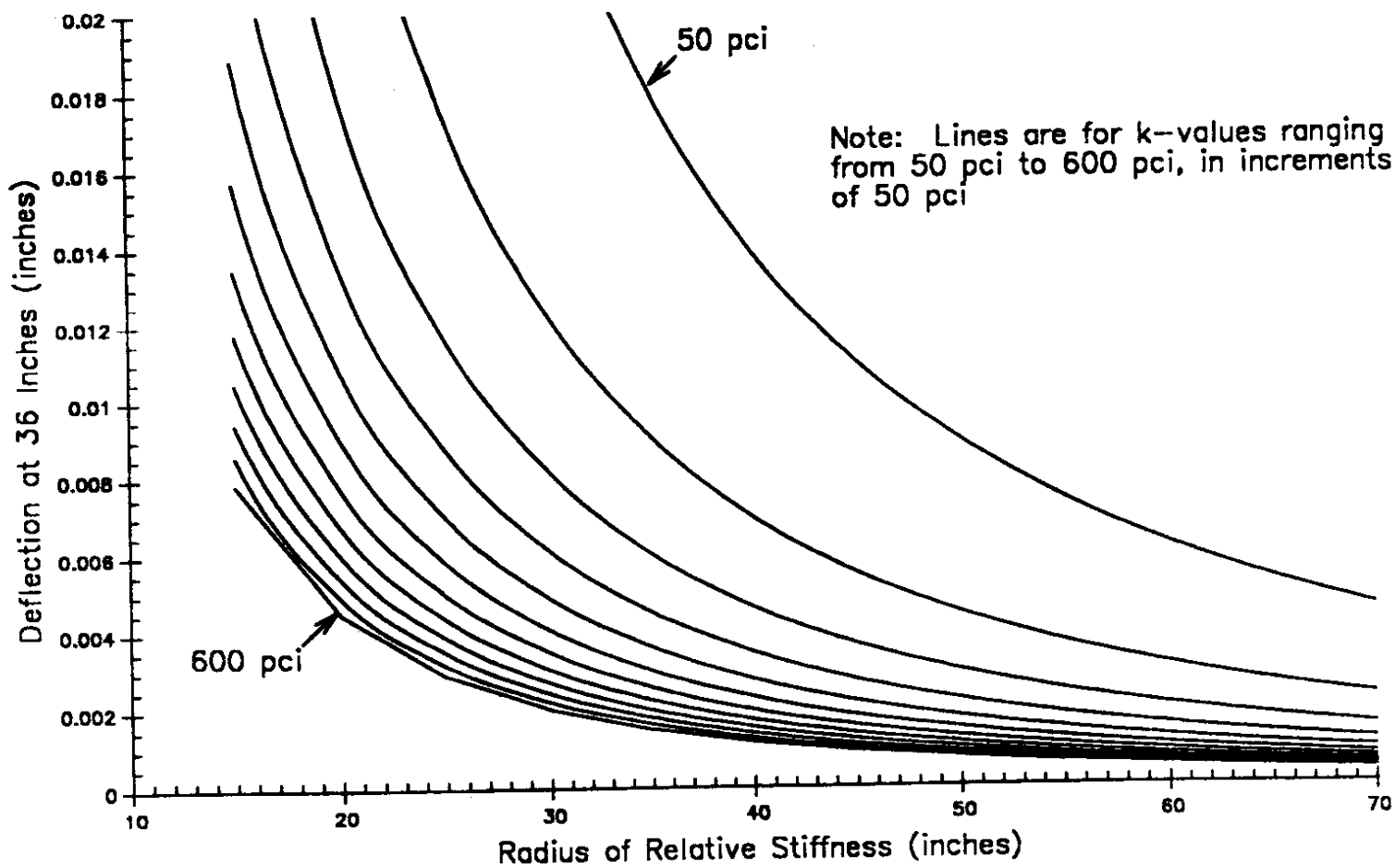


Figure 3.17. Prediction of k from Deflection at 36 Inches

5. Back calculate the slab elastic modulus, E, in psi, as follows:

$$E = (l^4(1-u^2)12k)/h \quad \text{Equation 3.12}$$

where: l = radius of relative stiffness, inches (from Step 3 above)
 u = Poisson's ratio, for PCC a value of 0.15 can be used
 k = modulus of subgrade reaction, pci (from Step 4 above)
 h = slab thickness, inches (given or assumed).

Alternatively, if the slab modulus, E, is known or assumed, the concrete slab thickness, h, in inches, can be back calculated from

$$h = [(12(1-u^2)kl^4)/E]^{1/3} \quad \text{Equation 3.13}$$

where the variables are the same as those listed above.

If Equation 3.11 is used instead of Figures 3.16 and 3.17 to calculate k, four determinations of each pavement system parameter (k, E, and h) are possible, each corresponding to a measured deflection, D_i .

Some conclusions presented in Reference 3.17, and reconfirmed during the data analyses conducted during this study, warrant repeating here. They are as follows:

1. For competent pavement systems ($l > 30$ inches), the k-value does not change in a statistically significant amount for different FWD applied load levels.
2. Figure 3.15 indicates that the normalized deflections, D_0 and D_1 , are relatively insensitive to changes in the value of l , compared to D_2 and D_3 . Thus, D_2 and D_3 will produce more reliable back calculated subgrade support values.
3. The coefficients of variation for the back calculated pavement layer parameters generally decrease as the load level increases. Thus, it is advisable to use the deflections from one of the higher load levels in the back calculation procedure.

4. E, k, and h are very sensitive to the deflection values measured; a small variation in deflection causes only a small change in area but can lead to significant variations (with COVs between 20 and 40 percent) in the back calculated parameter values.
5. The back calculated foundation stiffness, k, is independent of the assumed concrete elastic modulus and slab thickness values.
6. The concrete elastic modulus, E, is extremely sensitive to the assumed value for pavement thickness, h. In one case, a 1.4-inch change in thickness (15 percent) resulted in a 1,990,000 psi (35 percent) change in modulus. This large percentage of change in E indicates that E should be assumed and h should be calculated, which is contrary to current practice. Field slab moduli may be estimated from data obtained using nondestructive testing methods, including the Schmidt Hammer, which is discussed later.

Back calculated material properties were estimated for all four applied load levels for each test conducted at a slab center. The back calculations were done for three pavement thicknesses: the design pavement thickness, the mean pavement thickness, and the actual pavement thickness (estimated from the core measurements). In addition, the concrete thickness was back calculated from the elastic modulus calculated from the compressive strength tests.

3.3.4.2 SR 5. The back calculated concrete elastic moduli and subgrade support values are summarized in Table 3.12. Included in the table are the following:

1. the subgrade support value, k, which is independent of the concrete elastic modulus and slab thickness;
2. the concrete elastic moduli calculated for the 9.0-inch design thickness, the 9.06-inch average thickness, and the actual slab thickness obtained from the core closest to the FWD test point;

Table 3.12. Summary of Backcalculated E and k, SR 5

Row	Cracked/ Uncracked	Average Load (lbs)	Average k (pci)	E for Design Thickness of 9.0" (psi)	E for Average Thickness of 9.06" (psi)	h for Lab E ¹ (inches)	COV k (%)	COV E (%)	COV h (%)
2	Uncracked	15,389	217	4,953,000	4,859,000	8.28	31.0	34.5	14.2
2	Cracked	15,482	319	4,896,000	4,799,000	8.34	25.3	16.8	5.7
5	Uncracked	15,184	129	5,140,000	5,038,000	8.48	34.1	16.4	5.3
5	Cracked	15,223	145	6,099,000	5,985,000	8.91	35.5	37.5	12.6
2	All	15,443	277	4,920,000	4,824,000	8.32	32.3	24.3	9.5
5	All	15,197	134	5,460,000	5,354,000	8.62	33.4	26.6	8.3
All	Uncracked	15,263	163	5,068,000	4,969,000	8.40	41.8	23.3	9.1
All	Cracked	15,388	256	5,334,000	5,231,000	8.55	43.7	28.7	9.0
All	All	15,320	205	5,190,000	5,089,000	8.47	48.9	25.6	8.9
2	Uncracked	15,405	216	5,115,000 ²	—	—	35.8	2.3	—
5	Uncracked	15,183	129	5,057,000 ²	—	—	34.1	16.3	—
All	Uncracked	15,257	158	5,076,000 ²	—	—	43.4	13.0	—

¹E from compressive strength tests is 6,088,000 psi

²These values were calculated using the actual pavement thickness, obtained from the core nearest the test point. This evaluation was only conducted for uncracked slabs.

3. the concrete layer thickness calculated using the elastic modulus obtained from the compressive strength tests (6,088,000 psi); and
4. the coefficients of variation for each parameter.

The results presented are for tests made at approximately a 15,000 pound applied load level. This load level was selected because the results at this load level were less variable than those obtained at the lower three load levels. The modulus and support value calculated at each test point, for the 15,000 pound load level, are provided in Appendix E, Tables E.1 through E.3.

To evaluate the impact longitudinal slab cracking had on the back calculated concrete strength, the test points were divided into those conducted on uncracked slabs and those conducted on cracked slabs. The results in Table 3.12 are summarized accordingly. These results show that longitudinal cracking had no impact on the back calculated concrete

elastic modulus; the difference between the uncracked and cracked slab moduli was approximately 5 percent, which is negligible.

Several interesting observations can be made about the data presented in Table 3.12. First, the modulus of subgrade reaction for Row 2 (the outer lane) was about two times that for Row 5 (the inner lane). The k-values for Row 2, Slabs 19-21 and 25-27, were all greater than 300 pci, with an average of about 350 pci. This average was approximately 150 pci higher than the average for the other slabs in that row and about 220 pci greater than the average for Row 5. Several factors could have contributed to this difference, including a much thicker base course in that area or the presence of an old roadbed. Without additional investigation, the exact cause will remain unknown.

The back calculated elastic moduli are extremely sensitive to the assumed slab thickness value, as was mentioned above. In this case, a 0.7 percent increase in thickness (from 9.0 to 9.06 inches) caused a 1.9 percent decrease in the elastic moduli. A difference of this magnitude was expected because in the equation to back calculate E, the term h^3 appears. This large change indicates that it is critical to obtain accurate thickness measurements when back calculating for concrete stiffness.

The average concrete modulus was approximately 5,100,000 psi when calculated from both the average pavement thickness and the actual pavement thickness. This concrete modulus was about 1,000,000 psi (16 percent) less than the value calculated from the compressive strength test results. Again, there is no explanation for this discrepancy, since in fact the back calculated elastic moduli were expected to have been higher than the laboratory obtained elastic moduli because the back calculated elastic moduli are dynamic rather than static. Concrete moduli obtained under dynamic loading conditions are generally higher than concrete moduli obtained under static loading conditions. [3.5]

The results in Table 3.12 also indicate that the average pavement thickness, back calculated with the laboratory-determined concrete elastic modulus, was about 1/2-inch less than the 9.0-inch design thickness. The calculated thicknesses were also substantially less

than the thicknesses measured near each FWD test point. Again, there is no explanation for this difference, and the results did not agree with the results obtained for SR 90, which are discussed below.

The coefficients of variation for each parameter were the last areas of interest. The COV for k was almost two times that for E , which was about three times that for h . The high COV for k again indicated the tremendous variability in the back calculated subgrade support values. Perhaps of most interest was the COV for h , low in comparison to the other parameters. This low COV indicates that it may be most advantageous to estimate concrete elastic modulus in the field using a Schmidt Hammer or other similar device, and to back calculate the concrete layer thickness.

3.3.4.3 SR 90. The same data presented in Table 3.12 for SR 5 are presented in Table 3.13 for SR 90. The design thickness used for these calculations was 7.8 inches; the average thickness from the core data was 7.72 inches; and the concrete elastic modulus from the laboratory tests was 5,403,000 psi. The results are presented for the 15,000 pound load level. Tables E.5 through E.7 in Appendix E contain the back calculated parameters for each slab center FWD test points.

As at SR 5, the test data were divided according to whether the slab was cracked. The data were divided to evaluate the impact transverse slab cracking had on the back calculated concrete strength. The results presented in Table 3.13 indicate that transverse cracking did have an impact on the back calculated slab modulus. On the average, the cracked slabs had moduli approximately 30 percent less than the uncracked slabs. Engineers generally expect that cracked slabs will have lower elastic moduli, and this expectation is supported by the SR 90 data.

At this site the modulus of subgrade reaction was relatively consistent, with a COV of about 20 percent. The average k -value for all test points was 261 pci. Note that the COV for the k -value at this site was about 40 percent of that obtained at SR 5.

Table 3.13. Summary of Backcalculated E and k, SR 90

Row	Cracked/ Uncracked	Average Load (lbs)	Average k (pci)	E for Design Thickness of 7.8" (psi)	E for Average Thickness of 7.72" (psi)	h for Lab E ¹ (inches)	COV k (%)	COV E (%)	COV h (%)
1	Uncracked	15,342	249	5,250,000	5,414,000	7.67	16.1	26.5	8.9
1	Cracked	15,629	282	4,375,000	4,512,000	7.26	0.8	13.6	4.5
4	Uncracked	15,287	212	6,760,000	6,972,000	8.37	37.8	20.3	7.4
4	Cracked	15,219	279	3,945,000	4,068,000	6.99	18.6	23.1	6.9
1	All	15,429	254	5,115,000	5,276,000	7.60	15.2	25.8	8.5
4	All	15,233	266	4,508,000	4,649,000	7.26	23.5	33.6	10.4
All	Uncracked	15,364	239	5,652,000	5,830,000	7.85	22.2	26.6	9.2
All	Cracked	15,265	279	3,992,000	4,118,000	7.02	22.0	17.4	6.7
All	All	15,310	261	4,747,000	4,896,000	7.40	20.7	30.6	9.8
1	Uncracked	15,392	249	5,125,000 ²	—	—	16.1	20.8	—
4	Uncracked	15,286	210	6,497,000 ²	—	—	39.0	16.3	—
All	Uncracked	15,364	238	5,491,000 ²	—	—	22.6	21.9	—

¹E from compressive strength tests is 5,403,000 psi

²These values were calculated using the actual pavement thickness, obtained from the core nearest the test point. This evaluation was only conducted for uncracked slabs.

The back calculated elastic moduli were, as mentioned above, very sensitive to the value used for slab thickness. At this site, a 1 percent decrease in thickness (from 7.8 to 7.72 inches) caused a 3 percent increase in the elastic moduli. Again, a difference of this magnitude was expected because h^3 appears in the equation to back calculate E.

The average concrete modulus for SR 90, based on the average pavement thickness of all slabs, was approximately 4,896,000 psi. The average elastic modulus calculated from the actual slab thickness (obtained from the core nearest the FWD test point) was 5,491,000 psi. The former was about 400,000 psi (9 percent) less than the value calculated from the laboratory compressive strength tests (5,403,000 psi), and the latter was within 2 percent of this value. These results agree well, although the back calculated dynamic E and k were expected to be greater than the modulus calculated for compressive strength tests.

The average concrete layer thickness obtained using the elastic modulus from the compressive strength tests was 7.85 inches for the uncracked slabs and 7.02 inches for the cracked slabs. This uncracked slab thickness shows excellent agreement with the design pavement thickness of 7.8 inches. The lower value for the cracked slabs was expected and can be considered an "equivalent" pavement thickness (the pavement thickness for a design modulus value of 5,400,000 psi).

3.3.4.4 Schmidt Hammer. A recent laboratory investigation at the University of Illinois evaluated the feasibility of using a Schmidt Hammer to predict in-place concrete elastic moduli. Concrete test cylinders and beams were made from mixes designed to produce concrete having elastic moduli between 3 million and 5 million psi. The cylinders were used to conduct compressive strength tests from which the concrete elastic modulus was estimated ($E = 57000 (f_c)^{1/2}$). The beams were tested with the Schmidt Hammer and the results used to estimate elastic modulus.

The test hammer used for this project was a Forney Testing Machines Type I, with an impact energy of 0.075 mkg. This hammer was selected because the beams to be tested were small. A Type M hammer, with an impact energy of 3.0 mkg, would likely be more suitable for field applications.

The laboratory study results were developed into a regression equation ($y = 0.48687 + 0.8949 x$), which shows the relationship between the elastic modulus obtained from the compressive strength tests (y) and that obtained using the Schmidt Hammer (x). This relationship indicates that the Schmidt Hammer provides realistic elastic moduli.

A major study finding was that, for the Schmidt Hammer to give proper results, the concrete surface must be properly prepared. The study recommended that the in-place concrete surface be ground smooth before testing. This grinding can easily be accomplished with a light-weight, high-speed hand grinder with a cup wheel approximately 5 inches in diameter.

3.4 CLIMATOLOGICAL DATA

The climatological data collected during this study were used to develop typical thermal gradients that occur through a PCC slab for both western and eastern Washington. These thermal gradients were then used to estimate temperature-induced stresses in the slab. To properly model concrete pavement performance, load-induced stresses had to be coupled with temperature-induced stresses, since temperature-induced stresses alone can be large enough to cause cracking.

3.4.1 Thermal Gradients

The collected temperature, average monthly percentage of sunshine, and average monthly wind velocity data were used in the Climatic-Materials-Structural (CMS) Pavement Analysis Program developed by Dempsey at the University of Illinois. [3.18] This program uses a climate model to analyze multi-layered pavement systems. The program was developed because researchers recognized that field conditions (minimum and maximum air temperature, sunshine, wind velocity, precipitation, etc.) vary from site to site and that these field conditions influence pavement behavior and must be considered when pavement performance is evaluated.

The analysis technique incorporated in the CMS program is a one-dimensional forward-finite-difference, heat transfer model. Boundary conditions, including layer thicknesses, number of layers, material thermal characteristics (heat capacity, thermal conductivity, etc.), and the analysis time increment are required for program execution. The output CMS produces includes a temperature profile, the location and number of frost lines, subgrade moisture content, and pavement layer stiffness properties. For this study, the primary concern was to obtain the temperature profile through the slab so the temperature difference between the slab top and bottom could be estimated.

Three basic input files are required to use the CMS program. They are a pavement data file; a temperature, wind, and sunshine data file; and a radiation data file. The

requirements for each data file are described in detail in Reference 3.19. Typical input files for SR 5 and 90 are provided in Appendix F.

The CMS heat transfer model was verified in laboratory tests and through an evaluation of AASHTO Road Test data. Validation examples can be found in Reference 3.18.

The output obtained from the CMS program was the temperature profile through the slab depth, for each hour of the day, for each day of the year. To simplify these data analyses, the middle day of each month was selected as typical for that month. The temperature differential between the slab top and bottom was then recorded for each hour in the day.

The calculated temperature differentials between slab top and bottom showed that substantial variations occurred throughout the day, from a negative temperature differential (surface temperature lower than the temperature at the slab bottom) at night to a positive temperature differential during the day. The points of zero temperature differential appeared to occur at approximately 6 a.m. and 7 p.m. These variations are illustrated in Figures 3.18 and 3.19 for July 15th at the SR 5 and 90 test sections, respectively.

3.4.2 Thermal Stresses

Once the temperature differentials between the slab top and bottom have been estimated, the thermal stress caused by each differential was evaluated. To complete this evaluation, Westergaard's equation for thermal stress calculations was used. [3.20] This equation is as follows:

$$\sigma_y = \sigma_o [A (B + C)] \quad \text{Equation 3.14}$$

where:

σ_y	=	total thermal stress, psi
σ_o	=	$(E \cdot e_t \cdot t) / (2 (1 - u))$, psi
E	=	concrete elastic modulus, psi

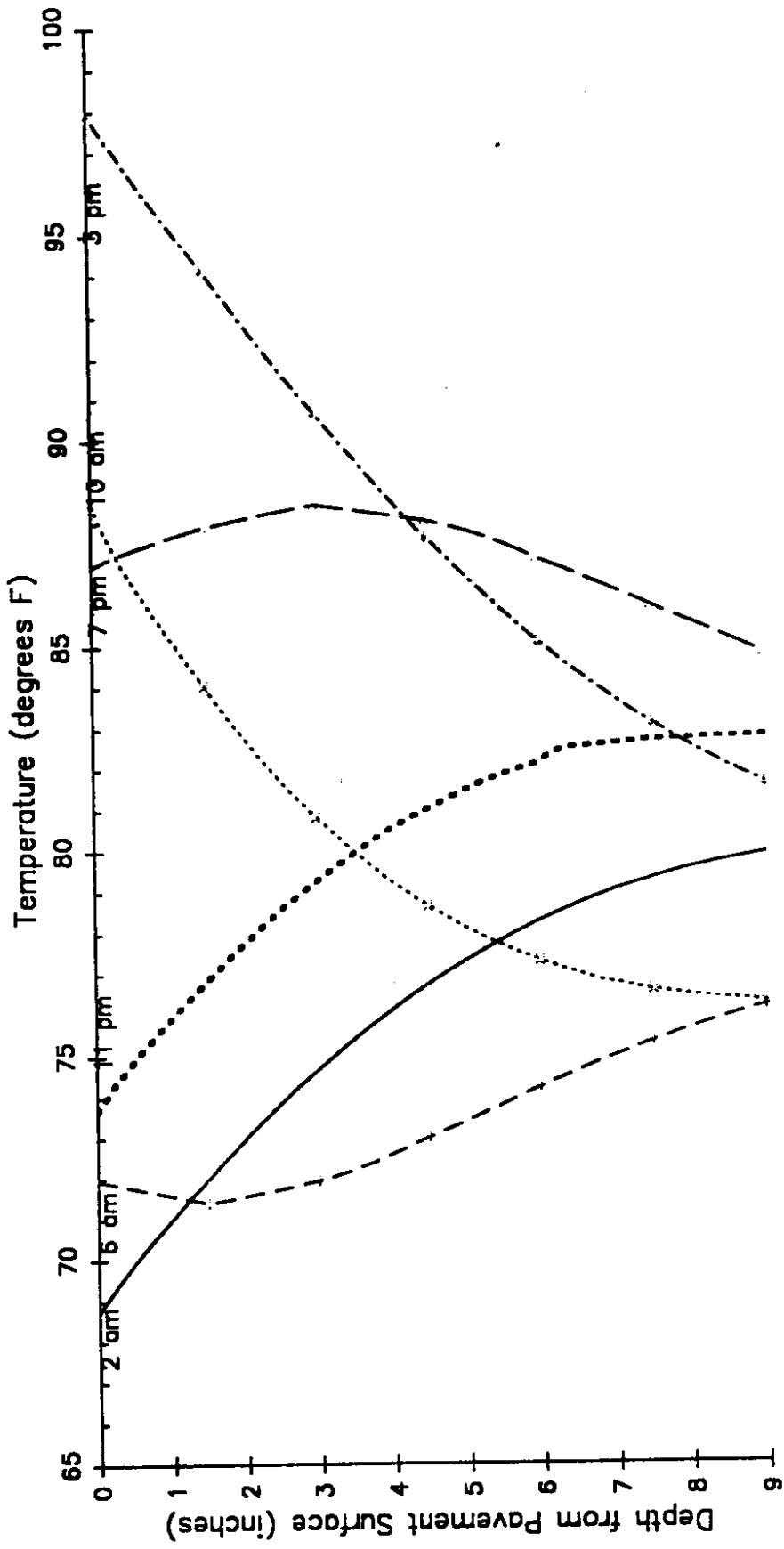


Figure 3.18 Temperature Change Through 9-Inch PCC Slab, July 15 - SR 5

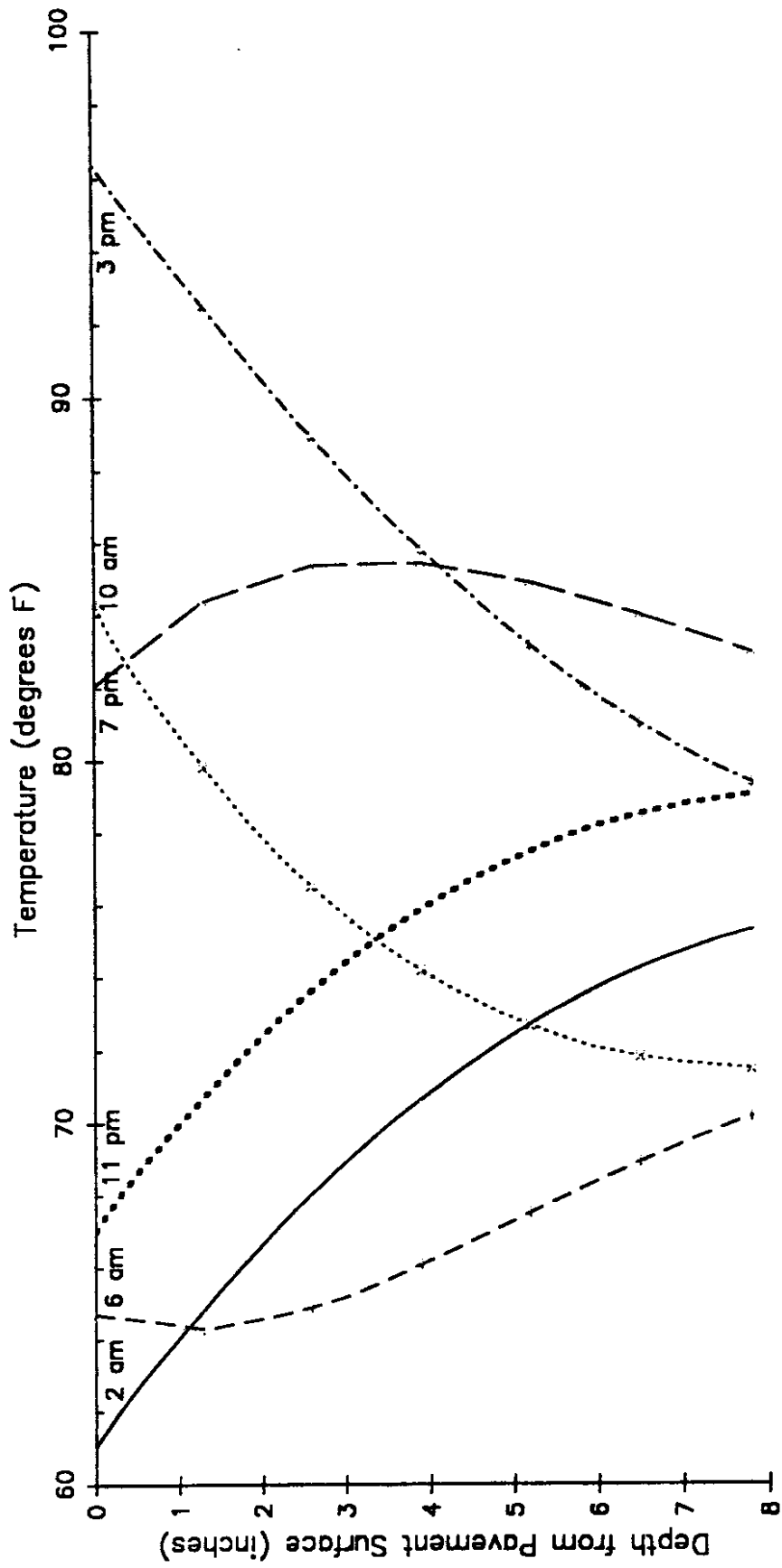


Figure 3.19 Temperature Change Through 7.8 -Inch PCC Slab, July 15 - SR 90

- e_t = concrete coefficient of thermal expansion, assumed to be 5.0×10^{-6} in/in/°F
- t = temperature differential between the slab top and bottom, °F
- u = Poisson's Ratio for concrete, assumed to be 0.15
- A = $1 - [(2\cos\lambda \cdot \cosh\lambda) / (\sin 2\lambda + \sinh 2\lambda)]$
- B = $(\tan\lambda + \tanh\lambda) \cdot \cos(y/l\sqrt{2}) \cdot \cosh(y/l\sqrt{2})$
- C = $(\tan\lambda - \tanh\lambda) \cdot \sin(y/l\sqrt{2}) \cdot \sinh(y/l\sqrt{2})$
- λ = $b / (l \cdot 8^{1/2})$
- b = slab width, inches
- l = radius of relative stiffness, inches.

The following assumptions were made in completing the evaluation:

1. The slab width, b , was assumed to be 180 inches (15 feet), or the slab length, because this slab width would provide the maximum stress along the pavement (longitudinal) edge, midway between the transverse joints.
2. y was assumed to equal 0, since the stress of interest was located at the pavement edge, midway between the transverse joints. Therefore, term C in the equation would be 0 and would not contribute to the thermal stress.
3. Westergaard's assumption that the slab length is infinity was considered true for this case. Slab length, which in this case was 12 feet rather than infinity, does have an effect on thermal stress; [3.21] however, this affect was ignored. The L/l ratios for SR 5 and 90 were not high enough to warrant the assumption about infinite slab length; [3.22] however, no closed-form solutions to this problem are currently available, and the error was felt to be acceptable considering the accuracy of the temperature predictions.

Using the Westergaard Equation and the above assumptions, the researchers calculated the thermal stresses over a 24-hour period for the middle day of each month. These stresses are presented in Appendix F.

Evaluating pavement fatigue on an hourly basis over 12 months would have been cumbersome; therefore, a typical monthly gradient was calculated that produces the same fatigue damage that would have been obtained if the fatigue had been summed over the 24-hour period. This evaluation was completed using Miner's Hypothesis [3.23] and by summing fatigue over the 24-hour period. An assumption about traffic distribution through the day was also made. The procedure assumed that truck traffic was a constant throughout any 24-hour period, and therefore each hour of the day could be evaluated identically.

The fatigue equation used to develop this "equivalent" gradient was that developed by Darter in the Zero-Maintenance Design study and is presented below: [3.6]

$$\log N_f = 16.61 - 17.61 (\text{Stress}/\text{MR}) \quad \text{Equation 3.15}$$

where:

- N_f = allowable repetitions to failure
- Stress = load-induced stress plus thermal stress, psi (the load stress was assumed to be 250 psi although any value assumed would have given the same results)
- MR = modulus of rupture, assumed to be 750 psi.

Note that any reasonably accurate fatigue equation could have been used and would have given the same results. The monthly gradients developed are provided in Tables 3.14 and 3.15 for SR 5 and 90, respectively. These tables also contain the equivalent thermal stress for the month and the temperature differential between the slab top and bottom.

The same procedure used to obtain equivalent monthly gradients was used to develop a typical temperature differential and gradient for the year. These results are also presented in Tables 3.14 and 3.15. The end result was that a typical gradient for western Washington was 1.231 degrees Fahrenheit per inch thickness, and for eastern Washington

Table 3.14. Temperature Differentials and Thermal Gradients — SR 5

Month	Thermal Stress (psi)	Temperature Differential (°F)	Thermal Gradient (°F/in)
January	30.15	3.383	0.376
February	50.09	5.620	0.624
March	80.48	9.030	1.003
April	97.80	10.973	1.219
May	107.70	12.084	1.343
June	111.05	12.460	1.384
July	120.48	13.518	1.502
August	115.14	12.919	1.435
September	92.18	10.342	1.149
October	59.03	6.623	0.736
November	25.13	2.820	0.313
December	10.70	1.201	0.133
Annual	98.75	11.080	1.231

Table 3.15. Temperature Differentials and Thermal Gradients — SR 90

Month	Thermal Stress (psi)	Temperature Differential (°F)	Thermal Gradient (°F/in)
January	5.56	0.485	0.062
February	58.75	5.124	0.657
March	106.75	9.310	1.194
April	129.36	11.281	1.446
May	141.61	12.349	1.583
June	153.25	13.364	1.713
July	170.33	14.854	1.904
August	160.31	13.980	1.792
September	125.40	10.936	1.402
October	79.42	6.926	0.888
November	4.88	0.426	0.055
December	-2.60	-0.227	-0.029
Annual	141.96	12.380	1.587

was 1.587 degrees Fahrenheit per inch thickness. These positive thermal gradients will result in tensile curl stresses that are additive to the load stresses. The western Washington gradient is valid for a 9-inch thick slab and the eastern Washington gradient for a 7.8-inch thick slab. The "annual" curl stress can be directly added to load stresses when fatigue analyses are conducted because it gives the same equivalent damage as the thermal stresses developed for each hour of the day for each month.

Using these typical gradients, the researchers calculated the thermal stress along the transverse joint and pavement edge for use in the fatigue analyses addressed Chapter 4.0. The results of the evaluation are presented in Figures 3.20 and 3.21 for SR 5 and Figures 3.22 and 3.23 for SR 90.

3.5 TRAFFIC

Traffic estimates were needed to develop the performance model discussed earlier. Estimates of the historical 18,000 pound equivalent single axle loads (ESALs) for each test section are provided in Tables 3.16 and 3.17 for SR 5 and 90, respectively. The total number of ESALs for SR 5 through 1987 was 13,048,000 and for SR 90 was 5,597,000.

The equivalency factors used to convert actual traffic to ESALs were developed from W-4 Table data for "rural interstate" sites. [3.24] WSDOT does not currently weigh trucks in urban areas, so the equivalencies developed using rural interstate data were used.

WSDOT did conduct a manual truck classification count near the SR 5 test section in 1984. This count confirmed the single unit and combination percentages obtained from the rural interstate data.

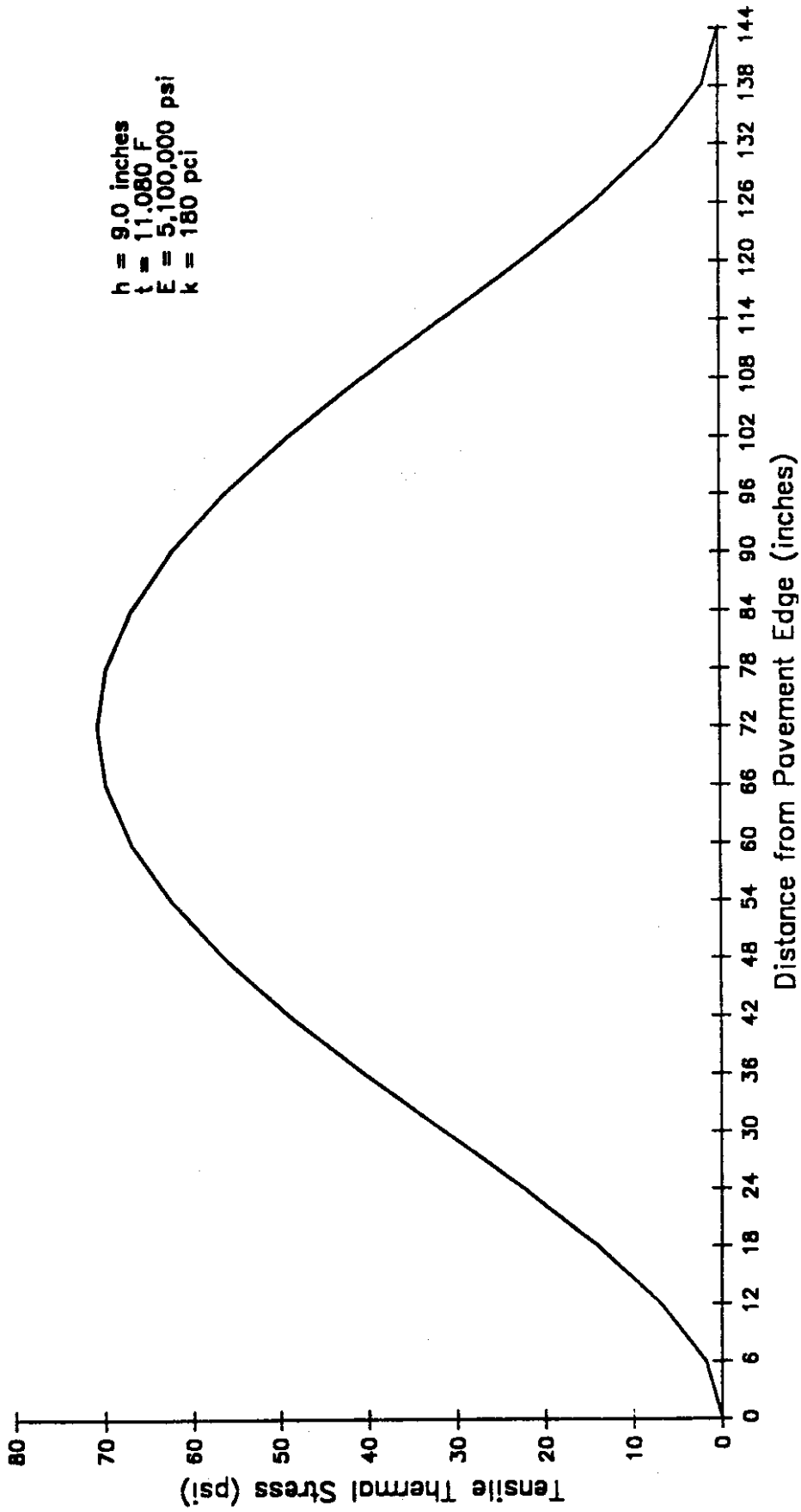


Figure 3.20 Curl Stress along the Transverse Joint - SR 5

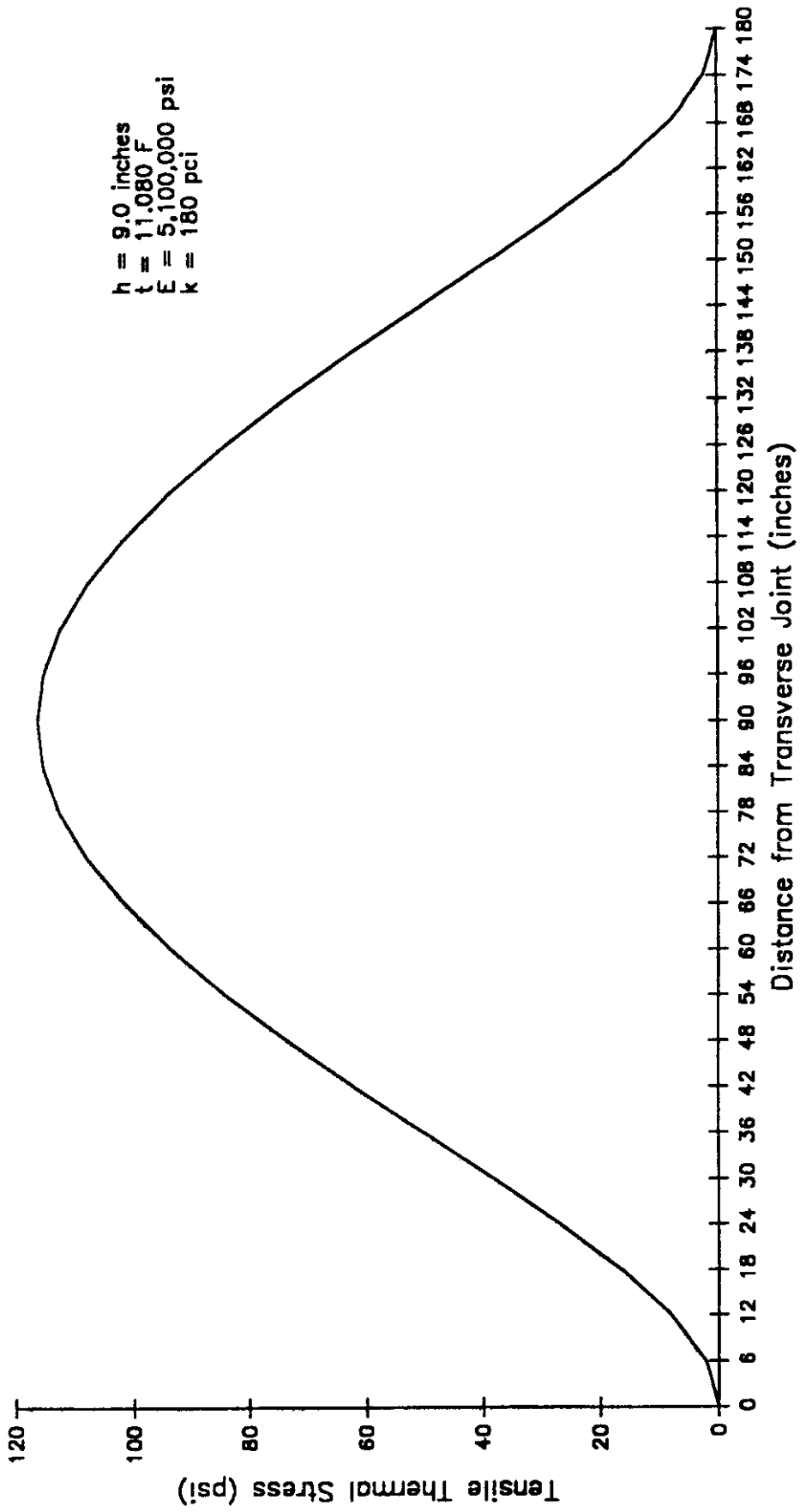


Figure 3.21 Curl Stress along the Pavement Edge - SR 5

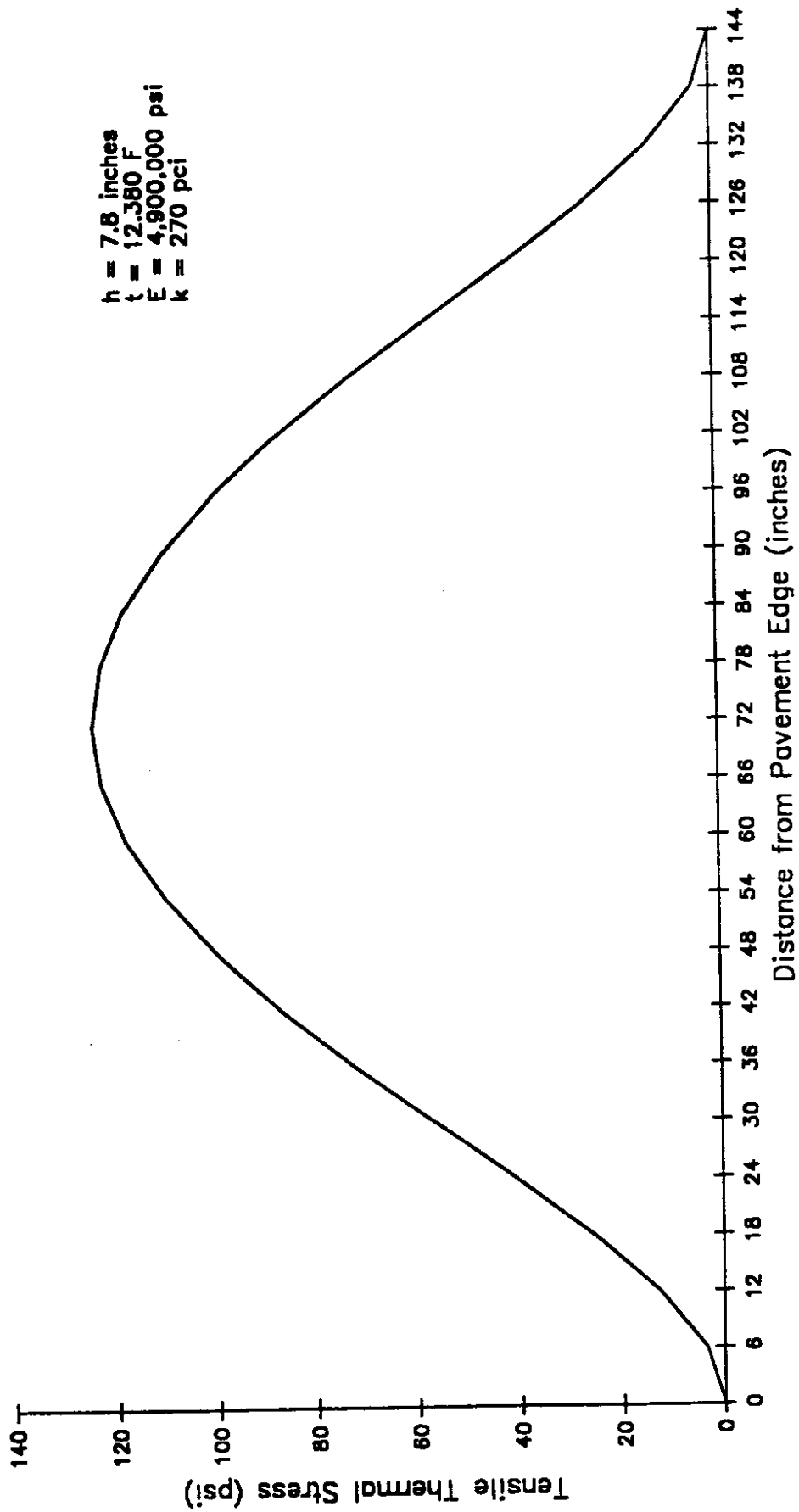


Figure 3.22 Curl Stress along the Transverse Joint - SR 90

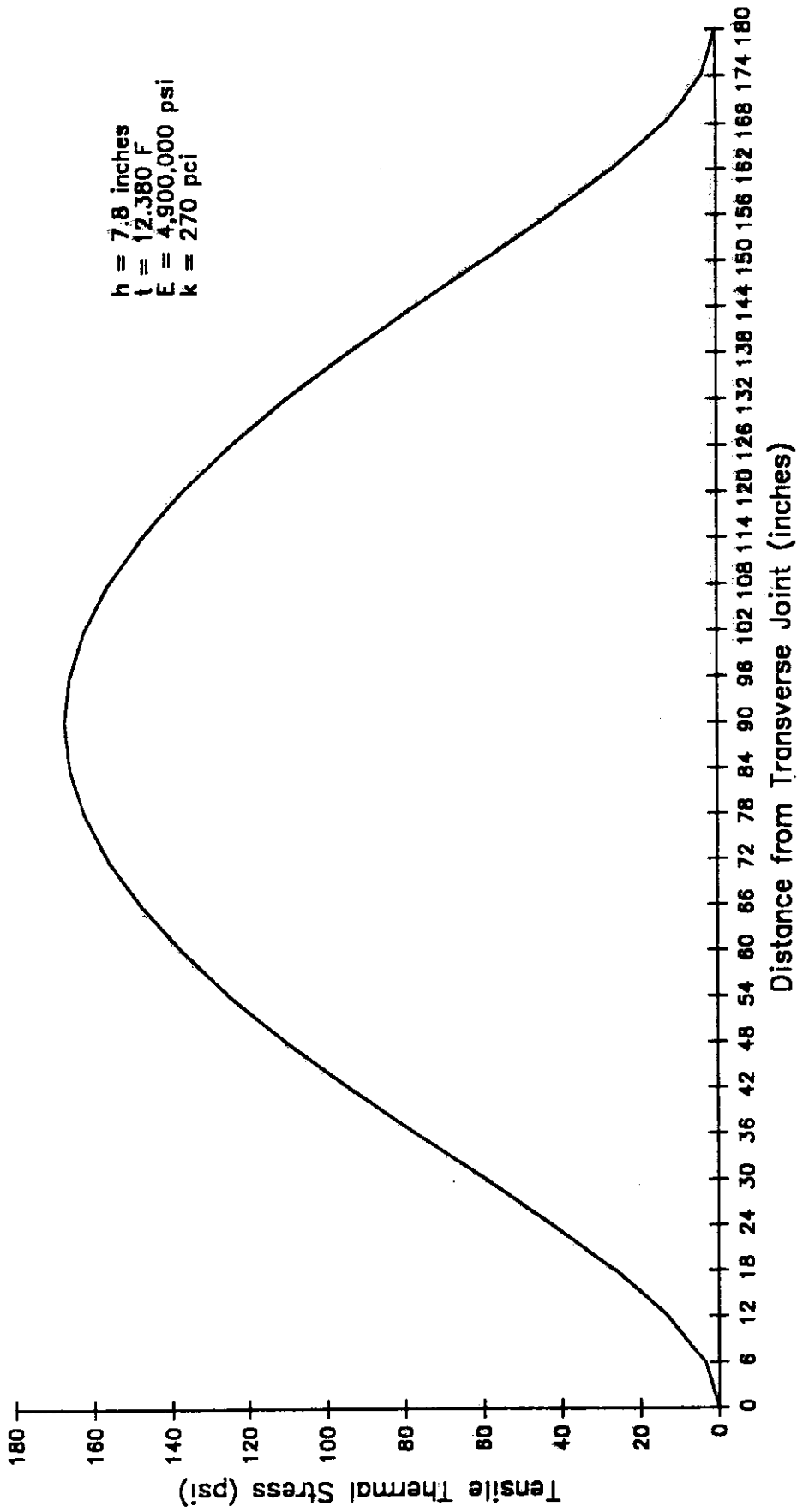


Figure 3.23 Curl Stress along the Pavement Edge - SR 90

Table 3.16. Equivalent Axle Load Estimate – SR 5, NE 175th (MP 176.35)

Year	ADT (two way)	Percent Trucks		Northbound Trucks				ESALs per yr.
		Single Units	Comb.	Daily Single Units	E.F.	Daily Comb.	E.F.	
1965	52,000	3	2	780	.13	520	.91	210,000
1966	57,700	3	2	866	.17	577	.91	245,000
1967	59,400	3	2	891	.17	594	.91	253,000
1968	66,600	3	2	999	.17	666	.91	283,000
1969	72,100	3	2	1082	.17	721	.84	288,000
1970	71,400	3	2	1071	.17	714	.84	285,000
1971	68,700	2	3	687	.17	1031	.84	359,000
1972	76,400	2	3	764	.18	1146	.88	418,000
1973	76,900	2	3	769	.18	1154	.88	421,000
1974	72,200	2	3	722	.20	1083	.90	408,000
1975	78,000	2	3	780	.20	1170	.90	441,000
1976	81,000	2	3	810	.22	1215	1.02	517,000
1977	85,900	2	3	859	.23	1288	1.02	552,000
1978	90,500	2	3	905	.12	1358	1.04	555,000
1979	101,800	2	3	1018	.23	1527	1.16	732,000
1980	129,200	2	3	1292	.24	1938	1.11	898,000
1981	133,100	2	3	1331	.24	1997	1.11	926,000
1982	135,800	2	3	1358	.24	2037	1.11	944,000
1983	113,200	2	3	1132	.24	1698	.99	713,000
1984	142,800	2	3	1428	.24	2142	.99	899,000
1985	147,000	2	3	1470	.24	2205	.99	926,000
1986	137,500	2	3	1375	.24	2062	.99	866,000
1987	144,400	2	3	1444	.24	2166	.99	909,000

Total ESALs = 13,048,000

Table 3.17. Equivalent Axle Load Estimate - SR 90, MP 279.26

Year	ADT (two way)	Percent Trucks		Northbound Trucks				ESALs per yr.
		Single Units	Comb.	Daily Single Units	E.F.	Daily Comb.	E.F.	
1965	11,200	2	7	112	.13	392	.91	136,000
1966	16,500	2	7	165	.17	578	.91	202,000
1967	17,800	2	7	178	.17	623	.91	218,000
1968	18,300	2	5	183	.17	458	.91	152,000
1969	19,400	2	5	194	.17	485	.84	161,000
1970	23,000	2	5	230	.17	575	.84	191,000
1971	24,300	4	4	486	.17	486	.84	179,000
1972	26,000	4	4	520	.18	520	.88	201,000
1973	28,200	4	4	564	.18	564	.88	218,000
1974	29,600	4	4	592	.20	592	.90	238,000
1975	28,600	4	4	572	.20	572	.90	230,000
1976	30,600	4	4	612	.22	612	1.02	277,000
1977	32,200	4	4	644	.23	644	1.02	294,000
1978	35,700	4	4	714	.12	714	1.04	302,000
1979	36,000	3	3	540	.23	540	1.16	274,000
1980	34,500	3	3	518	.24	518	1.11	255,000
1981	35,300	3	3	530	.24	530	1.11	261,000
1982	33,900	3	3	508	.24	508	1.11	250,000
1983	34,000*	4	4	680	.24	680	.99	305,000
1984	34,000*	4	4	680	.24	680	.99	305,000
1985	34,000*	4	4	680	.24	680	.99	305,000
1986	38,300	4	4	766	.24	766	.99	344,000
1987	33,300	4	4	666	.24	666	.99	299,000

* Estimate (missing data)

Total ESALs = 5,597,000

CHAPTER 4.0

PORTLAND CEMENT CONCRETE PAVEMENT PERFORMANCE EVALUATION

Using the data analysis results presented in Chapter 3.0, the researchers evaluated the PCC pavement performance of the two test sites included in this study. The results from these evaluations were intended to be applicable to other pavements in Washington state. Two major topics are addressed in this chapter. First, the mechanisms causing the distresses observed, namely transverse cracking, longitudinal cracking, and faulting, are discussed. Second, the remaining pavement life and crack and faulting propagation rates are discussed.

4.1 FAILURE MECHANISMS

Cracking is one of the primary structural distresses occurring in plain-jointed PCC pavements. Laboratory studies have shown that plain PCC pavement experiences fatigue failure when subjected to repetitive flexural stresses. [4.1-4.9] These studies have also shown that the load repetitions that can be applied to the concrete before fracturing has occurred are a function of the applied stress to flexural strength (modulus of rupture) ratio. As this ratio approaches 1.0 (applied stress equals flexural strength), the allowable load repetitions decreases.

Substantial work has been done to document the causes of transverse cracking and joint faulting in plain-jointed concrete pavements. This work is summarized here because it explains the failure mechanisms observed at the SR 90 test site. Very little work has been done to evaluate the causes of longitudinal cracking, even though this distress was observed at the AASHO Road Test and occurred before any other cracking in 30 of 91 test sections. [4.10] Longitudinal cracking also occurred at the Michigan Road Test. [4.11] In addition, longitudinal cracking was observed in Washington state and California in-service pavements that were evaluated as part of the Zero Maintenance Design study. [4.12] In

Washington state, longitudinal cracking is a commonly observed distress along the SR 5 corridor, and it is important to understand its cause (joint faulting is becoming increasingly more common, as well).

Because transverse cracking and faulting have been evaluated most extensively, and the longitudinal cracking evaluation logically follows a discussion on transverse cracking, the failure mechanisms at the SR 90 site will be described first.

4.1.1 SR 90

4.1.1.1 Transverse Cracking. After extensive analyses, several researchers have concluded that the critical fatigue damage location in a plain-jointed PCC pavement slab is midway between the transverse joints, at the pavement edge. [4.12] The critical tensile stress location and its direction are illustrated in Figure 4.1. Darter concluded that when the outer wheelpath traffic distribution centerline is less than 36 inches from the pavement edge, the critical fatigue damage point is at the slab edge. [4.12] This critical fatigue damage location indicates that cracking should initiate at the outer slab edge and that the cracking should propagate across the slab width (transverse cracking), as indicated by the tensile stress direction at the slab bottom (see Figure 4.1). This transverse crack initiation location has been documented in studies in which distress data for in-service pavements were collected.

Zollinger and Barenberg conducted extensive fatigue damage analyses while developing a jointed concrete pavement mechanistic design procedure for the Illinois Department of Transportation. [4.13] The analysis results indicated that the critical fatigue damage location was at the pavement edge midway between the transverse joints and that concrete fatigue was caused by a combination of load-induced stresses and thermal stresses (developed because of a temperature gradient through the slab depth). They also found that the traffic distribution across the pavement width controlled the fatigue damage occurring at this critical location.

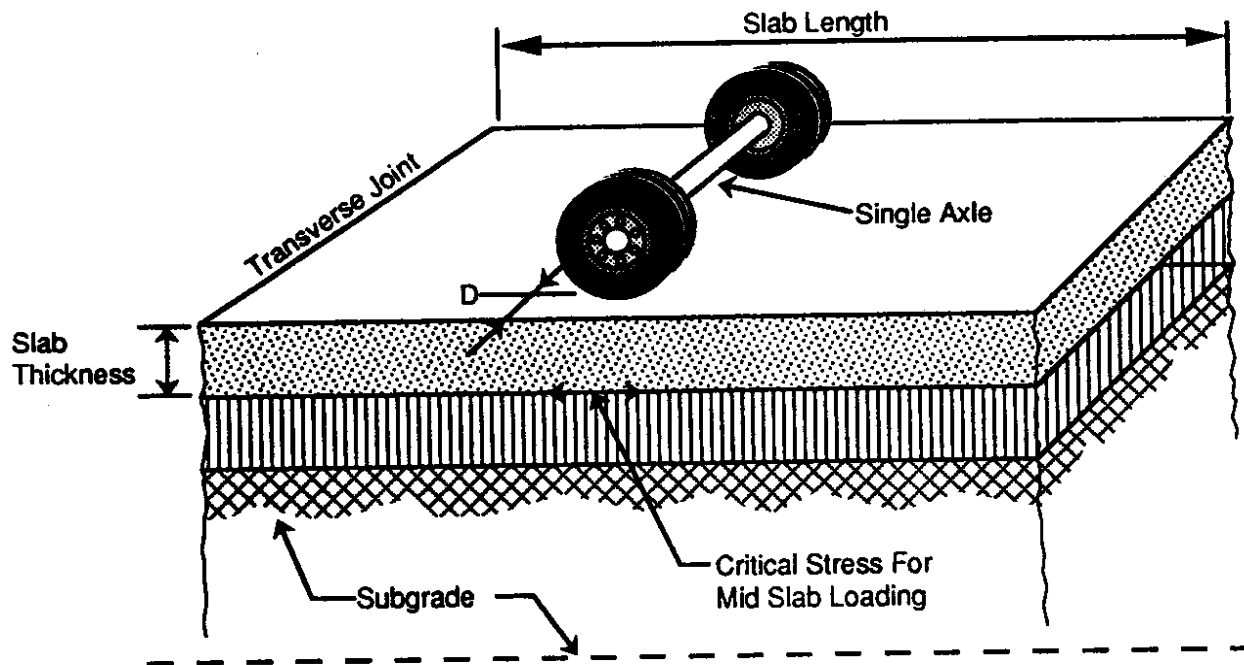


Figure 4.1 Critical Fatigue Damage Location and Tensile Stress Direction for Mid-Slab Loading

Thermal (curl) stresses contribute to fatigue damage and can be large enough to cause cracks in unloaded pavements. When the thermal gradient is positive (the surface temperature is greater than the slab bottom temperature), tensile stresses are induced at the slab bottom, as illustrated in Figure 4.2. These tensile stresses occur during the day and are in the same direction as load-induced stresses. Thus they are additive to the load stress, resulting in higher stresses at the critical stress location. In contrast, at night when the thermal gradient is negative, compressive stresses occur at the slab bottom, thereby reducing the load-induced stresses. Researchers have found that the daytime stresses (those additive to load stresses) are often substantially higher than the nighttime stresses. [4.14]

Curl stresses are highest at the pavement edge midway between the transverse joints. The curl stress distribution along the pavement edge at the SR 90 test site is shown in Figure 4.3. Because load stresses and thermal stresses are additive at the slab edge midway between the transverse joints, and because the thermal stresses are at a maximum, this location experiences the highest stresses and the maximum fatigue damage. Transverse cracks would be expected to initiate at this location, and they often do.

Where traffic loads occur across the slab, and how close they are to the pavement edge, are defined by a lateral traffic distribution curve. This characteristic distribution is important because the closer the wheel load is to the pavement edge, the higher are the tensile stresses created at the slab bottom and the greater the fatigue damage. Figure 4.4 shows load-induced tensile stresses at the slab bottom for wheel loads located across the pavement width. The lateral distance from the pavement edge to the outside edge of the outer truck tire has been designated "D"; this concept is further illustrated in Figure 4.5. The tensile stresses at the slab bottom are highest for a load at the pavement edge ($D = 0$), as shown in Figure 4.4.

All traffic does not occur at a constant distance, D, from the pavement edge but is distributed across the pavement. The mean distance from the pavement edge to the

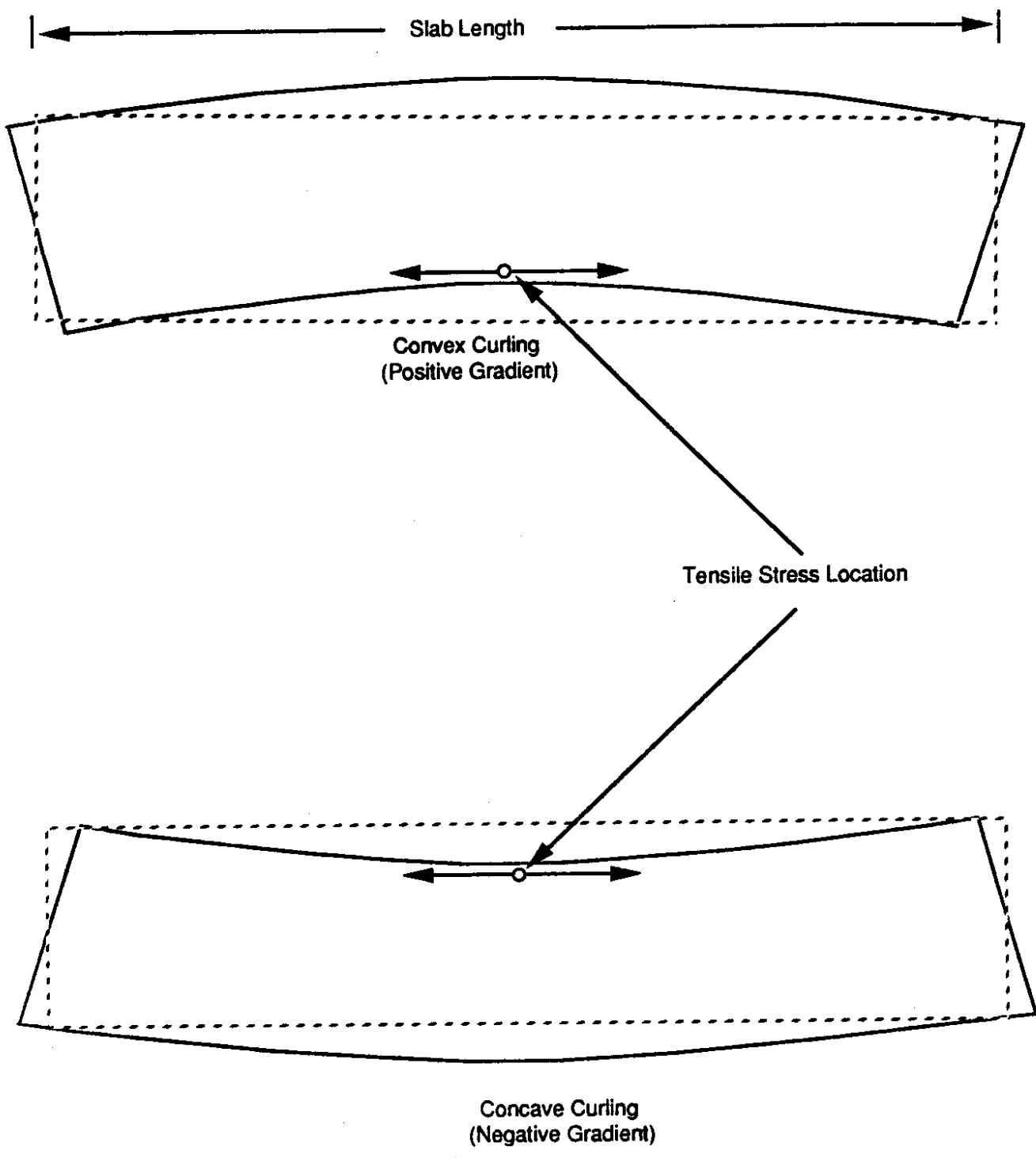


Figure 4.2 Deflected Slab Shape Under Temperature Gradient

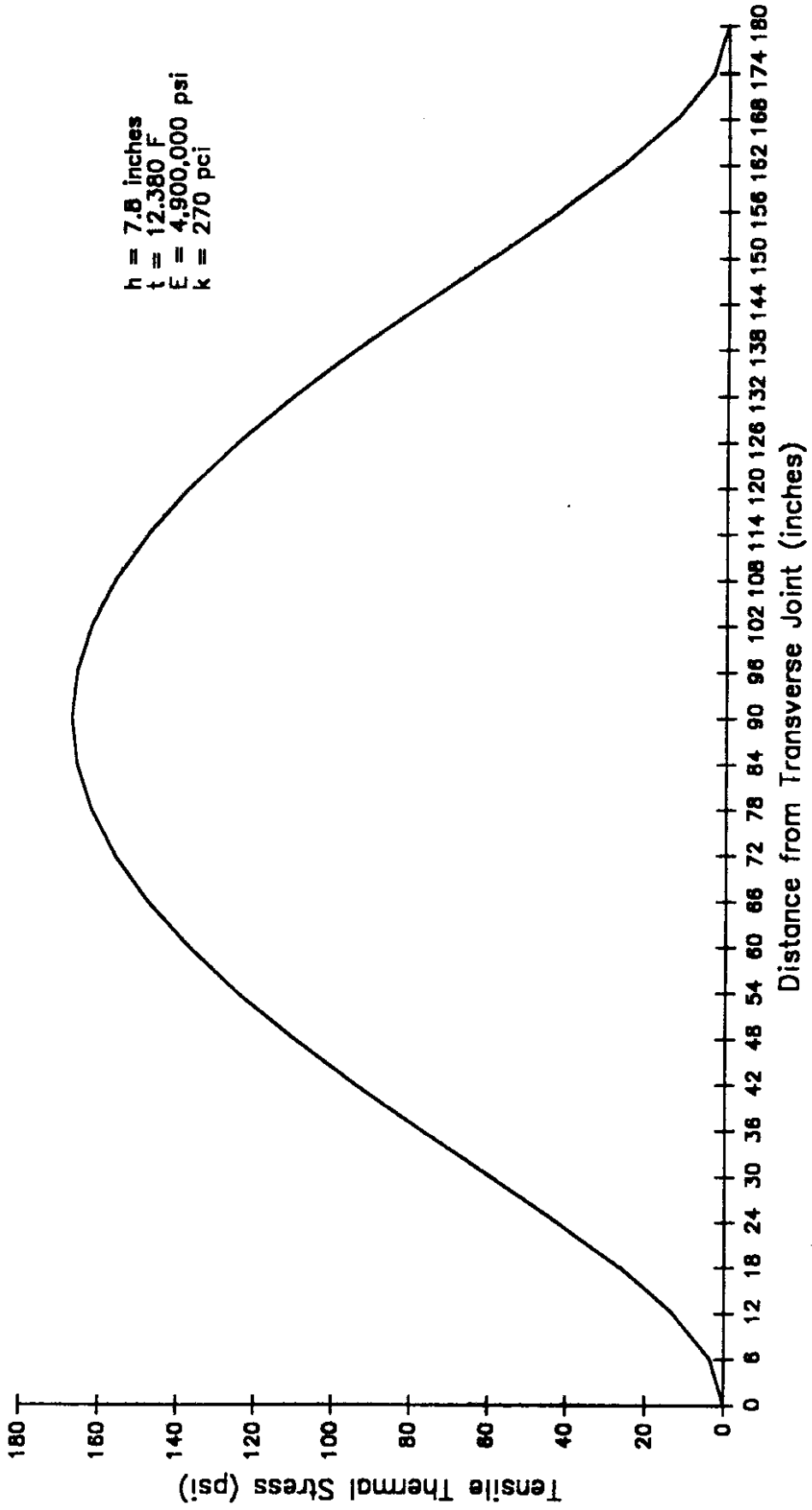


Figure 4.3 Curl Stress along the Pavement Edge - SR 90

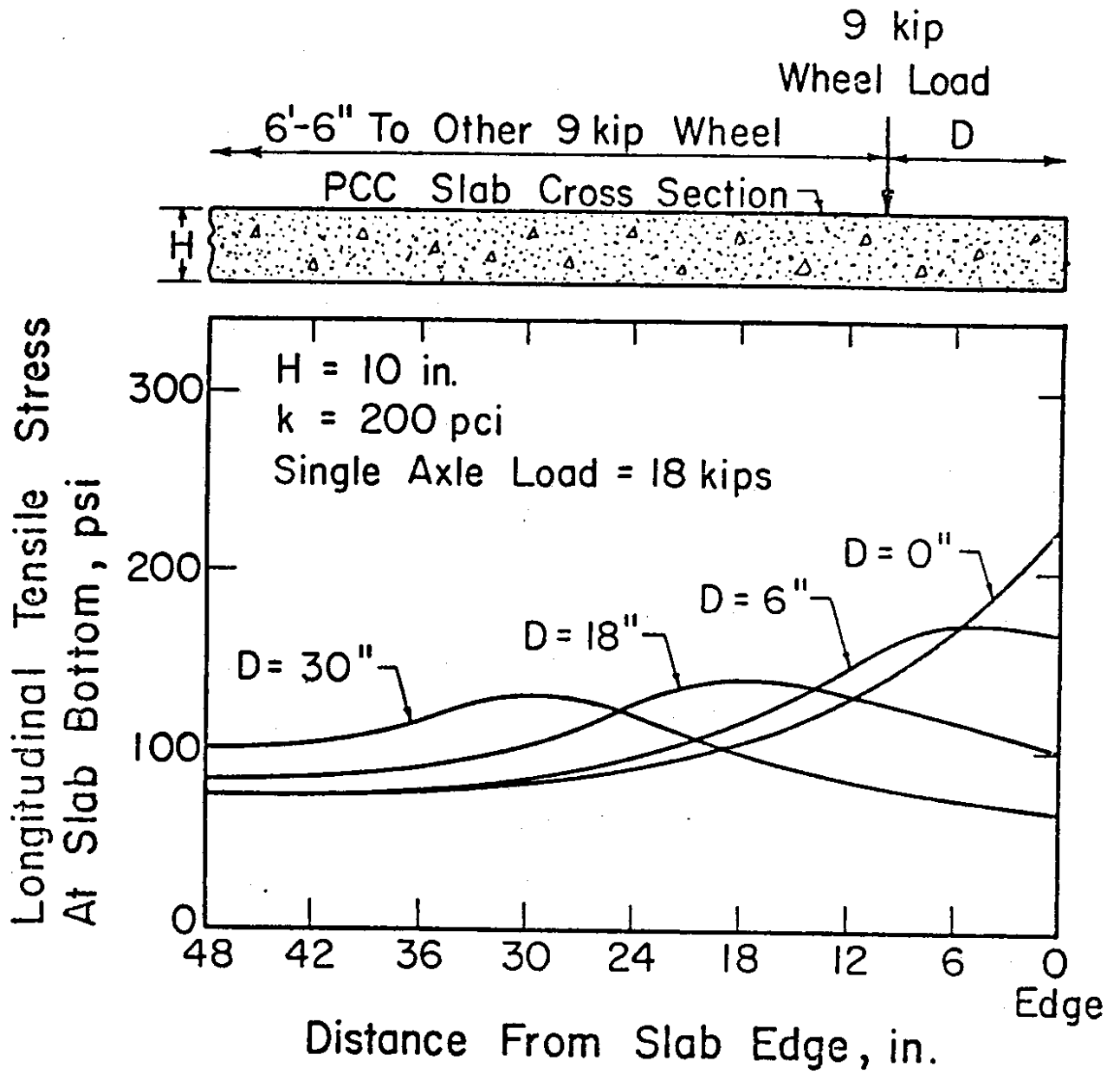
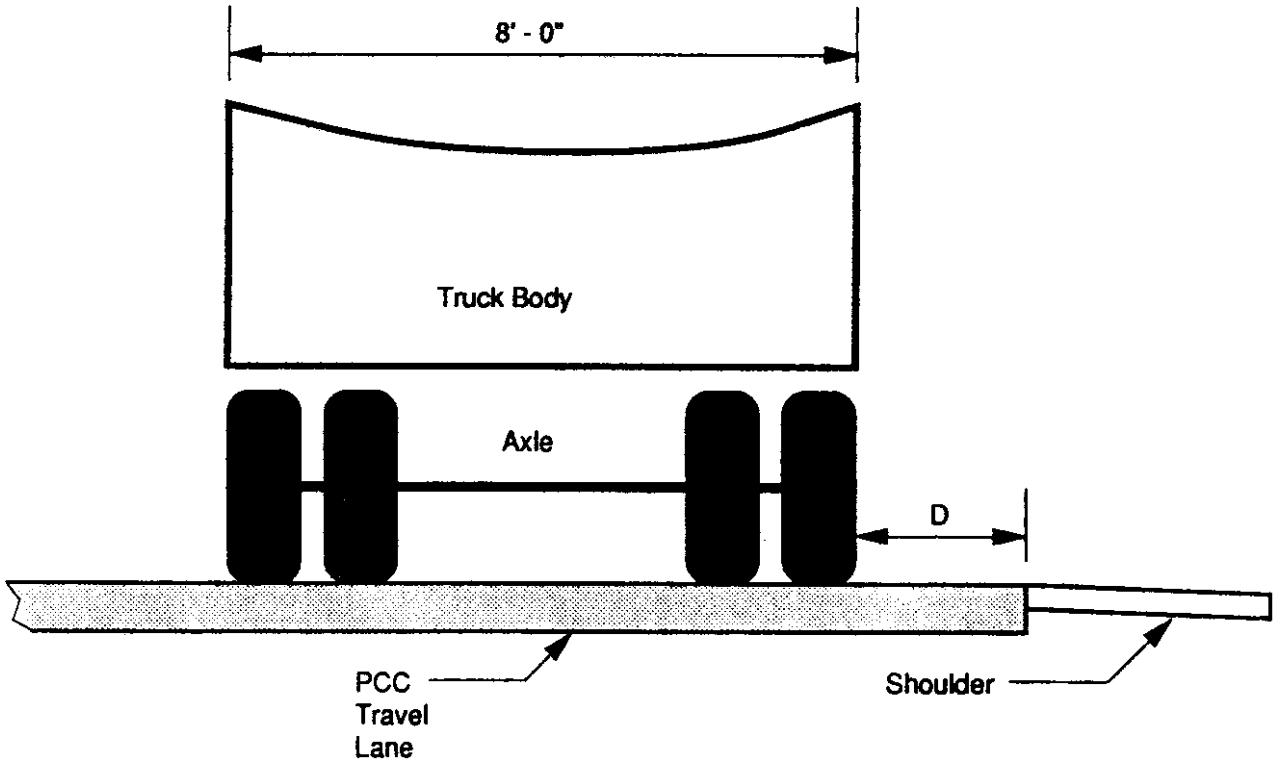


Figure 4.4 Computed Tensile Stresses Across Bottom of PCC Slab at Midpoint Between Transverse Joints for Various Transverse Positions of Axle Load [from Reference 4.12]



D = Distance from Slab Edge to Outside of Dual Tires

Figure 4.5. Illustration of the Mean Distance from Slab Edge to Outside of Dual Tires

centerline of such a distribution is designated D-bar. The lateral traffic distribution centerline varies with several factors, including traffic lane width, edge stripe location, whether shoulders are paved or unpaved, the presence of edge restraints along the pavement edge (for example, retaining walls), and whether a curb and gutter are present. [4.12]

Emery has shown that the lateral truck distribution on rural four-lane interstate highways is approximately normal and has a standard deviation of 10 inches. [4.15] Darter indicated that when no lateral obstructions exist and the shoulder is paved, the lateral traffic distribution centerline (D-bar) is between 12 and 21 inches. [4.12] Other studies have indicated that this value ranges from 16 to 18 inches. [4.15] Zollinger and Barenberg used the normal distribution proposed by Emery, and values of 12 and 18 inches for D-bar. A typical traffic distribution is shown in Figure 4.6 for a single axle with D-bar at 18 inches. The centerline for the outer wheelpath traffic distribution is at Point A (18 inches) and for the inner wheelpath is at Point B (102 inches).

All wheel loads applied to the pavement contribute to the fatigue damage accumulated at the pavement edge (the critical fatigue location). Research has shown that for traffic loading midway between the transverse joints, and for a traffic distribution centered at 18 inches, the fatigue damage accumulated at the pavement edge attributable to all traffic (ESALs) in the distribution is the same as the damage that would have been caused by 5 percent of the traffic applied at the pavement edge. In other words, 5 percent of the calculated ESALs must be applied at the critical fatigue location to produce the same fatigue damage as that caused by the full traffic distribution. The percentage of traffic at the pavement edge required to produce equivalent fatigue damage changes when the lateral traffic distribution centerline changes. The values obtained for each distribution centerline are essentially pass-to-coverage ratios, which Zollinger and Barenberg termed "equivalent damage ratios." When fatigue damage is evaluated on a pavement with a lateral traffic centerline at 18 inches, only 5 percent of the applied ESALs should be considered.

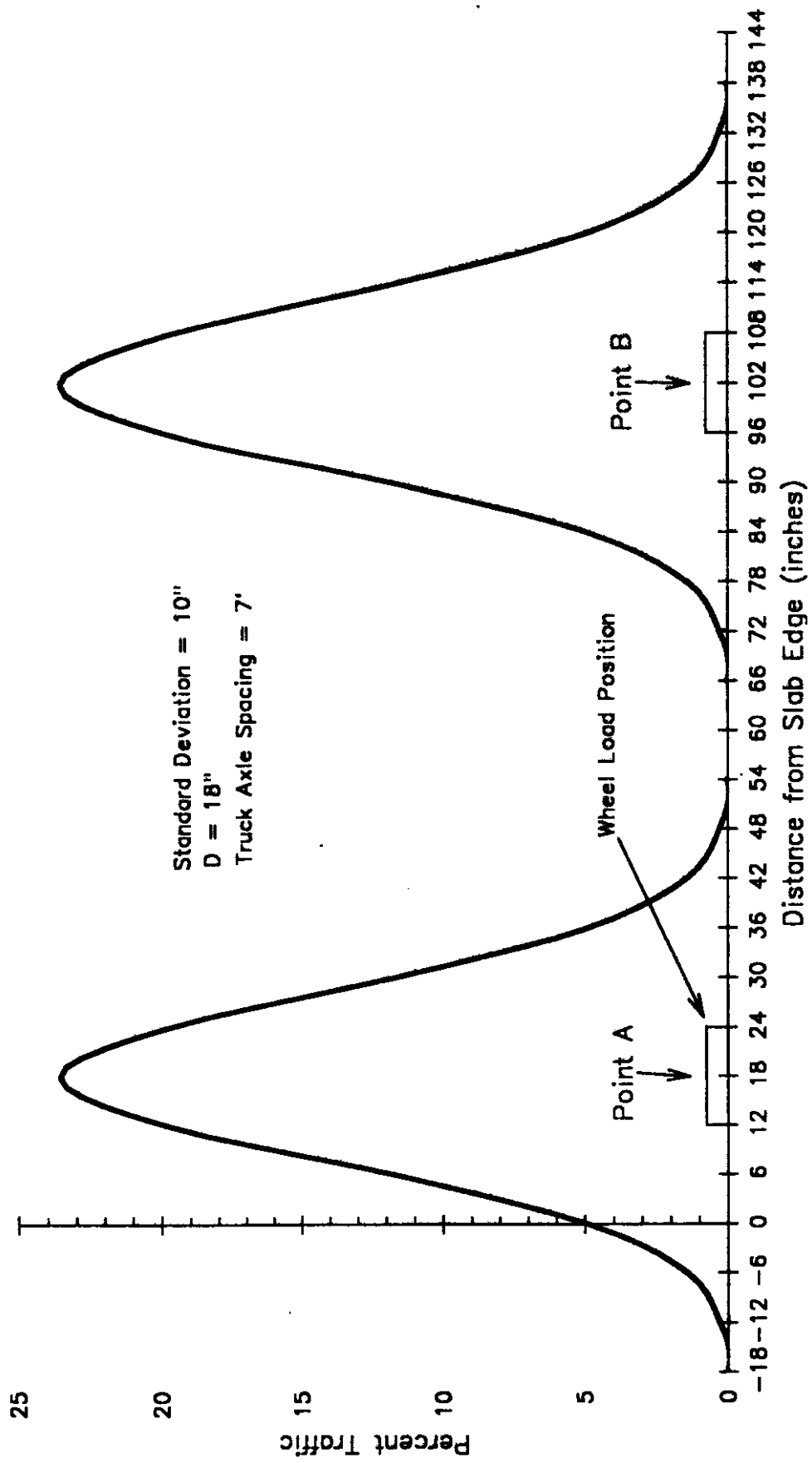


Figure 4.6 Lateral Traffic Distribution for a Single Axle

The conclusion to be drawn from the research is that the primary location for concrete fatigue should be at the pavement edge midway between the transverse joints, and the resulting cracks should be transverse cracks. This type of failure was exhibited at the SR 90 site, where transverse cracks were observed at approximately mid-slab.

4.1.1.2 Faulting. Two major field studies, one in California and one in Georgia, were conducted to evaluate the causes of faulting at the transverse joints in plain jointed concrete pavements. [4.16, 4.17] These studies concluded that faulting is created when loose material accumulates near the joints. Material is deposited under the approach slab when the leave slab is deflected by a wheel load and the free water under the joints moves rapidly backward, carrying loose material with it. Suction occurring when the load leaves the approach slab increases the force with which the free water moves. Observations of faulted joints have indicated that a thicker accumulation occurs under the approach slab, which causes this slab to lift, resulting in a faulted joint. The California study concluded that loose material comes from untreated shoulders and the cement treated base surface. [4.16] It also concluded that some material may result from abrasion at the joint interface and from material on the pavement surface moving downward through the joints.

Load transfer across the joints has a significant impact on whether faulting will occur. In general, the higher the load transfer efficiency is across the joint, the lower are the joint deflections and differential joint movements. Backward pumping of fines as a load passes over the joint is minimized when joint deflection and differential joint movement are minimized. Joint load transfer efficiency is affected by several factors, including joint opening, number and magnitude of load applications, foundation support, aggregate particle angularity, and whether load transfer devices are present. [4.18, 4.19, 4.20]

For joints without mechanical load transfer devices, joint load transfer efficiency occurs by aggregate interlock, which decreases significantly as the joints open. This

decrease is illustrated in Figure 4.7. Joint opening can be controlled most effectively by limiting the slab length. Laboratory and field studies have indicated that keeping joint openings less than 0.03 inch keeps the aggregate interlock at an acceptable level. With the assumption that the temperature difference between the time the SR 90 test section was paved (57.0 degrees Fahrenheit for April when construction was completed) and the mean monthly minimum temperature (19.6 degrees Fahrenheit for January), the joint opening was computed to be 0.034 inch by the following equation:

$$\Delta L = (C)(L)(\alpha T + e) \quad \text{Equation 4.1}$$

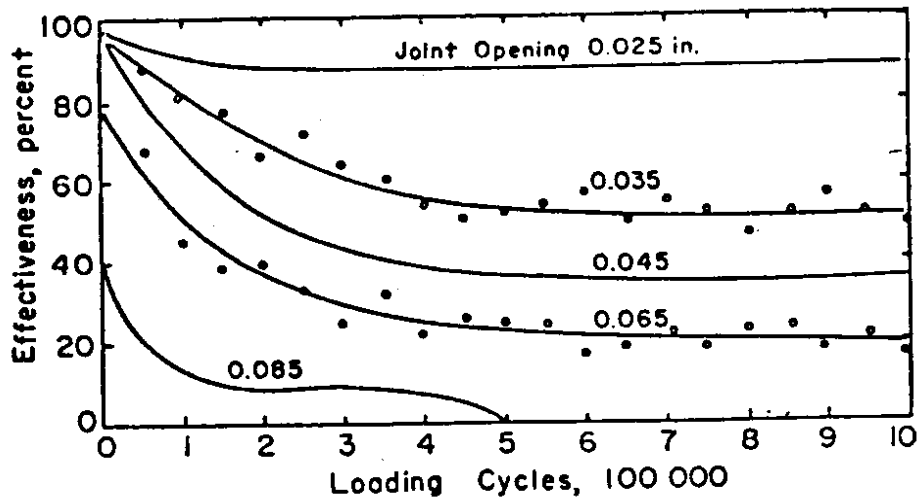
where:

- ΔL = joint opening caused by a temperature change T and concrete drying shrinkage, inches
- C = correction factor for subbase/slab frictional restraint (0.65 for stabilized subbase, 0.80 for granular subbase)
- L = joint spacing, inches
- α = concrete coefficient of thermal expansion, $5.0-6.0 \times 10^{-6}/^{\circ}\text{F}$
- T = the temperature when concrete was placed minus the lowest mean monthly temperature, degrees Fahrenheit
- e = concrete drying shrinkage coefficient, $0.2-0.8 \times 10^{-4}$ in/in.

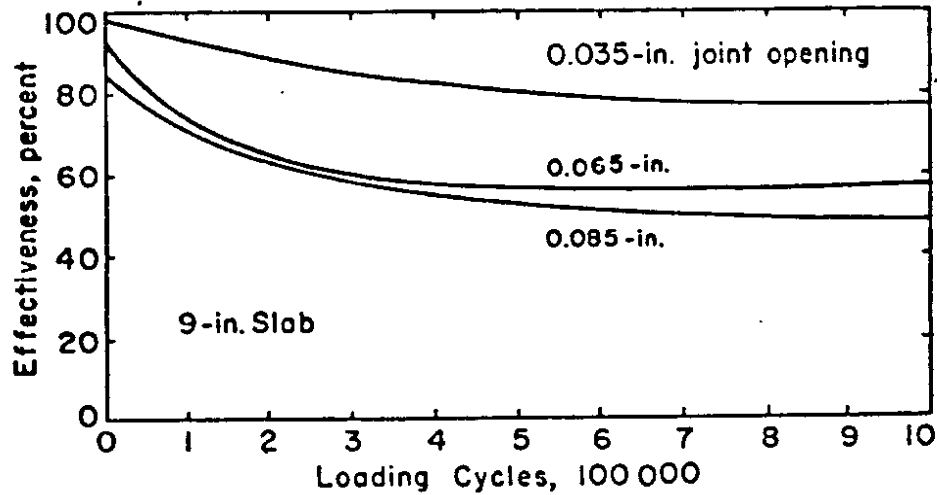
This joint opening was just slightly greater than the maximum allowable joint opening; however, the input temperatures were estimated and could have varied considerably from those assumed.

Joint load transfer efficiency decreases as the number of applied loads increases. Load transfer efficiency also decreases with increased load magnitude because of increased deflection and unit shear at the joint. [4.18, 4.19] These phenomena are illustrated in Figure 4.8.

Slab thickness and foundation support influence joint load transfer efficiency over time. Joint efficiency is maintained at a higher level as slab thickness increases. This improved joint efficiency may be due to reduced unit vertical shear across the joint

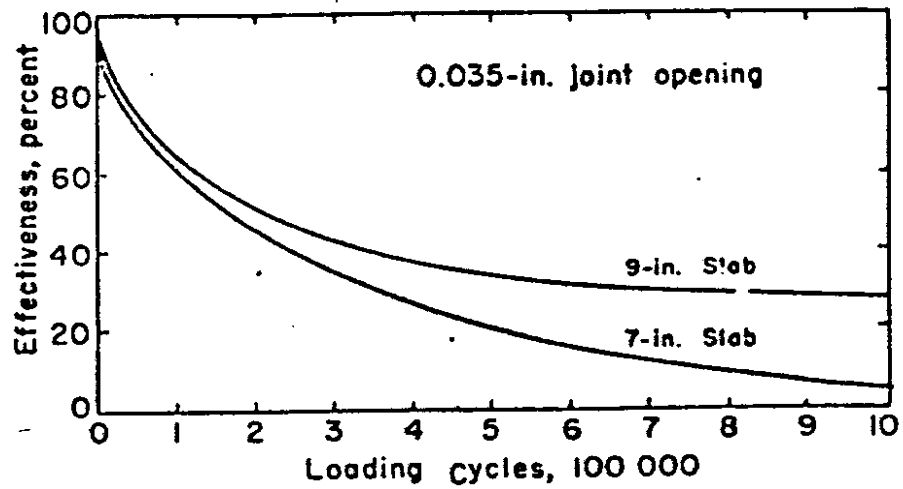


(a) Influence of joint opening on effectiveness
(9 in. slab, 6 in. gravel subbase, $k = 145$ psi)

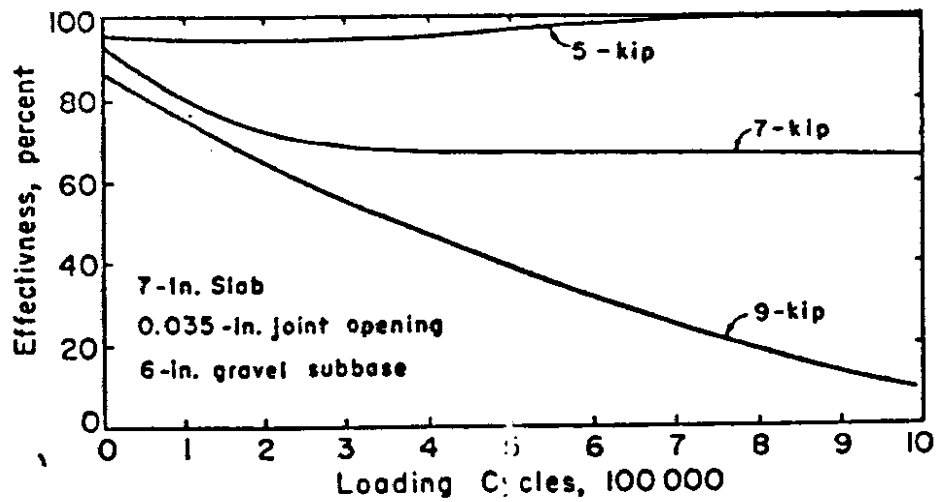


(b) Influence of joint opening on effectiveness
(9 in. slab., cement stabilized subbase,
 $k = 542$ pci)

Figure 4.7 Joint Load Effectiveness for Gravel and Cement Treated Subbase for Various Joint Openings [from Reference 4.18]



(a) Influence of slab thickness on effectiveness



(b) Influence of wheel load on effectiveness

Figure 4.8 Joint Load Effectiveness [from Reference 4.18]

face. [4.12] The corner deflection under load also decreases with increased slab thickness and foundation support. The less the deflection, the less the unit shear that must be transferred across the joint for a given load, and therefore joint efficiency remains higher for repeated load applications. The influence of slab thickness and foundation support on corner deflection is illustrated in Figure 4.9.

Mechanical load transfer devices (dowels) have been found to improve joint efficiency, particularly for large joint openings. [4.19, 4.21] Because joint efficiency is maintained at a higher level, joint faulting is reduced. The impact dowels have on load transfer efficiency is illustrated in Figure 4.10.

Once faulting has occurred, maintenance is required to reduce faulting to a level acceptable to the traveling public. The maintenance performed to correct faulting is often slab undersealing and grinding, or grinding alone. These activities are repairs and do not correct the pavement deficiencies that caused the faulting. Thus faulting often occurs again shortly after maintenance has been completed. This rapid faulting recurrence has been evidenced by WSDOT personnel on a section of SR 90 (Snoqualmie Pass) where joint grinding was completed. Within two years the joints were again faulted.

Because correcting faulting without extensive and costly maintenance is difficult and because the maintenance provided is, at best, a temporary fix, pavements are best designed and constructed with proper attention paid to the factors that influence faulting. Faulting can best be prevented by doing the following:

1. maintaining a high degree of joint load transfer efficiency throughout pavement life, by using mechanical load transfer devices or by using short joint spacing, which minimizes joint opening;
2. minimizing the water at the slab bottom near the joints by providing proper drainage, using an open-graded drainage layer, and adequately sealing joints; and,
3. using erosion resistant subbase materials.

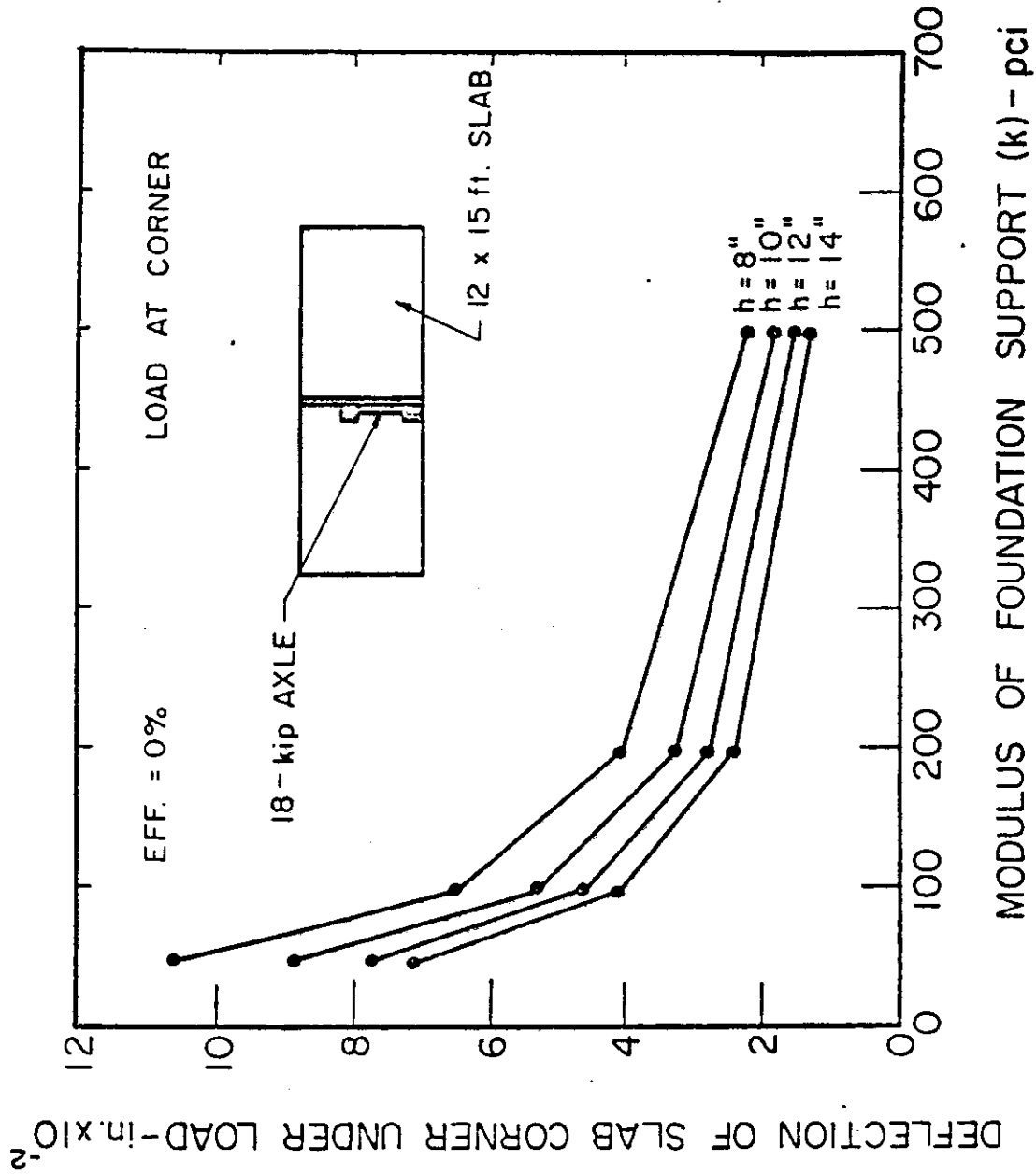


Figure 4.9 Influence of Slab Thickness and Foundation Support on Corner Deflection (Computed with F.E. Program) [from Reference 4.12]

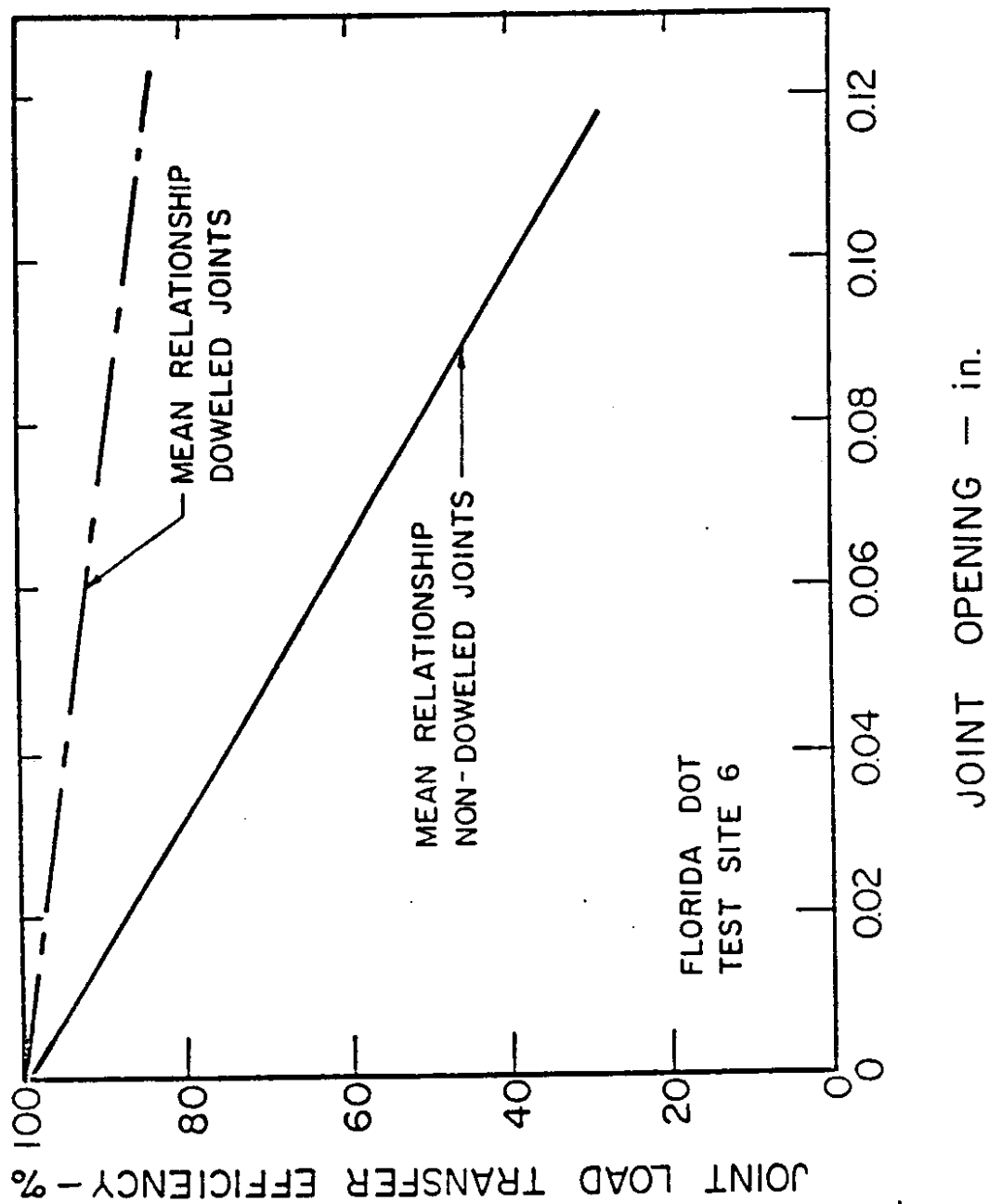


Figure 4.10 Influence of Mechanical Load Transfer Device on Joint Effectiveness after 12 Years of Service [from Reference 4.20]

4.1.2 SR 5 — Longitudinal Cracking

The longitudinal cracking observed in the SR 5 site is typical of the longitudinal cracking observed throughout Washington state. An issue to be investigated during this study was the longitudinal cracking mechanism, which appears to be load-related rather than caused by other factors such as improperly sawed longitudinal joints. WSDOT's and California's experiences have shown that this cracking appears frequently in the inner wheelpath, as well as the outer wheelpath. The longitudinal cracking observed at the AASHO Road Test occurred most often approximately 24 to 42 inches from the slab edge. [4.10]

As mentioned in the discussion on transverse cracking, research has shown that the critical fatigue location in a plain-jointed PCC pavement is at the pavement edge, midway between the transverse joints. The first step in investigating the mechanism causing longitudinal cracking was to look at differences between those pavements exhibiting longitudinal cracking and those exhibiting transverse cracking.

In evaluating the data collected at the SR 5 and SR 90 test sections, the most obvious difference between the two sites was the measured load transfer efficiency. These two pavement sections were tested at approximately the same temperature (60 degrees Fahrenheit), but the load transfer efficiency for all transverse joints at the SR 5 site averaged 91.6 percent with a COV of 8.0 percent, and at the SR 90 site averaged 67.0 percent with a COV of 33.8 percent. Because the two sites were tested at the same temperature, the measured load transfer efficiencies should have been similar, but they were not. Also, as evidenced by the COV values, the load transfer efficiencies varied only slightly at the SR 5 site, while they varied substantially at the SR 90 site.

The tight joints at SR 5 indicated that in-plane compressive forces parallel to the pavement centerline may have existed. To investigate whether other data supported this conclusion, the FWD deflection data were further evaluated. This evaluation found that, in

several instances, the deflections at the transverse joints were lower than those at the slab center (for the same slab). Theory indicates that the transverse joint deflection should be approximately 1.5 times higher than that at the slab center for 100 percent load transfer efficiency and should be 3.1 times higher for 0 percent load transfer efficiency (free-edge condition). The transverse joint to slab center deflection ratios are presented for SR 5 in Table 4.1 and for SR 90 in Table 4.2. The SR 90 ratios were calculated to determine whether differences existed between the two sites.

The data presented in Table 4.1 show that for about 30 percent of the cases, the transverse joint deflection was lower than the slab center deflection (ratios <1.0). The ratios at SR 5 varied from 0.65 to 4.17, with a mean of 1.49. A histogram of the ratio

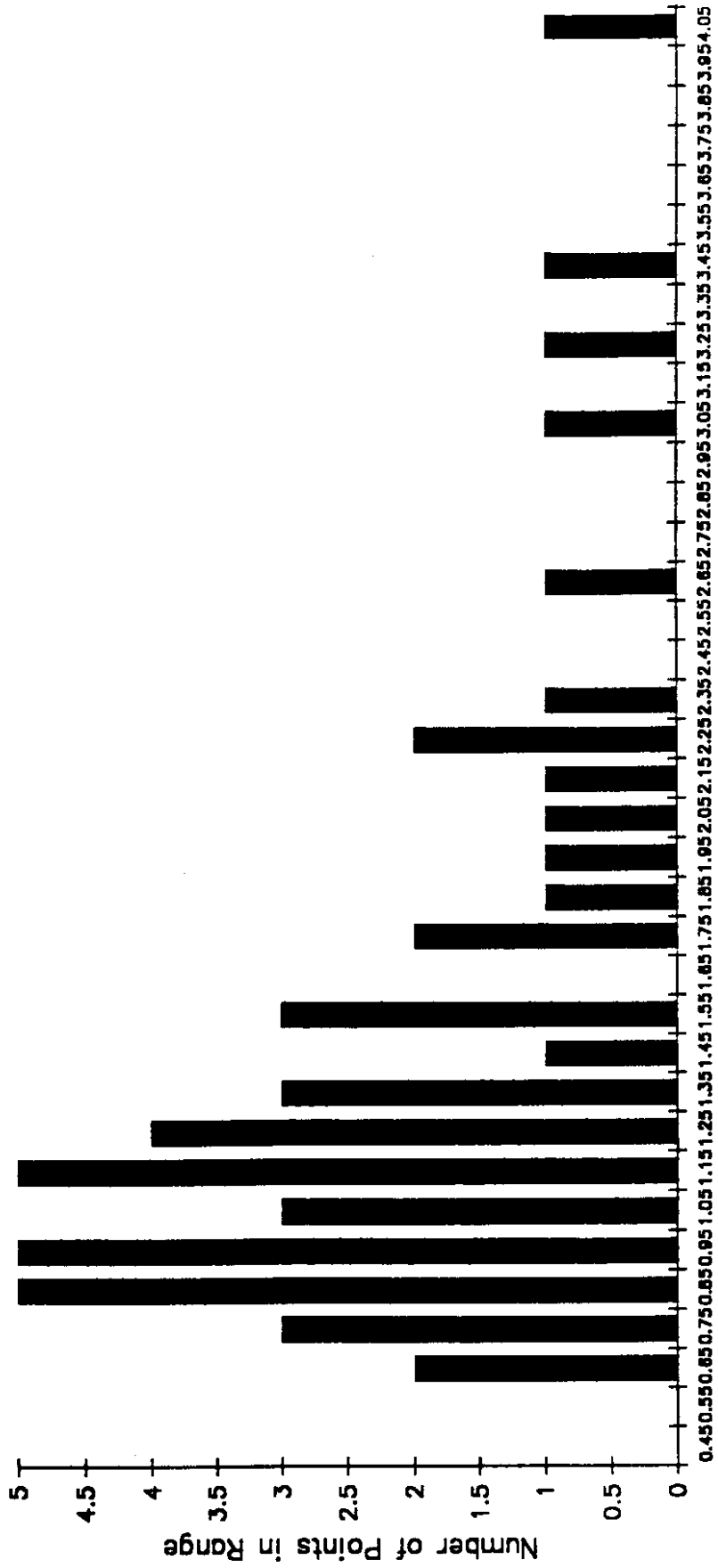
Table 4.1. Ratio of Transverse Joint Deflection to Slab Center Deflection — SR 5

Row	Slab	Transverse Joint 1	Transverse Joint 2
2	1	1.15	0.73
	2	0.93	0.86
	3	0.92	0.93
	4	0.97	1.13
	18	1.74	1.75
	19	2.61	1.24
	20	1.39	1.81
	21	1.97	2.08
	25	3.20	3.48
	26	4.17	2.20
	27	3.05	2.11
	28	1.06	1.12
5	1	0.77	0.86
	2	1.06	0.74
	3	0.65	0.88
	4	0.82	0.67
	18	1.04	0.96
	19	1.34	1.14
	20	1.36	1.47
	21	1.19	1.53
	25	1.27	1.56
	26	1.22	0.88
	27	1.24	2.36
	28	2.20	1.55

Table 4.2. Ratio of Transverse Joint Deflection to Slab Center Deflection — SR 90

Row	Slab	Transverse Joint 1	Transverse Joint 2
1	1	2.01	1.66
	2	1.86	1.58
	3	1.68	1.86
	4	1.76	1.40
	25	1.80	1.80
	26	1.65	1.47
	27	1.62	1.42
	28	1.67	1.83
	51a	1.19	1.22
	51b	1.33	1.59
	52	1.33	1.07
	53	1.28	1.24
	54	1.47	1.45
	4	1	1.65
2a		1.53	1.54
2b		1.66	1.63
3a		1.35	1.21
3b		1.31	1.24
4		1.27	1.22
25a		1.48	1.80
25b		1.48	1.68
26		2.00	1.88
27a		1.46	1.59
27b		1.65	1.53
28		1.58	1.71
51a		1.34	1.97
51b		1.37	1.18
52a		1.35	1.45
52b		1.38	1.25
53a		1.25	1.31
53b		1.39	1.25
54a		1.32	1.46
54b		1.39	1.26

distribution is shown in Figure 4.11. If the five highest ratios were considered outliers and were omitted, the mean ratio was 1.28. A histogram of the ratio distribution at SR 90 is shown in Figure 4.12. In no instances were the transverse joint to slab center deflection ratios less than 1.0 at the SR 90 site. The ratios varied from 1.07 to 2.01 at the SR 90 site, with a mean value of 1.50. The ratio distributions for both sites together are shown in Figure 4.13.



Transverse Joint Deflection/Slab Center Deflection Ratio

Figure 4.11 Transverse Joint Deflection to Center Slab Deflection Ratio - SR 5

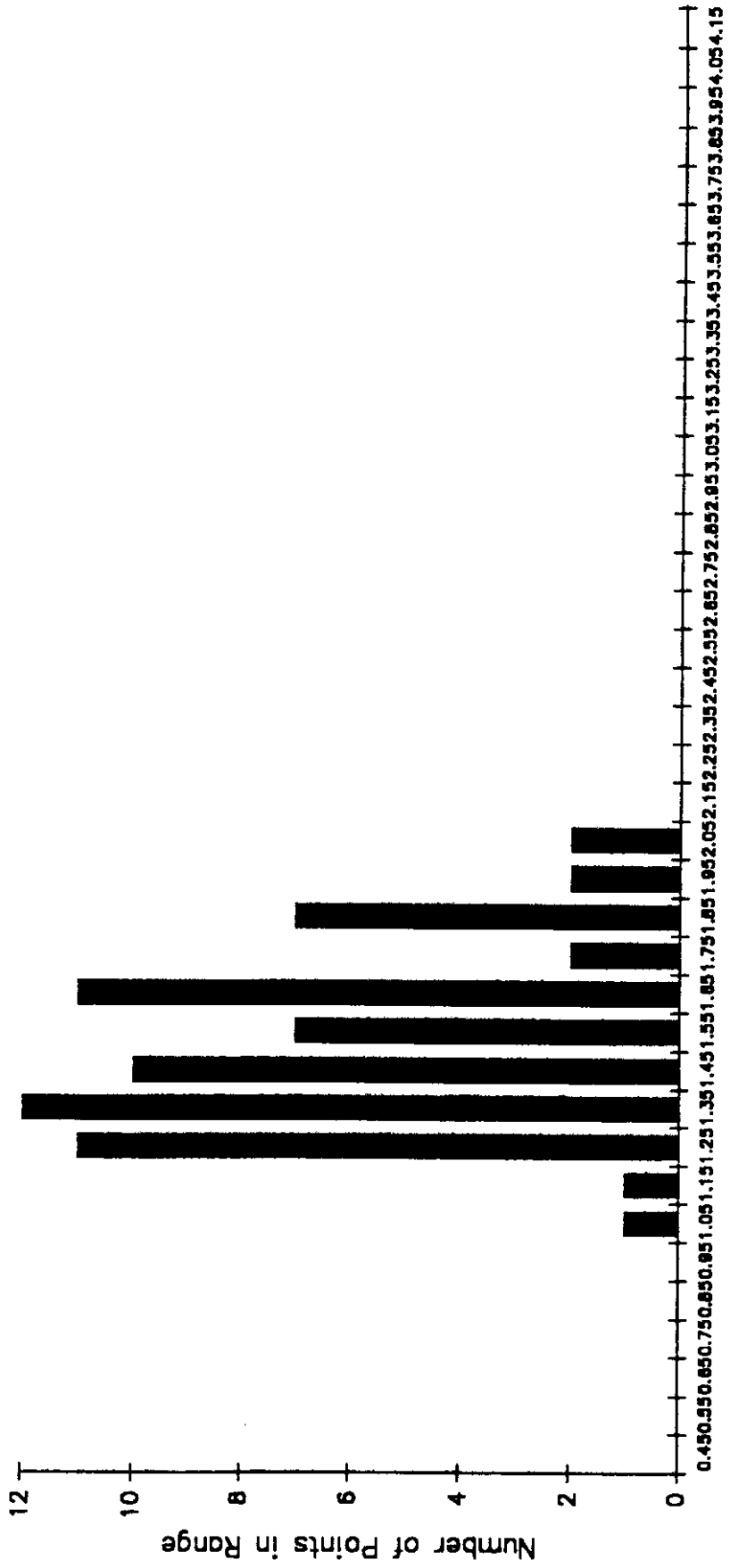
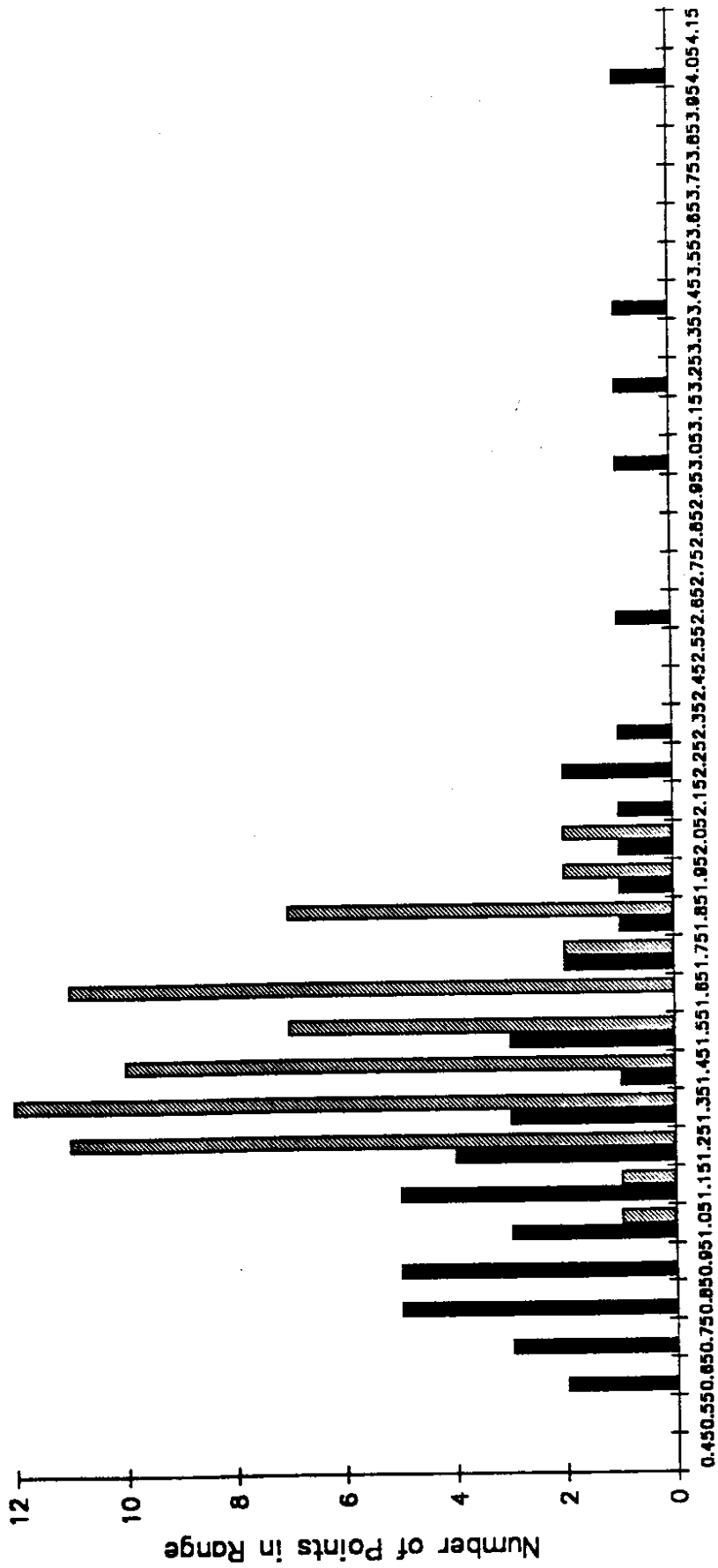


Figure 4.12 Transverse Joint Deflection to Center Slab Deflection Ratio - SR 90



Transverse Joint Deflection/Slab Center Deflection Ratio

Figure 4.13 Transverse Joint Deflection to Center Slab Deflection Ratio - All Data from SR 5 and SR 90

Note that the deflection testing at SR 5 was conducted between 11 p.m. and 4 a.m., when the temperature gradient was negative (temperature higher at the slab bottom than at the pavement surface), as illustrated in Figure 4.14. This temperature gradient would have caused a convex curvature in the slab, with the corners and joints curled up off the underlying supporting layer. This convex curvature should have resulted in higher transverse joint deflections and larger transverse joint to slab center deflection ratios, so the ratios measured at other times of the day may have been lower than those presented in Table 4.1.

There are two possible explanations for this phenomenon. The first is that large voids existed under the slab centers, resulting in high deflections, and the second is that significant in-plane compressive stresses existed. The researchers investigated the first alternative by plotting the load-deflection curves for deflections measured at the slab center. The results are presented in Table 4.3 and show that, according to the void detection process [4.23], voids did not exist under the slab centers. These results lended support to the second alternative that in-plane compressive stresses existed at this site.

If in-plane compressive stresses did exist, they would have reduced the tensile load-induced and thermal stresses occurring at the pavement edge midway between the

Table 4.3. Void Evaluation at Slab Centers — SR 5

Slab	Row 5	Void	Row 2	Void
1	1.19	no	-0.26	no
2	0.82	no	-0.36	no
3	0.50	no	-0.21	no
4	1.62	no	-0.65	no
18	0.63	no	-0.31	no
19	-0.22	no	-0.51	no
20	-0.30	no	-0.66	no
21	0.16	no	-0.56	no
25	0.10	no	-0.43	no
26	0.73	no	-0.36	no
27	-0.10	no	-0.52	no
28	0.31	no	0.78	no

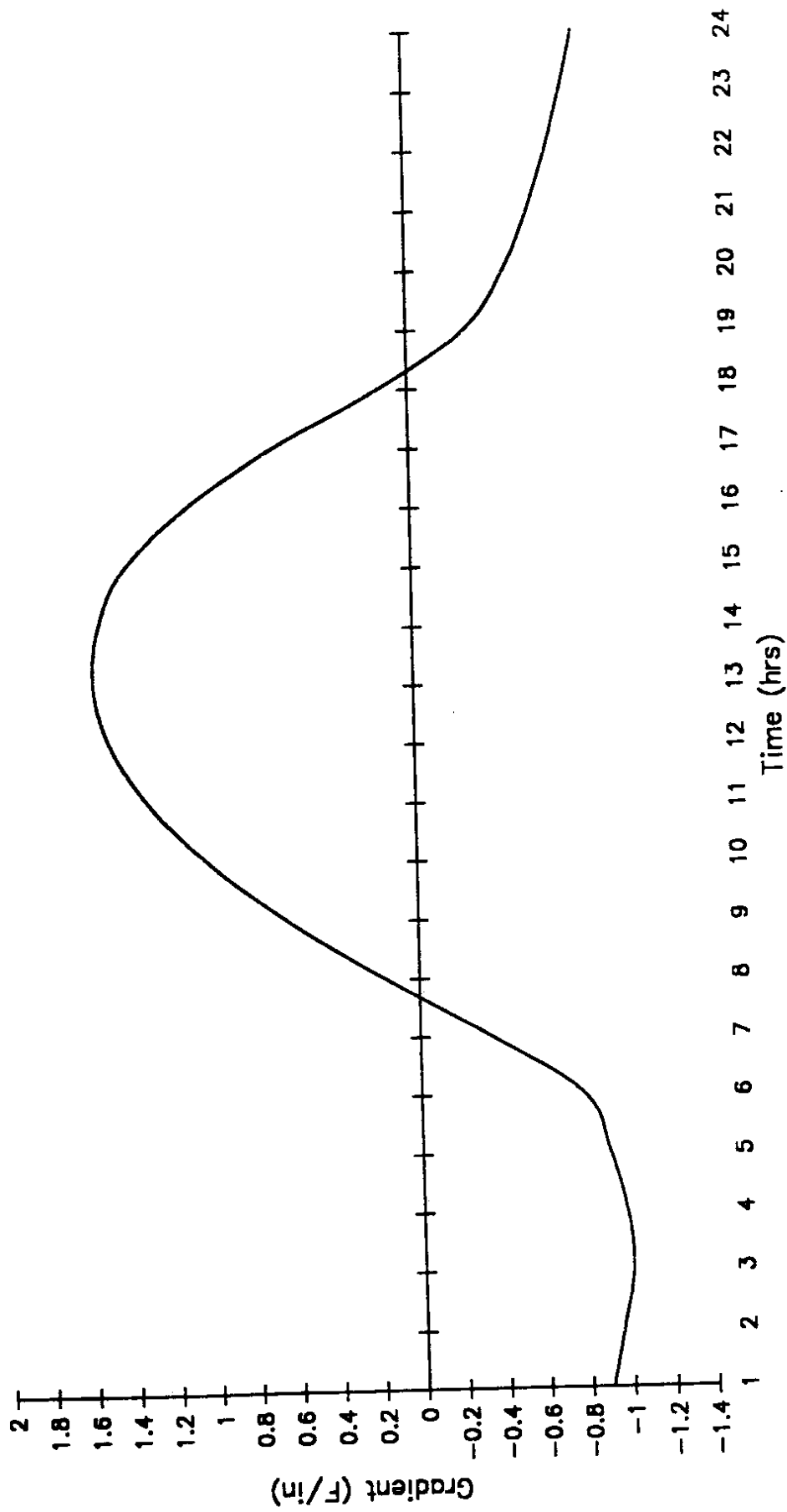


Figure 4.14 Temperature Gradient Through 9 Inch PCC Slab - SR 5

transverse joints. This reduction would have been caused by the compressive stresses being parallel to, but of opposite sign of, the load and thermal tensile stresses. In essence, the compressive stresses would have applied a prestressing along the slab length, reducing the effective tensile stress at the critical location.

To evaluate where along the pavement edge the longitudinal cracks should have occurred, and to estimate the in-plane compressive stresses necessary to make transverse joint loading critical, a fatigue damage evaluation was conducted. This evaluation was completed for a lateral traffic distribution centered 18 inches from the pavement edge, with a standard deviation of 10 inches, as illustrated in Figure 4.6. The inner wheelpath traffic distribution centerline was 102 inches from the outer slab edge (Point B on Figure 4.6). The traffic distributions were divided into 6-inch increments, as illustrated in Figure 4.15. The percentage of traffic in each 6-inch increment is indicated in the figure.

Load-induced stresses along the transverse joint were estimated with the ILLI-SLAB finite element computer program. Both wheel loads were placed on the slab, with each load equal to 9,000 pounds. The slab modulus was fixed at 4,000,000 psi, and the subgrade support value was set at 100 pci. ILLI-SLAB runs were completed for the outer wheel centered at 6, 12, 18, 24, 30, 36, 42, 48, and 54 inches from the pavement edge. Each load location was evaluated with aggregate interlock factors of 10^3 , 10^4 , 10^5 , 10^6 , and 10^8 to span all expected field load transfer efficiencies. The load transfer efficiencies corresponding to these aggregate interlock factors were 22.2, 70.3, 91.8, 95.5, and 96.1 percent, respectively.

Figure 4.16 shows the load-induced stresses along the transverse joint for the outer wheel load centered at 6, 18, 30, 42, and 54 inches from the pavement edge. These stresses were for an aggregate interlock factor of 10^5 (LTE=91.8 percent). For loads centered at 6, 18, and 30 inches, the stress under the inner wheel was greater than the stress under the outer wheel. Thus for a typical lateral traffic distribution centered at 12 or

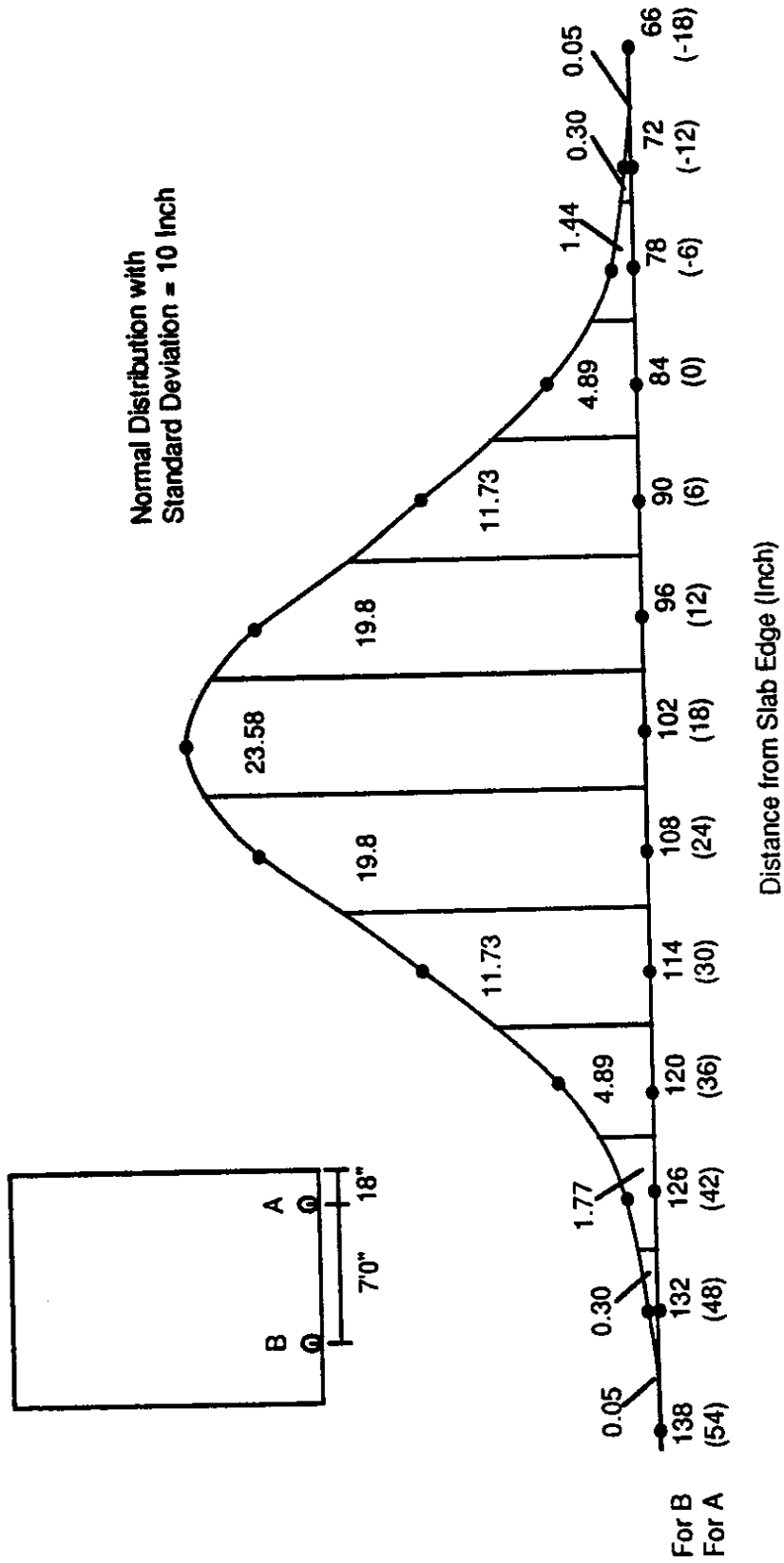


Figure 4.15 Percent Traffic in Each 6 Inch Increment

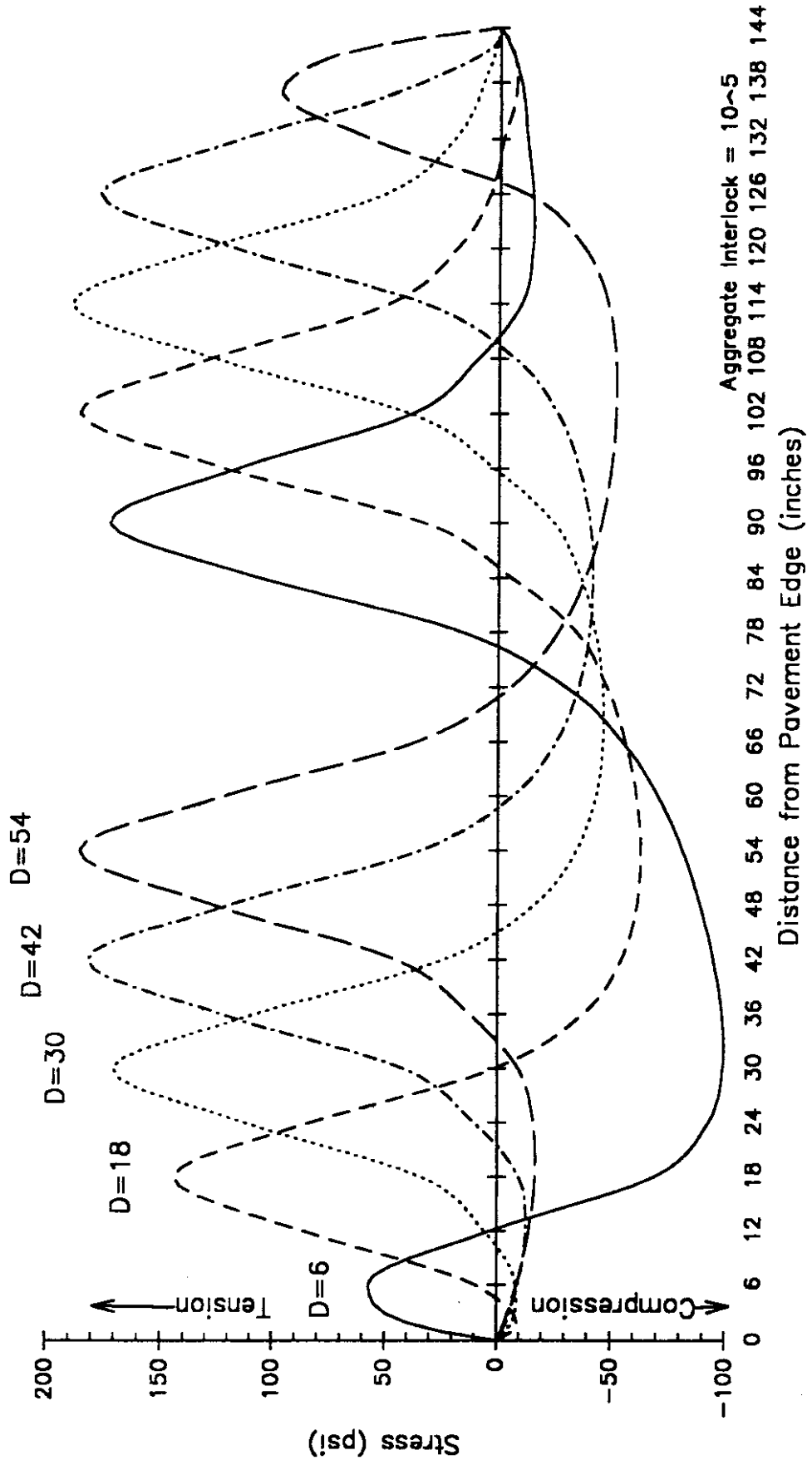


Figure 4.16 Load Stresses for Different Load Locations Along the Transverse Joint

18 inches, the load stresses under the inner wheel were higher than the load stresses under the outer wheel.

As indicated in the discussion on transverse cracking, curl stresses also contribute to fatigue damage. Figure 4.17 shows the curl stresses along the transverse joint, estimated with the typical temperature gradient developed for SR 5. As at the pavement edge, the curl stress is greatest midway along the joint. Because truck traffic is not centered on the pavement (if it were centered, the lateral traffic distribution centerline would be at 24 inches), the curl stress at the center of each traffic distribution is not the same. Figure 4.18 shows the load stress, the curl stress, and the combined stress along the transverse joint for traffic distributions centered at 18 and 102 inches. This figure clearly shows that the highest stress occurred under the inner wheel load, 102 inches from the pavement edge, and was about 80 psi higher than the stress under the outer wheel.

While the stresses were highest under the wheel loads, it was necessary to define the point along the transverse joint at which the maximum fatigue accumulated. This location would define where the longitudinal crack initiation should have occurred. To determine this location, a fatigue analysis was completed. The fatigue damage accumulated under each traffic distribution curve (centered at Points A and B) for loads applied at different locations on the transverse joint was calculated. To describe the procedure used, an example calculation will be described for loads centered at 6 inches and 90 inches.

The ILLI-SLAB computer program outputs for wheel loads centered at 6 and 90 inches were used. The stress at the center of each 6-inch interval along the transverse joint was recorded for those intervals covered by the lateral traffic distributions (0 through 54 inches for the outer wheel, and 66 through 138 inches for the inner wheel). This stress was added to the thermal stress at the middle of the 6-inch interval to obtain total stress. The combined load plus curl stress was used in a fatigue equation to calculate the allowable repetitions to failure, N_f .

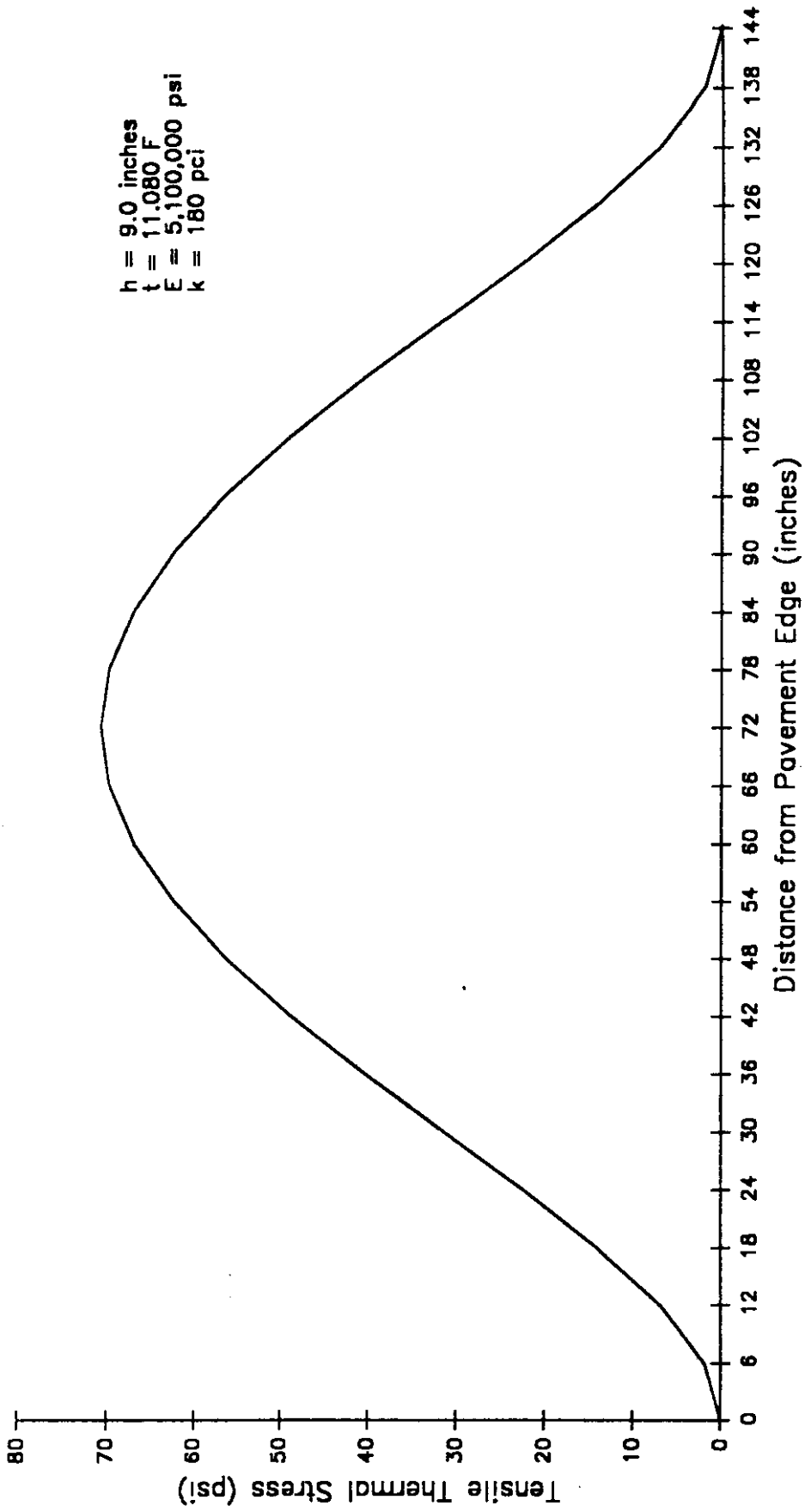


Figure 4.17 Curl Stress Along the Transverse Joint - SR 5

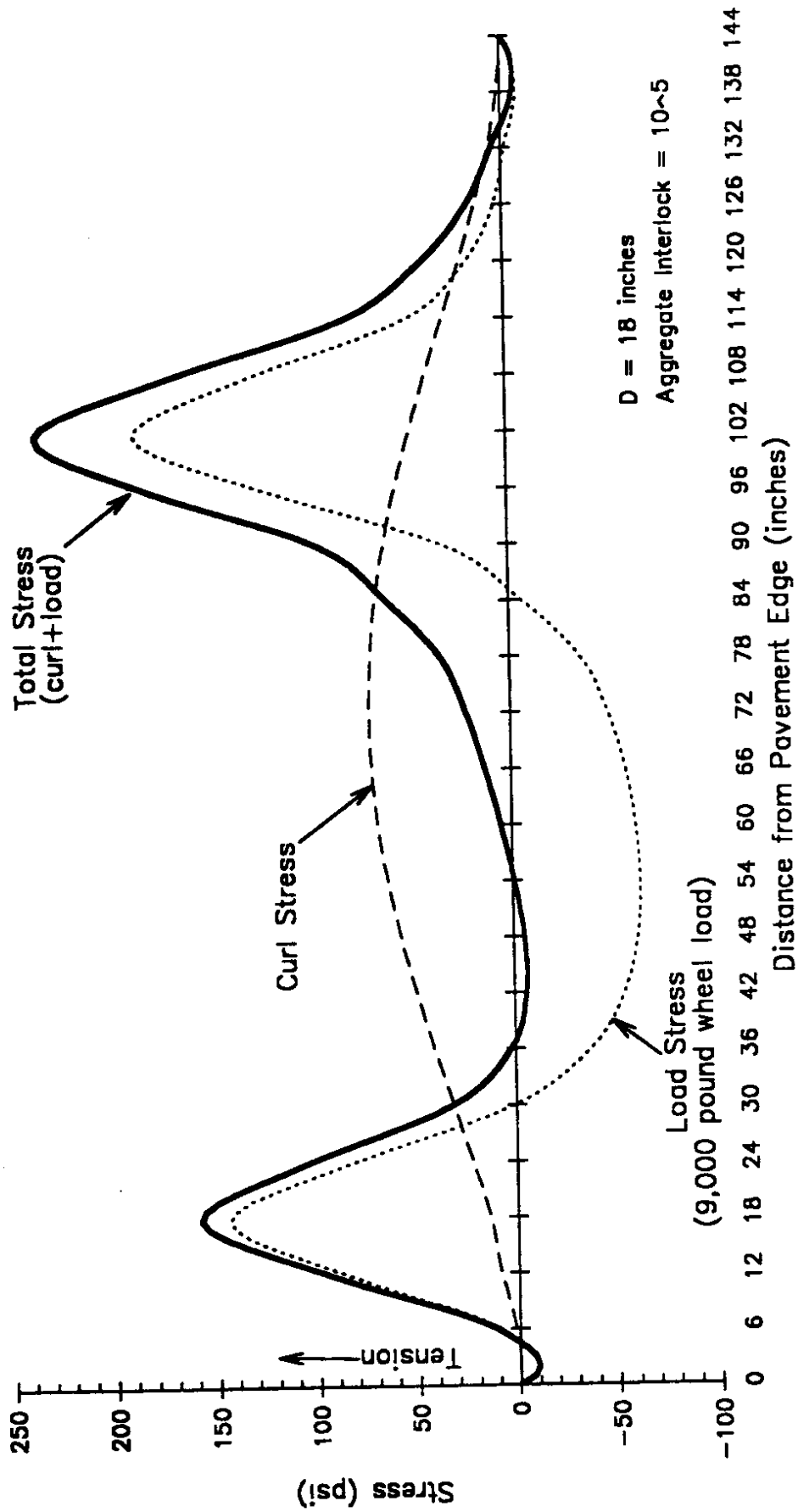


Figure 4.18 Load, Curl and Total Stress Along the Transverse Joint - SR 5

For this evaluation the total traffic was assumed to be 1,000 ESALs. The percentage of traffic in each 6-inch interval (see Figure 4.15) was multiplied by 1,000 to get the number of ESALs applied in that interval. This total was divided by N_f , calculated using the total stress in the interval, to get fatigue damage. The fatigue damage for all intervals included under each entire traffic distribution was summed using Miner's Hypothesis [4.23] to get the total accumulated fatigue under the distribution. The process described above was completed for loads moved at 6-inch intervals along the transverse joint.

The same fatigue damage evaluation was completed for all aggregate interlock values considered. The results are plotted in Figure 4.19 for aggregate interlock values of 10^8 (LTE=96.1 percent) and 10^4 (LTE=70.3 percent). The results in Figure 4.19 show that the critical fatigue location for lateral traffic distributions centered at 18 and 102 inches was under the inner wheel load 102 inches from the pavement edge. A secondary critical fatigue location existed at 30 to 36 inches from the pavement edge (its location varied between these two points as the aggregate interlock values changed). These results indicated that primary longitudinal cracking should be initiating in the middle of the inner wheelpath, with secondary cracking at 30 to 36 inches from the pavement edge. Field observations have shown that most longitudinal cracking originates in the inner wheelpath, as would be expected from the analyses conducted for this study.

The next step in the analysis was to determine the percentage of traffic that had to be applied at the traffic distribution centerline (18 and 102 inches) for each applied load location to produce the same fatigue damage as that accumulated under the entire lateral traffic distribution curve. This analysis involved calculating the number of ESALs, placed at the distribution centerline, that would result in the same fatigue damage as that accumulated under the total distribution. The load plus curl stresses at 18 and 102 inches were used in a fatigue equation to calculate allowable repetitions to failure, N_f , at that location. This N_f value was then multiplied by the accumulated fatigue damage summed

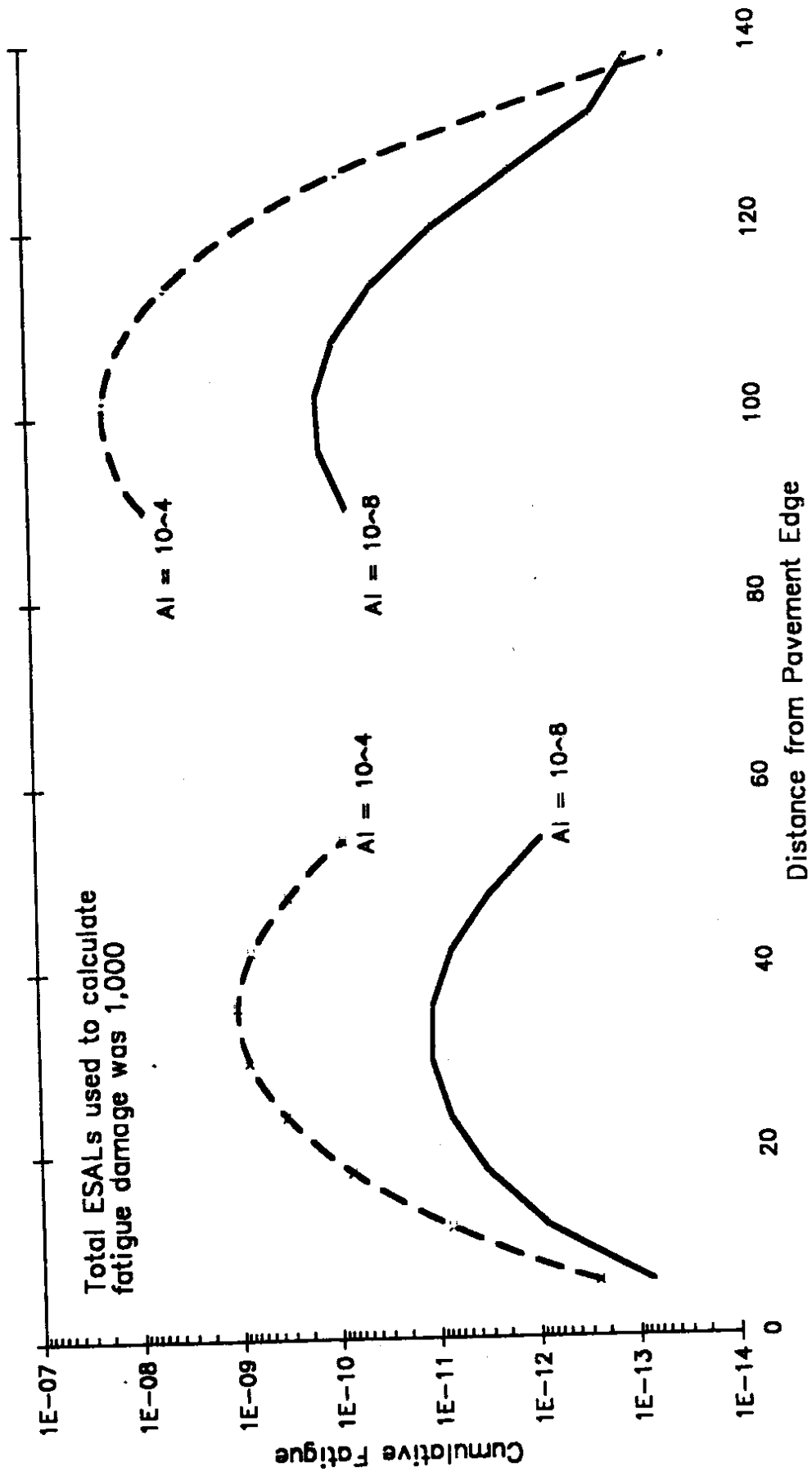


Figure 4.19 Lateral Distribution of Fatigue Damage (18,000 Pound Single Axle)

over the entire distribution to get ESALs ($n = N_f \times$ accumulated fatigue damage). The value of n was then divided by 1,000 (the total number of ESALs assumed in the evaluation) to determine the percentage of traffic that had to be applied at the traffic distribution centerlines to give the same total fatigue damage. This calculation yields essentially a pass-to-coverage ratio. The analysis results are presented in Table 4.4 and show that the maximum percentage of traffic required to produce equal fatigue occurred at 18 inches for the outer traffic distribution and at 102 inches for the inner traffic distribution. The pass-to-coverage ratios for both locations were about 26 percent. This value varied slightly as the aggregate interlock value changed. The pass-to-coverage ratios obtained suggest that when accumulated fatigue is evaluated along the transverse joint, only 26 percent of the actual traffic (ESALs) should be used in the calculation.

Table 4.4. Pass-to-Coverage Ratios Along the Transverse Joint

Load Centered At (inches)	Pass-to-Coverage Ratio				
	AI = 10 ³	AI = 10 ⁴	AI = 10 ⁵	AI = 10 ⁶	AI = 10 ⁸
<u>Point A</u>					
6	0.123	0.124	0.134	0.165	0.177
12	0.210	0.212	0.218	0.230	0.251
18	0.249	0.250	0.254	0.267	0.288
24	0.208	0.209	0.211	0.222	0.238
30	0.124	0.124	0.125	0.132	0.142
36	0.052	0.052	0.053	0.056	0.061
42	0.016	0.016	0.016	0.017	0.019
48	0.0033	0.0034	0.0034	0.0038	0.0045
54	0.0006	0.0006	0.0006	0.0007	0.0009
<u>Point B</u>					
90	0.126	0.125	0.126	0.134	0.145
96	0.208	0.208	0.210	0.225	0.235
102	0.247	0.247	0.251	0.262	0.280
108	0.208	0.209	0.213	0.225	0.245
114	0.125	0.126	0.129	0.140	0.157
120	0.054	0.054	0.056	0.063	0.076
126	0.017	0.017	0.018	0.022	0.030
132	0.004	0.004	0.005	0.009	0.016
138	0.003	0.003	0.009	0.044	0.066

The final step in the evaluation was to estimate the in-plane compressive stress required to make the transverse joint the critical loading location and longitudinal cracking the primary distress. The researchers accomplished this evaluation by calculating the total stress (load plus curl) at the critical fatigue location along the transverse joint (102 inches from the pavement edge). That stress was used to calculate allowable repetitions to failure. To calculate fatigue damage, 26 percent of the total traffic assumed in the analysis was used. This percentage of traffic was the pass-to-coverage ratio developed during this study.

The total stress for the critical fatigue location midway between the transverse joints at the pavement edge was calculated, and this stress was used to compute fatigue damage. For this latter case, 5 percent of the assumed ESALs were used (the pass-to-coverage ratio for the pavement edge critical loading location). The fatigue damage occurring at the pavement edge was greater than that occurring at the transverse joint. The stress reduction required at the pavement edge to produce the same fatigue damage as that at the transverse joint critical fatigue location was calculated.

The evaluation showed that, for an aggregate interlock value of 10^5 (LTE=91.8 percent), a 125 psi reduction in total stress at the pavement edge yielded the same fatigue damage as that calculated at the transverse joint. Therefore, the in-plane compressive stress required to make the transverse joint the critical fatigue location resulting in longitudinal cracks was about 125 psi. The required in-plane forces varied with the aggregate interlock factor. For an aggregate interlock of 10^8 (LTE=96.1 percent), in-plane forces of 180 psi were required, and for an aggregate interlock of 10^3 (LTE=22.2 percent), in-plane forces of 70 psi were required.

The conclusions drawn from these analyses are as follows:

1. the critical transverse joint fatigue location is in the inner wheel path 102 inches from the pavement edge for a lateral traffic distribution centered at 18 inches;

2. a secondary fatigue location exists at approximately 30 to 36 inches from the pavement edge;
3. the pass-to-coverage ratio, or the percentage of traffic (ESALs) to consider in a typical fatigue damage evaluation is 26 percent; and
4. the in-plane compressive forces required to make the transverse joint the critical fatigue location and longitudinal cracking the primary distress is 125 psi for an aggregate interlock of 10^5 (LTE=91.8 percent).

4.2 DISTRESS PROPAGATION RATES — CRACKING

The "generic" performance curve developed in Chapter 3.0 and reproduced in Figure 4.20 can be used to predict crack propagation rates. However, to make this evaluation process easier, the performance curve was converted to a percentage of cracking versus cumulative ESALs curve. This conversion was the result of multiplying the fatigue damage at each point used to develop the performance curve by a constant number of ESALs. For this evaluation the number of ESALs was 1,000,000. The resulting curve is shown in Figure 4.21. As the figure shows, this curve is identical in shape to the performance curve.

The curve presented in Figure 4.21 can be used to estimate the number of ESALs that will occur between two cracking levels. The following example illustrates how this can be accomplished. Assume that 20 percent of an in-service pavement's slabs have been cracked after 2,000,000 ESAL applications and that one needs to know the amount of time until 50 percent of the slabs will be cracked. The first step in estimating when 50 percent of the slabs will be cracked is to plot the point corresponding to 20 percent cracking and 2,000,000 ESALs on Figure 4.21. The procedure is illustrated in Figure 4.22.

Next, the performance curve is shifted, parallel to its current location, until it intersects the plotted point, as shown. This shifting is valid because the shape of the curve does not change. Then, the difference in ESALs between 20 percent cracking and

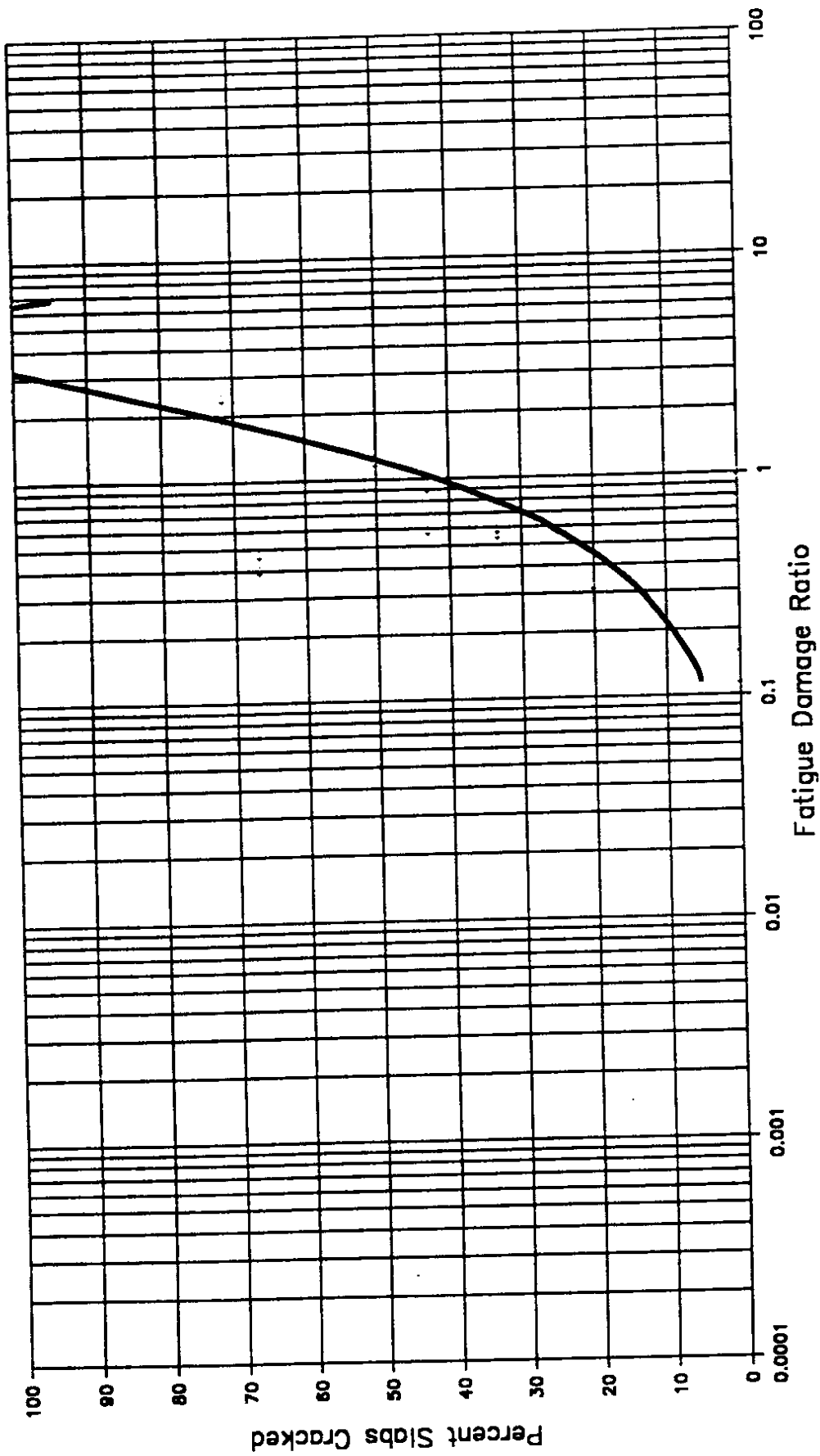


Figure 4.20 "Generic" Performance Curve

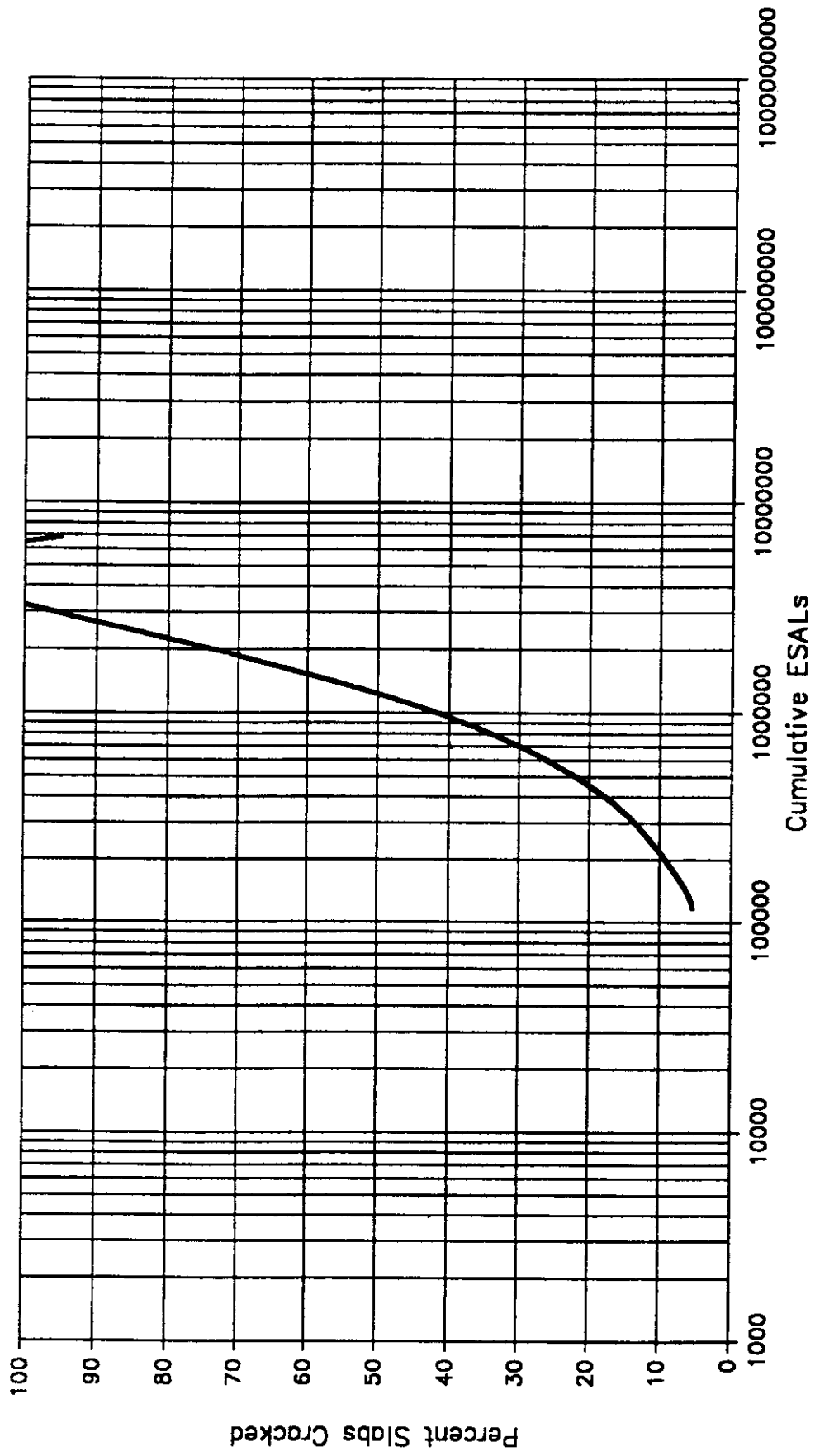


Figure 4.2.1 Percent Slabs Cracked versus Cumulative ESALs

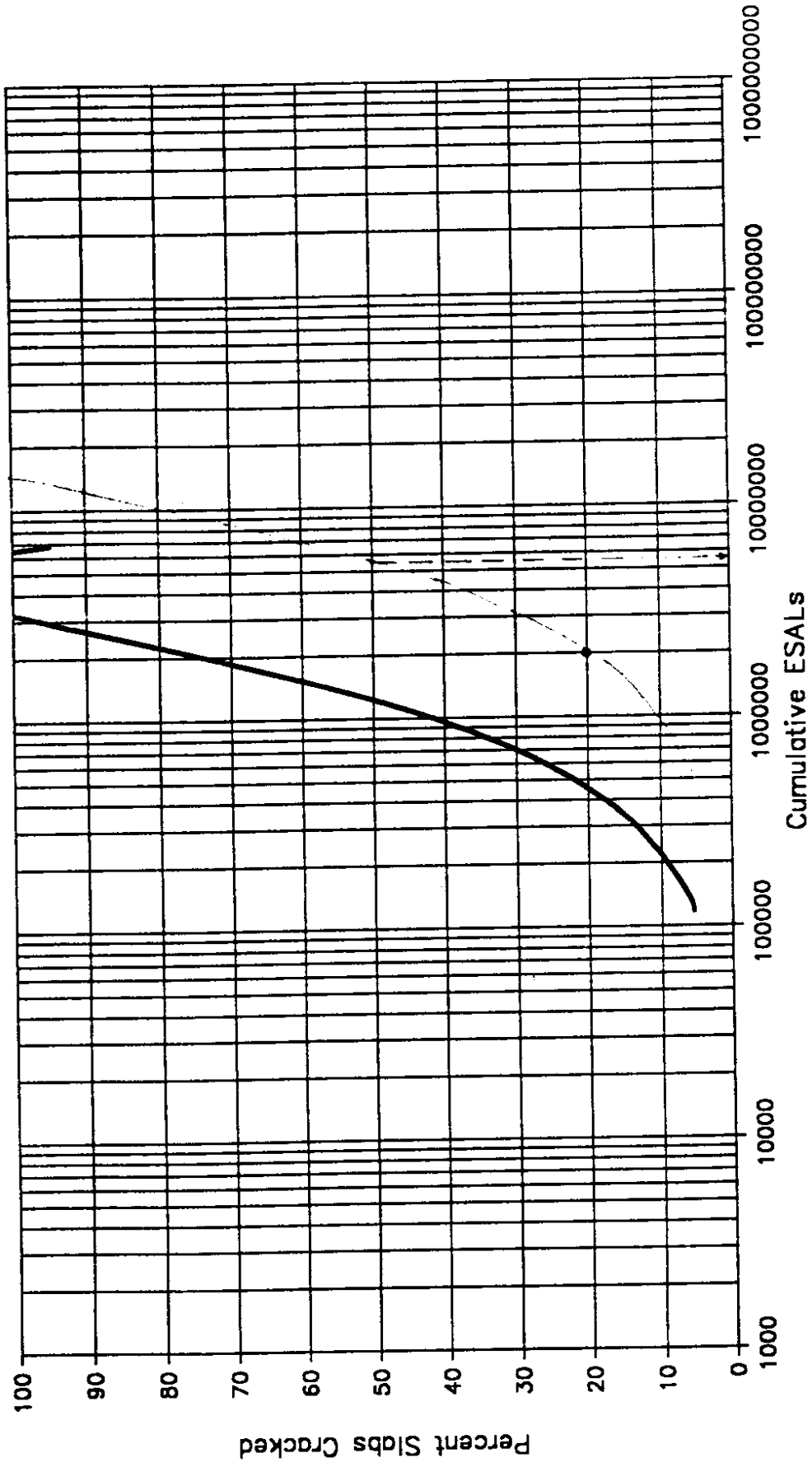


Figure 4.22 Crack Propagation Rate Example

50 percent cracking can be estimated, keeping in mind that the x-axis scale is a log scale. For this example the difference in ESALs between 20 percent cracking and 50 percent cracking is approximately 3,500,000 (5,500,000 - 2,000,000). Thus the pavement can withstand approximately 3,500,000 more ESAL applications before cracking reaches the 50 percent level. If the number of ESALs per year is known, the amount of time until 50 percent of the slabs become cracked can be estimated.

Note that the percentage of cracking versus cumulative ESAL curve presented in Figure 4.22 is only valid if truck characteristics do not change and the method of computing ESALs remains constant. If the number of ESALs per truck changes, or the method used to convert actual truck traffic to ESALs changes, this crack propagation rate estimating technique is not valid. New performance curves and a new cracking versus ESAL curve would then have to be developed.

Also note that pavement performance can be impacted by factors other than concrete fatigue, including environmental factors. Thus the curve in Figure 4.22, which was based on accumulated fatigue, does not include all factors that contribute to cracking. Therefore, pavement performance predicted by this curve may not be totally accurate. However, this is the best available method for predicting crack propagation rates and will provide general guidelines for scheduling concrete pavement rehabilitation projects. It is therefore a useful planning tool.

CHAPTER 5.0

PORTLAND CEMENT CONCRETE REHABILITATION ALTERNATIVES

Many PCC pavements in Washington have reached or are nearing the end of their design lives. These pavements will require either reconstruction or rehabilitation to ensure they continue to provide acceptable service. It is critical that proper decision-making tools are used to evaluate whether the proper course of action is reconstruction or rehabilitation. If the pavement is to be rehabilitated and not reconstructed, then the rehabilitation technique selected must repair existing deterioration and prevent future deterioration. The alternative chosen must provide the longest life for the least cost.

This chapter provides a general discussion on reconstruction and rehabilitation alternatives considered to be feasible for the concrete pavements in Washington state. The techniques discussed are

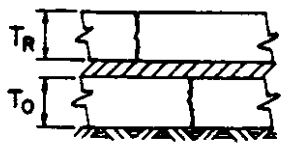
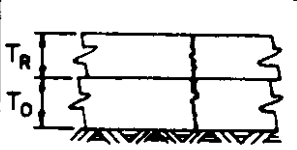
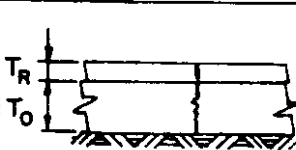
1. portland cement concrete overlays,
2. asphalt concrete overlays, and
3. reconstruction, including concrete pavement recycling.

After these alternatives have been discussed in general, the specific alternatives feasible for both SR 5 and 90 will be addressed.

5.1 PORTLAND CEMENT CONCRETE OVERLAYS

Portland cement concrete overlays are generally of three types: bonded, partially bonded, and unbonded. These overlays can be plain-jointed, reinforced, or continuously reinforced (must be unbonded). Each overlay type has its own advantages and disadvantages, which are described below. Figure 5.1 summarizes pertinent facts about these three concrete overlay types.

CONCRETE OVERLAYS ON CONCRETE PAVEMENT

TYPE OF OVERLAY		UNBONDED OR SEPARATED OVERLAY	PARTIALLY BONDED OR DIRECT OVERLAY	BONDED OR MONOLITHIC OVERLAY	
					
PROCEDURE		CLEAN SURFACE DEBRIS AND EXCESS JOINT SEAL PLACE SEPARATION COURSE-PLACE OVERLAY CONCRETE.	CLEAN SURFACE DEBRIS AND EXCESS JOINT SEAL AND REMOVE EXCESSIVE OIL AND RUBBER-PLACE OVERLAY CONCRETE	SCARIFY ALL LOOSE CONCRETE,CLEAN JOINTS,CLEAN AND ACID ETCH SURFACE-PLACE BONDING GROUT AND OVERLAY CONCRETE.	
MATCHING OF JOINTS IN OVERLAY & PAVEMENT		LOCATION } NOT NECESSARY TYPE } NOT NECESSARY	REQUIRED } NOT NECESSARY }	REQUIRED } REQUIRED }	
REFLECTION OF UNDERLYING CRACKS TO BE EXPECTED		NOT NORMALLY	USUALLY	YES	
REQUIREMENT FOR STEEL REINFORCEMENT		REQUIREMENT IS INDEPENDENT OF THE STEEL IN EXISTING PAVEMENT OR CONDITION OF EXISTING PAVEMENT.	REQUIREMENT IS INDEPENDENT OF THE STEEL IN EXISTING PAVEMENT. STEEL MAY BE USED TO CONTROL CRACKING WHICH MAY BE CAUSED BY LIMITED NON-STRUCTURAL DEFECTS IN PAVEMENT.	NORMALLY NOT USED IN THIN OVERLAYS. IN THICKER OVERLAY STEEL MAY BE USED TO SUPPLEMENT STEEL IN EXISTING PAVEMENT.	
FORMULA FOR COMPUTING THICKNESS OF OVERLAY (T_R) NOTE: T IS THE THICKNESS OF MONOLITHIC PAVEMENT REQUIRED FOR THE DESIGN LOAD ON THE EXISTING SUPPORT C IS A STRUCTURAL CONDITION FACTOR T_R SHOULD BE BASED ON THE FLEXURAL STRENGTH OF		$T_R = \sqrt{T^2 - CT_0^2}$ OVERLAY CONCRETE	$T_R = \sqrt[1.4]{T^{1.4} - CT_0^{1.4}}$ OVERLAY CONCRETE	$T_R = T - T_0$ EXISTING CONCRETE NOTE: THE ABILITY OF THE OVERLAID SLAB TO TRANSFER LOAD AT THE JOINTS SHOULD BE ASSESSED SEPARATELY	
MINIMUM THICKNESS		6"	5"	1"	
APPLICABILITY OF VARIOUS OVERLAY TYPES	STRUCTURAL CONDITION OF EXISTING PAVEMENT	NO STRUCTURAL DEFECTS $C=1.0^*$	YES	YES	YES
		LIMITED STRUCT. DEFECTS $C=0.75^*$	YES	ONLY IF DEFECTS CAN BE REPAIRED	ONLY IF DEFECTS CAN BE REPAIRED
		SEVERE STRUCT. DEFECTS $C=0.35^*$	YES	NO	NO
	SURFACE CRACKS, SCALING, SPALLING AND SHRINKING AGE CRACKS	NEGLECTIBLE	YES	YES	YES
		LIMITED	YES	YES	YES
		EXTENSIVE	YES	NO	YES

* C VALUES APPLY TO STRUCTURAL CONDITION ONLY, AND SHOULD NOT BE INFLUENCED BY SURFACE DEFECTS.

Figure 5.1. Summary of Concrete Overlay on Existing Pavements [from Reference 5.2]

5.1.1 Bonded Overlays

This overlay method involves bonding a thin concrete layer to an existing concrete pavement to form a monolithic layer. Bonded concrete overlays can be used to improve the existing pavement structural capacity and also to correct existing pavement surface deficiencies (such as studded tire wear). The minimum thickness recommended for a bonded concrete overlay is 3 inches. [5.1]

Bonded concrete overlays are most successful on concrete pavements that have not significantly deteriorated, but that require improved load carrying capacity or an improved surface condition. If the existing pavement shows significant distress, and in particular working cracks and joint faulting, repairs must be made to the existing pavement before overlay placement. Bonded concrete overlays should not be placed on existing plain-jointed concrete pavements that have working cracks measuring more than 100 lineal feet/mile unless the cracks have been repaired with full-depth patches and joints have been formed in the overlay at these patch edges. [5.3] Several excellent references are available that document concrete pavement repair methods [5.3, 5.4, 5.5, 5.6].

Working cracks in the existing pavement will rapidly reflect through the overlay and will quickly reach the severity of the underlying crack if they are not repaired. Reflection crack severity can be somewhat controlled by overlay thickness and by the use of reinforcing steel across the underlying cracks. Cracks reflect through the overlay because the layers are bonded together, and stress relief at the bond interface is not possible. Two mechanisms cause reflection cracking: horizontal movement due to slab expansion and contraction, and vertical movement due to applied traffic loads.

Bonded concrete overlays do not significantly reduce pumping or joint faulting. The overlay does not provide increased load transfer because joints in the bonded overlay are sawed completely through the overlay thickness. If the existing pavement has faulting that averages more than 0.15-inch, steps to reduce water at the slab/subbase interface must

be taken. [5.3] If not corrected by pre-overlay activities, faulting is likely to progress at the same rate it did before the overlay was placed. Note that bonded concrete overlays do reduce corner deflections, which may reduce the faulting rate slightly.

Bonded concrete overlays increase pavement life by reducing tensile edge stresses and corner deflections. [5.1, 5.7] The reduced tensile stresses result in reduced fatigue damage per load application and thus a longer pavement life. For equivalent bonded concrete and asphalt concrete overlay thickness, the edge load stresses are considerably lower with concrete overlays than with the asphalt concrete overlays. [5.3]

The cost-effectiveness of bonded concrete overlays depends on required pre-overlay repair, surface preparation techniques, required overlay thickness, traffic control measures necessary during construction, and overlay design life. A bonded overlay may not be a cost-effective alternative if more than 10 percent of the pavement area must be repaired. [5.3]

Design procedures for determining required bonded concrete overlay thicknesses are provided in references 5.7, 5.8, and 5.9.

The major advantages of bonded concrete overlays are as follows:

1. The new overlay corrects existing surface irregularities and provides increased structural life with a minimum change in surface elevation.
2. Bridge clearance problems are minimized, as are costs associated with matching other pavement surfaces (shoulders) and raising appurtenances such as guardrails.

The major disadvantages of a bonded concrete overlay are as follows:

1. A sound existing concrete pavement surface is required or existing distress will rapidly reflect through the new overlay.
2. Surface preparation is critical, and excellent quality control is required to ensure bonding. If debonding occurs the overlay will rapidly fail.

3. Joints in the existing pavement must be matched (including full-depth repair joints and longitudinal joints).

A summary of bonded concrete overlay performance can be found in References 5.3 and 5.10.

5.1.2 Partially Bonded Overlays

When concrete is placed directly on an existing concrete surface without extensive surface preparation, the result is a partially bonded overlay. Some bonding between the overlay and the underlying pavement occurs in this overlay type because no steps are taken to prevent a bond. Because some bond does occur, current design practice results in overlay thicknesses that are less than those required for an unbonded overlay. The minimum thickness for partially bonded overlays is usually between 5 and 7 inches. [5.1] As with the bonded concrete overlay, all working cracks must be eliminated.

If a partially bonded overlay is constructed, joint spacing in the overlay should be kept as short as possible, and joints in the overlay should match joints in the underlying pavement. Joint spacing should not exceed, in feet, 1.5 to 1.75 times the slab thickness, in inches. This is because of the stiff underlying concrete slab, which causes increased thermal stresses.

Questions remain regarding partially bonded overlay design reliability, and therefore partially bonded overlays are not recommended for use in rehabilitating WSDOT PCC pavements.

5.1.3 Unbonded Overlays

Unbonded concrete overlays can help to correct many existing concrete pavement deficiencies and are typically used when the existing pavement is badly deteriorated. These overlays are most often employed to improve load-carrying capacity. To prevent bonding, separation layers between the existing pavement and the overlay are required. The most common separation layer material is hot-mix asphalt concrete. This separation layer is

usually less than 2 inches thick and allows independent movement between the original slab and overlay. This independent movement results in reduced reflection cracking, which increases the overlay life expectancy and results in a more cost-effective rehabilitation alternative. Reflection cracking can occur if the separation layer is too thin or too stiff.

Unbonded concrete overlays, if properly designed, can substantially improve load-carrying capacity. This overlay behaves like a new pavement built on a very strong subbase. Thus, load-induced stresses and pavement deflections are reduced. Reduced load stresses result in longer fatigue life, and lower deflections result in less pumping, loss of support, and joint faulting.

Faulting in this overlay type is not often observed. [5.3] Faulting is controlled by highly non-erodible layers under the overlay (existing concrete and separation layer), dowels in the overlay, and mismatching overlay joints. [5.3] Joints in the overlay need not be matched to joints in the underlying pavement. In fact, the overlay joints are recommended to be offset at least 3 feet from existing transverse joints and/or working cracks. [5.3] These mismatched joints decrease pumping and minimize the impact existing faulting has on pavement performance. Mismatched joints inhibit faulting and pumping by providing improved load transfer at the overlay joints, as illustrated in Figure 5.2. [5.3] In addition, existing slab deflection is reduced by the overlay, which limits pumping, subsequent voids, and faulting.

One problem with unbonded concrete overlays is the potential for large thermal (curl) stresses to develop in the overlay. Separation layers can also have high friction factors, which can cause stresses in the overlay. Curl stress magnitude is impacted by overlay slab length, thickness, and support. The thinner the slab and the higher the subgrade support, the larger the curl stress. [5.11] Curl stresses can be controlled, in part, by using short joint spacings. Maximum joint spacing, in feet, should be no greater than 1.5 times the slab thickness, in inches. If short joint spacings are not used, the pavement should be heavily reinforced to keep cracks tight.

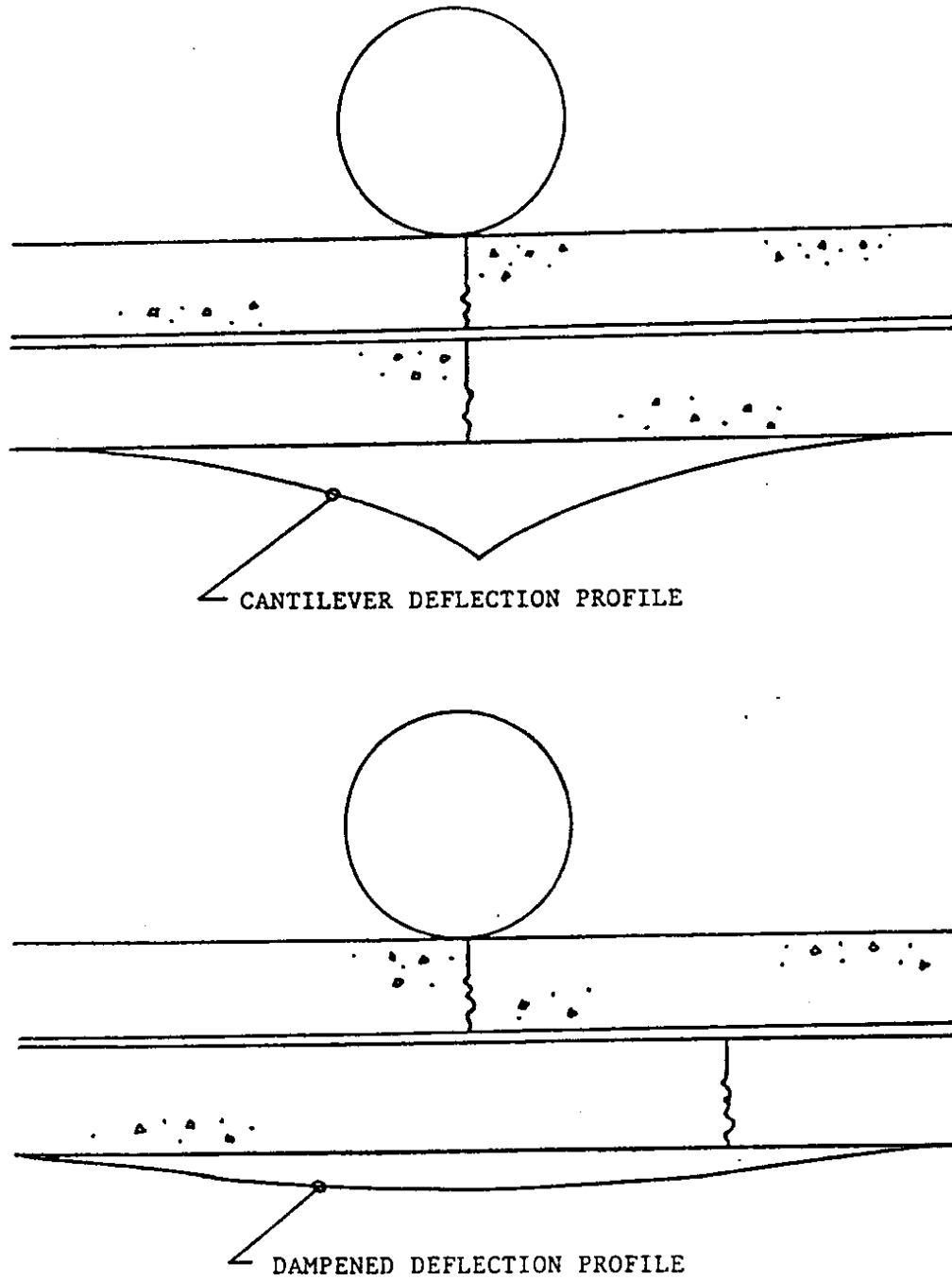


Figure 5.2. The Effectiveness of Mismatched Joints in Inhibiting the Development of Faulting and Pumping [after Reference 5.3]

Unbonded overlays can be a cost-effective rehabilitation alternative when the existing pavement is structurally deficient and badly deteriorated, overhead clearances are not critical, and matching the overlay joints with joints in the existing pavement is not economical. [5.5, 5.6] The separation material used, the required overlay thickness, and additional costs generated from increased pavement surface elevation also impact unbonded concrete overlay cost effectiveness. The additional pavement thickness needed for this overlay type requires that shoulder grades be raised, as well as many appurtenances (for example, guardrails).

Unbonded overlays are constructed with the same construction techniques as those used for new pavements. Very little pre-overlay repair is required. If the slabs in the existing pavement rock badly, crack and seating should be considered. Guidelines for pre-overlay repair are provided in Reference 5.3.

The major advantages of an unbonded concrete overlay are as follows:

1. existing pavement joints do not have to be matched in the overlay (in fact, they should not be), which simplifies construction;
2. existing pavement surface preparation is minimal; and
3. conventional construction techniques are used as are conventional design procedures.

The major disadvantages of an unbonded overlay are as follows:

1. the greatest overlay thickness is required (of the three concrete overlay types);
2. a debonding medium must be constructed; and
3. overhead clearances may be a problem.

5.2 ASPHALT CONCRETE OVERLAYS

Asphalt concrete overlays are one of the most commonly used rehabilitation techniques available and can provide additional load-carrying capacity and improve

pavement surface condition. Minimum required asphalt concrete overlay thicknesses have been established by many agencies, and these thicknesses are based on the need to level the pavement surface, prevent debonding, and retard reflection cracking. Asphalt concrete overlays intended to improve structural load-carrying capacity must be at least 2.5 inches thick. [5.7] WSDOT has typically used 0.3-foot (3.6 inches) to 0.35 foot (4.2 inches) asphalt concrete overlays over existing concrete pavements. [5.12] Experience in other states has shown that asphalt concrete overlays less than 3 inches thick often develop potholes because the overlay debonds.

Perhaps the major benefit provided by asphalt concrete overlays is a reduction in curl stress in the concrete pavement. In a study conducted for South Carolina, Dempsey found that a 6-inch asphalt concrete overlay reduced the thermal gradient through the concrete pavement by about 66 percent. This reduction in gradient results in a significant decrease in curl stress. Reduced curl stress means that the concrete fatigue life is increased, resulting in a longer pavement life.

Two primary problems that normally occur in asphalt concrete overlays over PCC pavements are rutting and reflection cracking. As overlay thickness increases, the rutting problem increases and the reflection cracking problem decreases. Ultimately, the rutting problem must be controlled through proper mix designs. Attempts to control reflection cracking have included completing pre-overlay repairs to the concrete pavement, using stress-relieving interlayers, using crack-arresting interlayers, and using fabrics. [5.7] These techniques are discussed in this section.

The major advantages of asphalt concrete overlays over concrete pavements are as follows:

1. curl stresses are substantially reduced, resulting in longer concrete fatigue life; and
2. this alternative probably entails the shortest construction duration, least disruption to traffic during construction, and the lowest initial cost.

The major disadvantages are as follows:

1. there is strong potential for rutting to occur in the asphalt concrete overlay;
2. studded tire wear in the asphalt concrete is much greater than for portland cement concrete pavements; and
3. the average expected design life is about 12 years (based on WSDOT experience) and rehabilitation is sometimes required sooner than 12 years to correct surface rutting and raveling problems.

5.2.1 Pre-Overlay Repair

Pre-overlay repairs conducted before an asphalt concrete overlay has been placed include pressure grouting, cracking and seating the concrete, and retro-fitting load transfer devices. Each technique is discussed below.

5.2.1.1 Pressure Grouting. Pressure grouting restores support under a concrete slab or subbase where pumping of fines has created a small void. The resulting loss of support causes large deflections and increased slab stresses, which lead to joint faulting, corner breaks, and finally complete slab break-up. [5.6] Pressure grouting is performed to fill the voids, thereby stabilizing the concrete slab. When the voids have been filled, deflections are reduced and the structural integrity of the slab is restored. This benefit will likely diminish over time, at which point additional pressure grouting or other rehabilitation may be required. [5.4] Note that pressure grouting does not correct depressions, increase structural capacity, or eliminate faulting. If these voids are not filled before an asphalt concrete overlay has been placed, rapid reflection cracking and overlay deterioration will occur.

Pressure grouting involves pumping grout material under the slab. Research conducted in NCHRP Project 1-21 [5.6] and verified in other studies has shown that pressure grouting should only be performed at joints or cracks where loss of support can be demonstrated, usually using nondestructive deflection testing results. If a joint or crack

exhibits low deflections and is pressure grouted, the deflections will remain the same or, more likely, will increase. The grouting will usually raise the slab, causing a loss of uniform support. Pumping too much grout under the slab, even when voids exist, can cause slabs to crack because of uneven support. Thus, the pressure grouting operation requires adequate quality control to ensure that pavement is not damaged.

5.2.1.2 Crack and Seat. The Federal Highway Administration Rehabilitation Manual states that

The intent of pavement cracking and seating is to create concrete pieces that are small enough to reduce horizontal slab movement to a point where thermal stresses which contribute to reflective cracking will be greatly reduced, yet still large enough and still have some aggregate interlock between pieces so that the majority of the original structural strength of PCC pavement is retained. Seating of the broken slabs after cracking is intended to reestablish support between the subbase and the slab where voids may have existed. [5.4]

Current practice is generally to crack the concrete pavement into 2- to 3-foot long pieces and place a 3- to 5-inch thick asphalt concrete overlay on the cracked pavement surface. Cracking and seating is a viable alternative for concrete pavements constructed on strong subgrades. It is critical that through-slab cracking is achieved during the cracking/breaking process. If through-cracking is not achieved, reflection cracking is likely to occur rapidly.

Several studies have been conducted to evaluate the field performance of crack and seat projects. [5.13, 5.14, 5.15] These study results are summarized in NCHRP Synthesis Number 144, "Breaking/Cracking and Seating Concrete Pavements." Most studies have found that cracking and seating reduces or at least delays reflection cracking, thereby extending service life and resulting in a more cost-effective rehabilitation alternative.

Cracking and seating can be a cost-effective rehabilitation alternative. However, there are many unknowns in completing crack and seat projects. The NCHRP Synthesis indicated that at present there are no guidelines for quantifying how much cracking/breaking is achieved during construction, and no procedure is currently available

to evaluate the impact slab segment geometry has on overall pavement performance. In addition, no appropriate method for evaluating the cracked slab structural capacity is available, nor is a mechanistic design procedure for the asphalt concrete overlay.

Even with the lack of formal evaluation techniques and design procedures, cracking and seating should be considered a viable alternative for rehabilitating concrete pavements. Caltrans has used this rehabilitation technique extensively on its Interstate PCC pavement with good initial success (refer to Appendix I, Paragraph I.3.4).

5.2.1.3 Load Transfer Devices. Load transfer devices can be retro-fitted into concrete pavements to control differential joint and crack movement. Load transfer restoration has been recommended for faulted transverse joints or cracks that show poor load transfer efficiency (0 to 50 percent) in cool weather. It has also been recommended if an asphalt concrete overlay is to be placed over a concrete pavement in which joints and cracks have faulted or have otherwise exhibited poor load transfer efficiency. This repair method retards reflection cracking incidence and severity, spalling, and overlay deterioration. [5.7] If load transfer has not been established and the asphalt concrete overlay is placed, reflection cracking can rapidly occur in the overlay, resulting in premature failure (depends on the AC overlay thickness as well).

Two methods have been used to restore load transfer: shear devices and dowels. [5.16] Reference 5.16 provides a detailed description of each device and its field performance to date. Dowel installation was evaluated under an FHWA contract in Georgia and in a study at the University of Illinois. Results showed that dowels have performed well even after nine years of traffic.

5.2.2 Stress-Relieving Interlayers

Reflection cracking is caused by joint or crack movement in the underlying concrete pavement. These movements are caused by low temperatures, daily temperature cycles, and traffic loads. Stress-relieving interlayers are primarily used to minimize required

overlay thickness and to retard reflection cracking. The layers are "soft" and constructed to dissipate stresses developed during joint or crack movement. These interlayers are generally a rubber or polymer-modified asphalt and are constructed directly on the concrete surface.

The results from several analytical studies have shown that an asphalt-rubber interlayer effectively reduces stresses at the existing pavement/asphalt concrete overlay interface. [5.17] However, the field study results have been mixed. The Minnesota Department of Transportation has constructed several projects to study asphalt-rubber interlayer performance. [5.18] One project showed that a 4-inch overlay with normal asphalt concrete exhibited significantly less reflection cracking than a 3-inch overlay with an asphalt-rubber interlayer. In contrast, a study conducted for the Federal Highway Administration [5.19] found that "the asphalt-rubber when placed as a seal coat (SAM) will control reflection of fatigue cracks and is an [alternative] to a major overlay. When placed as a SAMI, it will effectively control reflection of all cracks." [5.17]

Stress-relieving interlayers have performed well in some instances and have performed poorly in others. Caution must be exercised when these layers are used to prevent reflection cracking.

5.2.3 Crack-Arresting Interlayers

Crack-arresting layers are granular layers that are placed on the existing concrete before the asphalt concrete overlay has been placed. These layers retard reflection cracking by providing large void spaces that effectively blunt the crack propagation. [5.7] These interlayers have performed well when properly installed. However, if they are improperly constructed, instability often results in the asphalt concrete mix, and rutting occurs.

5.2.4 Fabrics

Synthetic fabrics act as a reinforcing layer in the asphalt concrete overlay. Fabric interlayers are used to retard reflection cracking and to waterproof the pavement structure.

Fabrics in overlays physically restrain movement in the overlay as the cracks and joints in the underlying pavement open. This physical restraint presumably minimizes reflection cracking. To ensure that physical restraint occurs, fabrics should be placed in the overlay, not at the concrete surface. [5.20, 5.21] Fabrics have had mixed success in retarding reflection cracking and in some instances have worsened overlay performance.

5.2.5 Performance of Asphalt Concrete Projects in Washington State

The PCC rehabilitation projects for which performance data exist in the state of Washington are limited to AC overlays with fabric interlayers or asphalt-rubber interlayers, and AC overlays with no pre-rehabilitation treatment (there was no inclusion of a stress-relieving interlayer or a surface treatment). (The AC overlays were WSDOT Class B gradation (5/8 inch top size) with AR 4000 binder.) A survey conducted on the current surface course rehabilitation projects (Table 5.1) found that the average expected performance (when the PCR is equal to 50, determined using the WSDOT Pavement Management System) of an AC overlay with fabric interlayer is 19.3 years, with a standard deviation of 3.5 years; the average expected performance of an AC overlay with asphalt-rubber interlayer is 14.8 years, with a standard deviation of 0.8 year; and that of an AC overlay with no pre-rehabilitation treatment is 14.3 years, with a standard deviation of 3.7 years (however, the calculated PCR is based only on alligator, longitudinal, transverse cracking and patching and not rutting). The corresponding AC overlay thickness for these three strategies ranged from 3.6 inches to 4.8 inches over the fabric interlayer (northbound average thickness = 4.2 inches and standard deviation = 0.5 inch for 18 projects; southbound average thickness = 4.2 inches and standard deviation = 0.5 inch for 16 projects), 1.8 inches to 4.8 inches for the asphalt-rubber interlayer (northbound average thickness = 3.9 inches and standard deviation = 1.4 inches for 4 projects; southbound average thickness = 4.4 inches and standard deviation = 0.6 inch for 8 projects), and from 0.7 inch to 9.6 inches for the AC overlay with no pre-rehabilitation treatment (northbound

Table 5.1a. Performance of AC Overlays on

Mileposts	AC Overlay Surface Course			Layer 2			Layer 3			Co
	Year Constructed	Type	Thickness (ft)	Year Constructed	Type	Thickness (ft)	Year Constructed	Type	Thickness (ft)	
7.53 - 7.64	1984	SAMI	0.15	1962	PCCP	0.75				
7.67 - 7.91	1981	ACP	0.15	1969	ACP	0.33	1962	PCCP	0.75	
7.91 - 9.51	1981	ACP	0.15	1969	ACP	0.33	1955	PCCP	0.75	
9.53 - 14.58	1981	ACP	0.15	1969	ACP	0.33	1955	PCCP	0.75	
14.58 - 17.04	1981	ACP	0.15	1970	ACP	0.15	1956	PCCP	0.75	
17.04 - 17.34	1981	ACP	0.15	1970	ACP	0.67	1956	PCCP	0.75	
17.34 - 18.18	1981	ACP	0.15	1970	ACP	0.15	1956	PCCP	0.75	
18.41 - 18.73	1981	ACP	0.15	1970	ACP	0.15	1956	PCCP	0.75	
18.73 - 19.50	1981	ACP	0.15	1970	ACP	0.35	1956	PCCP	0.75	
20.11 - 20.78	1984	SAMI	0.40	1970	PCCP	0.75				
20.85 - 22.12	1984	SAMI	0.40	1964	PCCP	0.75				
33.20 - 33.41	1974	ACP	0.15	1973	ACP	0.80				
33.41 - 33.46	1974	ACP	0.60	1952	PCCP	0.75	1952	PCCP	0.75	
33.46 - 34.75	1974	ACP	0.80	1952	PCCP	0.75				
37.23 - 37.45	1977	FABRIC	0.35	1971	ACP	0.15	1952	PCCP	0.75	
37.45 - 38.08	1981	ACP	0.35	1977	SAMI	0.35	1971	ACP	0.35	
52.90 - 56.80	1981	ACP	0.15	1970	ACP	0.60	1953	PCCP	0.75	
56.80 - 57.13	1977	FABRIC	0.40	1953	PCCP	0.75				
57.13 - 57.84	1977	FABRIC	0.40	1953	PCCP	0.75				
57.84 - 59.06	1977	FABRIC	0.40	1956	PCCP	0.75				
59.20 - 59.41	1978	FABRIC	0.30	1956	PCCP	0.75				
59.72 - 60.86	1981	ACP	0.30	1956	PCCP	0.75				
60.86 - 60.89	1981	ACP	0.30	1978	FABRIC	0.30				
60.89 - 61.31	1981	ACP	0.30	1956	PCCP	0.75	1956	PCCP	0.75	
61.35 - 63.49	1981	ACP	0.30	1977	FABRIC	0.35				
63.49 - 64.84	1977	FABRIC	0.40	1956	PCCP	0.75	1956	PCCP	0.75	
64.84 - 68.12	1981	ACP	0.30	1956	PCCP	0.75				
68.12 - 68.93	1984	SAMI	0.34	1981	ACP	0.30				
68.93 - 69.34	1981	ACP	0.30	1956	PCCP	0.75	1956	PCCP	0.75	
69.34 - 69.39	1981	ACP	0.30	1978	FABRIC	0.30				
69.39 - 72.29	1978	FABRIC	0.30	1956	PCCP	0.75	1956	PCCP	0.75	
72.29 - 73.28	1990	ACP	0.18	1976	ACP	0.40				
73.28 - 73.92	1979	FABRIC	0.30	1956	PCCP	0.75	1956	PCCP	0.75	
73.92 - 74.01	1979	FABRIC	0.30	1968	ACP	0.09				
74.01 - 76.04	1979	FABRIC	0.30	1956	PCCP	0.75	1956	PCCP	0.75	
76.04 - 76.36	1979	FABRIC	0.40	1956	PCCP	0.75				
76.36 - 77.14	1979	FABRIC	0.30	1956	PCCP	0.75				
77.23 - 77.42	1979	FABRIC	0.40	1956	PCCP	0.75				
77.42 - 77.55	1979	FABRIC	0.30	1956	PCCP	0.75				
77.55 - 78.35	1981	ACP	0.30	1956	PCCP	0.75				
78.35 - 78.38	1984	ACP	0.35	1981	ACP	0.30	1956	PCCP	0.75	
78.38 - 78.44	1984	ACP	0.35	1973	ACP	0.35	1956	PCCP	0.75	
78.44 - 79.07	1990	ACP	0.18	1973	ACP	0.35	1956	PCCP	0.75	
79.07 - 79.09	1973	ACP	0.35	1956	PCCP	0.75				
79.09 - 79.19	1990	ACP	0.18	1973	ACP	0.35				
83.04 - 83.23	1990	ACP	0.18	1973	ACP	0.15	1956	PCCP	0.75	
83.23 - 83.28	1990	ACP	0.33	1990	Grind	0.15	1956	PCCP	0.75	
83.35 - 83.36	1976	FABRIC	0.35	1956	PCCP	0.75	1973	ACP	0.15	
83.36 - 83.70	1982	ACP	0.06	1976	FABRIC	0.35				
83.70 - 84.91	1976	FABRIC	0.35	1956	PCCP	0.75	1956	PCCP	0.75	
84.91 - 85.16	1982	ACP	0.06	1976	FABRIC	0.35				
85.16 - 85.51	1976	FABRIC	0.35	1956	PCCP	0.75	1956	PCCP	0.75	
85.51 - 87.96	1976	FABRIC	0.35	1956	PCCP	0.75				

¹ PCR based on WSPMS deduct values (distress types of alligator cracking, longitudinal cracking, transverse cracking and patching).

² A=Alligator Cracking
 L=Longitudinal Cracking
 T=Transverse Cracking
 R=Rutting
 P=Patchings

³ Deepest rut (both wheelpaths measured).

District 4 PCCP — SR 5 Northbound

Layer 4			Performance							
Year Constructed	Type	Thickness (ft)	Traffic (1989)		1990		Distress Types ²	Rutting ³		Predicted Life ¹ to PCR = 50
			ADT	% Trk	AGE	PCR ¹		Depth (in)	No. Measurements	
1952	PCCP	0.75	27469	7.8	6	99	None	—	—	13 (1997)
			27469	7.8	9	99	None	—	—	16 (1997)
			27469	7.8	9	99	None	—	—	16 (1997)
			41888	7.3	9	92	R	—	—	14 (1995)
			43263	10.5	9	91	R/T	—	—	14 (1995)
			41100	10.8	9	100	R	—	—	17 (1998)
			40016	11.0	9	99	R	—	—	16 (1997)
			40016	11.0	9	99	R	—	—	16 (1997)
			40016	11.0	9	98	R	—	—	15 (1996)
			40016	11.0	6	99	R	—	—	15 (1999)
			38026	11.2	6	99	None	—	—	15 (1999)
			43271	10.5	16	59	R/P/L	0.75	3	16 (1990)
			43271	10.5	16	59	R/P/L	0.75	1	17 (1991)
			43271	10.5	16	82	R/P/L	0.63	5	20 (1994)
			40413	13.5	13	69	R/P	—	—	14 (1991)
			37529	17.1	9	73	R/P	—	—	12 (1993)
			24649	16.5	9	89	R/T	0.43	11	13 (1994)
			24583	16.5	13	99	R	0.69	4	22 (1999)
			26446	15.9	13	100	R	0.61	7	23 (2000)
			28455	15.3	13	100	R	0.74	7	23 (2000)
			28520	15.3	12	100	R	—	—	22 (2000)
			26138	15.4	9	99	R	0.53	8	18 (1999)
			25981	15.6	9	99	R	—	—	18 (1999)
			25761	15.8	9	99	R	0.57	4	18 (1999)
			25028	16.3	9	99	R	0.61	21	18 (1999)
			23143	15.5	13	100	R	0.74	13	23 (2000)
			22733	15.3	9	100	R	—	—	19 (2000)
			26526	13.3	6	100	R	—	—	16 (2000)
			30317	11.9	9	100	R	—	—	19 (2000)
			30411	11.8	9	100	R	—	—	19 (2000)
			30496	12.0	12	83	R/T	0.84	16	16 (1994)
			31807	12.0	14	-5	R/A/T/L	—	—	11 (2001)
			33064	11.6	11	70	R/A/T/L	—	—	14 (1993)
33064	11.6	11	96	R/L	—	—	19 (1998)			
33064	11.6	11	99	R	—	—	20 (1999)			
33317	11.6	11	99	R	—	—	20 (1999)			
34910	11.6	11	99	R	—	—	20 (1999)			
36264	11.5	11	98	R	—	—	19 (1998)			
36264	11.5	11	98	R	—	—	19 (1998)			
39423	11.8	9	99	R	—	—	18 (1999)			
39764	11.8	6	99	R	—	—	15 (1999)			
38066	11.8	6	99	R	—	—	15 (1999)			
39650	11.6	17	79	R/T	—	—	11 (2001)			
40248	11.6	17	79	R/T	—	—	21 (1994)			
40734	11.5	17	79	R/T	—	—	11 (2001)			
36225	10.5	17	84	R/T	—	—	11 (2001)			
37331	10.6	17	84	R/T	—	—	13 (2003)			
38770	10.8	14	85	R/T	—	—	19 (1995)			
38770	10.8	8	85	R/T	—	—	11 (1993)			
38770	10.8	14	86	R/T	—	—	19 (1995)			
38770	10.8	8	89	R/T	—	—	11 (1993)			
38770	10.8	14	89	R/T	—	—	19 (1995)			
38770	10.8	14	98	R	—	—	23 (1999)			

Table 5.1b. Performance of AC Overlays

Mileposts	AC Overlay Surface Course			Layer 2			Layer 3			
	Year Constructed	Type	Thickness (ft)	Year Constructed	Type	Thickness (ft)	Year Constructed	Type	Thickness (ft)	
7.54	7.61	1984	SAMI	0.40	1962	PCCP	0.75			
7.91	7.98	1984	SAMI	0.40	1969	PCCP	0.75			
20.78	20.91	1984	SAMI	0.40	1970	ACP	0.58	1942	PCCP	0.58
20.91	21.39	1984	SAMI	0.40	1964	PCCP	0.75			
21.39	21.88	1984	SAMI	0.40	1947	PCCP	0.75			
36.30	36.85	1977	FABRIC	0.35	1971	ACP	0.15	1952	PCCP	0.75
37.11	37.27	1977	FABRIC	0.35	1971	ACP	0.15	1952	PCCP	0.75
42.67	43.36	1976	ACP	0.35	1971	ACP	0.15	1954	PCCP	0.75
43.36	43.39	1985	ACP	0.15	1976	ACP	0.35	1971	ACP	0.15
44.72	44.82	1985	SAMI	0.29	1976	PCCP	0.75			
44.82	44.93	1985	ACP	0.25	1976	PCCP	0.75			
44.93	45.44	1985	SAMI	0.29	1976	PCCP	0.75			
50.40	50.88	1976	ACP	0.75	1971	ACP	0.15	1952	PCCP	0.75
52.92	56.80	1981	ACP	0.15	1970	ACP	0.60	1953	PCCP	0.75
56.80	57.13	1977	FABRIC	0.40	1953	PCCP	0.75			
57.13	57.84	1977	FABRIC	0.40	1953	PCCP	0.75			
57.84	59.06	1977	FABRIC	0.40	1956	PCCP	0.75			
59.20	61.31	1981	ACP	0.30	1956	PCCP	0.75			
61.35	68.12	1981	ACP	0.30	1956	PCCP	0.75			
68.12	68.93	1984	SAMI	0.34	1981	ACP	0.30	1956	PCCP	0.75
68.93	68.96	1981	ACP	0.30	1956	PCCP	0.75			
68.96	69.34	1985	ACP	0.06	1981	ACP	0.30	1956	PCCP	0.75
69.34	69.39	1985	ACP	0.06	1981	ACP	0.30	1978	FABRIC	0.30
69.39	70.61	1985	ACP	0.06	1978	FABRIC	0.30	1956	PCCP	0.75
70.61	72.29	1978	FABRIC	0.30	1956	PCCP	0.75			
72.29	73.28	1990	ACP	0.18	1976	FABRIC	0.40	1956	PCCP	0.75
73.28	73.82	1979	FABRIC	0.30	1956	PCCP	0.75			
73.82	73.90	1979	FABRIC	0.30	1968	ACP	0.09	1956	PCCP	0.75
73.90	76.04	1979	FABRIC	0.30	1956	PCCP	0.75			
76.04	76.36	1979	FABRIC	0.40	1956	PCCP	0.75			
76.36	77.14	1979	FABRIC	0.30	1956	PCCP	0.75			
77.23	77.42	1979	FABRIC	0.40	1956	PCCP	0.75			
77.42	77.55	1979	FABRIC	0.30	1956	PCCP	0.75			
77.55	78.35	1981	ACP	0.30	1956	PCCP	0.75			
78.35	78.38	1984	ACP	0.35	1981	ACP	0.30	1956	PCCP	0.75
78.38	78.44	1984	ACP	0.35	1981	ACP	0.30	1956	PCCP	0.75
78.44	79.07	1990	ACP	0.18	1973	ACP	0.35	1956	PCCP	0.75
79.07	79.09	1990	ACP	0.15	1973	ACP	0.35	1956	PCCP	0.75
79.09	79.19	1990	ACP	0.18	1973	ACP	0.35	1956	PCCP	0.75
83.04	83.25	1990	ACP	0.18	1973	ACP	0.15	1956	PCCP	0.75
83.25	83.28	1990	ACP	0.33	1990	Grind	0.15	1973	ACP	0.15
83.36	83.70	1982	ACP	0.06	1975	FABRIC	0.35	1956	PCCP	0.75
83.70	84.91	1975	FABRIC	0.35	1956	PCCP	0.75			
84.91	85.16	1982	ACP	0.06	1975	FABRIC	0.35	1956	PCCP	0.75
85.16	85.51	1975	FABRIC	0.35	1956	PCCP	0.75			
85.51	87.96	1976	FABRIC	0.35	1956	PCCP	0.75			

¹ PCR based on WSPMS deduct values (distress types of alligator cracking, longitudinal cracking, transverse cracking and patching).

² A=Alligator Cracking
 L=Longitudinal Cracking
 T=Transverse Cracking
 R=Rutting
 P=Patching

³ Deepest rut (both wheelpaths measured).

n District 4 PCCP -- SR 5 Southbound

Year Constructed	Layer 4		Traffic (1989)		1990		Distress Types ²	Performance		Predicted Life ¹ to PCR = 50
	Type	Thickness (ft)	ADT	% Trk	AGE	PCR ¹		Rutting ³		
								Depth (in)	No. Measurements	
1954	PCCP	0.75	27469	7.8	6	99	R	—	—	15 (1999)
			27489	7.8	6	99	R	—	—	15 (1999)
			40016	11.0	6	99	None	—	—	15 (1999)
			38026	11.2	6	99	None	—	—	15 (1999)
			38026	11.2	6	99	None	—	—	15 (1999)
			40413	13.5	13	95	R/L	0.42	6	23 (2000)
			37529	17.1	13	95	R/L	0.44	2	23 (2000)
			33174	13.0	14	66	R/P	0.75	7	15 (1991)
			31288	12.1	5	65	R/P	0.38	—	6 (1991)
			31288	12.1	5	99	None	—	—	14 (1999)
			31288	12.1	5	99	None	—	—	14 (1999)
			31288	12.1	5	99	None	—	—	14 (1999)
			24649	16.5	14	99	R	0.73	5	23 (1999)
			24649	16.5	9	88	R/T	0.44	21	13 (1994)
			24583	16.5	13	100	R	0.67	3	23 (2000)
			26446	15.9	13	99	R	0.57	7	22 (1999)
			28455	15.3	13	99	R	0.78	12	22 (1999)
			25761	15.8	9	99	R	0.66	18	18 (1999)
			25028	16.3	9	99	R	0.53	63	18 (1999)
			1956	PCCP	0.76	26526	13.3	6	99	R
29131	12.3	9				100	R	—	—	19 (2000)
30411	11.8	5				100	R	—	—	12 (1997)
30411	11.8	5				100	R	—	—	12 (1997)
30411	11.8	5				100	R	0.50	7	12 (1997)
30560	12.2	12				22	R/A/L/T	—	—	10 (1988)
30624	12.3	14				25	R/A/L/T	—	—	11 (2001)
33064	11.6	11				100	R	—	—	21 (2000)
33064	11.6	11				100	R	—	—	21 (2000)
33064	11.6	11				99	R	—	—	20 (1999)
33317	11.6	11				94	R/T	—	—	18 (1997)
34892	11.6	11				90	R/T	—	—	17 (1996)
36264	11.5	11				69	R/P	—	—	13 (1992)
36264	11.5	11				69	R/P	—	—	13 (1992)
39423	11.8	9				72	R/P	—	—	11 (1991)
38609	11.9	6				74	R/P	—	—	9 (1993)
38609	11.9	6				74	R/P	—	—	9 (1993)
39650	11.6	17				49	R/A/T	—	—	11 (2001)
40248	11.6	17				49	R/A/T	—	—	11 (2001)
40734	11.5	17				49	R/A/T	—	—	11 (2001)
1956	PCCP	0.75	36323	10.5	17	74	R/A/T	—	—	11 (2001)
			37970	10.7	17	74	R/A/T	—	—	13 (2003)
			38770	10.8	8	94	R/T	—	—	12 (1994)
			38770	10.8	15	95	R/T	—	—	22 (1997)
			38770	10.8	8	49	R/T/P	—	—	8 (1990)
			38770	10.8	15	45	R/T/P	—	—	15 (1990)
			38770	10.8	14	85	R/L/T	—	—	19 (1995)

average thickness = 3.0 inches and standard deviation = 1.8 inches for 31 projects; southbound average thickness = 2.8 inches and standard deviation = 1.9 inches for 22 projects). Table 5.1 also includes the results of condition surveys. These surveys show that the performance of these strategies in reducing crack reflection (transverse) ranged from fair to excellent, typically, fair performance was the result of construction practices or the thinness of the overlay. Good performance generally was observed in the thicker overlays and particularly those with the SAMI pretreatment.

The survival lives of the original AC overlays (no fabric or SAMI) placed on PCCP were examined. For the northbound overlays, the average time to resurfacing was 12.1 years (standard deviation 3.4 years) with an average AC overlay thickness of 3.7 inches (standard deviation 1.9 inches) for 17 projects. For southbound overlays, the average time to resurfacing was 13.1 years (standard deviation 4.7 years) with an average AC overlay thickness of 3.8 inches (standard deviation 2.1 inches) for 10 projects.

A separate survey to measure rutting was conducted during May 1990. These results show rather extensive rutting (ranging from about 0.4 to 0.8 inch in the wheelpaths). By dividing the total rut for each section by the overlay age, an estimate of the rutting rate can be made. These rates ranged from 0.07 to 0.04 inch/year in the northbound lane (Table 5.1a) and 0.10 to 0.03 inch/year in the southbound lane (Table 5.1b). Overall, the mean rates of rutting along with the associated standard deviations were

Northbound: \bar{x} = 0.055 inch/year
s = 0.010 inch/year
n = 12

Southbound: \bar{x} = 0.057 inch/year
s = 0.019 inch/year
n = 12

Combining these data along with an approximate ESALs/year of about 700,000 results in a rutting rate of about 8.0×10^{-8} inches/ESAL. Thus, a new AC overlay, for this location and traffic, can be expected to incur ruts of about 0.5 inch or greater 10 years after placement of the overlay. Based on ESALs, about 0.08 inch of rutting can be expected for

every 1,000,000 ESALs. Thus, the currently used AC overlays in District 4 will become marginal due to rutting after about 10 years of service or 7,000,000 ESALs (needless to say that age alone cannot cause rutting but, in this case, the 10 year limitation is based on the existing traffic on this portion of SR 5). The rutting rates and associated limiting ages and ESALs are only very approximate, but these values are important in examining the limitations of AC overlay performance on PCC Interstate pavements.

An examination of rutting rates for the various AC mixtures used along this section of SR 5 would, undoubtedly, be informative. This is particularly important since rutting in this location is the principal cause of surfacing failure. It is interesting to note that some of the AC overlays lasted up to 17 years before resurfacing was done.

5.3 RECONSTRUCTION

When a pavement reaches or nears the end of its life, it may be so badly deteriorated that reconstruction, rather than resurfacing or restoration, becomes the most cost-effective alternative. The following conditions may dictate that reconstruction is the best alternative: [5.7]

1. extensive cracking has occurred, which indicates the pavement has little, if any, remaining structural life;
2. extensive slab settlement, heave, rocking or cracking has occurred;
3. extensive joint deterioration has occurred. Reconstruction may be particularly cost-effective for short-jointed pavements in which a large number of joints would have to be repaired if other resurfacing or restoration techniques were used; and
4. extensive concrete deterioration, caused by poor concrete durability and excessive joint movement, has occurred.

Reconstruction may also be warranted when only the outer traffic lane (the truck lane) has deteriorated to a point requiring rehabilitation. Consideration should then be

given to reconstructing only this outer traffic lane. Reconstruction becomes a viable alternative in this case because resurfacing cannot be completed over one lane only. Added benefits of reconstruction are that geometrics can be improved, subgrade problems can be corrected, and drainage conditions can be improved.

The major advantages of reconstruction are as follows:

1. it creates a new pavement, with an expected design life of a new pavement and a new surface to resist studded tire wear;
2. it presents the opportunity to correct geometric and drainage deficiencies and to improve or repair subgrade conditions; and
3. relatively low risk is associated with design and construction.

The major disadvantages are the following:

1. a long construction duration and major traffic disruption, and
2. relatively high initial cost.

Once reconstruction has been chosen as a viable alternative, new pavement design procedures are used to develop the required pavement thickness. Design features that were not considered when the existing pavement was designed and constructed can now be considered and included in the new pavement. These design features may include subbase types, shoulder types, joint spacing, load transfer devices, and proper joint construction.

Three basic areas that should be considered in new pavement design are discussed in this section. They are subbase type, shoulder type, and joint design. In addition, concrete pavement recycling is addressed.

5.3.1 Subbase Type

Subbases in concrete pavements are constructed to prevent supporting layer erosion, facilitate drainage, provide a stable construction platform, provide uniform slab support, and control frost penetration depth. Three subbase types are generally considered

when a new pavement is designed. They are granular; cement-treated, including econocrete or lean concrete; and asphalt-treated.

Perhaps the most significant subbase requirement is that the material be non-erodible. Erodible materials result in loss of support, pumping, voids, and joint faulting. In wet climates subbase erosion can be a problem because excess water can accumulate at the subbase/slab interface. For a granular base to be non-erodible it must be open-graded and should have a D_{60}/D_{10} ratio greater than 4 to ensure stability under construction traffic. [5.22] This layer must also have sufficient permeability to prevent pore-pressure build-up and should be designed as a drainage layer. To prevent pore-pressure build-up, the layer should have a permeability greater than 1,000 feet/day. [5.23] To achieve this permeability, nearly all fines should be removed from the material, and the minus No. 4 sieve fraction should be kept below 7 percent. Caltrans practice with permeable subbases is presented in Appendix I.

Cement-treated materials have generally performed poorly in Washington state. Econocrete or lean concrete have not performed significantly better than cement-treated. A major disadvantage of cement-treated, econocrete, or lean concrete subbases is their stiffness. Very stiff subbases result in increased curl stress. These higher stresses result in increased curl at the slab edges. The curl allows debris to infiltrate under the slab. The slab is thus prevented from returning to full contact with the subbase surface when the temperature gradient reverses. The inability to return full contact can result in voids with concomitant stress concentrations, which can cause corner breaks and can also result in loss of support.

Well-designed asphalt-treated mixes have been found to be virtually non-erodible. [5.23] Asphalt stabilized materials can tolerate asphalt cement contents greater than the optimum required for maximum stability because stability is not an issue for a subbase under a PCC pavement. These materials should be compacted to a high relative density to minimize porosity. [5.23] Asphalt-treated materials are not as stiff as cement-treated

materials. Their lower stiffness means that curl stresses are lower, and the subbase can deform to accommodate the debris that infiltrates between the slab and the subbase. Thus, overall pavement performance is improved.

Subbase thicknesses should be sufficient to create a stable working platform that can support construction traffic. Its presence should not be considered a justification for raising the modulus of subgrade reaction value used in design. However, asphalt-treated bases, cement-treated bases, and lean concrete bases tend to reduce load stresses and thereby provide a slight increase in pavement life.

5.3.2 Shoulder Type

Several field studies have shown that shoulders constructed with full-depth concrete have performed well and have improved traffic lane performance. [5.11] Asphalt shoulders have also worked well as long as the longitudinal joint has been well-maintained. Zollinger and Barenberg evaluated the relative benefits of asphalt shoulders, 10-foot tied shoulders (with high and medium load transfer) and a 2-foot extended driving lane. [5.22] The required concrete pavement thickness developed for each shoulder type for varying traffic levels is shown in Figure 5.3. The results show that the asphalt concrete shoulder required the greatest concrete pavement thickness, while the 2-foot extended and 10-foot tied (with high load transfer) shoulders required the least concrete thickness.

Shoulder type should be considered when new pavement designs are being completed. The shoulder type selected will be determined by economic considerations and by the ability of local contractors to construct widened lanes. If concrete shoulders are used, the following recommendations should be followed:

1. The shoulder thickness at the traffic lane/shoulder interface should be the same as that of the traffic lanes.
2. The tie bar sizes and spacing should be selected with consideration for joint type and the required load transfer.

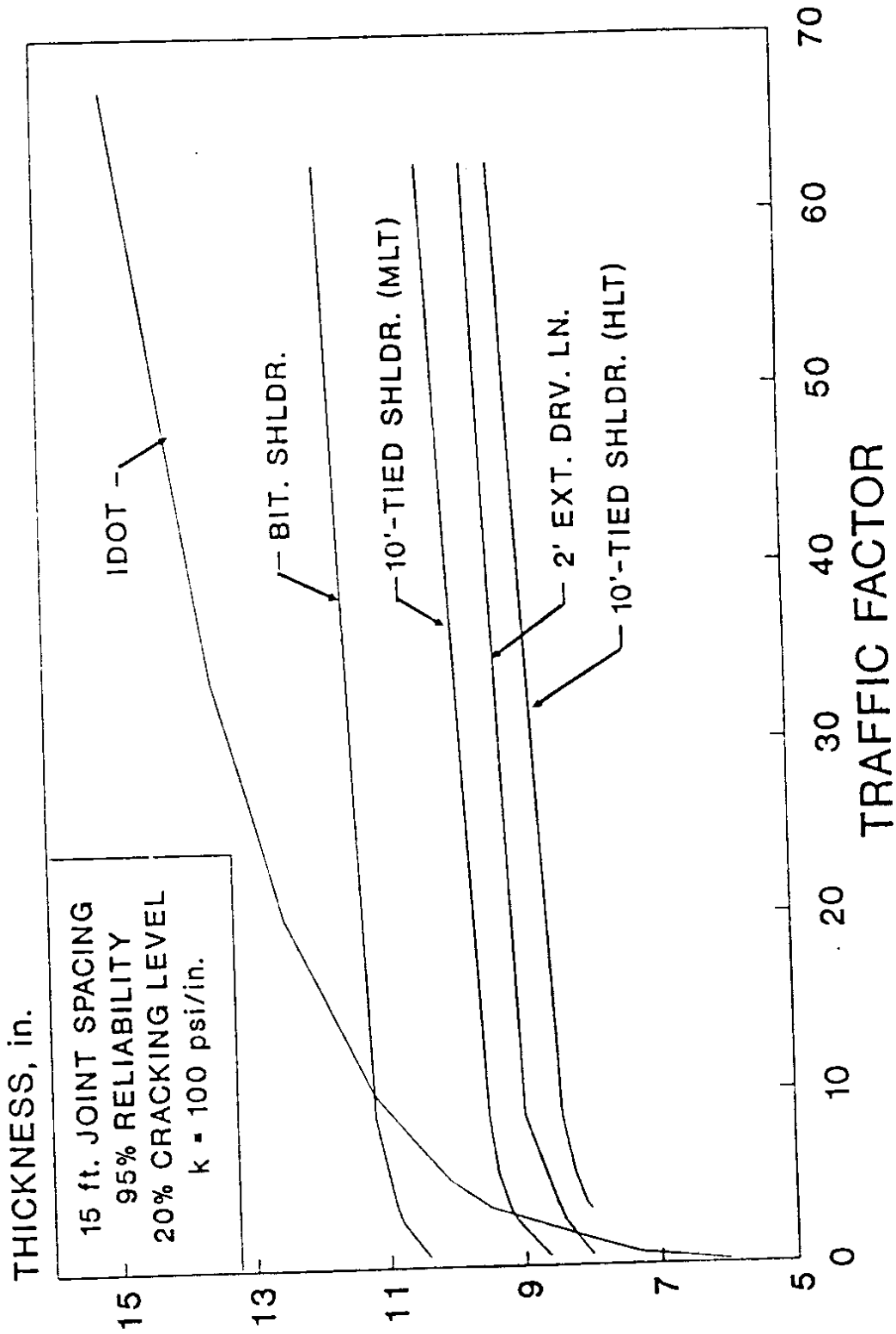


Figure 5.3 Design Curve Comparing Present IDOT Thicknesses with the Mechanistic Based Procedure for Various Shoulder Types [from Reference 5.22]

3. Transverse joints should be matched with, and have the same spacing as, those in the traffic lanes.
4. The longitudinal joint should be saw-cut and properly sealed.

5.3.3 Joint Design

Transverse joint spacing affects the curl stress magnitude induced in the pavement. As transverse joint spacing increases, the thermal stresses induced along the pavement edge increase. These higher thermal stresses result in an increased incidence of transverse cracking. Experience indicates that transverse joint spacing should be kept to 20 feet or less for pavements in the thickness range under consideration. Therefore, the current variable transverse joint spacings of 9, 10, 13, and 14 feet (average 11.5 feet) used in Washington state are satisfactory.

Several sections of SR 5 and 90 have experienced joint faulting (mostly nonskewed 15 ft. joint spacing). Joint faulting can be minimized by installing mechanical load transfer devices in the pavement when it is constructed or by retro-fitting these devices into an existing pavement as a rehabilitation alternative. Policy decisions up to 1989 generally dictated that mechanical load transfer devices were not needed. This policy made short joint spacings, such as those currently used, all the more critical. WSDOT currently will allow dowel bars on a case-by-case basis. Whenever dowel bars are used in future PCC pavements, experience to date suggests that the joint skew can be eliminated. The random spacing should be retained.

5.3.4 Recycling

In most cases when reconstruction is justified, agencies can reduce the construction costs by recycling the existing concrete pavement. Concrete recycling involves breaking up the existing concrete to produce aggregate that can be used in place of virgin aggregate when a new concrete pavement is constructed.

Concrete recycling versatility and cost effectiveness have been demonstrated on several projects. The following statements are based on this experience. [5.7]

1. Concrete recycling can result in substantial cost savings on reconstruction projects, particularly when high-quality virgin aggregates are not available, or are expensive; disposal sites for the existing concrete are not available; or reconstruction is on a tight schedule.
2. Recycled concrete aggregate may replace virgin aggregate in all pavement layers.
3. Recycled concrete aggregate performs as well as virgin aggregate in portland cement concrete, as long as the mix design is modified to achieve required strength and workability. A water-reducing admixture and exclusion of crushed concrete fines may be required.

Reference 5.4 provides detailed information, including guide specifications, about concrete pavement recycling.

Given the optimistic views on recycled PCC, recent experience in states such as Michigan suggest caution. It is prudent for WSDOT to monitor such developments and not plan, at this time, widespread use of recycled PCC in new slabs.

5.4 FEASIBLE REHABILITATION ALTERNATIVES

5.4.1 Bridge Clearances

The bridge clearance data presented in Appendix B show that, for the most part, bridge clearances are not a problem along the Interstate corridors for which data were collected. If bridge clearances are a problem at one or two locations in the area to be rehabilitated, it may be feasible and cost effective to remove the existing pavement under the obstruction and reconstruct it while feathering the rehabilitation chosen for the area to match grades. If several bridges present clearance problems, other rehabilitation alternatives, including reconstruction, should be considered.

5.4.2 Life-Cycle Cost Analysis of Rehabilitation Strategies

When the life-cycle cost analysis was conducted, construction items that were not rehabilitation strategy specific were not included in the analysis. These factors included such items as removing striping, lane markers, traffic buttons, and guard rails. Also excluded from the analysis were the rehabilitation of the bridge decks and approaches and any access ramps; the analysis only included the main lanes of the facility. Further, disposal costs of PCC were estimated but not included in the cost summaries.

In addition to the assumptions which follow, other uncertainties exist. For example:

- It is assumed that PCC remove and replace and PCC overlay will have a performance period without rehabilitation of 40 years. This may be a bit long particularly in light of surface wear largely caused by studded tires (hence lower than desirable surface friction). On the other hand, whether studded tires will continue to be used is unclear.
- All traffic control and user costs are very site specific. It is difficult to estimate these costs with much confidence for this report. Directly related to such costs is the estimated construction period for each rehabilitation alternative. The periods assumed may differ significantly with actual projects.
- It is yet unclear as to the benefits of periodic pavement resurfacing to reduce roadway generated traffic noise. Thus, no provision was made for such in these cost estimates.

The rehabilitation strategies included in the life-cycle cost analysis consisted of the following:

1. **Remove and Replace**
 - (a) Tied shoulders and Asphalt Treated Base (ATB)
 - (b) Asphalt shoulders and ATB

2. Asphalt Concrete Overlay
 - (a) Without interlayer
 - (b) With Fabric
 - (c) With Asphalt-Rubber Interlayer
 - (d) Following Cracking and Seating
3. Unbonded Concrete Overlay

Rehabilitation Project Specifications

- This analysis was for the rehabilitation of I-5 at 175th Street, in the Seattle area.
- Project Length = 5 miles
- Lane Width = 12 feet
- Number of Lanes = 4
- Shoulder Width = 11 feet (right), 5 feet (left)
- Original Concrete Thickness = 9 inches
- Initial ADT = 133,500
- Construction Period —
 - Remove and Replace PCC: 6:00 a.m. - 6:00 p.m. over 3 months (90 days)
 - PCC Overlay: 6:00 a.m. - 6:00 p.m. over 2 months (60 days)
 - AC Overlay: 10:00 p.m. - 6:00 a.m. over 1.5 months (4.2 inch AC overlay) and 2.2 months (6.0 inch AC overlay)

The selection of the construction period for the remove and replace option was based on a project constructed in the Detroit Area on the Lodge Freeway. There, 8.7 miles of a six-lane (three lanes each way) divided freeway was reconstructed in six months. [5.26] (Northbound lanes reconstructed in 97 days.) Therefore, the assumption was made that for the

above scenario, 5 miles, 4 lanes in one direction, could be constructed in Washington state in 3 months (90 days).

The determination for the construction period for an AC overlay was based on the calculation of conservative asphalt concrete production rates, which are shown in Appendix H.

- Construction would occur in one direction at a time
- The construction costs that are listed below do not include any unique costs that might be associated with nighttime construction.

Remove and Replace — Construction Costs¹

(See Appendix H for all cost calculations)

Roadway Excavation Including Haul	\$6.71/C.Y.
Removing Cement Concrete Pavement	\$7.20/S.Y.
Removing Asphalt Concrete Pavement	\$3.37/S.Y.
Cement Concrete Pavement (14-day cure)	
10 inch section	\$21.00/S.Y.
12 inch section	\$22.24/S.Y.
15 inch section	\$29.70/S.Y.
Asphalt Concrete Pavement Cl. B (including paving asphalt)	\$27.79/ton
Tie bars	\$0.54/lb.
Dowel Bar	\$6.82 each
Asphalt Treated Base	\$24.96/ton
Labor for Traffic Control	\$19.75/hour
Sequential Arrow Sign	\$6.52/hour
Plastic Drums	\$62.00 each
Temporary Concrete Barrier	\$9.81/L.F.

¹WSDOT Unit Bid Analysis for March 1, 1988, to February 28, 1990. All price listings are for District 1 and are the average values for each item listed.

Asphalt Concrete Overlay — Construction Costs¹

(See Appendix H for all cost calculations)

Asphalt for Tack Coat	\$214.17/ton
Planing Bituminous Pavement	\$3.37/S.Y.
Asphalt Concrete Pavement Cl. B (including Paving Asphalt)	\$27.79/ton
Crack Sealing (Estimate)	\$1.00/L.F.
Labor for Traffic Control	\$19.75/hour
Sequential Arrow Sign	\$6.52/hour
Crack and Seat ² [5.27]	\$1.00/S.Y.
Fabric Interlayer	\$1.00/S.Y.
Asphalt-Rubber Interlayer	\$2.00/S.Y.
Plastic Drums	\$62.00/each

Rehabilitation Costs

Assumptions

- The future overlay construction costs were assumed to be the same as in year 1.
- For the future AC overlays, it was assumed rutting would be present requiring milling of the surface to remove. The new AC overlay was assumed to be the same thickness as the initial AC overlay (either 4.2 or 6.0 inches thick).

¹ WSDOT Unit Bid Analysis for March 1, 1988, to February 28, 1990. All price listings are for District 1 and are the average values for each item listed.

²This cost may be underestimated for the construction of the first crack and seat project by the WSDOT; California's first crack and seat project had a bid price of \$12.50/square yard, including 5-inch AC overlay. [5.28]

Life-Cycle Cost Analysis

Assumptions

- Expected life to failure:
Remove and Replace PCC = 40 years
AC Overlay
12.5 years then the overlay is milled and new overlay placed
10.0 years then the overlay is milled and new overlay placed
PCC Overlay = 40 years
- Analysis Period = 40 years
- Discount Rate = 4%
- Assume Traffic (ADT) will increase at a rate of 2.74% per year.
[5.29]

Present Worth Analysis

Table 5.2 illustrates the results of the present worth analysis of this study. Table 5.2 is divided into the three categories previously mentioned, which include remove and replace PCC, AC overlays, and PCC overlays.

User Delay Costs

Though large uncertainties are involved in the determination of costs associated with the users of the facility during construction, an attempt must be made. The calculation of user costs is very site specific and must be performed for each section of the project where major changes of traffic flow or volumes take place.

TABLE 5.2. PRESENT WORTH COST SUMMARY

Remove and Replace PCCP	Construction Costs	Rehabilitation Costs	Total Costs
ATB with Tied Shoulders			
10 inches	\$8,827,000	\$0.00	\$8,827,000
12 inches	\$9,229,000	\$0.00	\$9,229,000
15 inches	\$11,245,000	\$0.00	\$11,245,000
ATB with Asphalt Shoulders			
10 inches	\$7,405,000	\$0.00	\$7,405,000
12 inches	\$7,708,000	\$0.00	\$7,708,000
15 inches	\$9,217,000	\$0.00	\$9,217,000
AC Overlay	Construction Costs	Rehabilitation Costs	Total Costs
No Pre-Rehabilitation Treatment			
4.2 inches	\$1,783,000	\$2,814,000	\$4,597,000
6.0 inches	\$2,306,000	\$3,374,000	\$5,680,000
Fabric Interlayer			
4.2 inches	\$1,971,000	\$3,016,000	\$4,987,000
6.0 inches	\$2,494,000	\$3,576,000	\$6,070,000
Asphalt-Rubber Interlayer			
4.2 inches	\$2,159,000	\$3,217,000	\$5,376,000
6.0 inches	\$2,682,000	\$3,778,000	\$6,460,000
Following Crack and Seat			
4.2 inches	\$1,971,000	\$3,016,000	\$4,987,000
6.0 inches	\$2,494,000	\$3,576,000	\$6,070,000

Note: For AC overlay options, costs assume AC overlay is milled after 12.5 years of service and new AC overlay placed (at 12.5, 25.0, and 37.5 years).

Table 5.2. Present Worth Cost Summary (Continued)

AC Overlay	Construction Costs	Rehabilitation Costs	Total Costs
No Pre-Rehabilitation Treatment			
4.2 inches	\$1,783,000	\$3,786,000	\$5,569,000
6.0 inches	\$2,306,000	\$4,539,000	\$6,845,000
Fabric Interlayer			
4.2 inches	\$1,971,000	\$4,057,000	\$6,028,000
6.0 inches	\$2,494,000	\$4,810,000	\$7,304,000
Asphalt-Rubber Interlayer			
4.2 inches	\$2,159,000	\$4,328,000	\$6,487,000
6.0 inches	\$2,682,000	\$5,081,000	\$7,763,000
Following Crack and Seal			
4.2 inches	\$1,971,000	\$4,057,000	\$6,028,000
6.0 inches	\$2,494,000	\$4,810,000	\$7,304,000
<p>Note: For AC overlay options, costs assume AC overlay is milled after 10.0 years of service and new overlay placed (at 10.0, 20.0, and 30.0 years).</p>			
PCC Overlay	Construction Costs	Rehabilitation Costs	Total Costs
With Concrete Shoulders			
10 inches	\$6,022,000	\$0.00	\$6,022,000
With Asphalt Concrete Shoulders			
10 inches	\$5,008,000	\$0.00	\$5,008,000

Table 5.3. Present Worth of User Costs

Rehabilitation Type	Texas A&M Method	CalTrans Method
Remove and Replace PCC	\$5,879,000	\$4,224,000
PCC Overlay	\$3,919,000	\$2,816,000
AC Overlay		
every 12.5 years		
4.2 inches	\$1,241,000	\$930,000
6.0 inches	\$1,780,000	\$1,334,000
every 10.0 years		
4.2 inches	\$1,347,000	\$968,000
6.0 inches	\$1,933,000	\$1,389,000

The following is a list of general assumptions that were made to conduct an analysis of the costs associated with the user of the facility. The selection of the design speeds before and during the construction was not based on specific calculations. The development of an accurate estimation of these traffic speeds and volumes should be modeled to assure a reasonable estimate of costs associated with delay and vehicle operation for each section of roadway to be rehabilitated.

General Assumptions

- No stopping of vehicles (progression would occur at a reduced speed) through the construction area.
- The percentage of total ADT that would occur during the construction period was estimated on the basis of a volume versus time graph for the particular section of roadway, in this case, on SR 5 at 175th Street. These traffic volumes were located in the "Ramp and Roadway Traffic Volumes," Summary Report, January/June 1986, by Traffic Operations — District 1, Washington State Department of Transportation.
- For the remove and replace and the PCC overlay, the amount of ADT occurring during the construction period was estimated to be 75 percent of total ADT; the corresponding value for the AC overlays was estimated to be 10 percent of total ADT.
- Reference 5.29, "The Status of the Nation's Highways: Condition and Performance," says, "the states have estimated that travel will increase at a rate of 2.74 percent per year through the year 2000." Since it was not the intent of this study to perform an analysis on future traffic levels, a 2.74 percent increase in the traffic volume was

also used after the year 2000. To estimate the user costs associated with a rehabilitation project, an attempt must be made to determine future traffic volumes.

- Appendix H shows calculations of user delay and operating costs.

Using the methods presented in Appendix A, and the above assumptions, an attempt was made to quantify the costs associated with the user of the facility. These costs are shown in Table 5.3.

5.4.3 SR 5

On the basis of the discussions presented in this chapter, the feasible rehabilitation alternatives for this site appear to be the following: asphalt overlay, crack and seat with asphalt overlay, and reconstruction. The subbase material should be asphalt-treated base, and the variable joint spacing currently constructed should be used. Careful consideration should be given to extended or tied concrete shoulders for this section.

In addition, concrete pavement recycling or an unbonded concrete overlay might be feasible alternatives. The unbonded concrete overlay might create problems with bridge clearances, and all appurtenances would have to be raised to the new grade. Raising all appurtenances would be costly for an urban area Interstate pavement.

This study estimated that the initial annual ESALs in 1965 were 210,000 and increasing to 909,000 in 1987. This is an annual ESAL growth rate of about 7 percent. Further, recent FHWA statistics [5.25] suggest that an annual growth rate for rural Interstate pavements (based on data from 1970 to 1986) is as much as 9 percent. Thus, the use of annual growth rates of 3.5, 7.0, and 9.0 percent results in 30-year analysis ESALs (assuming an initial annual ESAL rate of 1,000,000 for SR 5 in Seattle) of 52,000,000, 94,000,000, and 136,000,000, respectively. Since the authors do not expect these combined large increases in annual ESAL growth rates, the true design value probably lies between 50,000,000 and 100,000,000 ESALs.

5.4.4 SR 90

The feasible rehabilitation alternatives for this site appear to be crack and seat with an asphalt concrete overlay, and reconstruction. Currently used joint spacings for new construction are satisfactory. Consideration should be given to extended or tied concrete shoulders and the use of dowels at the transverse joints.

Concrete pavement recycling or an unbonded concrete overlay might also be feasible for the SR 90 pavements. The clearance problems and cost of raising the shoulder grades and appurtenances might not be as great for this site, and therefore an unbonded concrete overlay might be a viable alternative.

This study estimated that the initial annual ESALs for SR 90 in 1965 were 136,000 and increased to 299,000 in 1987, resulting in an annual growth rate of about 3.5 percent. If 3.5 percent and 7.0 percent (double the current rate) are used to estimate the ESALs over a 30-year analysis period (starting with a base year ESAL rate of 350,000), then the design traffic loading ranges between 18,000,000 and 33,000,000.

CHAPTER 6.0

CONCLUSIONS AND RECOMMENDATIONS

6.1 CONCLUSIONS

Since the PCC pavement rehabilitation that has occurred in the state of Washington has been limited, the need for an increase in new test sections to explore cracking and seating and portland cement concrete overlays is obvious. However, the addition of these new test sections may not be cost effective, especially if studies have been conducted in other areas with similar conditions.

The state of California has performed extensive cracking and seating testing (details provided in Appendix I). Since the traffic volumes, subgrade support, small changes in the seasonal temperatures, and non-reinforced portland cement concrete pavements are characteristic of both California and western Washington, a crack and seat project can be expected to perform as well in western Washington as it has in California. The only problem is the potential reduction of the structural capacity of the existing concrete slabs and the rate of rutting in AC overlays.

Though several stress-relieving interlayers have been constructed in the state, the added costs for a fabric or rubber-asphalt interlayer may be better spent as an increase in the thickness of an asphalt concrete overlay.

With the past and continuing performance of the existing portland cement concrete pavements, the same or longer performance period, 30+ years, can be expected to result if the removal and replacement option is selected. (Note that the performance of PCC pavements which have been overlaid, as illustrated in Table 5.1, "survived," on average, 20 years prior to resurfacing. The majority of these specific pavements were built during the 1950s (mostly 1956) and their "survival" lives may not be exclusively indicative of structural performance due to Interstate geometric upgrading, surface friction, etc.) In addition, the use of an asphalt treated base should improve the service life of the pavement and reduce the need for future maintenance of the PCC pavement.

When future rehabilitation projects of the PCC Interstate freeways take place, the selection of a "wrong" strategy will have a very high impact on not only the funding for initial construction but also problem correction, not to mention the additional costs that users of the facility will have to endure. Therefore, the authors assume that WSDOT will likely select either the option of removal and replacement, asphalt concrete overlay with no pre-rehabilitation treatment, or a crack and seat project with asphalt concrete overlay. (However, single lane rehabilitation on multi-lane highways will undoubtedly result in other types of rehabilitation strategies.) The results of the cost analysis for these three options, including user costs, are shown in Table 6.1. The user costs calculated by the Caltrans method were selected only for illustrative purposes. (Details for Table 6.1 were developed in Chapter 5.0 and Appendices A and H.)

Table 6.1 shows that the total construction costs for a removal and replacement project with concrete shoulders and an asphalt treated base, over a 5-mile, 4-lane project, would range from \$8.8 to \$11.2 million, depending on the slab thickness. The costs of an asphalt concrete overlay for the same project, using no pre-rehabilitation treatment, would range from \$4.6 to \$5.7 million for a 4.2-inch and 6.0 inch-overlay, respectively, and the cracking and seating would cost from \$5.0 to \$6.1 million. A comparison of construction costs for all three options shows that the removal and replacement of PCC option is about

**TABLE 6.1. SUMMARY OF TOTAL REHABILITATION COSTS
(Cost per Lane-Mile)**

	Construction Costs	User Costs	Total Costs
Remove and Replace with Tied Shoulders and ATB			
10 inches	\$441,000	\$211,000	\$652,000
12 inches	\$461,000	\$211,000	\$672,000
15 inches	\$562,000	\$211,000	\$773,000
AC Overlay with No Pre-Rehabilitation Treatments (12.5 yr cycle)			
4.2 inches	\$230,000	\$46,000	\$276,000
6.0 inches	\$284,000	\$67,000	\$351,000
AC Overlay following Cracking and Seating of Concrete Slabs			
4.2 inches	\$249,000	\$46,000	\$295,000
6.0 inches	\$303,000	\$67,000	\$370,000

40 to 50 percent more costly than the other two options. If user costs are considered, the remove and replace PCC option is about 50 to 60 percent more costly.

Considering that the Washington state Interstate system is composed of approximately 400 miles of PCC pavement, all of which is rapidly approaching the end of its initial performance period, the selection of the rehabilitation strategy could have a funding impact exceeding \$700 million if the entire system was rehabilitated with an asphalt concrete overlay. On the other hand, if the entire system was removed and replaced with a slab thickness of 12 inches, for example, then the total costs could exceed \$1.25 billion. These two considerations may be extreme, and the rehabilitation of these pavements will not occur at the same time, but the impact of whatever type of rehabilitation used will be significant. Engineering knowledge and experience will be needed as part of this decision process.

In reviewing the above costs, the reader should keep in mind the following assumptions:

1. It is possibly a bit optimistic that both the remove and replace with PCC and the PCC overlay were assumed to perform 40 years without resurfacing. Given the emphasis on increasing safety (as illustrated by surface friction) and reducing noise (for example, by periodic resurfacings), some type of intermediate resurfacing may be necessary (say at about 20 to 25 years). Such resurfacings were not considered in the cost analyses. Additionally, any unique costs associated with processing the removed PCC slabs into either new pavement materials or disposal in a landfill were not considered in the cost summaries (however, disposal costs were estimated and are contained in Appendix H). Similarly, any unique construction costs associated with nighttime construction of AC overlays were not made.
2. The AC overlay option was examined based on two recurring performance periods: overlays every 10 or 12.5 years. These two performance periods

were based on observed overlay performance on the WSDOT route system. It was assumed that rutting will be present when resurfacing occurs, thus requiring milling (or possibly AC levelup). It was further assumed that to insure another complete performance period that the future AC overlays would be constructed with a depth of new AC equal to the original (either 4.2 or 6.0 inches). Thus, the total depth of AC over the original PCC could exceed the original AC overlay thickness (depends on the actual depth of milling). Under this scenario, it is assumed no further, significant degradation of the original PCC slabs takes place after overlay. Actual pavement performance suggests that this is not unreasonable for up to two overlay cycles. The uncertainty increases beyond that.

3. The construction durations which are necessary to estimate user costs for each rehabilitation option are probably a bit optimistic. Clearly, an improved understanding of construction durations in urban areas is of significant interest to WSDOT. The construction durations that were used did not assume significant additional work such as safety improvements, etc.

Are the above assumptions realistic? In time, this will become clearer. The primary goal of the cost analyses is to suggest a process for estimating such costs.

The results of the load transfer analysis made apparent that the presence of voids beneath the PCC slabs is not of concern in the Seattle area, and therefore no corrective action need be performed (at the current time). On the other hand, the load transfer results for SR 90 showed signs of voids and faulting of the PCC slabs. Therefore, if an overlay is to be the selected rehabilitation strategy, action will be needed to prevent slab movement, or reflection cracking will likely occur within a few years after paving, reducing pavement performance.

6.2 RECOMMENDATIONS

The authors will not make "hard and fast" recommendations as to which rehabilitation type is best. Clearly, such a decision is a function of numerous project-specific factors. However, the analyses and related information contained in this report should be of direct benefit to those who will make the decisions.

REFERENCES

CHAPTER 2.0

- 2.1 Mahoney, J.P., and N.C. Jackson, "A Proposal Entitled Portland Cement Concrete Pavement Performance and Rehabilitation," submitted by the Washington State Transportation Center, to the Research Office, Washington State Department of Transportation, September 4, 1985 revised November 4, 1985.
- 2.2 Nelson, T.L., and LeClerc, R.V., "Development and Implementation of Washington State's Pavement Management System," Research Report WA-RD 50.1, Washington State Department of Transportation, Olympia, Washington, September 1982.
- 2.3 Cinquemani, V., J.R. Owenby, Jr., and R.G. Baldwin, "Input Data for Solar Systems," Prepared for the U.S. Department of Energy, Interagency Agreement No. E949-26-1041, November 1978.
- 2.4 Personal Communication with the National Oceanic and Atmospheric Administration, Weather Service Division, March 1988.
- 2.5 1987 Bridge List, Washington State Department of Transportation, Olympia, Washington.

CHAPTER 3.0

- 3.1 Lary, J.A., "LTM Site Models and A Comparison of Field and Laboratory Resilient Moduli," Washington State Department of Transportation, Field Order No. F772559, December 1983.
- 3.2 American Concrete Institute, "Building Code Requirements for Reinforced Concrete," ACI Standard 318-63, June 1963.
- 3.3 Hammit, G.M. II, "Concrete Strength Relationships," U.S. Army Waterways Experiment Station, Vicksburg, Mississippi, December 1971.
- 3.4 Troxell, G.E., H.E. Davis, and J.W. Kelly, Composition and Properties of Concrete, 2nd Edition, McGraw-Hill, 1968.
- 3.5 Mindess, S., and J.F. Young, Concrete, Prentice-Hall, Inc., Englewood Cliffs, N.J., 1981.
- 3.6 Darter, M.I., "Design of Zero-Maintenance Plain Jointed Concrete Pavement: Vol. I - Development of Design Procedures," Federal Highway Administration, Report No. FHWA-RD-77-111, June 1977.
- 3.7 Zollinger, D.G., and E.J. Barenberg, "Development of Mechanistic Based Design Procedure for Jointed Concrete Pavements," Transportation Research Laboratory, Department of Civil Engineering, University of Illinois at Urbana-Champaign,

Research Report 518-2, Project IHR-518, Illinois Cooperative Highway Research Program, 1988.

- 3.8 Shahin, M.Y., and S.D. Kohn, "Pavement Maintenance Management for Roads and Parking Lots," United States Army Corps of Engineers, Construction Engineering Research Laboratory, Technical Report M-294, October 1981.
- 3.9 Tabatabaie-Raissi, A.M., "Finite-Element Analysis of Cracked Concrete Pavements," Highway Research Record 671, Transportation Research Board, Washington, D.C., 1978.
- 3.10 Ioannides, A.M., J. Donnelly, M.R. Thompson, and E.J. Barenberg, "Analysis of Slabs-on-Grade for a Variety of Loading and Support Conditions," AFOSR-83-0143, Air Force Office of Scientific Research, Washington, D.C., September 1984.
- 3.11 Foxworthy, P.T., "Concepts for the Development of a Nondestructive Testing and Evaluation System for Rigid Airfield Pavements," Ph.D. Thesis, University of Illinois at Urbana-Champaign, June 1985.
- 3.12 Colley, B.E., and H.A. Humphrey, "Aggregate Interlock at Joints in Concrete Pavements," Highway Research Record No. 189, Highway Research Board, Washington, D.C., 1967.
- 3.13 Stelzenmuller, W.B., L.L. Smith, and T.J. Larson, "Load Transfer at Contraction Joints in Plain Portland Cement Concrete Pavements," Research Report 90-D, Florida Department of Transportation, April 1973.
- 3.14 Darter, M.I., and J.A. Crovetti, "Void Detection Procedures - Appendix C," NCHRP 1-21, National Cooperative Highway Research Program, Transportation Research Board, Washington, D.C., March 1985.
- 3.15 Hoffman, M.S., and M.R., Thompson, "Mechanistic Interpretation of Nondestructive Pavement Testing Deflections," Civil Engineering Studies, Transportation Engineering Series No. 32, Illinois Cooperative Highway and Transportation Research Program Series No. 190, University of Illinois at Urbana-Champaign, 1981.
- 3.16 Ioannides, A.M., "Dimensional Analysis in NDT Rigid Pavement Evaluation," submitted to the Journal of Transportation Engineering, American Society of Civil Engineers, 1988.
- 3.17 Ioannides, A.M., E.J. Barenberg, and J.A. Lary, "Interpretation of Falling Weight Deflectometer Results Using Principles of Dimensional Analysis," to be presented at the Fourth International Conference on Concrete Pavement Design and Rehabilitation, Purdue University, West Lafayette, Indiana, April 1989.
- 3.18 Dempsey, B.J., "A Heat-Transfer Model for Evaluating Frost Action and Temperature Related Effects in Multilayered Pavement Systems," Ph.D. Dissertation, University of Illinois, Urbana, Illinois, 1969.

- 3.19 Herlache, W.A., A.J. Patel, and B.J. Dempsey, "The Climatic-Materials-Structural Pavement Analysis Program - User's Manual," prepared for the Federal Highway Administration, Contract No. DTFH 61-80-C-00013 - Phase II, Washington, D.C., April 1984.
- 3.20 Westergaard, H.M., "Analysis of the Stresses in Concrete Roads Caused by Variations in Temperature," *Public Roads*, Vol.8, No. 3, May 1927, pp. 54-60.
- 3.21 Ioannides, A.M., M.R. Thompson, and E.J. Barenberg, "Westergaard Solutions Reconsidered," *Transportation Research Record* 1043, Transportation Research Board, National Research Council, Washington, D.C., pp. 13-23.
- 3.22 Ioannides, A.M., and R.A. Salsilli-Murua, "Temperature Curling in Rigid Pavements: An Application of Dimensional Analysis," to be Presented at the 1989 Annual Meeting of the Transportation Research Board, Washington, D.C., January 1989.
- 3.23 Miner, M.A., "Cumulative Damage in Fatigue," *Transactions, American Society of Mechanical Engineers*, Vol. 67, 1945, pp. A159-A164.
- 3.24 Weigh Station Data, W-4 Tables, published by the Washington State Department of Transportation.

CHAPTER 4.0

- 4.1. Murdock, J.W., "A Critical Review of Research on Fatigue of Plain Concrete," *Engineering Experiment Station, University of Illinois, Bulletin* 476, 1965.
- 4.2. Nordby, G.M., "Fatigue of Concrete - A Review of Research," *Proceedings, American Concrete Institute*, Vol. 55, 1959, pp. 191-220.
- 4.3. Hilsdorf, H.K., and C.E. Kesler, "Fatigue Strength of Concrete Under Varying Flexural Stresses," *Proceedings, American Concrete Institute*, Vol. 63, 1966, pp. 1059-1076.
- 4.4. Raithby, K.W., and A.C. Whiffin, "Failure of Plain Concrete Under Fatigue Loading - A Review of Current Knowledge," *Road Research Laboratory, Report LR 231*, Berkshire, England, 1968.
- 4.5. McCall, J.T., "Probability of Fatigue Failure of Plain Concrete," *Proceedings, American Concrete Institute*, Vol. 55, 1959, pp. 233-245.
- 4.6. Murdock, J.W. and C.E. Kesler, "Effect of Range of Stress on Fatigue Strength of Plain Concrete Beams," *Proceedings, American Concrete Institute*, Vol. 55, 1959, pp. 221-231.
- 4.7. Ople, F.S., Jr, and C.L. Hulsbos, "Probable Fatigue Life of Plain Concrete with Stress Gradient," *Proceedings, American Concrete Institute*, Vol. 63, 1966, pp. 59=81.
- 4.8. Clemmer, H.F., "Fatigue of Concrete," *Proceedings, American Society of Testing and Materials*, Vol. 22, Part II, 1922, pp. 408-419.

- 4.9. Kesler, C.E., "Effect of Speed of Testing on Flexural Strength of Plain Concrete," Proceedings, Highway Research Board, Vol. 32, 1953, pp. 251-258.
- 4.10. The AASHO Road Test - Report 5 - Pavement Research," Special Report 51E, Highway Research Board, Washington, D.C., 1962.
- 4.11. Finney, E.A., and L.T. Oehler, "Final Report on Design Project, Michigan Test Road," Proceedings, Highway Research Board, Vol. 38, 1959.
- 4.12. Darter, M.I., "Design of Zero-Maintenance Plain Jointed Concrete Pavement: Vol. I — Development of Design Procedures," Federal Highway Administration, Report No. FHWA-RD-77-111, June 1977.
- 4.13. Zollinger, D.G., and E.J. Barenberg, "Development of Mechanistic Based Design Procedure for Jointed Concrete Pavements," Transportation Research Laboratory, Department of Civil Engineering, University of Illinois at Urbana-Champaign, Research Report 518-2, Project IHR-518, Illinois Cooperative Highway Research Program, 1988.
- 4.14. Teller, L.W., and Southerland, E.C., "The Structural Design of Concrete Pavements, Part 3 - A Study of Concrete Pavement Cross Sections," Public Roads, Vol. 16, No. 10, 1935.
- 4.15. Emery, D.K., "A Preliminary Report on the Transverse Lane Displacement for Design Trucks on Rural Freeways," paper presented to the ASCE Pavement Design Speciality Conference, Atlanta, Georgia, June 1975.
- 4.16. Spellman, D.L., T.H. Woodstrom, and B.F., Neal, "Faulting of Portland Cement Concrete Pavements," Highway Research Record No. 407, Highway Research Board, Washington, D.C., 1972.
- 4.17. Gulden, W., "Pavement Faulting Study," Final Report Project 7104, Georgia Department of Transportation, 1975.
- 4.18. Colley, B.E., and H.A. Humphrey, "Aggregate Interlock at Joints in Concrete Pavements," Highway Research Record No. 189, Highway Research Board, Washington, D.C., 1967.
- 4.19. Stelzenmuller, W.B., L.L. Smith, and T.J. Larson, "Load Transfer at Contraction Joints in Plain Portland Cement Concrete Pavements," Research Report 90-D, Florida Department of Transportation, April 1973.
- 4.20. "Design, Construction, and Maintenance of PCC Pavement Joints," Synthesis of Highway Practice No. 19, National Cooperative Highway Research Program, Washington, D.C., 1973.
- 4.21. Evaluation of the Performance of Doweled Contraction Joints Placed on Three Types of Subbase Courses," Report No. 30, unpublished internal reports, Georgia Department of Transportation, February 1974.

- 4.22. Darter, M.I., and J.A. Crovetti, "Void Detection Procedures - Appendix C," NCHRP 1-21, National Cooperative Highway Research Program, Transportation Research Board, Washington, D.C., March 1985.
- 4.23. Miner, M.A., "Cumulative Damage in Fatigue," Transactions, American Society of Mechanical Engineers, Vol. 67, 1945, pp. A159-A-164.

CHAPTER 5.0

- 5.1 Hutchinson, R.L., "Resurfacing with Portland Cement Concrete," NCHRP Synthesis of Highway Practice No. 99, Transportation Research Board, Washington, D.C., December 1982.
- 5.2 Ray, G.K., "Design of Concrete Overlays for Pavements," ACI Journal 325.1R-67, ACI Manual of Concrete Practice, Part 2, 1988.
- 5.3 Voigt, G.F., S.H. Carpenter, and M.I. Darter, "Rehabilitation of Concrete Pavement — Volume 3 — Overlay Rehabilitation Techniques," USDOT, Federal Highway Administration, Contract No. DTFH-61-85-C-00004, June 1987.
- 5.4 "Pavement Rehabilitation Manual," published by the U.S. Department of Transportation, Federal Highway Administration, Washington, D.C., March 1988.
- 5.5 Ortiz, D., E.J. Barenberg, M.I. Darter, and J. Darling, "Effectiveness of Existing Rehabilitation Techniques for Jointed Concrete Pavements," Project HPR-3(6), Transportation Research Laboratory, Department of Civil Engineering, Engineering Experiment Station, University of Illinois, Urbana, Illinois, August 1986.
- 5.6 Darter, M.I., E.J. Barenberg, and W.A. Yrjanson, "Joint Repair Methods for Portland Cement Concrete Pavements — Research Report, Design and Construction Guidelines and Guide Specifications, Final Report," prepared for the National Cooperative Highway Research Program, Project 1-21, Transportation Research Board, Washington, D.C., February 1985.
- 5.7 ERES Consultants, Inc., "Techniques for Pavement Rehabilitation," Participants Notebook, National Highway Institute/Federal Highway Administration, Washington, D.C., 1987 Revised Edition.
- 5.8 Tayabji, S.D., and P.A. Okamoto, "Thickness Design of Concrete Resurfacing," Portland Cement Association, Presented at the Third International Conference on Concrete Pavement Design and Rehabilitation, Purdue University, 1985.
- 5.9 "AASHTO Pavement Design Guide, 1986," American Association of State Highway and Transportation Officials, 1986.
- 5.10 "Status of Thin-Bonded Concrete Overlays," Federal Highway Administration, Publication FHWA EP-02-01, Washington, D.C., 1988.
- 5.11 Darter, M.I., "Design of Zero-Maintenance Plain Jointed Concrete Pavement: Vol. 1 — Development of Design Procedures," Federal Highway Administration, Report No. FHWA-RD-77-111, June 1977.

- 5.12 Pierce, L.M., "A Life-Cycle Cost Analysis for the Rehabilitation of Portland Cement Concrete Pavements in Washington State," Master's Thesis, University of Washington, Seattle, Washington, 1988.
- 5.13 Eckrose, R.A., and W.E. Poston, Jr., "Asphalt Overlays on Cracked and Seated Concrete Pavements," Information Series 83, National Asphalt Pavement Association, 1982.
- 5.14 "Crack and Seat Performance," Review Report, Federal Highway Administration, Demonstration Projects Division and Pavement Division, May 1987.
- 5.15 Drake, E.B., "Pavement Rehabilitation by Breaking and Seating Existing Portland Cement Concrete Pavement Prior to Bituminous Concrete Overlays," presented at the 1988 Annual Transportation Research Board Meeting, Washington, D.C., January 1988.
- 5.16 Darter, M.I., E.J. Barenberg, W.A. Yrjanson, and J.F. Daleiden, "Design and Construction Guidelines and Guide Specifications for Repair of Jointed Concrete Pavement — Appendix A," NCHRP No. 1-21, National Cooperation Highway Research Program, Transportation Research Board, June 1984.
- 5.17 Coetzee, N.F., and C.L. Monismith, "Analytical Study of Minimization of Reflection Cracking in Asphalt Concrete Overlays by Use of a Rubber-Asphalt Interlayer," Transportation Research Record 700, Transportation Research Board, Washington, D.C., 1979, pp. 100-108.
- 5.18 Allen, H.S., and K.P. Keel, "Evaluation of an Asphalt Rubber Interlayer," Special Study No. 383, Construction/Interim Report, Minnesota Department of Transportation, August 1985.
- 5.19 Kudd, S.Q., "Asphalt Rubber Stress Absorbing Membrane Interlayers," Interim Report, Report No. FHWA-DP-37, Federal Highway Administration, Washington, D.C., June 1981.
- 5.20 Noonan, J.E. and McCullough, F.R., "Reduction of Reflection Cracking in Bituminous Overlays on Rigid Pavements," Report No. 78, New York State Department of Transportation, 1980.
- 5.21 Dykes, J.W., "The Use of Fabric Interlayers to Retard Reflective Cracking," Proceedings of the Association of Asphalt Pavement Technologists, Volume 49, 1980.
- 5.22 Zollinger, D.Z., and E.J., Barenberg, "Development of Mechanistic Based Design Procedure for Jointed Concrete Pavements," Transportation Research Laboratory, Department of Civil Engineering, University of Illinois at Urbana-Champaign, Research Report 518-2, Project IHR-518, Illinois Cooperative Highway Research Program, 1988.
- 5.23 Van Wijk, A.J., "Rigid Pavement Pumping: (1) Subbase Erosion (2) Economic Modeling," Ph.D. Thesis, School of Civil Engineering, Purdue University, 1985.

- 5.24 Woodstrom, J.H., "Concrete Pavement Drainage in California," presented at the International Seminar on Drainage and Erodibility at the Concrete Slab-Subbase-Shoulder Interface, Paris, France, March 24-25, 1983.
- 5.25 Federal Highway Administration, "Highway Statistics — 1986," Washington, D.C., 1986.
- 5.26 American Concrete Pavement Association, "Take Out the Old . . . Put in 7-Miles of New 6-Lane Concrete Pavement in Just 6 Months," Concrete Pavement Progress, American Concrete Pavement Association Volume 23, No. 3, Arlington Heights, Illinois, May/June 1987.
- 5.27 Donohue & Associates, Inc., "Does PCC Cracking and Seating Work?" National Asphalt Paving Association, Better Roads, January 1986.
- 5.28 U.S. DOT, "Concrete Pavement Restoration and Crack and Seat Rehabilitation Performance Evaluation Reports," U.S. Department of Transportation, Federal Highway Administration, Washington, D.C., May 22, 1987.
- 5.29 "The Status of the Nation's Highways: Condition and Performance," Report of the Secretary of Transportation to the U.S. Congress, Washington, D.C., June 1985.

APPENDIX A
LITERATURE REVIEW

APPENDIX A

LITERATURE REVIEW

A.1 INTRODUCTION

This literature review will concentrate only on the rehabilitation of short-jointed, unreinforced, undoweled PCC pavements (the most common of the PCC pavements constructed in Washington state on the Interstate system).

When an existing pavement, rigid or flexible, requires rehabilitation, a structural analysis of not only the existing pavement but also of the rehabilitation strategy is necessary. The remaining life of the existing pavement, the definition of the failure mode(s), and the determination of future traffic levels are essential for the design of the rehabilitation strategy.

The rehabilitation strategies that will be reviewed in this appendix include the following:

- PCC Overlays
 - Bonded
 - Partially bonded
 - Unbonded
- Asphalt Concrete (AC) Overlays
 - Treatments to the existing surface
 - Crack filling
 - PCC slab subsealing
 - Cracking and seating
- Stress relieving interlayers
 - Fabrics
 - Asphalt rubber
- Removal and replacement
 - No changes to the base material
 - Concrete stabilized base
 - Asphalt treated base

- Drainage considerations
- Maintenance
- A life cycle analysis of the rehabilitation strategies

A.2 OVERLAYS

Overlays are used in pavement rehabilitation to restore pavement distresses. Often overlays are used to correct a loss in skid resistance, decrease pavement surface roughness, improve surface drainage, arrest structural deterioration, and meet a need to increase the load carrying capacity of the facility. The type of overlay needed for each pavement depends on the function of the overlay and the type and condition of the existing pavement. [A.1] The principal types of overlays to be considered are PCC (rigid) overlays (bonded, partially bonded, and unbonded) and AC (flexible) overlays.

All types of overlays provide a smooth wearing surface, increase serviceability, and decrease user costs. Therefore, additional information must be obtained to determine which overlay type is most appropriate in the rehabilitation of the pavement structure. First, the structural adequacy of the existing pavement must be determined. The type of overlay is highly dependent on the structural soundness of the existing pavement. If the surface distress is light, then several overlay options are available, and the life-cycle cost analysis is the primary factor in the selection process. On the other hand, if the surface distress is heavy, the overlay options are limited and the selection process is based not only on the life-cycle cost analysis but also the structural adequacy of the overlay. Secondly, the amount of load transfer that exists across the joints and any existing cracks also limits the types of overlays to be considered because of the process of crack reflectance. Other factors that should be considered include the following: "initial construction costs, life-cycle costs, overhead clearance problems, curb clearances, traffic control constraints during construction, design reliability and expected performance, future maintenance options,

material availability, energy and environmental constraints" [A.1], and the effect the rehabilitation will have on the user of the facility and on the state's economy.

Upon completion of the existing pavement evaluation, as described above, a decision must be made about whether the overlay should be rigid or flexible. This decision must be based not only on the structural performance of the overlay but also the cost of the rehabilitation strategy. Both material types offer benefits, and these benefits will be discussed in detail in the following sections.

A.3 PCC OVERLAYS

There are essentially three types of rigid overlays. As discussed earlier, they include bonded, partially bonded, and unbonded. Each form has advantages and limitations.

A bonded overlay corrects existing surface irregularities such as studded tire wear and construction related pavement roughness. Because of the minimum overlay thickness (2 to 3 inches), problems associated with overhead clearances, and the need to match other pavement surfaces such as shoulders is minimized. Some disadvantages associated with a bonded overlay include the requirement of a structurally sound existing pavement, critical surface preparation to ensure adequate bonding, exact alignment of the existing joints with the joints of the overlay, and high initial construction costs. Because of the requirement that the existing pavement be structurally sound, this form of overlay is not suitable as a rehabilitation alternative, since both SR 5 in Seattle and SR 90 in Spokane are exhibiting structural defects (longitudinal and transverse cracking, joint faulting).

Partially bonded PCC overlays generally have a minimum thickness range of 5 to 7 inches and require no special design considerations for bonding the overlay to the existing PCC pavement. A disadvantage associated with this type of overlay is that if structural defects exist in the underlying pavement, they will tend to reflect through the overlay. Furthermore, with the bonded overlay, the construction of the partially bonded overlay

requires the alignment of the existing joints with the joints of the overlay. In addition, overhead clearances may not allow overlays of this thickness.

The third and final type of rigid overlay is the unbonded PCC overlay. The minimum thickness of a unbonded overlay is about that of the partially bonded overlay (5 to 7 inches), but often it is thicker (approximately equivalent to new PCC pavements on a stiff subgrade). This type of overlay is acceptable on existing PCC pavements that are exhibiting some form of structural distress. Alignment of joints and extensive surface preparation is not necessary, and unbonded overlays offer the greatest potential for long-term, relatively maintenance-free performance. However, with these advantages come disadvantages, such as the fact that the construction of an unbonding medium (usually a layer of AC) is required. Construction of the unbonded overlay requires the longest construction period duration. It has the highest construction cost in comparison to all the overlays considered, and overhead clearances may be a problem.

A.4 FLEXIBLE OVERLAYS

The primary objective of any overlay design is to provide a highway with adequate performance over a maximum useful life with a minimum amount of required maintenance. [A.2] AC overlays are the most widely used and accepted form of roadway surfacing because of their low initial costs, relative ease of application, improvements to the surface rideability, and increases to the load carrying capacity of the roadway.

When engineers consider the use of a flexible overlay over an existing PCC pavement, their main concern is reflection cracking. A reflection crack will develop when there are horizontal and/or vertical movements between the existing PCC pavement and the AC overlay. AC has low strength under low rates of loading; therefore a crack may develop in the overlay where there is significant movement in the underlying slab. [A.3] The horizontal movements are due to the expansion and contraction of the existing slab caused by temperature and moisture changes. [A.2] The differential vertical movements are

a function of the load transfer ability at the cracks and/or joints. The load transfer ability of the cracks and joints is dependent on the slab temperature; the amount of slab support; the efficiency of dowels, when present; the traffic loadings; the amount of curling of the slabs; the amount of aggregate interlock; and the presence or absence of moisture in the supporting layers. The majority of reflection cracking is caused by movements in the slab due to thermal effects. [A.3]

The prevention of crack reflectance is critical in obtaining the expected performance period of the AC overlay. Once the crack and/or joints have reflected through the overlay and are subjected to repeated traffic loadings, ravelling and spalling of the crack may occur. These may lead to water intrusion. Water intrusion can loosen the bond between the surface and the underlying pavement, which can result in premature fatigue cracking and/or pumping of fine material and a decrease in the amount of subgrade support.

Several methods have been tried to prevent or at least minimize reflection cracking of the AC overlay. As of yet, there is no proven overlay method that can be successfully applied to completely prevent reflection cracking in the AC overlay. Methods that have been partially successful include the following: greater thickness of the overlay, treatments to the existing pavement before overlaying (crack and joint sealing, subsealing, and cracking and seating), and stress-relieving interlayers (asphalt rubber, membranes, fabrics, and open-graded AC). [A.3] These methods to reduce crack reflection are discussed further below.

A.4.1 Thickness of the Overlay

There is evidence that reflection cracking may be reduced by increasing the thickness of the overlay. [A.4, A.5] The thickness of the AC overlay required to retard reflection cracking on PCC pavement is dependent on the amount of load transfer at the joints and/or cracks. One can assume that the thicker the overlay is, the greater will be the load transfer capabilities over the crack and/or joint, and the longer will be the life of the

overlay before cracks will be reflected to the surface. [A.6] A cost analysis should be conducted when significant thickness is required to restore the structural capacity of the roadway. However, "the results of several reflection cracking studies, where the overlay varied from 1-1/2 to 10 inches, all showed some degree of reflection cracking." [A.7] Unfortunately, increasing only the thickness of the AC overlay does not necessarily eliminate reflection cracking.

A.4.2 Treatment of Existing Pavements

When a PCC pavement is prepared for an asphalt concrete overlay, essentially three treatments can be applied to the existing PCC surface. These include crack filling, stabilizing PCC slabs by subsealing, and cracking and seating of PCC slabs.

A.4.2.1 Crack Filling. Little experimentation has been reported on the effect of crack filling on reflection cracking. [A.6] For almost every overlay process, cracks greater than 1/4- or 3/8-inch wide should be filled before overlaying. [A.6] Wyoming constructed an experimental AC overlay using 90 percent CRS-2 emulsion and 10 percent latex rubber as the crack sealant. [A.8] The study concluded that the crack sealer did not significantly reduce reflection cracking. In Texas, a sulfur compound was used as a crack filler on an auxiliary PCC runway at Kelly AFB. [A.9] The study reported that the crack sealer minimized reflection cracking. These variations may have been due to the type of crack filler used, construction practices, and/or traffic loadings experienced on each project. To not fill significant cracks (1/4 or 3/8 inch) is an error, for the purpose of filling cracks is to restrict surface water from entering the supporting base and/or subgrade. [A.6] A base and/or subgrade with reduced moisture provide greater load support, less surface deflection under load, and consequently, less potential for reflection cracking. [A.6]

Caution is warranted in that joint sealants and crack filling materials and associated application techniques must be compatible with AC overlays. Experience with construction of an AC overlay on SR 90 near Spokane during 1989 further suggests this.

A.4.2.2. Subsealing. The necessity in stabilizing PCC slabs by subsealing is to minimize the differential slab movements at a joint or crack. The slightest differential movements of the PCC slab can cause reflection cracking in the AC overlay. [A.6]

The loss of support near transverse joints and working cracks caused by the pumping of base and/or subgrade fines is one of several major causes of concrete pavement deterioration. [A.10] As further loadings are applied, the pumping action increases and the void increases in size. As the void size increases, corner loadings along the outer edge force the leave slab to act in a cantilever fashion, which generally leads to serious faulting, corner breaks, and or diagonal cracks across the slab. [A.10]

In many states it has become standard practice to subseal slabs by injecting a grout mixture. What is lacking in this procedure is the determination of the locations where loss of support exists. This deficiency has led many agencies to subseal on a "blanket coverage" (all joints and working cracks) basis. [A.10] This "blanket coverage" creates several problems: (1) it is not possible to determine whether and where any voids exist; (2) an estimate of the grout quantity required to fill existing voids is unknown; and (3) the extent to which the voids were filled and support restored is questionable. The difficulty involved with subsealing slabs is in the determination of the location and size of these underlying voids. Several methods have been developed to measure the size of these voids. Two methods, in particular, were developed by Crovetti and Darter. [A.11] The first method uses NDT (non-destructive testing) deflection measurements and a graphical plot of the load versus deflection to rapidly detect, in the field, the "presence of voids by analysis of the load/deflection response at slab corners." [A.11] The second method determines "the existence of a void and an estimate of its horizontal area using deflection measurements from center slab and corner locations" [A.11] and standardized adjustment factors. These two methods were developed using the ILLISLAB finite element computer program computer and models of loadings. Though continued research is still necessary

for these methods, this is an interesting approach in the determination of voids beneath slab joints and cracks.

A.4.2.3 Cracking and Seating. The concept behind cracking and seating PCC slabs, before AC overlay, is to minimize the amount of horizontal and differential vertical movements at the slab joints and cracks. Breaking the slab into smaller sections reduces localized horizontal movements, and seating the slab reduces differential deflections at the joints and cracks caused by the presence of voids. [A.7] The benefits of cracking and seating, followed by an AC overlay, is that reflection cracking can be prevented or delayed; service life can be extended; maintenance costs are reduced; and traffic disruptions are minimized in comparison to other rehabilitation alternatives (e.g., removal and replacement of PCC overlay).

Essentially two pieces of equipment are used in cracking and seating the existing PCC slabs, an impact hammer and a heavy roller. The impact hammer should be capable of delivering enough energy to break the pavement without causing spalling. Enough energy has been developed when the cracking technique results in a fine crack that runs through the complete depth of the slab. Because of excessive surface spalling, machines with sharp cracking tools should not be used, and impacts should not be made within one foot of another crack or joint. [A.12] To prevent surface spalling, "the breaker shall be equipped with a plate-type shoe designed to prevent penetration into the existing surface." [A.13] Pneumatic rollers weighing 15 tons or more, with five passes, provide the best seating effect. [A.12] A pneumatic-tired roller is specified because of steel drum rollers and vibratory rollers tend to bridge over the cracked pieces and do not effectively seat the slabs and therefore are generally not used for seating purposes. Adequate seating of the slabs is critical to the performance of the overlay. Without proper seating, the broken slabs may rock and cause reflection cracking in the AC overlay, while "overworking" the slabs tends to cause loosening and drastically reduces the load carrying capacity of the PCC. Because of the variation in equipment, slab thickness, subgrade characteristics, and

contractors, a test section should be used so that the necessary amount of energy to crack the slabs and the required weight and number of passes of the roller can be established.

The optimum size of the cracked pieces is still a matter of debate. Several studies have been performed to determine the optimum size of the cracked pieces, but depending on the governing agency and the characteristics of the test site, these dimensions vary. In pavements with reasonably firm subgrades or bases, cracked sizes of 2 to 3 feet with 3 to 5 inches of AC overlay thickness have performed best to date. [A.14] The California Transportation Laboratory in Sacramento reported that the nominal cracked dimension of 4 ft by 6 ft and 4.2 inches of AC overlay with a fabric interlayer has performed the best (additional details on Caltrans practice can be found in Appendix I).

Joint inspection should be made before cracking and seating operations. Badly deteriorated joints or cracks may require repair and should also serve as a warning that voids may be under the joint or crack and may need subsealing. The Asphalt Institute recommends stabilization and subsealing if the mean deflection at the joint is greater than 0.014 inches and if the differential deflection is greater than 0.002 inches. [A.15]

Another major concern with cracking and seating of PCC pavements is whether traffic should be allowed to travel on the cracked pavement before seating and overlaying. The current practice in California is to not allow traffic on newly cracked PCC, nor on the leveling course of asphalt for up to 15 days. In addition, California's specifications state that cracked pavements have to be seated not more than 24 hours before overlaying. Most differential vertical displacement reduction is achieved during the pavement cracking operation, before seating efforts. [A.16] This suggests that it is ineffective to seat the pavement immediately after cracking. However, traffic using the cracked pavement has been found to cause some "unseating," probably due to rocking of the slab segments. [A.16] Therefore, if traffic is to be allowed on the cracked pavement, seating should be done just before to overlay paving and after traffic exposure. [A.16]

After the concrete has been cracked, support must rely on the aggregate interlock and base or subgrade support to prevent vertical movement of the individual slab pieces. [A.17] Selection of a project for cracking and seating is dependent upon the support and drainability of the pavement base or subgrade. [A.17] Recent experience has indicated that non-reinforced pavements that have been cracked and are then seated into a poor base or subgrade are susceptible to rocking or vertical movements of some of the pavement pieces. [A.17] If a section of roadway has a history of frost heaving or other base or subgrade deficiencies, cracking and seating plus an AC overlay will not improve the condition. [A.17]

The use of cracking and seating with an AC overlay should be approached with caution. Of 22 projects, only four showed less reflection cracking than the control sections. [A.7] Reduction is obvious in the first few years, but after four or five years the crack and seated section exhibits approximately the same amount of reflection cracking as the control sections. A significant reduction in reflective cracking occurred on projects in Florida and California. [A.12] These states found that cracking and seating had the best performance under the same limitations as other methods used to reduce crack reflectance. These limitations include the following: (1) construction on a strong base or subgrade, (2) location in areas where there are small changes in the seasonal temperature, and (3) non-reinforced pavement. [A.12] A strong base will help by minimizing the differential deflections of each pavement piece. Small changes in the seasonal temperature understandably result in less thermal movement in the slab, thereby reducing tensile stress in the AC overlay and the possibility of reflective cracking. [A.12] With non-reinforced pavements, the aggregate interlock is the controlling factor in resisting differential deflection or vertical movement. [A.12] In addition, non-reinforced pavements generally have shorter slab lengths (15 - 20 feet) than reinforced pavements, which reduces the thermal movement at the joints and should reduce reflective cracking.

The reduction of the structural capacity of the existing pavement is an undesirable feature of the cracking and seating procedure. Cracking and seating of the cracked sections has a direct relationship to the structural capacity of the pavement. [A.18] According to the 1986 AASHTO Design Guide, the suggested structural coefficients of the cracked and seated pavement are as follow:

<u>Crack Spacing</u>	<u>Structural Layer Coefficients</u>
1 foot	0.25
2 feet	0.35
3 feet	0.45

Since the structural capacity of the existing pavement is reduced, more overlay thickness is required to maintain the same structural number as the non-cracked pavement. [A.12] Using an overlay analysis procedure such as AASHTO's would result typically in the need for at least 3 inches to maintain equivalent structural capacity. [A.12] The additional cost of the additional overlay thickness, the cracking and seating operation, and other required work must be evaluated to determine whether these costs are justified.

In conclusion, cracking and seating may provide benefits under some conditions by delaying, not eliminating, reflection cracking. These benefits are limited to pavements that are non-reinforced, have relatively strong bases or subgrades, and are in areas that have small changes in the seasonal temperature.

A.4.3 Stress-Relieving Interlayers

The principal objectives of a stress-relieving interlayer is to minimize the thickness of the overlay needed to rehabilitate a roadway surface and to prevent or slow the process of reflection cracking. Although laboratory experimentation and theoretical analyses have determined that interlayers can reduce the high stresses developed at a crack or joint, as of yet, a proven design method to utilize stress-relieving interlayers to the fullest advantage has not been developed. [A.6] Several interlayer methods have been studied and tried, and

these include, but are not limited to, the use of an asphalt-rubber interlayer, fabric interlayer, and fiber reinforcement.

A.4.3.1 Asphalt-Rubber Interlayer. In the late 1960s experiments were conducted in Sweden on the effects of mixing rubber particles into asphaltic pavements. A system incorporating 3 to 4 percent by weight of relatively large (1/16 to 1/4) rubber particles into an asphalt pavement was developed to increase skid resistance and durability, and it was found to provide a new form of wintertime ice control. [A.19] Initially, in the United States, the primary reason for using rubber in AC overlays was to find a suitable way of disposing of a waste material, discarded rubber tires.

Several analytical studies have been conducted that show that the asphalt-rubber interlayer is an effective mean of reducing the stresses that develop at the interface of the existing pavement and that of the AC overlay. One particular study reported that, an approach to relieving these stresses that appears to be promising is the placement of a thin (1/4- to 3/8-inch) asphalt-rubber membrane of low stiffness and high deformability. [A.20] This study showed that the asphalt-rubber interlayer significantly reduced the developed stresses. The stresses in a pavement that contained the asphalt-rubber interlayer were one-sixth to one-eighth those in a pavement that did not contain such a layer. [A.20] The thickness of the AC overlay significantly affected the stress at the crack tip in the pavement that did not have a rubber-asphalt layer, but had little effect on the pavement that did. [A.20] For a given situation, the study found that "a pavement that does not have an asphalt-rubber interlayer would require a total of 5.5 inches of AC to achieve the same crack-tip stress level as 2 inches of AC and a 1.6 inch rubber-asphalt interlayer." [A.20] Even though an analytical study has determined that the use of an asphalt-rubber interlayer effectively reduces the possibility of reflective cracking, field testing will be the deciding key to its success.

As with all methods of reducing reflective cracking, the performance of asphalt-rubber interlayers varies from state to state. The Minnesota Department of Transportation

has conducted several field studies on the performance of asphalt-rubber interlayers. [A.21] In one study, the results showed that a 4-inch AC overlay had significantly less reflective cracking than did a 3-inch AC overlay with an asphalt-rubber interlayer. The Minnesota Department of Transportation concluded that "the asphalt-rubber interlayer has not significantly reduced the amount of reflective cracking in the new AC overlay when compared to the test section with no asphalt-rubber interlayer." [A.21] In contrast, a study was conducted for the Federal Highway Administration that found "The addition of recycled rubber to certain asphaltic materials not only has provided a means of disposing of waste material, but a beneficial use has been demonstrated in field tests." [A.22] This study concluded that "the asphalt-rubber when placed as a seal coat (SAM) will control reflection of fatigue cracks and is an alternate to a major overlay. When placed as a SAMI, it will effectively control reflection of all cracks." [A.20] The obvious advice in this situation is to construct field test sites, and on the basis of their performance, determine how effective asphalt-rubber interlayers are in limiting the process of reflective cracking.

A.4.3.2 Fabric Interlayer. Starting in the late 1960s and continuing through the 1970s, synthetic fabrics have been increasingly used under AC overlays. [A.6] The fabrics are manufactured from polypropylene, glass, nylon, polyester, or a combination of the above. The principal fabrics currently in use in the United States for pavement rehabilitation are polypropylene and polyester. [A.6] These fabrics are manufactured by several processes, including needle-punched, spunbonded, woven, and in various combinations of the above. [A.23] Fabric interlayers are used to retard or prevent reflection cracking and to waterproof the pavement structure to prevent surface water from entering the AC overlay. [A.6] As with most overlay construction procedures, proper surface preparation is critical to the performance of the overlay. Proper surface preparation includes sealing of all joints and cracks where necessary, and the stabilization of slabs so that vertical movements are minimized. [A.24]

As was discussed previously, the best way to determine the effectiveness of a particular method in reducing reflection cracking is the construction of a test site. In Georgia, testing was performed on the effectiveness of placing an 18-inch wide strip of Bituthene, a prefabricated membrane, over the transverse and longitudinal center-line and shoulder joints of PCC pavements. [A.6] The strips were covered with AC overlays of 2, 4, and 6 inches. After 15 months of service, the 2-inch section was performing well, while 88 percent of the joints from the corresponding control section reflected through the overlay. [A.25] After four years, the material is still performing well, particularly under the 4- and 6-inch overlays. [A.25] The performance of this system should be viewed cautiously, and one should ask whether the performance is based on the action of the fabric strip or on the thickness of the overlay. Virginia reported on the effect of fabric on crack reflection where there is differential vertical movement at the cracks. [A.24, A.26] The following conclusions were based on the study's results:

1. Neither sand as a bond breaker nor high strength fabrics as stress relieving layers are effective in reducing reflection cracking where vertical joint movement is a significant factor.
2. When differential deflections are greater than about 0.002 inches, reflection cracks form early. Such cracking is delayed for lower differential deflection but may occur as the magnitude and frequency of wheel loadings increase.
3. An asphalt impregnated polypropylene fabric or an unwoven, spun-bonded nylon fabric have been found to sustain the formation of reflection cracking when placed to span the joints of an existing PCC pavement and then covered with an AC overlay.
4. An asphalt impregnated polypropylene fabric spanning the joints in PCC pavements, and placed between the pavement and an asphaltic overlay, may be effective in reducing the infiltration of surface water to pavement sub-

layers. There is some evidence that pavement pumping may be reduced by this method.

5. Both an asphalt impregnated polypropylene fabric and an unwoven, spun-bonded nylon fabric can delay the formation of reflection cracking. There is strong evidence, however, that such cracking is fatigue cracking and will eventually develop under the application of repetitive wheel loadings.

Iowa has tested the performance of three fabrics placed under a 3-inch AC overlay on an existing 20-foot wide PCC pavement that was widened to 24 feet. [A.27] Iowa reported that in comparison to the control (the report did not report the thickness of the control section, but 3 inches can be assumed) the use of fabrics reduced reflection cracking, and that reflection cracking over the pavement widening crack was nearly eliminated. [A.6] In tests conducted in Louisiana, "the use of two fabrics on PCC failed to eliminate or reduce cracking in comparison to the control sections." [A.28] In Georgia a test involving the use of Mirafi and Petromat over PCC showed the benefit of thicker overlays over fabric in comparison to the control sections. [A.25, A.29]

Further evaluation is necessary before the use of fabrics can be included in design concepts. [A.6] The benefits of asphalt-saturated fabrics in retarding penetration of water have been recognized by some agencies, but the benefits have not been quantified. [A.6]

A.4.3.3 Fiber Reinforcement. As with the above two methods for reducing reflection cracking, standardized methods for using fibers in asphalt pavements need to be defined on the basis of an understanding of the interactions that occur as a result of the introduction of fibers. [A.30] A study was conducted in Texas on the use of eight types of chopped synthetic (polypropylene and polyester) fibers. From this study the following conclusions were drawn: [A.30]

1. The addition of fibers to an asphalt paving mixture normally requires (or allows) a slight increase in the optimum design asphalt content. The

increase in asphalt content is dependent upon the quantity and surface area per unit weight of fibers added and the type and gradation of the aggregate.

2. The stability of a given fiber mixture does not decrease as rapidly as the nonfiber mixture when the asphalt content exceeds optimum.
3. A given dense, graded, asphalt paving mixture containing synthetic fibers requires more compactive effort to produce a pavement density equal to that normally obtained without fibers.
4. According to results from resilient modulus tests, stiffness of the fiber mixtures is not appreciably different from that of the control (no fibers) mixture at any temperature from -10° F to 100° F.
5. Indirect tension tests revealed that, overall, the addition of fibers to a paving mixture causes a slight decrease in tensile strength and a slight increase in tensile strain (elongation) at failure. The increased tensile strain is likely due to the additional asphalt, as well as the fibers in these mixtures, and shows that fibers and additional asphalt add flexibility to the asphalt concrete mixture.
6. Generally, a mixture containing fibers is less susceptible to moisture induced damage than a similar mixture containing no fibers.
7. On the basis of a limited number of constant-stress flexural fatigue tests, it appears that synthetic fibers have the potential to increase fatigue performance of asphalt concrete paving mixtures. Fibers appear to be most beneficial at high strain levels.
8. Laboratory tests on fiber and nonfiber asphalt mixtures at 33° and 77° F indicate that fiber mixtures will exhibit significantly greater resistance to crack propagation at relatively high strain levels. Apparently, the fibers aid in distributing the stresses away from the crack site.

9. Pavement performance predicted with mathematical models have shown that properly designed asphalt paving mixtures containing fibers have the potential to increase overall pavement service life. Further, fiber mixtures exhibited the capacity to reduce rutting but not cracking in an asphalt pavement.
10. Review of field tests conducted by other agencies has indicated that synthetic fibers in hot mixed asphalt concrete will often reduce reflection cracking. However, fibers have not been established as a cost effective construction alternative.
11. Fibers can be successfully employed in drum mix plants using modified fines feeding equipment. Fibers can also be mixed in the asphalt cement before it is introduced into the drum; however, this process requires special equipment.

In a study conducted by the city of Tacoma in November of 1983, the city replaced three major arterial intersections that were showing signs of deterioration with 3 inches of fiber (BoniFibers) reinforced ACP. It also replaced one control intersection with 3 inches of Washington State Department of Transportations standard Class B AC. As of October 1987, the BoniFiber section is performing the same as the control section, neither of which are showing signs of distress.

Though the importance of reducing the degree of reflection cracking is necessary for the performance of the AC overlay, careful consideration must be made to include the costs associated with each method. This fact cannot be overemphasized. When an AC overlay is designed with one of the previously mentioned methods, one must consider whether using an interlayer or treating the surface is as cost effective as increasing the thickness of the overlay. The cost of an interlayer or a surface treatment may be more expensive than the addition of an extra inch of AC where both may have the same effect in reducing reflection cracking. Until a guaranteed method of minimizing reflection cracking

can be developed, the designer will be responsible for using good engineering judgment and cost analysis in the selection of the rehabilitation strategy when an AC overlay is being incorporated into the rehabilitation design.

A.5 REMOVE AND REPLACE

When a PCC pavement is restored through removal of the existing material and replacement with the same, several benefits and disadvantages become apparent. The benefits of a removal and replacement project are based on the amount of capital required for initial construction and on the funding limitations. These benefits and disadvantages are briefly discussed in the following paragraphs.

Obviously, when a PCC pavement is removed, the concern of reflection cracking is totally eliminated. Though reflection cracking is no longer a problem, the overriding constraint is that of the initial construction costs and the length of the construction period. The length of the construction period has the largest impact on the user of the facility. User costs can approach the costs associated with the costs of initial construction.

When a PCC pavement is to be restored, the pavement life of the replaced material, assuming it is concrete, is expected to equal or exceed the life of the pavement it is replacing. This expectation for increased life is based on the improvements in materials (the use of high strength and more durable concrete), increased pavement thickness, the knowledge of previous performance, and the adjustments that can be made to improve any future projects. In addition, the knowledge of using a stabilized base material beneath the concrete slabs significantly affects future performance levels. The California Department of Transportation, Caltrans, has installed several miles of PCC pavements over concrete stabilized base. The performance of these slabs has not been as well as expected. Pumping and faulting of the slabs have been the prevalent failures and have lead to the conclusion of poor pavement performance when concrete stabilized base was used in this type of environment. On the other hand, the Washington State Department of

Transportation and other agencies have found the performance of PCC pavements that are over an asphalt treated base (ATB) to be excellent (WSDOT would likely use a Class E specification). It is expected that an ATB will offer several years to the life of the PCC pavement. Therefore, consideration should be given to the inclusion of an ATB, for though the initial construction costs are higher, the benefits of reduced or no future maintenance and increased service life are positive attributes that need recognition.

Another consideration that needs to be addressed when a PCC pavement is restored is whether to recycle the removed concrete and use it as aggregate for the "new" pavement. Although high-quality aggregate is still available in Washington State, environmental, energy, and other factors could affect the future availability and costs of the aggregate. The problems (i.e., cost and environmental) associated with the disposal of the removed concrete must also be considered.

The mix design of the new (recycled) concrete is still a critical item, and all of the variables must be taken into account. [A.31] These variables include the following:

1. the type of aggregate used in the original pavement,
2. the condition of the existing pavement (i.e., the presence of D-cracking),
3. the amount of recycled fines to be permitted in the new concrete,
4. the use of fly ash, and
5. the amount of water reducer-super plasticizer in the mix.

A study conducted by agencies such as the Army Corps of Engineers [A.32, A.33], Waterways Experimentation Station, the Iowa Department of Transportation [A.34], Massachusetts Institute of Technology [A.35], the Minnesota Department of Transportation, Michigan Department of Transportation, and the Federal Highway Administration, produced the following findings [A.35]:

1. The aggregate particles produced by crushing concrete have good particle shape, high absorptions, and low specific gravity in comparison with conventional mineral aggregates.

2. The use of crushed concrete as a coarse aggregate had no significant effect on mixture proportions or workability of the mixtures in comparison with the control mixtures.
3. When the crushed concrete was used as a fine aggregate, the mixture was less workable and required more cement because of the water demand. The study found that the substitution of a natural (well-rounded) sand for a portion of the fine aggregate was required to produce a workable concrete. Iowa uses about 30 percent natural sand to obtain the workability of its standard pavement mixture, which contains a 50-50 mixture of coarse and fine aggregate.
4. Research has shown a substantial increase in frost resistance of concrete made from recycled aggregates when it is compared to concrete made from normal conventional aggregate.
5. The durability of concrete made with aggregate subject to "D" cracking can be substantially improved by recycling.
6. The use of recycled aggregate did not have any significant effect on the volume response of specimens to temperature and moisture effects.
7. The use of low strength recycled concrete as aggregate need not be detrimental to the compressive strength of concrete mixtures that contain this aggregate.
8. The use of concrete aggregate from building rubble that contains excessive amounts of contaminating sulfate resulted in deleterious sulfate reactions. Therefore, the amount of sulfate should be restricted to one percent or less of the total aggregate by weight to be safe.
9. The use of water reducing admixtures to lower the water content is effective in increasing strengths of concrete mixtures that contain recycling concrete as aggregate.

On a removal and replacement project in Oklahoma [A.37], "Engineers estimated that the work would have cost \$6 million if virgin aggregate had been used. About \$800,000 was saved (a savings of approximately 13 percent) by recycling the old pavement and thus avoiding the purchase of 63,000 tons of virgin aggregate." To be cost effective, the recycled pavement must remain serviceable for as many years as a pavement produced with virgin aggregate. [A.37] The Michigan Department of Transportation reported a reduction in aggregate costs of 50 to 65 percent by using recycled concrete instead of virgin aggregate. [A.31]

The potential impact of the use of recycled concrete pavements will increase because of the shortage of materials in certain areas (mainly urban); the problem of solid waste disposal; the increased cost of materials, and hauling of materials to the job site; and savings in energy and initial construction costs.

A.6 DRAINAGE

The importance of a good drainage system can not be overstated. It is well known that the intrusion of surface water into the pavement decreases the performance of the supporting soils, which have a great effect on the expected life of the entire pavement system. The decrease in performance caused by inadequate drainage can cause premature distress such as cracking, faulting, increased roughness, and a relative rapid decrease in the level of serviceability. [A.38]

When a rehabilitation strategy includes that of an overlay, drainage improvements are difficult because of construction practices. Edge drains may be installed, but because of the dimensions of the drainage trench, adequate compaction may be difficult to achieve. Adequate compaction is required to prevent the settlement of the overlying pavement or shoulder under the impact loading of traffic. [A.38] Care must be taken not to cause damage or disruption of the collector pipe system during the compaction process. If the overlay involves the use of a fabric interlayer, it may improve the drainage of the pavement

for a couple of years. However, beyond this time frame performance is questionable because of possible clogging of the fabric with fine material or possibly a tear in the fabric due to the high stresses between the PCC slab and the interlayer.

If the rehabilitation strategy will result in the selection of removal and replacement, then improvement of the drainage system will not have any significant impact on construction practices and should be designed according to new construction.

A.7 MAINTENANCE

Maintenance of each particular rehabilitation strategy is important to the performance of the pavement, as well as the economic comparisons of all strategies. It is obvious that, depending on the type of rehabilitation, the amount of maintenance required will vary from strategy to strategy. For example, an AC overlay will require more maintenance than if the pavement is completely removed and replaced. There is also a difference in maintenance practices if a stabilized base is used. Unfortunately, the data required to effectively determine the amount, the timing, and the location of maintenance practices is still difficult to quantify and qualify.

A.8 LIFE-CYCLE COST ANALYSIS

The purpose of a life-cycle cost analysis is to evaluate the economics of a paving project. A life-cycle analysis "should be made of the potential design alternatives, each capable of providing the required performance." [A.39] If all other things are equal, the alternative that is the least expensive over time should be selected; that is, the design engineer should try to find the design that will serve the needs of the traffic volume and loads for a given level of service for the lowest cost over time. [A.40] A life-cycle cost analysis is one that considers the cost of construction, operation, and maintenance of a facility over the entire analysis period.

Several economic methods can be used to evaluate the alternative rehabilitation strategies. For the purpose of this study, a present worth procedure was used and is discussed below.

A.8.1 Present-Worth Method

The present-worth method is an economic method that involves the conversion of all present and future expenses to a base of today's costs. [A.41] The present worth of some planned future expenditure is equivalent to the amount of money that would need to be invested now at a given compound interest rate for the original investment, plus interest to equal the expected cost at the time it is needed. [A.39] All costs are predicted and they are then reduced to one single cost in the present. [A.39] The totals of these present-worth costs are then compared, one with another, and the lowest cost alternative is chosen, providing all other factors are equal. [A.42]

"Equation (1) is for the single present worth of a future sum of money for a given number of years with a given discount rate. This equation is for nonrecurring costs." [A.39]

Basic Components

$$PW = F \frac{1}{(1 + i)^n} \quad (1)$$

where,

- PW = Present Worth.
- F = Future sum of money at the end of "n" years from now that is equal to PW with a discount rate of i.
- n = Number of years.
- i = Discount rate per time period.
- SPW = Single-payment present worth factor = $\frac{1}{(1 + i)^n}$

The present worth of a single future value F, can be determined by multiplying it by the single-payment present-worth factor (SPW). [A.39] Values for SPW are located in the economic tables in Appendix C.

Equation (2) is used to determine the present worth of a series of end-of-the-year payments for a given number of years with a given discount rate. This equation is for recurring costs. [A.39]

$$PW = \frac{A(1+i)^n - 1}{i(1+i)^n} \quad (2)$$

where,

PW = Present Worth

A = End-of-year payments in a uniform series for "n" years that is equivalent to PW at discount rate i.

n = Number of years.

i = Discount rate per time period.

UPW = Uniform present worth factor. $= \frac{(1+i)^n - 1}{i(1+i)^n}$

The present-worth of a series of annual payments, A, can be determined by multiplying A by the uniform present-worth factor (UPW) for given values of n and i. Values of UPW are located in the economic tables in Appendix C.

In summary, the general equation to be used in determining the life-cycle cost for a given rehabilitation alternative is illustrated in the following equation:

$$PW = \text{Initial Construction} + (\text{Maintenance Costs})(UPW) + (\text{Rehabilitation Costs})(SPW) + (\text{User Costs})(UPW) + (\text{Salvage Value})(SPW)$$

The factors that incorporate and influence the outcome of the life-cycle cost analysis include the analysis period, construction costs, maintenance costs, rehabilitation costs, user costs, salvage value, energy costs, interest and inflation, and discount rates. The following paragraphs briefly define the above factors.

A.8.2 Analysis Period

The analysis period is the time period used for comparing design alternatives. An analysis period may contain several maintenance and rehabilitation activities during the life cycle of the pavement being evaluated. For the present worth procedure, all alternatives should be evaluated over the same analysis period. [A.39]

A.8.3 Construction Costs

The construction costs include "the costs for building a section of pavement in accordance with the plans and specifications." [A.39]

A.8.4 Maintenance Costs

Maintenance costs are "those costs associated with maintaining a pavement at or above some predetermined performance level. This includes both corrective and preventive maintenance but does not include rehabilitation." [A.39] As a general rule, the Washington State Department of Transportation does not perform significant pavement structure maintenance on the interstate PCC pavements; the cost analysis in Chapter 5.0 therefore did not include the costs due to maintenance.

A.8.5 Rehabilitation Costs

Rehabilitation costs are those "costs (that) cover the types of activities performed as part of rehabilitating or restoring the pavement. These represent periodic costs at future dates used to restore the pavement to an acceptable performance level." [A.39]

A.8.6 User Costs

User costs are those "costs (that) are accumulated by the user of the facility as related to pavement type, pavement condition, maintenance activities, or rehabilitation work." [A.39] These may be in the form of delay costs (due to speed changes, speed reductions, and idling time), operating costs (fuel consumption, tire wear, vehicle maintenance), costs due to accidents (fatal, non-fatal, and property damage), and user

discomfort costs. The cost associated with denial-of-use is also part of this item. [A.39] The user costs may reach such high values that its neglect can result in major errors in the economic evaluation of pavement rehabilitation alternatives.

During the course of research for this project, essentially two methods were located in determining the costs associated with the user of the facility. The first method was developed by Texas A & M University [A.43] in 1975. This study generated costs associated with time and operating due to speed changes, traveling at uniform speed, and idling. These operating and time costs are shown in Tables A.1 through A.4, with respect to the speed of travel. A factor of 2.08 was applied to these values to reflect costs as of October 1987. This factor was determined by dividing the Consumer Price Index (all items) for December of 1975 (166.3) into the Consumer Price Index (all items) for October of 1987 (345.3). [A.44]

A second method was developed by the Caltrans Highway Operations Branch, District 04. [A.45] The intent of this report was to document the traffic performance of the existing freeway system. This study used a "floating car" method to collect field data on freeway congestion. The floating cars were equipped with tachographs that recorded the car speed as the car traveled along the section of freeway under study. The data recorded on the tach cards were then reduced and plotted on travel time and speed profile charts. From these results, Caltrans has determined that the average value of time is equal to \$6.25 per vehicle-hour of delay and an average cost of fuel is \$1.00 per gallon.

A.8.7 Salvage Value

This is the value of the pavement at the end of the life cycle or analysis period. Salvage value can be either positive or negative, depending on whether the material has some economic value or the cost of demolition or removal exceeds any salvageable value [A.39]

Table A.1. Dollars of Excess Operating and Time Costs of Speed Change Cycles — Excess Cost above Continuing at Initial Speed, Rural Roads

Initial Speed MPH	Dollars Per 1,000 Cycles					
	Speed Reduced To and Returned From (MPH)					
	0	10	20	30	40	50
10	22.17					
20	47.62	24.63				
30	82.54	56.23	29.70			
40	131.75	103.63	74.36	41.32		
50	203.89	194.04	141.06	104.50	59.16	
60	315.38	279.88	241.95	198.89	147.57	84.99

Table A.2. Dollars of Excess Operating and Time Costs of Speed Change Cycles — Excess Cost Above Continuing at Initial Speed, Urban Roads

Initial Speed MPH	Dollars Per 1,000 Cycles					
	Speed Reduced To and Returned From (MPH)					
	0	10	20	30	40	50
10	15.35					
20	30.79	14.66				
30	51.02	33.64	17.01			
40	78.57	60.00	41.80	22.52		
50	117.74	97.68	77.47	56.11	31.02	
60	177.56	154.34	128.49	105.28	76.81	42.99

Table A.3. Dollars of Operating and Time Cost per 1,000 Vehicle Miles at Uniform Speeds

Uniform Speed MPH	Dollars per 1,000 Miles	
	Rural Roads	Urban Roads
10	1029.40	948.19
20	561.26	515.56
30	408.26	373.00
40	337.58	305.68
50	302.19	270.09
60	288.20	253.07

Table A.4. Dollars of Operating and Time Cost of Delay (or Idling) per 1,000 Vehicle Hours

Type of Delay Cost	Dollars per 1,000 Hours	
	Rural Roads	Urban Roads
Operating	345.92	321.50
Time	8,810.24	8,215.52
Total	9,156.16	8,537.02

A.8.8 Energy Cost

"The relative energy consumption for different competing alternatives is a factor that may be considered. The dollar cost associated with this item is generally part of construction, maintenance, or rehabilitation costs." [A.39] Due to the difficulty in quantifying this cost, it is often neglected in the life-cycle cost analysis.

A.8.9 Interest and Inflation

When present worth analysis is used, the comparison of two alternatives depends to a large extent upon the rate of interest applied in the study. A higher interest rate results in a lower life-cycle cost for the lower first-cost pavement rehabilitation alternative, while a lower interest rate (or no interest rate) favors the higher first-cost pavement rehabilitation alternative. In addition, with the increase in the inflation rate over the past several years, the concern over whether to include the inflation rate in the analysis is unclear. Since the final outcome is significantly affected by both the interest and the inflation rates, there has been a general consensus to use a discount rate in the life-cycle cost analysis. [A.39, A.46, A.47]

A.8.10 Discount Rate

The discount rate is used as a means of comparing the alternative uses for funds by reducing the future expected costs or benefits to present-day terms. [A.38] The discount rate is sometimes referred to as the real discount rate [A.48] or the real cost of capital. [A.49, A.50] There is general agreement that the discount rate, or real discount rate should be the difference between the market interest rate and inflation using constant dollars. [A.48, A.49, A.50, A.51, A.52, A.53] There has been a general consensus that a discount rate of four percent should be used in the life-cycle cost analysis. [A.49, A.50, A.53]

REFERENCES

- A.1 Federal Highway Administration, Techniques for Pavement Rehabilitation, Training Course, Participant Notebook, U.S. Department of Transportation, Contract No. DOT-FH-11-9580, prepared by ERES Consultants, Inc., revised March 1987.
- A.2 Treybig, H.J., McCullough, B.F., Smith, P., and H.V. Quintus, "Overlay Design and Reflection Cracking Analysis for Rigid Pavements," Report No. FHWA-RD-77-66, Federal Highway Administration, Washington, D.C., August 1977.
- A.3 Crawford, Cambell, Controlled Cracking and Seating of Portland Cement Concrete Pavement Prior to Asphalt Overlay," Paving and Transportation Conference, Proceedings, 23rd Conference, University of New Mexico, 1980, pp. 217-240.
- A.4 Bone, A.J., and L.W. Crump, "Current Practices and Research on Controlling Reflection Cracking," Highway Research Board Bulletin 123, Highway Research Board, 1956.
- A.5 Zube, E., "Wire Mesh Reinforcement in Bituminous Resurfacing," Highway Research Board Bulletin 131, Highway Research Board, 1956.
- A.6 Sherman, George B., NCHRP Synthesis of Highway Practice No. 92, "Minimizing Reflection Cracking of Pavement Overlays," Transportation Research Board, National Research Council, Washington, D.C., 1982.
- A.7 Treybig, H.J. McMullough, F.B., Smith, P., H. Von Quintus, "Overlay Design and Reflection Cracking Analysis for Rigid Pavements," Volume 1, Development of New Design Criteria, Report No. FHWA-RD-77-66, Federal Highway Administration, Washington, D.C., August 1977.
- A.8 Wyoming Highway Department, "Soft Asphalt Cushion and Rubberized Crack Filler for Minimizing Reflection Cracking," No. I-80-5(43)323, Happy Jack — East, 1975.
- A.9 Ludwig, A.C., and L.N. Pena, Jr., "Reflective Cracking Control," Public Works, May 1970.
- A.10 Tabatabraie, A.M. and E.J. Barenberg, "Longitudinal Joint System in Slip-Formed Rigid Pavements," Report No. FAA-RD-77-4, Volume III — User's Manual, Federal Aviation Administration and Federal Highway Administration, November 1979.
- A.11 Crovetti, J.A. and M.I. Darter, "Void Detection for Jointed Concrete Pavements," prepared for the Annual Meeting of the Transportation Research Board, Washington, D.C., January 1985.
- A.12 U.S. DOT, "Concrete Pavement Restoration and Crack and Seat Rehabilitation Performance Evaluation Reports, U.S. Department of Transportation, Federal Highway Administration, Washington, D.C., May 22, 1987.

- A.13 Drake, E.B., "Breaking-Seating and Bituminous Concrete Overlay of Existing Portland Cement Concrete Pavements," Engineering Bulletin of Purdue University, Procedures of the 70th Annual Road School, March 6-8, 1984.
- A.14 Donohue & Associates, Inc., "Does PCC Cracking and Seating Work?" National Asphalt Paving Association, Better Roads, January 1986.
- A.15 "Asphalt Overlays for Highway and Street Rehabilitation," MS-17, The Asphalt Institute, June 1983.
- A.16 Smith, R.E., "California Implements Crack-&-Seat Strategy," Roads & Bridges, May 1985.
- A.17 Welke, R.A., Webb, A.B. Jr., and C. Van Deusen, "Cracking and Seating of Jointed PCC Pavements in Michigan," A presentation for the Association of Asphalt Paving Technologists 59th Annual Meeting, April 11, 1984.
- A.18 AASHTO, "AASHTO Guide for Design of Pavement Structures," American Association of State Highway and Transportation Officials, Washington, D.C., 1986.
- A.19 Esch, D.C., "Asphalt Pavements Modified with Coarse Rubber Particles — Design, Construction, and Ice Control Observations," Report No. FHWA-AK-RD-85-07, Federal Highway Administration, Washington, D.C., August 1984.
- A.20 Coetzee, N.F., and C.L. Monismith, "Analytical Study of Minimization of Reflection Cracking in AC Overlays by Use of a Rubber-Asphalt Interlayer," Transportation Research Record 700, Transportation Research Board, Washington, D.C., 1979, pp. 100-108.
- A.21 Allen, H.S., and K.P. Keel, "Evaluation of an Asphalt-Rubber Interlayer," Special Study No. 383, Construction/Interim Report, Minnesota Department of Transportation, August 1985.
- A.22 Kudd, S.Q., "Asphalt Rubber Stress Absorbing Membrane Interlayers," Interim Report, Report No. FHWA-DP-37, Federal Highway Administration, Washington, D.C., June 1981.
- A.23 Dykes, J.W., "The Use of Fabric Interlayers to Retard Reflective Cracking," Proceedings of the Association of Asphalt Paving Technologists, Volume 49, 1980.
- A.24 McGhee, K.H., "Efforts to Reduce Reflection Cracking of Bituminous Concrete Overlays of Portland Cement Concrete Pavements," Virginia Highway and Transportation Research Council, November 1975.
- A.25 Gulden, W., "Rehabilitation of Plain Portland Cement Concrete Pavements with Asphaltic Concrete Overlays," Proceedings of the Association of Asphalt Paving Technologists, Volume 47, February 1978.
- A.26 Virginia Highway and Transportation Research Council, "Minimization of Reflection Cracking in Flexible Pavements," July 1977.

- A.27 Iowa Highway Research Board, "Prevention of Reflection Cracking in Asphalt Overlays with Stuctofors, Petromat, and Cerex, December 1977.
- A.28 Carey, D.E., "Evaluation of Synthetic Fabrics for the Reduction of Reflective Cracking," Final Report, Report No. 70-1B(B), Research and Development Section, Louisiana Department of Highways, March 1975.
- A.29 Tyner, H.L., Gulden, W., and D. Brown, "Resurfacing of Plain Jointed-Concrete Pavements," Transportation Research Record 814, pp. 41-45, 1981
- A.30 Button, J.W and T.G. Hunter, "Synthetic Fibers in Asphalt Paving Mixtures," Report No. FHWA/TX-85/73+319-1F, Federal Highway Administration, Washington, D.C., November 1984.
- A.31 McCarthy, G.J., "Recycling of Concrete Freeways by Michigan Department of Transportation," Transportation Research Record 1040, Transportation Research Board, National Research Council, Washington, D.C., 1985.
- A.32 Buck, A.D., "Recycled Concrete," Miscellaneous paper C-72-14, U.S. Army Engineer, Waterways Experimentation Station, C.E., Vicksburg, Mississippi.
- A.33 U.S. Army Engineer Waterways Experimentation Station, C.E., "Handbook of Concrete & Cement," August 1949, with quarterly supplements, Vicksburg, Mississippi.
- A.34 Bergren, J.V., and R.A. Britson, Iowa Department of Transportation, Division of Highways, "Portland Cement Concrete Utilizing Recycled Pavement," January 1977.
- A.35 Frondistou-Yannas, Stanatia, Taichi Itoh, Massachusetts Institute of Technology, "Economic Feasibility of Concrete Recycling," Journal of ASCE Structural Division, April 1977.
- A.36 Yrjanson, W.A., "Recycling Portland Cement Concrete," St. Louis, 1981.
- A.37 Hankins, R.B., and T.M. Borg, "Recycling PCC Roadways in Oklahoma," Transportation Research Record 986, Transportation Research Board, National Research Council, Washington, D.C., 1984.
- A.38 U.S. Department of Transportation, "Highway Subdrainage Design," Report No. FHWA-TS-80-224, Federal Highway Administration, Washington, D.C., August 1980.
- A.39 Peterson, Dale E., NCHRP Synthesis of Highway Practice No. 122: "Life-Cycle Cost Analysis of Pavements," Highway Research Board, National Research Council, Washington, D.C., 1985.
- A.40 Winfrey R. and C. Zellner, NCHRP Report No. 122: "Summary and Evaluation of Economic Consequences of Highway Improvements," Highway Research Board, National Research Council, Washington, D.C., 1971.
- A.41 Dell'Isola, A.J. and S.J. Kirk, Life-Cycle Costing For Design Professionals, McGraw-Hill, New York, 1981.

- A.42 Keely, B.J. and J.W. Griffith, "Life Cycle Cost-Benefit Analysis. A Basic Course in Economics Decision Making," Report No. HEW/OFEPM-75/06. Department of Health, Education, and Welfare, Washington, D.C., 1975.
- A.43 Lytton, R.L., McFarland, W.F., and D.L. Schafer, NCHRP Report No. 160, "Flexible Pavement Design and Management Systems Approach Implementation," Transportation Research Board, National Research Council, Washington, D.C., 1975.
- A.44 U.S. Department of Labor, "Detailed Report, October 1987," U.S. Department of Labor, Bureau of Labor, October 1987.
- A.45 Lindley, J.A., "Quantification of Urban Freeway Congestion and Analysis of Remedial Measures," Draft Report, Federal Highway Administration, Washington, D.C., June 1986.
- A.46 Federal Highway Administration, "Proceedings, Workshop in Pavement Rehabilitation," Federal Highway Administration, Report No. FHWA-TS-84-224, Washington, D.C., March 1985.
- A.47 Ray, Gordon K., "Life-Cycle Cost Studies for Pavements," for presentation to the Association of Cost Engineers First Annual Region IV Seminar, Chicago - O'Hare Marriott Hotel, May 7, 1983.
- A.48 Roy, R. and G.K. Ray, Discussion of "A Comparative Economic Analysis of Asphalt and Concrete Pavements," Florida Department of Transportation. Portland Cement Association, Skokie, Ill., 1984.
- A.49 Epps, J.A. and C.V. Wootan, "Economic Analysis of Airport Pavement Rehabilitation Alternatives — An Engineering Manual," Report No. DOT-FAA-RD-81-78, Federal Aviation Administration, Department of Transportation, Washington, D.C., 1981.
- A.50 Standing Committee on Highways, A Manual on User Benefit Analysis of Highway and Bus-Transit Improvements, American Associations of State Highway and Transportation Officials, Washington, D.C. 1977.
- A.51 "A Comparative Economic Analysis of Asphalt and Concrete Pavements," Florida Department of Transportation, 1984.
- A.52 Weed, R.M., "Basic Engineering — Economics Concepts," Memorandum Report, New Jersey Department of Transportation, 1984.
- A.53 Oglesby, C.H., and R.G. Hicks, *Highway Engineering*, 4th Edition, Wiley, New York, pp. 97-159, 791-793, 1982.

APPENDIX B
BRIDGE CLEARANCES

Required Clearances:

Resurfacing, Interstate	14.5 feet
Safety Improvements, Interstate	16.0 feet

Minimum Bridge Heights for both SR 5 and SR 90 where taken from the WSDOT 1987 Bridge List.

SR 5 - Bridge Height listings begin at the Pacific Avenue Interchange in Tacoma and end with the junction of SR 5 and SR 542 in Bellingham.

Table B.1. Minimum Bridge Clearances (SR 5)

<u>BRIDGE NUMBER</u>	<u>CROSSING NAME</u>	<u>VERTICAL CLEARANCES (ft)</u>		<u>ALLOWABLE OVERLAY THICKNESS (ft)</u>	
		<u>NORTH</u>	<u>SOUTH</u>	<u>NORTH</u>	<u>SOUTH</u>
5/441	Tacoma Ave UC	33.33	29.00	18.83	14.50
5/444	Pacific Ave UC	22.83	17.00	8.33	2.50
5/448	McKinley Hill UC	20.00	17.50	5.50	3.00
5/451	E.L. St UC	43.00	33.17	28.50	18.67
5/457	PO Tacoma Rd UC	19.25	16.67	4.75	2.17
99/400	SR 99	16.83	16.92	2.33	2.42
5/461	Ardena Rd UC	16.33	17.33	1.83	2.83
514/8	SR 514 UC	16.25	16.42	1.75	1.92
5/501	So. 376th St UC	16.75	18.83	2.25	4.33
161/102	SR 161 UC	17.08	16.08	2.58	1.58
5/505	So. 320th St UC	16.83	15.83	2.33	1.33
5/513	So. 216th St UC	20.33	18.17	5.83	3.67
5/515	Military Rd UC	19.50	19.67	5.00	5.17
5/518	So. 178th St UC	18.25	16.08	3.75	1.58
5/520E	Frontage Rd UC	16.17		1.67	
SR 405	SR 405 UC	16.17	20.58	1.67	6.08
5/524	So. 144th St UC	17.25	16.58	2.75	2.08
5/525N-N	N-N Ramp UC)/	16.50	16.75	2.00	2.25
5/526.1	Steel Hill UC	18.50	16.92	4.00	2.42
900/13W	SR 900 UC	18.67	16.83	4.17	2.33
900/12W	SR 900 UC	17.08	16.50	2.58	2.00
5/528	So. 107th St UC	17.08	18.50	2.58	4.00
5/532.5	Albro St UC	16.33	16.67	1.83	2.17
5/533E-N	E-N Ramp UC	16.33	16.50	1.73	2.00
5/536N-W	N-W Ramp UC	19.25	28.42	4.75	13.92

Table B.1. Minimum Bridge Clearances (SR 5) (Continued)

<u>BRIDGE NUMBER</u>	<u>CROSSING NAME</u>	<u>VERTICAL CLEARANCES (ft)</u>		<u>ALLOWABLE OVERLAY THICKNESS (ft)</u>	
		<u>NORTH</u>	<u>SOUTH</u>	<u>NORTH</u>	<u>SOUTH</u>
5/537S	EB Spokane St UC	28.42	29.33	13.92	14.83
5/537E-N	E-N Ramp UC	16.67	24.58	2.17	10.08
5/537W-S	W-S Ramp UC	40.67	44.00	26.17	29.50
5/537N	WB Spokane St UC	37.75	37.25	23.25	22.75
5/538S-E	S-E Ramp UC	16.25	18.75	1.75	4.25
5/539.5	Beacon-Holgate UC	16.83	26.25	2.33	11.75
5/540N-W	N-W Ramp UC	17.00	40.08	2.50	25.58
90/10W-S	W-S Ramp UC	16.92	16.42	2.42	1.92
90/10	SR 90, future UC	19.00	17.92	4.50	3.42
90/10E-N	E-N Ramp UC	17.92	24.83	3.42	10.33
5/542S-E	S-E Ramp UC	28.00	20.25	13.50	5.75
5/544	Yesler St UC	23.17	15.50	8.67	1.00
5/546	Madison St UC	22.33	39.25	7.83	24.75
5/547	Spring St UC	21.42	31.42	6.92	16.92
5/545N-W	N-Seneca UC SB		20.33		5.83
5/548PS	So Park Plaza UC	16.42	26.58	1.92	12.08
5/548	Seneca St UC	15.25	25.92	0.75	11.42
5/548PN	No Park Plaza UC	16.92	18.92	2.42	4.42
5/549E-N	Univ Ramp UC SB		18.92		4.42
5/549	8th Ave UC	26.75	33.83	12.25	19.33
5/550	Pike St UC	16.75	18.92	2.25	4.42
5/551	Pine-Boren UC	28.25	36.00	13.75	21.50
5/552	Olive Way UC	15.42	18.00	0.92	3.50
5/553	Denny Way UC	15.92	19.58	1.42	5.08
5/564	Lakeview Blvd UC	24.75	18.00	10.25	3.50
520/1W-S	W-S Ramp UC	15.50		1.00	
5/569	Roanoke St UC	14.92	16.92	0.42	2.42
5/572	NE 45th St UC	15.83	20.67	1.33	6.17
5/574	NE 50th St UC	14.75	16.17	0.25	1.67
5/580	NE 70th St UC	29.67	20.33	15.17	5.83
5/580RNE	N-E Exp Ramp UC	22.67		8.17	
522/14W-S	Ramp UC SR 522	23.33	25.67	8.83	11.17
5/582	5th Ave NE UC	17.25	18.25	2.75	3.75
5/583	NE 80th St UC	19.00	19.50	4.50	5.50
5/584N-W	N-85th Ramp UC	18.42	16.50	3.92	2.00
5/585	NE 92nd St UC	17.75	16.08	3.25	1.58
5/589	NE 117th St UC	18.25	17.00	3.75	2.50
5/590	NE 130th St UC	16.25	17.00	1.75	2.50
513/32	SR 513 UC	16.42	20.33	1.92	5.83
5/596	NE 185th	16.25	20.25	1.75	5.75
5/598	Pedestrian UC	21.08	18.08	6.58	3.58
5/602	236th St SW UC	18.50	18.50	4.00	4.00

Table B.1. Minimum Bridge Clearances (SR 5) (Continued)

<u>BRIDGE NUMBER</u>	<u>CROSSING NAME</u>	<u>VERTICAL CLEARANCES (ft)</u>		<u>ALLOWABLE OVERLAY THICKNESS (ft)</u>	
		<u>NORTH</u>	<u>SOUTH</u>	<u>NORTH</u>	<u>SOUTH</u>
5/603	228th St SW UC	17.33	20.92	2.83	6.42
5/605	220th St SW UC	16.33	19.33	1.83	4.83
524/10	SR 524 UC	16.25	16.25	1.75	1.75
405/112E	SR 405 UC	18.67	19.17	4.17	4.67
405/112W	SR 405 UC	18.75	20.00	4.25	5.50
5/613	Maple Rd UC	18.50	17.00	4.00	2.50
5/615	165th St SW UC	16.25	19.17	1.75	4.67
5/618	Post Rd UC	16.17	17.17	1.67	2.67
5/620E	Stockshow Rd UC	15.67		1.17	
5/620W	Stockshow Rd UC		16.92		2.42
99/610	SR 99 UC	17.67	16.33	3.17	1.83
527/120SR 527 UC		20.25	17.75	5.75	3.25
5/622N-W	N-W Ramp UC	50.00	50.00	35.50	35.50
5/624	Juniper Dr UC	18.33	17.33	3.83	2.83
5/629	Cascade View UC	16.42	18.83	1.92	4.33
5/630	41st St UC	16.50	19.75	2.00	5.25
5/642	23rd St UC	17.33	16.25	2.83	1.75
5/646	12th Ave NE UC	16.75	16.83	2.25	2.33
5/655	Tulalip RR UC	16.25	16.33	1.75	1.83
5/656	Marshall Rd UC	16.42	16.25	1.92	1.75
5/657	Stimson Rd UC	16.50	16.92	2.00	2.42
5/661	Lk Goodwin Rd UC	16.17	16.17	1.67	1.67
5/662	King Thompson UC	17.50	19.50	3.00	5.00
530/115	SR 530 UC	16.25	16.42	1.75	1.92
5/671	Jackson Rd UC	19.75	17.33	5.25	2.83
5/701	Milltown Rd UC	19.50	19.92	5.00	5.42
530/1	SR 530 UC	16.42	16.33	1.92	1.83
5/704	So Mt Vernon IC	17.50	18.00	3.00	3.50
5/706	Anderson Rd UC	16.83	17.17	2.33	2.67
5/707	Blackburn St UV	15.33	15.75	<u>0.83</u>	1.25
5/709	2nd St UC	14.33	15.50	<u>-0.17</u>	1.00
5/712.5	Hopper Rd UC	16.67	16.58	2.17	2.08
11/1	SR 11 UC	15.42	15.83	<u>0.92</u>	1.33
5/717	Cook Rd UC	16.42	16.42	1.92	1.92
5/722	Bow Hill Rd UC	16.25	16.50	1.75	2.00
5/725	Alger Rd UC	18.75	16.67	4.25	2.17
5/803	Samish Inn UC	16.67	22.75	2.17	8.25
5/807	So Bellingham UC	17.17	17.00	2.67	2.50
5/814	Alabama St U	15.17	15.17	<u>0.67</u>	<u>0.67</u>
5/815	BN RR UC	17.08	16.83	2.58	2.33
5/816	Milwaukee RR UC	14.75	14.92	<u>0.25</u>	<u>0.42</u>
5/817	Pedestrian UC	15.50	16.17	1.00	1.25

Seattle Reversible Express Lanes

Table B.1. Minimum Bridge Clearances (SR 5) (Continued)

<u>BRIDGE NUMBER</u>	<u>CROSSING NAME</u>	<u>VERTICAL CLEARANCES (ft)</u>		<u>ALLOWABLE OVERLAY THICKNESS (ft)</u>	
		<u>NORTH</u>	<u>SOUTH</u>	<u>NORTH</u>	<u>SOUTH</u>
542/1	SR 542	16.17	15.75	1.67	1.25
5/553R	Tunnel	14.42	14.42	-0.08	-0.08
520/1W-S	W-S Ramp UC	15.17	15.17	<u>0.67</u>	<u>0.67</u>
5/569	Roanoke St UC	15.92	15.92	1.42	1.42
5/570	Ship Canal UC	17.58	17.58	3.08	3.08
5/572	NE 45th St UC	18.17	18.17	3.67	3.67
5/574	NE 50th St UC	15.42	15.42	<u>0.92</u>	<u>0.92</u>
5/580	NE 70th St UC	27.58	27.58	13.08	13.08
5/580RNE	N-E Ramp UC	22.42	22.42	7.92	7.92
522/14W-S	W-S UC SR 522	22.25	22.25	7.75	7.75
5/583	NE 80th St	16.58	16.58	2.08	2.08

SR 90 - Bridge height listings begin at the junction of SR 902 and end at the junction of SR 27.

Table B.2. Minimum Bridge Clearances (SR 90)

<u>BRIDGE NUMBER</u>	<u>CROSSING NAME</u>	<u>VERTICAL CLEARANCES (ft)</u>		<u>ALLOWABLE OVERLAY THICKNESS (ft)</u>	
		<u>NORTH</u>	<u>SOUTH</u>	<u>NORTH</u>	<u>SOUTH</u>
902/10	SR 902 UC	16.92	16.33	2.42	1.83
90/529	Geiger Rd UC	17.00	16.25	2.50	1.75
2/618S	SR2 UC	18.00	16.75	3.50	2.25
2/618N	SR2 UC	20.92	19.42	6.42	4.92
90/533	Garden Spr Rd UC	20.67	18.33	6.17	3.83
90/535	Rosamond Ave UC	16.58	18.08	2.08	3.58
90/536	BN RR UC	22.83	22.83	8.33	8.33
90/537	Lindeke St UC	18.17	16.67	3.67	2.17
90/538	BN RR UC	25.00	25.00	10.50	10.50
90/538	UP RR UC	16.83	16.42	2.33	1.92
195/124W	SR 195 UC	17.58	17.92	3.08	3.42
195/124E	SR 195 UC	18.08	18.75	3.58	4.25
90/548	Sherman St UC	19.08	18.25	4.58	3.75
90/550	Arthur St UC	16.67	16.83	2.17	2.33
90/562EW	E-W Ramp UC	17.58	16.92	3.08	2.42
90/564	Pedestrian UC	19.92	19.58	5.42	5.08
90/567	Pedestrian UC	14.75	15.50	<u>0.25</u>	1.00
90/568	Thor St UC	16.75	16.67	2.25	2.17
90/569	Freya St UC	15.58	15.67	1.08	1.17
90/571	Pedestrian UC	15.75	15.25	1.25	<u>0.75</u>
90/577	Broadway Ave UC	17.83	16.42	3.33	1.92
90/579W	Argonne Rd UC	16.42	16.25	1.92	1.75
90/579E	Argonne Rd UC	17.33	15.42	2.83	<u>0.92</u>
27/124E	SR 27 UC		16.25		1.75
27/124W	SR 27 UC		15.67		1.17

APPENDIX C
CORE THICKNESSES,
LOAD TRANSFER EFFICIENCIES,
PLAY, VOIDS

Table C-1. Core Thickness -- SR 5

CORE NUMBER	LOCATION/DESCRIPTION	THICKNESS (in.)
6	Slab 2, longitudinal crack	8-3/8
7	Slab 2/3, contraction joint	9-1/2
8	Slab 3, longitudinal crack	8-9/16
10	Slab 3/4, contraction joint	9-1/8
11	Slab 4, pavement edge	9-3/8
12	Slab 4/5, contraction joint	9-5/8
13	Slab 17/18, contraction joint	9-5/16
14	Slab 18, mid-panel	9-7/16
15	Slab 18/19, contraction joint	9-1/2
17	Slab 19, longitudinal crack	9
18	Slab 19/20, contraction joint	9-9/16
19	Slab 20, longitudinal crack	9-1/8
21	Slab 20/21, contraction joint	9-9/16
23	Slab 21/22, contraction joint	9-1/2
24	Slab 24/25, contraction joint	9-1/2
26	Slab 25, mid-crack	8-7/8
27	Slab 25/26, contraction crack	9-7/16
28	Slab 26, mid-crack	8-3 /4
29	Slab 1, mid-panel, long. joint	8-7/8
30	Slab 3, mid-panel, long. joint	8-7/8
31	Slab 5, mid-panel, long. joint	8-3/4
32	Slab 18, mid-panel, long. joint	9-1/8
33	Slab 20, mid-panel, long. joint	9
34	Slab 25, mid-panel, long. joint	8-3/4
35	Slab 27, mid-panel, long. joint	8-1/4
36	Slab 26, mid-panel	8-3/8
38	Slab 26, mid-panel	8-1/2
40	Slab 28/29, contraction joint	9

Table C-2. Core Thickness -- SR 90

CORE No.	LOCATION/DESCRIPTION	THICKNESS (in.)	Average (in.)
1	Slab 1, transverse joint	7.75, 8.0, 7.88	7.88
2	Slab 1, edge joint	7.75, 7.63	7.69
3	Slab 1, main lane, edge	8.0, 8.0, 7.88	7.96
4	Slab 1, main lane, mid-panel	8.0, 8.0, 7.88	7.96
5	Slab 1/2, transverse joint	7.75	7.75
6	Slab 2, transverse crack	7.75	7.75
7	Slab 2/3, transverse joint	7.75 to 7.88	7.81
8	Slab 2/3, between long. and edge joint	8.0	8.00
9	Slab 3, between tran. joint and crack	7.88, 7.88, 8.0	7.92
10	Mid-panel crack	7.75, 7.88, 7.88	7.83
11	Slab 3/4, transverse joint	7.88, 7.88, 8.0	7.92
12	Slab 4, main lane, edge	8.25, 7.88, 7.88	8.04
13	Slab 4, mid-panel	8.38, 8.25, 8.0	8.21
14	Slab 4/5, transverse joint	7.75, 7.75, 7.88	7.79
15	Slab 24/25, pavement edge	7.75, 7.75, 7.5	7.67
16	Slab 25, pvmt. edge, mid-panel crack	7.38, 7.38, 7.5	7.42
17	Slab 25/26, mid-panel crack/tran. jt.	7.88, 7.88, 7.75	7.83
18	Joint at main lane edge and gutter	7.38, 7.5, 7.63	7.50
19	Slab 25/26, transverse joint	7.5, 7.75	7.62
20	Slab 26, mid-panel	7.63, 7.63, 7.5	7.58
21	Slab 26/27, transverse joint	7.5, 7.5, 7.75	7.58
22	Slab 27, mid-panel crack	7.38, 7.38, 7.75	7.42
23	Slab 27, mid-panel	7.88, 7.88, 7.75	7.83
24	Slab 27/28, transverse joint	7.75, 7.0	7.38
25	Slab 28, mid-panel, pvmt. edge	7.75, 7.88, 8.0	7.88
28	Slab 50/51, transverse joint	7.5, 7.5, 7.63	7.52
29	Slab 51, mid-panel crack, pvmt. edge	7.5, 7.63, 7.63	7.58
30	Slab 51/52, mid-panel crack/tran. jt.	7.75, 7.63, 7.63	7.67
32	Slab 51/52, transverse joint	7.38, 7.38, 7.75	7.50
33	Slab 52, tran. joint/mid-panel crack	7.25	7.25
34	Slab 52, mid-panel crack	7.25	7.25
35	Slab 52/53, transverse joint	7.25, 7.38, 7.38	7.33
36	Slab 53, mid-panel crack	7.5, 7.38, 7.38	7.42
37	Slab 53/54, mid-panel crack/tran. jt.	7.5, 7.5, 7.38	7.46
38	Slab 53/54, transverse joint	7.38	7.38
39	Slab 54, tran. joint/mid-panel crack	7.5, 7.5, 7.63	7.54
40	Mid-panel	7.63, 7.63, 7.5	7.58
41	Mid-panel crack	7.5, 7.38	7.44

42	Slab 54, longitudinal crack	7.5	7.50
43	Slab 54/55, transverse joint	7.5, 7.5, 7.38	7.46
44	Slab 1, longitudinal joint (lane 1)	6.88, 6.88, 6.5	6.75
	(lane 2)	8.5	8.50
45	Slab 2, longitudinal joint (lane 1)	7.88, 7.88, 8.0	7.92
	(lane 2)	8.25	8.25
46	Slab 3, longitudinal joint (lane 1)	7.25, 7.38, 7.0	7.21
	(lane 2)	8.25, 8.25, 8.5	8.33
47	Slab 4, longitudinal joint (lane 1)	8.5, 8.5, 8.0	8.33
	(lane 2)	8.0	8.00
48	Slab 26, longitudinal jt. (lane 1)	8.13, 8.0, 8.13	8.08
	(lane 2)	8.13, 8, 7.88	8.00
49	Slab 27, longitudinal jt. (lane 1)	8.0	8.00
	(lane 2)	7.75, 7.88, 7.75	7.79

Table C-3. Load Transfer Efficiencies - SR 5.

Row	Joint or Crack	Joint or Crack Number	Approach or Leave	Mean LTE ¹ (%)	Stdev. (%)	COV (%)
1	Joint	0/1	Approach	85.9	0.35	0.40
			Leave	92.1	0.50	0.55
1	Joint	1/2	Approach	86.9	0.65	0.75
			Leave	95.0	1.21	1.27
1	Joint	2/3	Approach	89.8	0.38	0.42
			Leave	97.0	0.96	0.99
1	Joint	3/4	Approach	84.4	0.67	0.80
			Leave	91.5	0.79	0.86
1	Joint	4/5	Approach	91.0	0.57	0.62
			Leave	96.5	0.42	0.43
1	Joint	17/18	Approach	97.2	0.74	0.77
			Leave	92.9	0.44	0.47
1	Joint	18/19	Approach	98.2	1.00	1.02
			Leave	98.8	0.24	0.24
1	Joint	19/20	Approach	95.0	1.01	1.06
			Leave	92.6	1.20	1.29
1	Joint	20/21	Approach	94.9	0.99	1.05
			Leave	96.3	1.12	1.17
1	Joint	21/22	Approach	>100.0	1.00	0.98
			Leave	89.2	0.85	0.95
1	Joint	24/25	Approach	96.8	0.94	0.97
			Leave	96.1	1.12	1.16
1	Joint	25/26	Approach	98.6	3.08	3.13
			Leave	92.1	1.09	1.19
1	Joint	26/27	Approach	92.3	2.94	3.19
			Leave	85.9	0.92	1.07
1	Joint	27/28	Approach	94.6	0.78	0.82
			Leave	94.4	0.79	0.84
1	Joint	28/29	Approach	52.8	2.14	4.05
			Leave	63.5	6.53	10.27
2	Joint	0/1	Approach	91.5	0.69	0.76
			Leave	93.3	0.40	0.43
2	Joint	1/2	Approach	87.2	1.22	1.40
			Leave	91.4	1.76	1.93
2	Joint	2/3	Approach	88.9	1.81	2.04
			Leave	94.4	1.07	1.13
2	Joint	3/4	Approach	86.1	1.16	1.35
			Leave	95.2	1.13	1.19
2	Joint	4/5	Approach	89.2	2.57	2.88
			Leave	92.4	1.67	1.81

¹ The load transfer provided is the average load transfer measured for all eight drops completed with the Falling Weight Deflectometer.

Table C-3. Continued.

Row	Joint or Crack	Joint or Crack Number	Approach or Leave	Mean LTE (%)	Stddev. (%)	COV (%)
2	Joint	17/18	Approach	98.9	0.72	0.73
			Leave	97.0	0.69	0.71
2	Joint	18/19	Approach	98.7	0.73	0.74
			Leave	95.6	0.79	0.82
2	Joint	19/20	Approach	96.7	1.16	1.21
			Leave	83.8	2.12	2.53
2	Joint	20/21	Approach	98.3	0.56	0.57
			Leave	92.2	1.10	1.19
2	Joint	21/22	Approach	>100.0	0.63	0.61
			Leave	90.3	2.79	3.09
2	Joint	24/25	Approach	98.4	1.25	1.27
			Leave	88.8	1.98	2.23
2	Joint	25/26	Approach	97.4	1.49	1.53
			Leave	87.6	1.82	2.08
2	Joint	26/27	Approach	97.0	2.85	2.94
			Leave	89.6	1.24	1.38
2	Joint	27/28	Approach	93.7	1.92	2.04
			Leave	84.2	1.14	1.36
2	Joint	28/29	Approach	81.2	0.89	1.10
			Leave	-	-	-
3	Joint	0/1	Approach	89.0	0.22	0.24
			Leave	93.4	1.24	1.33
3	Joint	1/2	Approach	92.5	0.88	0.95
			Leave	94.9	0.44	0.46
3	Joint	2/3	Approach	90.8	1.19	1.31
			Leave	91.0	0.87	0.96
3	Joint	3/4	Approach	89.9	0.70	0.78
			Leave	92.2	0.68	0.74
3	Joint	4/5	Approach	87.2	0.81	0.93
			Leave	91.0	1.35	1.48
3	Joint	17/18	Approach	93.6	0.65	0.69
			Leave	96.8	0.60	0.62
3	Joint	18/19	Approach	92.5	0.62	0.67
			Leave	96.2	0.91	0.95
3	Joint	19/20	Approach	92.2	1.04	1.13
			Leave	96.1	1.27	1.32
3	Joint	20/21	Approach	-	-	-
			Leave	92.2	0.54	0.58
3	Joint	21/22	Approach	96.2	0.34	0.36
			Leave	94.8	0.79	0.83
3	Joint	24/25	Approach	89.7	0.94	1.05
			Leave	99.2	1.07	1.07
3	Joint	25/26	Approach	94.6	1.27	1.34
			Leave	89.4	0.88	0.98

Table C-3. Continued.

Row	Joint or Crack	Joint or Crack Number	Approach or Leave	Mean LTE (%)	Stdev. (%)	COV (%)
3	Joint	26/27	Approach	88.2	1.19	1.35
			Leave	93.5	0.98	1.05
3	Joint	27/28	Approach	95.6	0.70	0.73
			Leave	97.5	1.30	1.33
3	Joint	28/29	Approach	96.6	0.57	0.59
			Leave	97.6	1.07	1.10
4	Joint	0/1	Approach	90.3	0.51	0.56
			Leave	96.7	0.70	0.74
4	Joint	1/2	Approach	94.2	0.68	0.73
			Leave	96.1	1.05	1.09
4	Joint	2/3	Approach	90.4	1.19	1.31
			Leave	90.6	0.40	0.44
4	Joint	3/4	Approach	85.6	0.37	0.44
			Leave	90.2	0.52	0.58
4	Joint	4/5	Approach	88.4	0.57	0.64
			Leave	95.8	1.01	1.05
4	Joint	17/18	Approach	49.0	1.72	3.51
			Leave	69.9	5.72	8.18
4	Joint	18/19	Approach	95.0	0.39	0.41
			Leave	93.0	1.15	1.24
4	Joint	19/20	Approach	93.3	1.26	1.35
			Leave	95.8	1.38	1.44
4	Joint	20/21	Approach	97.1	0.58	0.60
			Leave	87.0	0.65	0.75
4	Joint	21/22	Approach	96.1	0.75	0.78
			Leave	99.9	1.18	1.18
4	Joint	24/25	Approach	92.9	0.47	0.51
			Leave	95.8	1.49	1.56
4	Joint	25/26	Approach	>100.0	0.43	0.43
			Leave	88.1	0.54	0.62
4	Joint	26/27	Approach	85.2	0.63	0.74
			Leave	>100.0	1.54	1.53
4	Joint	27/28	Approach	76.1	1.55	2.04
			Leave	82.6	1.84	2.22
4	Joint	28/29	Approach	98.0	0.98	1.00
			Leave	94.7	1.06	1.11
5	Joint	0/1	Approach	88.0	1.07	1.22
			Leave	95.4	0.75	0.79
5	Joint	1/2	Approach	92.1	1.35	1.46
			Leave	93.1	0.68	0.73
5	Joint	2/3	Approach	87.3	1.06	1.21
			Leave	90.5	0.77	0.85

Table C-3. Continued.

Row	Joint or Crack	Joint or Crack Number	Approach or Leave	Mean LTE (%)	Stdev. (%)	COV (%)
5	Joint	3/4	Approach	90.1	2.12	2.35
			Leave	92.8	1.18	1.28
5	Joint	4/5	Approach	85.5	1.33	1.56
			Leave	93.4	1.19	1.27
5	Joint	17/18	Approach	80.8	0.67	0.83
			Leave	88.1	0.83	0.94
5	Joint	18/19	Approach	92.9	1.06	1.14
			Leave	93.4	0.92	0.99
5	Joint	19/20	Approach	94.2	1.47	1.56
			Leave	93.3	0.83	0.89
5	Joint	20/21	Approach	97.1	1.26	1.30
			Leave	92.3	0.56	0.61
5	Joint	21/22	Approach	94.7	1.01	1.07
			Leave	87.8	0.97	1.11
5	Joint	24/25	Approach	94.0	0.55	0.59
			Leave	89.1	1.38	1.54
5	Joint	25/26	Approach	91.8	0.83	0.90
			Leave	94.3	0.98	1.04
5	Joint	26/27	Approach	88.7	0.51	0.57
			Leave	94.7	1.09	1.15
5	Joint	27/28	Approach	97.6	0.98	1.00
			Leave	92.6	1.10	1.19
5	Joint	28/29	Approach	97.7	0.94	0.97
			Leave	85.8	1.88	2.19
-	Longitudinal Joint - Corner	Slab 2	Approach	21.6	7.51	34.77
			Leave	37.7	2.07	5.49
	Longitudinal Joint - Center	Slab 2	Approach	35.7	8.41	23.55
			Leave	51.2	4.86	9.49
	Longitudinal Joint - Corner	Slab 2	Approach	96.7	2.43	2.51
			Leave	92.3	3.96	4.29
-	Longitudinal Crack - Corner	Slab 2	Approach	51.9	2.88	5.55
			Leave	85.7	3.08	3.60
	Longitudinal Crack - Center	Slab 2	Approach	92.2	2.02	2.20
			Leave	94.0	4.01	4.27
	Longitudinal Crack - Corner	Slab 2	Approach	94.5	2.99	3.17
			Leave	74.4	1.56	2.10
-	Longitudinal Joint - Corner	Slab 25	Approach	66.8	1.14	1.70
			Leave	73.9	5.07	6.87
	Longitudinal Joint - Center	Slab 25	Approach	98.6	1.25	1.27
			Leave	70.4	2.72	3.86

Table C-3. Continued.

Row	Joint or Crack	Joint or Crack Number	Approach or Leave	Mean LTE (%)	Stdev. (%)	COV (%)
	Longitudinal Joint - Corner	Slab 25	Approach Leave	74.8 86.6	5.63 1.63	7.53 1.89
-	Longitudinal Crack - Corner	Slab 25	Approach Leave	56.8 13.4	3.17 3.70	5.58 27.58
	Longitudinal Crack - Center	Slab 25	Approach Leave	- 63.3	- 3.03	- 4.80
	Longitudinal Crack - Corner	Slab 25	Approach Leave	88.5 27.0	5.54 1.33	6.26 4.94

Table C-4. Load Transfer Efficiencies - SR 90.

Row	Joint or Crack	Joint or Crack Number	Approach or Leave	Mean LTE ¹ (%)	Stdev. (%)	COV (%)
1	Joint	0/1	Approach	54.7	2.54	4.64
			Leave	84.1	1.43	1.70
1	Joint	1/2	Approach	77.4	3.61	4.66
			Leave	84.3	2.17	2.58
1	Joint	2/3	Approach	86.7	1.64	1.89
			Leave	87.1	1.54	1.76
1	Joint	3/4	Approach	50.7	3.18	6.27
			Leave	72.1	5.93	8.22
1	Joint	4/5	Approach	81.8	3.22	3.93
			Leave	88.2	4.13	4.68
1	Joint	24/25	Approach	58.8	3.26	5.54
			Leave	83.5	2.09	2.50
1	Joint	25/26	Approach	65.7	2.41	3.68
			Leave	84.2	1.12	1.33
1	Joint	26/27	Approach	63.0	4.14	6.58
			Leave	83.0	1.72	2.08
1	Joint	27/28	Approach	76.6	1.27	1.66
			Leave	83.1	0.96	1.15
1	Joint	28/29	Approach	46.1	0.57	1.23
			Leave	75.3	4.43	5.88
1	Joint	50/51	Approach	90.6	0.80	0.88
			Leave	91.2	0.49	0.54
1	Joint	51/52	Approach	89.6	0.48	0.54
			Leave	89.6	2.42	2.70
1	Joint	52/53	Approach	89.0	0.82	0.93
			Leave	85.4	0.96	1.13
1	Joint	53/54	Approach	86.0	1.13	1.31
			Leave	85.6	1.20	1.40
1	Joint	54/55	Approach	85.2	0.90	1.06
			Leave	88.0	0.85	0.96
1	Crack	Slab 51	Approach	87.5	1.32	1.50
			Leave	94.5	0.81	0.86
2	Joint	0/1	Approach	81.4	2.02	2.48
			Leave	90.8	0.52	0.58
2	Joint	1/2	Approach	29.8	5.73	19.22
			Leave	65.7	5.16	7.85

¹ The load transfer provided is the average load transfer measured for all eight drops completed with the Falling Weight Deflectometer.

Table C-4. Continued.

Row	Joint or Crack	Joint or Crack Number	Approach or Leave	Mean LTE (%)	Stdev. (%)	COV (%)
2	Joint	2/3	Approach	42.8	4.40	10.28
			Leave	71.8	3.62	5.04
2	Joint	3/4	Approach	81.5	0.75	0.92
			Leave	85.7	1.49	1.73
2	Joint	4/5	Approach	90.3	1.63	1.80
			Leave	91.3	1.29	1.42
2	Joint	24/25	Approach	33.2	4.26	12.85
			Leave	75.0	7.11	9.48
2	Joint	25/26	Approach	45.9	4.87	10.61
			Leave	84.1	4.13	4.91
2	Joint	26/27	Approach	34.5	5.32	15.43
			Leave	71.2	12.89	18.10
2	Joint	27/28	Approach	68.7	1.54	2.24
			Leave	75.2	8.53	11.34
2	Joint	28/29	Approach	87.5	0.82	0.93
			Leave	89.8	1.34	1.49
2	Joint	50/51	Approach	89.6	1.85	2.06
			Leave	94.0	1.38	1.47
2	Joint	51/52	Approach	93.7	1.22	1.30
			Leave	92.2	0.65	0.70
2	Joint	52/53	Approach	91.3	1.21	1.33
			Leave	89.2	0.79	0.89
2	Joint	53/54	Approach	84.6	0.44	0.51
			Leave	95.7	1.33	1.40
2	Joint	54/55	Approach	87.4	0.51	0.59
			Leave	93.3	1.53	1.64
2	Crack	Slab 51	Approach	89.9	0.67	0.75
			Leave	93.7	1.50	1.60
3	Joint	0/1	Approach	14.4	2.42	16.82
			Leave	87.5	2.28	2.61
3	Joint	1/2	Approach	11.4	2.10	18.36
			Leave	47.0	9.11	19.37
3	Joint	2/3	Approach	15.4	0.79	5.11
			Leave	69.3	3.43	4.95
3	Joint	3/4	Approach	15.0	4.26	28.47
			Leave	38.0	7.84	20.63
3	Joint	4/5	Approach	12.8	1.09	8.48
			Leave	40.8	11.82	28.97
3	Joint	24/25	Approach	82.0	1.61	1.96
			Leave	84.9	1.18	1.39
3	Joint	25/26	Approach	45.4	2.27	5.00
			Leave	87.2	1.67	1.92

Table C-4. Continued.

Row	Joint or Crack	Joint or Crack Number	Approach or Leave	Mean LTE (%)	Stdev. (%)	COV (%)
3	Joint	26/27	Approach	80.7	1.95	2.42
			Leave	88.3	1.61	1.83
3	Joint	27/28	Approach	47.1	2.84	6.02
			Leave	91.9	2.05	2.23
3	Joint	28/29	Approach	80.6	0.99	1.22
			Leave	84.2	0.53	0.63
3	Joint	50/51	Approach	84.8	2.14	2.52
			Leave	94.2	3.02	3.20
3	Joint	51/52	Approach	91.3	1.82	1.99
			Leave	91.0	0.93	1.03
3	Joint	52/53	Approach	93.8	2.36	2.52
			Leave	89.6	6.25	6.98
3	Joint	53/54	Approach	84.5	4.65	5.50
			Leave	90.3	1.25	1.39
3	Joint	54/55	Approach	50.1	2.70	5.38
			Leave	67.2	1.17	1.74
3	Crack	Slab 2	Approach	46.8	5.73	12.25
			Leave	49.0	7.83	15.98
3	Crack	Slab 3	Approach	38.3	5.58	14.56
			Leave	37.5	7.56	20.16
3	Crack	Slab 25	Approach	73.8	3.10	4.20
			Leave	78.8	3.07	3.90
3	Crack	Slab 27	Approach	72.2	1.01	1.40
			Leave	61.0	5.02	8.23
3	Crack	Slab 51	Approach	81.8	2.78	3.39
			Leave	92.9	1.74	1.87
3	Crack	Slab 52	Approach	80.8	0.46	0.57
			Leave	87.4	0.99	1.13
3	Crack	Slab 53	Approach	89.2	2.68	3.01
			Leave	89.8	5.04	5.61
3	Crack	Slab 54	Approach	82.5	0.91	1.10
			Leave	88.1	4.02	4.57
4	Joint	0/1	Approach	52.4	1.56	2.99
			Leave	61.8	3.59	5.81
4	Joint	1/2	Approach	68.9	2.19	3.18
			Leave	76.0	0.91	1.20
4	Joint	2/3	Approach	60.3	1.10	1.82
			Leave	77.0	3.64	4.72
4	Joint	3/4	Approach	77.9	0.69	0.89
			Leave	84.5	1.75	2.07
4	Joint	4/5	Approach	76.0	1.04	1.37
			Leave	80.8	0.95	1.17

Table C-4. Continued.

Row	Joint or Crack	Joint or Crack Number	Approach or Leave	Mean LTE (%)	Stdev. (%)	COV (%)
4	Joint	24/25	Approach	30.0	1.37	4.58
			Leave	77.6	1.27	1.64
4	Joint	25/26	Approach	21.3	0.98	4.58
			Leave	32.5	7.16	22.05
4	Joint	26/27	Approach	27.3	0.67	2.45
			Leave	66.6	5.05	7.58
4	Joint	27/28	Approach	33.3	3.57	10.71
			Leave	44.6	10.73	24.04
4	Joint	28/29	Approach	34.0	1.12	3.29
			Leave	48.0	4.80	10.00
4	Joint	50/51	Approach	58.7	0.82	1.39
			Leave	73.8	2.80	3.79
4	Joint	51/52	Approach	79.3	1.93	2.44
			Leave	84.1	1.52	1.81
4	Joint	52/53	Approach	82.5	0.67	0.81
			Leave	83.1	0.83	0.99
4	Joint	53/54	Approach	76.4	1.70	2.22
			Leave	74.4	0.82	1.11
4	Joint	54/55	Approach	46.6	1.97	4.23
			Leave	56.5	2.87	5.08
4	Crack	Slab 2	Approach	62.7	2.05	3.27
			Leave	71.0	3.01	4.24
4	Crack	Slab 3	Approach	84.0	0.44	0.52
			Leave	89.1	2.62	2.94
4	Crack	Slab 25	Approach	21.4	1.37	6.40
			Leave	49.4	9.31	18.84
4	Crack	Slab 27	Approach	28.4	2.62	9.22
			Leave	41.0	6.89	16.84
4	Crack	Slab 51	Approach	38.9	4.06	10.44
			Leave	50.8	1.31	2.58
4	Crack	Slab 52	Approach	74.3	0.37	0.50
			Leave	78.4	1.09	1.39
4	Crack	Slab 53	Approach	62.8	0.96	1.52
			Leave	63.8	1.23	1.93
4	Crack	Slab 54	Approach	75.2	1.41	1.87
			Leave	55.9	8.37	14.97
5	Joint	0/1	Approach	49.9	1.37	2.74
			Leave	56.6	3.42	6.05
5	Joint	1/2	Approach	56.2	1.38	2.46
			Leave	54.6	0.27	0.49
5	Joint	2/3	Approach	58.8	2.72	4.62
			Leave	78.5	5.31	6.77

Table C-4. Continued.

Row	Joint or Crack	Joint or Crack Number	Approach or Leave	Mean LTE (%)	Stdev. (%)	COV (%)
5	Joint	3/4	Approach	71.8	1.44	2.01
			Leave	72.7	3.04	4.18
5	Joint	4/5	Approach	75.0	1.50	2.00
			Leave	77.5	1.19	1.54
5	Joint	24/25	Approach	39.5	3.25	8.23
			Leave	61.9	4.55	7.35
5	Joint	25/26	Approach	26.0	0.49	1.88
			Leave	44.5	7.95	17.88
5	Joint	26/27	Approach	33.6	1.90	5.65
			Leave	56.3	8.19	14.55
5	Joint	27/28	Approach	25.6	1.73	6.79
			Leave	33.8	4.97	14.72
5	Joint	28/29	Approach	24.6	0.35	1.43
			Leave	36.5	4.79	13.13
5	Joint	50/51	Approach	26.0	3.67	14.11
			Leave	50.6	7.76	15.35
5	Joint	51/52	Approach	49.1	2.27	4.63
			Leave	58.3	3.80	6.52
5	Joint	52/53	Approach	71.8	0.36	0.50
			Leave	76.7	5.95	7.76
5	Joint	53/54	Approach	54.1	3.43	6.34
			Leave	51.0	6.12	12.01
5	Joint	54/55	Approach	36.7	1.07	2.91
			Leave	58.4	1.79	3.07
5	Crack	Slab 2	Approach	79.3	1.35	1.70
			Leave	79.1	7.00	8.84
5	Crack	Slab 3	Approach	69.2	1.38	2.00
			Leave	71.3	3.13	4.39
5	Crack	Slab 25	Approach	28.8	3.41	11.86
			Leave	36.9	8.23	22.29
5	Crack	Slab 27	Approach	66.9	1.74	2.60
			Leave	53.6	5.11	9.51
5	Crack	Slab 51	Approach	43.5	4.26	9.78
			Leave	42.9	6.40	14.93
5	Crack	Slab 52	Approach	71.4	1.11	1.56
			Leave	84.5	2.25	2.66
5	Crack	Slab 53	Approach	50.6	1.38	2.72
			Leave	51.2	6.65	12.98
5	Crack	Slab 54	Approach	73.9	1.31	1.78
			Leave	68.2	6.19	9.08

Table C-5. Play - SR 5.

Row	Joint or Crack	Joint or Crack Number	Approach or Leave	Mean Play ¹ (mils)	Stdev. (mils)
1	Joint	0/1	Approach	0.30	0.10
			Leave	-0.10	0.03
1	Joint	1/2	Approach	0.14	0.04
			Leave	-0.18	0.08
1	Joint	2/3	Approach	0.03	0.02
			Leave	-0.28	0.09
1	Joint	3/4	Approach	0.29	0.11
			Leave	-0.04	0.02
1	Joint	4/5	Approach	-0.03	0.03
			Leave	-0.27	0.11
1	Joint	17/18	Approach	-0.40	0.11
			Leave	-0.16	0.06
1	Joint	18/19	Approach	-0.52	0.12
			Leave	-0.58	0.16
1	Joint	19/20	Approach	-0.19	0.04
			Leave	-0.09	0.03
1	Joint	20/21	Approach	-0.24	0.04
			Leave	-0.32	0.06
1	Joint	21/22	Approach	-0.74	0.20
			Leave	0.11	0.09
1	Joint	24/25	Approach	-0.40	0.06
			Leave	-0.37	0.05
1	Joint	25/26	Approach	-0.65	0.21
			Leave	-0.08	0.21
1	Joint	26/27	Approach	-0.09	0.13
			Leave	0.37	0.21
1	Joint	27/28	Approach	-0.20	0.06
			Leave	-0.19	0.04
1	Joint	28/29	Approach	2.72	0.95
			Leave	2.00	-.08
3	Joint	0/1	Approach	0.07	0.02
			Leave	-0.11	0.02
3	Joint	1/2	Approach	-0.09	0.05
			Leave	-0.21	0.06
3	Joint	2/3	Approach	0.00	0.04
			Leave	-0.01	0.02
3	Joint	3/4	Approach	0.02	0.03
			Leave	-0.07	0.02
3	Joint	4/5	Approach	0.21	0.05
			Leave	-0.01	0.07

¹ Mean play is the play averaged over the eight Falling Weight Deflectometer drops conducted at each test point.

Table C-5. Continued.

Row	Joint or Crack	Joint or Crack Number	Approach or Leave	Mean Play (mils)	Stdev. (mils)
3	Joint	17/18	Approach	-0.22	0.04
			Leave	-0.44	0.11
3	Joint	18/19	Approach	-0.12	0.02
			Leave	-0.34	0.07
3	Joint	19/20	Approach	-0.06	0.03
			Leave	-0.22	0.04
3	Joint	20/21	Approach	-	-
			Leave	-0.10	0.02
3	Joint	21/22	Approach	-0.25	0.20
			Leave	-0.10	0.44
3	Joint	24/25	Approach	-0.04	0.22
			Leave	-0.20	0.43
3	Joint	25/26	Approach	-0.12	0.08
			Leave	0.01	0.09
3	Joint	26/27	Approach	-0.08	0.05
			Leave	-0.08	0.03
3	Joint	27/28	Approach	-0.36	0.06
			Leave	-0.48	0.06
3	Joint	28/29	Approach	-0.45	0.11
			Leave	-0.53	0.06
4	Joint	0/1	Approach	0.01	0.03
			Leave	-0.31	0.06
4	Joint	1/2	Approach	-0.23	0.03
			Leave	-0.36	0.09
4	Joint	2/3	Approach	0.01	0.04
			Leave	-0.00	0.01
4	Joint	3/4	Approach	0.30	0.09
			Leave	0.02	0.03
4	Joint	4/5	Approach	0.10	0.05
			Leave	-0.25	0.05
4	Joint	17/18	Approach	3.89	0.80
			Leave	1.70	0.06
4	Joint	18/19	Approach	-0.36	0.08
			Leave	-0.20	0.05
4	Joint	19/20	Approach	-0.61	0.06
			Leave	-0.32	0.04
4	Joint	20/21	Approach	-0.44	0.11
			Leave	0.28	0.12
4	Joint	21/22	Approach	-0.44	0.08
			Leave	-0.74	0.11
4	Joint	24/25	Approach	-0.11	0.02
			Leave	-0.23	0.04
4	Joint	25/26	Approach	-0.54	0.14
			Leave	0.15	0.07

Table C-5. Continued.

Row	Joint or Crack	Joint or Crack Number	Approach or Leave	Mean Play (mils)	Stdev. (mils)
4	Joint	26/27	Approach	0.29	0.12
			Leave	-0.47	0.09
4	Joint	27/28	Approach	1.23	0.18
			Leave	0.85	0.18
4	Joint	28/29	Approach	-0.54	0.09
			Leave	-0.32	0.02
-	Longitudinal Joint - Corner	Slab 2	Approach	4.98	0.67
			Leave	2.70	0.80
	Longitudinal Joint - Center	Slab 2	Approach	3.68	0.40
			Leave	1.99	0.26
	Longitudinal Joint - Corner	Slab 2	Approach	-0.23	0.03
			Leave	-0.01	0.08
-	Longitudinal Crack - Corner	Slab 2	Approach	1.48	0.40
			Leave	0.12	0.05
	Longitudinal Crack - Center	Slab 2	Approach	-0.04	0.06
			Leave	-0.03	0.05
	Longitudinal Crack - Corner	Slab 2	Approach	-0.18	0.14
			Leave	0.57	0.15
-	Longitudinal Joint - Corner	Slab 25	Approach	0.89	0.30
			Leave	0.54	0.10
	Longitudinal Joint - Center	Slab 25	Approach	-0.25	0.05
			Leave	0.70	0.33
	Longitudinal Joint - Corner	Slab 25	Approach	0.79	0.43
			Leave	0.12	0.12
-	Longitudinal Crack - Corner	Slab 25	Approach	0.98	0.32
			Leave	9.35	1.62
	Longitudinal Crack - Center	Slab 25	Approach	-0.45	0.10
			Leave	1.02	0.46
	Longitudinal Crack - Corner	Slab 25	Approach	-0.56	0.14
			Leave	4.99	1.41

Table C-6. Play - SR 90.

Row	Joint or Crack	Joint or Crack Number	Approach or Leave	Mean Play ¹ (mils)	Stdev. (mils)
2	Joint	0/1	Approach	0.97	0.40
			Leave	-0.62	1.11
2	Joint	1/2	Approach	5.53	1.05
			Leave	1.48	0.12
2	Joint	2/3	Approach	3.83	0.80
			Leave	0.81	0.15
2	Joint	3/4	Approach	0.57	0.22
			Leave	-0.27	0.15
2	Joint	4/5	Approach	0.04	0.10
			Leave	-0.62	0.25
2	Joint	24/25	Approach	7.82	1.17
			Leave	0.95	1.10
2	Joint	25/26	Approach	5.46	0.63
			Leave	-0.28	0.41
2	Joint	26/27	Approach	5.44	0.88
			Leave	0.95	1.56
2	Joint	27/28	Approach	1.77	0.37
			Leave	0.53	0.59
2	Joint	28/29	Approach	0.24	0.12
			Leave	-0.64	0.08
2	Joint	50/51	Approach	0.08	0.11
			Leave	-0.81	0.16
2	Joint	51/52	Approach	-0.18	0.02
			Leave	-0.66	0.15
2	Joint	52/53	Approach	-0.03	0.04
			Leave	-0.37	0.09
2	Joint	53/54	Approach	0.40	0.14
			Leave	-0.90	0.20
2	Joint	54/55	Approach	0.19	0.08
			Leave	-0.66	0.15
2	Crack	Slab 51	Approach	0.04	0.04
			Leave	-0.73	0.18
3	Joint	0/1	Approach	9.62	1.89
			Leave	0.25	0.13
3	Joint	1/2	Approach	3.72	0.46
			Leave	3.88	0.25
3	Joint	2/3	Approach	9.72	2.26
			Leave	2.10	0.50
3	Joint	3/4	Approach	6.85	1.37
			Leave	4.78	0.59

¹ Mean play is the play averaged over the eight Falling Weight Deflectometer drops conducted at each test point.

Table C-6. Continued.

Row	Joint or Crack	Joint or Crack Number	Approach or Leave	Mean Play (mils)	Stdev. (mils)
3	Joint	4/5	Approach	7.06	1.73
			Leave	4.57	0.16
3	Joint	24/25	Approach	0.86	0.22
			Leave	0.68	0.40
3	Joint	25/26	Approach	5.24	1.11
			Leave	0.48	0.44
3	Joint	26/27	Approach	1.72	0.46
			Leave	2.88	0.42
3	Joint	27/28	Approach	1.16	0.75
			Leave	-0.01	0.63
3	Joint	28/29	Approach	4.26	0.78
			Leave	-0.09	0.10
3	Joint	50/51	Approach	0.66	0.21
			Leave	0.28	0.24
3	Joint	51/52	Approach	0.95	0.63
			Leave	-0.30	-0.46
3	Joint	52/53	Approach	0.18	0.29
			Leave	0.34	0.82
3	Joint	53/54	Approach	0.75	0.13
			Leave	0.16	0.38
3	Joint	54/55	Approach	4.54	0.90
			Leave	2.32	0.64
3	Crack	Slab 2	Approach	9.12	1.92
			Leave	5.58	0.08
3	Crack	Slab 3	Approach	4.51	0.76
			Leave	6.81	0.44
3	Crack	Slab 25	Approach	1.75	0.29
			Leave	1.12	0.14
3	Crack	Slab 27	Approach	0.83	0.32
			Leave	0.32	0.38
3	Crack	Slab 51	Approach	0.61	0.24
			Leave	0.54	0.41
3	Crack	Slab 52	Approach	-0.04	0.17
			Leave	0.03	0.22
3	Crack	Slab 53	Approach	-0.23	0.16
			Leave	0.00	0.45
3	Crack	Slab 54	Approach	0.65	0.71
			Leave	0.10	0.28
5	Joint	0/1	Approach	2.50	0.78
			Leave	2.00	0.48
5	Joint	1/2	Approach	2.16	0.69
			Leave	2.23	0.79

Table C-6. Continued.

Row	Joint or Crack	Joint or Crack Number	Approach or Leave	Mean Play (mils)	Stdev. (mils)
5	Joint	2/3	Approach	1.69	0.46
			Leave	0.53	0.07
5	Joint	3/4	Approach	0.77	0.22
			Leave	0.72	0.20
5	Joint	4/5	Approach	0.58	0.21
			Leave	0.56	0.19
5	Joint	24/25	Approach	2.86	0.77
			Leave	1.56	0.23
5	Joint	25/26	Approach	3.80	1.27
			Leave	2.31	0.39
5	Joint	26/27	Approach	2.56	0.92
			Leave	1.47	0.20
5	Joint	27/28	Approach	3.70	1.46
			Leave	3.16	0.86
5	Joint	28/29	Approach	4.24	1.44
			Leave	3.25	0.88
5	Joint	50/51	Approach	4.87	1.09
			Leave	2.70	0.86
5	Joint	51/52	Approach	2.51	0.65
			Leave	1.89	0.37
5	Joint	52/53	Approach	0.92	0.29
			Leave	0.62	0.23
5	Joint	53/54	Approach	2.01	0.47
			Leave	2.47	0.39
5	Joint	54/55	Approach	3.47	1.04
			Leave	1.72	0.61
5	Crack	Slab 2	Approach	0.57	0.28
			Leave	0.64	0.56
5	Crack	Slab 3	Approach	0.98	0.30
			Leave	0.90	0.26
5	Crack	Slab 25	Approach	3.49	0.99
			Leave	3.12	0.46
5	Crack	Slab 27	Approach	0.89	0.27
			Leave	1.57	0.37
5	Crack	Slab 51	Approach	2.86	0.58
			Leave	2.76	0.48
5	Crack	Slab 52	Approach	0.97	0.27
			Leave	0.39	0.31
5	Crack	Slab 53	Approach	2.06	0.58
			Leave	1.99	0.41
5	Crack	Slab 54	Approach	0.81	0.24
			Leave	1.06	0.15

Table C-7. Void Evaluation - SR 5.

Row	Joint/ Crack	Intersect Approach (mils)	Intersect Leave (mils)	Indicated Void	Adjacent Slab Cracked
1	0/1	1.4	1.2	no	no/no ¹
	1/2	-0.2	-0.3	no	no/yes
	2/3	0.5	0.5	no	yes/yes
	3/4	0.2	0.0	no	yes/no
	4/5	-0.2	-0.3	no	no/no
	17/18	0.7	0.9	no	no/no
	18/19	1.8	2.1	yes	no/yes
	19/20	0.1	0.1	no	yes/yes
	20/21	0.8	0.6	no	yes/no
	21/22	0.9	1.3	no	no/no
	24/25	2.0	2.2	yes	no/yes
	25/26	5.2	6.0	yes	yes/yes
	26/27	1.5	2.3	yes	yes/yes
	27/28	1.0	1.0	no	yes/no
	28/29	2.7	5.0	yes	no/no
2	0/1	-0.5	-0.4	no	no/no
	1/2	-0.6	-0.4	no	no/yes
	2/3	-0.2	-0.3	no	yes/yes
	3/4	-0.5	-0.4	no	yes/no
	4/5	-0.8	-0.5	no	no/no
	17/18	0.3	0.4	no	no/no
	18/19	0.7	-1.3	no	no/yes
	19/20	-0.5	-2.0	no	yes/yes
	20/21	-0.1	-0.1	no	yes/no
	21/22	-0.1	-0.2	no	no/no
	24/25	1.6	1.9	no	no/yes
	25/26	3.2	5.0	yes	yes/yes
	26/27	0.7	0.9	no	yes/yes
	27/28	0.4	0.6	no	yes/no
	28/29	1.5	-	no	no/no
3	0/1	0.7	0.5	no	no/no
	1/2	0.9	1.6	no	no/yes
	2/3	-0.3	-0.1	no	yes/yes
	3/4	1.2	0.8	no	yes/no
	4/5	2.1	0.6	yes	no/no

¹ the first yes or no is for the approach slab, the second yes or no is for the leave slab.

Table C-7. Continued.

Row	Joint/ Crack	Intersect Approach (mils)	Intersect Leave (mils)	Indicated Void	Adjacent Slab Cracked	
3	17/18	2.5	2.6	yes	no/no	
	18/19	2.2	2.4	yes	no/yes	
	19/20	0.7	0.6	no	yes/yes	
	20/21	-	2.8	yes	yes/no	
	21/22	1.9	1.8	no	no/no	
	24/25	0.7	0.6	no	no/yes	
	25/26	0.6	0.5	no	yes/yes	
	26/27	-0.1	0.0	no	yes/yes	
	27/28	3.7	4.4	yes	yes/no	
	28/29	3.8	4.5	yes	no/no	
	4	0/1	2.1	2.1	yes	no/no
		1/2	3.3	3.3	yes	no/no
2/3		0.2	0.2	no	no/no	
3/4		2.3	2.5	yes	no/no	
4/5		0.7	1.1	no	no/no	
17/18		6.0	5.0	yes	no/no	
18/19		4.1	4.8	yes	no/no	
19/20		2.9	2.3	yes	no/no	
20/21		2.5	3.8	yes	no/no	
21/22		4.1	4.9	yes	no/no	
24/25		0.8	0.8	no	yes/yes	
25/26		0.7	1.9	no	yes/yes	
26/27		1.6	1.3	no	no/yes	
27/28		7.2	8.1	yes	yes/yes	
28/29		4.2	5.1	yes	yes/yes	
5		0/1	0.4	0.2	no	no/no
		1/2	0.4	0.7	no	no/no
		2/3	-0.3	-0.5	no	no/no
	3/4	0.1	0.4	no	no/no	
	4/5	-0.3	-0.3	no	no/no	
	17/18	0.4	0.6	no	no/no	
	18/19	0.7	0.9	no	no/no	
	19/20	0.1	0.3	no	no/no	
	20/21	0.2	0.6	no	no/no	
	21/22	1.6	2.4	yes	no/no	

Table C-7. Continued.

Row	Joint/ Crack	Intersect Approach (mils)	Intersect Leave (mils)	Indicated Void	Adjacent Slab Cracked
5	24/25	0.1	0.2	no	yes/yes
	25/26	0.7	1.0	no	yes/yes
	26/27	0.2	0.2	no	yes/no
	27/28	2.6	3.0	yes	yes/yes
	28/29	1.8	2.0	yes	yes/yes
	Longit. Joint	2-corner	4.4	1.3	yes
	2-center	4.6	3.1	yes	no/yes
	2-corner	-0.3	-0.6	no	no/yes
	25-corner	-0.3	-0.8	no	yes/yes
	25-center	-0.7	-1.4	no	yes/yes
	25-corner	-0.1	-0.3	no	yes/yes
Longit. Crack	2-corner	0.2	0.6	no	yes/yes
	2-center	-0.4	-0.5	no	yes/yes
	2-corner	-0.4	0.1	no	yes/yes
	25-corner	-0.5	10.0	yes	yes/yes
	25-center	-0.7	-1.5	no	yes/yes
	25-corner	-0.3	2.7	yes	yes/yes

Table C-8. Void Evaluation - SR 90.

Row	Joint/ Crack	Intersect Approach (mils)	Intersect Leave (mils)	Indicated Void	Adjacent Slab Cracked
1	0/1	1.1	1.4	no	no/no ¹
	1/2	-0.7	1.3	no	no/no
	2/3	-0.1	0.4	no	no/no
	3/4	-0.2	0.3	no	no/no
	4/5	-0.5	0.0	no	no/no
	24/25	0.5	1.3	no	no/no
	25/26	0.9	1.2	no	no/no
	26/27	-0.4	1.0	no	no/no
	27/28	0.2	0.3	no	no/no
	28/29	0.3	0.7	no	no/no
	50/51	0.6	1.0	no	no/yes
	crack	0.9	0.7	no	-
	51/52	1.4	1.2	no	yes/no
	52/53	0.3	0.4	no	no/no
	53/54	0.5	0.4	no	no/no
	54/55	0.0	0.0	no	no/no
2	0/1	4.8	7.0	yes	no/no
	1/2	4.6	4.5	yes	no/no
	2/3	3.4	4.0	yes	no/no
	3/4	1.3	1.4	no	no/no
	4/5	1.3	1.9	no	no/no
	24/25	11.4	12.3	yes	no/no
	25/26	10.5	7.7	yes	no/no
	26/27	6.6	8.1	yes	no/no
	27/28	4.6	5.8	yes	no/no
	28/29	3.6	4.2	yes	no/no
	50/51	2.7	3.1	yes	no/yes
	crack	2.8	2.8	yes	-
	51/52	2.4	3.1	yes	yes/no
	52/53	1.0	1.5	no	no/no
	53/54	2.4	2.6	yes	no/no
	54/55	1.5	1.6	no	no/no
3	0/1	9.7	5.3	yes	no/no
	1/2	5.6	7.0	yes	no/yes
	crack	8.1	12.2	yes	-

¹ the first yes or no is for the approach slab, the second yes or no is for the leave slab.

Table C-8. Continued.

Row	Joint/ Crack	Intersect Approach (mils)	Intersect Leave (mils)	Indicated Void	Adjacent Slab Cracked
3	2/3	8.9	5.6	yes	yes/yes
	crack	4.4	12.4	yes	-
	3/4	5.5	5.0	yes	yes/no
	4/5	5.5	7.0	yes	no/no
	24/25	7.7	7.5	yes	no/yes
	crack	8.1	6.8	yes	-
	25/26	8.5	6.5	yes	yes/no
	26/27	4.8	5.5	yes	no/yes
	crack	4.1	4.8	yes	-
	27/28	7.6	8.1	yes	yes/no
	28/29	6.7	2.9	yes	no/no
	50/51	2.9	3.2	yes	no/yes
	crack	1.4	1.9	no	-
	51/52	8.9	10.0	yes	yes/yes
	crack	5.8	6.3	yes	-
	52/53	6.6	7.0	yes	yes/yes
	crack	3.3	4.3	yes	-
	53/54	4.8	4.2	yes	yes/yes
	crack	2.8	5.5	yes	-
	54/55	6.4	4.4	yes	yes/no
4	0/1	0.5	1.0	no	no/no
	1/2	0.4	0.4	no	no/yes
	crack	0.9	0.8	no	-
	2/3	8.2	0.9	yes	yes/yes
	crack	0.0	0.0	no	-
	3/4	0.3	0.1	no	yes/no
	4/5	0.0	-0.2	no	no/no
	24/25	1.3	0.8	no	no/yes
	crack	1.7	1.5	no	-
	25/26	1.0	2.2	yes	yes/no
	26/27	0.0	0.7	no	no/yes
	crack	0.7	0.9	no	-
	27/28	0.5	0.9	no	yes/no
	28/29	0.7	0.6	no	no/no
	50/51	0.5	0.8	no	no/yes
	crack	2.0	0.6	yes	-
	51/52	0.2	0.6	no	yes/yes
	crack	0.6	0.7	no	-
	52/53	0.4	0.6	no	yes/yes
	crack	0.3	0.6	no	-
53/54	0.2	0.4	no	yes/yes	

Table C-8. Continued.

Row	Joint/ Crack	Intersect Approach (mils)	Intersect Leave (mils)	Indicated Void	Adjacent Slab Cracked
4	crack	0.4	3.1	yes	-
	54/55	1.1	0.6	no	yes/no
5	0/1	0.9	0.6	no	no/no
	1/2	0.1	-0.1	no	no/yes
	crack	-0.9	0.3	no	-
	2/3	0.7	0.9	no	yes/yes
	crack	0.3	0.1	no	-
	3/4	0.5	0.2	no	yes/no
	4/5	0.0	-0.1	no	no/no
	24/25	0.9	1.3	no	no/yes
	crack	1.1	2.8	yes	-
	25/26	1.2	1.4	no	yes/no
	26/27	0.4	1.2	no	no/yes
	crack	0.3	0.7	no	-
	27/28	1.4	1.1	no	yes/no
	28/29	1.2	1.1	no	no/no
	50/51	3.8	2.6	yes	no/yes
	crack	2.4	2.2	yes	-
	51/52	2.1	2.4	yes	yes/yes
	crack	1.8	1.9	no	-
	52/53	1.3	1.1	no	yes/yes
	crack	0.8	1.5	no	-
53/54	1.7	2.3	yes	yes/yes	
crack	0.9	2.0	no	-	
54/55	2.4	0.8	yes	yes/no	

APPENDIX D
BACKCALCULATION PROCEDURE DESCRIPTION

INTRODUCTION

To determine the in-situ Portland Cement Concrete (PCC) and foundation support moduli an accurate, easy-to-use and efficient interpretation scheme for Falling Weight Deflectometer (FWD) data was used in this study. This closed-form backcalculation procedure has been presented by Ioannides (1988). It is based on a consistent and theoretically rigorous approach utilizing the principles of dimensional analysis, and is applicable to two-layer, rigid pavement systems. The backcalculation process also utilizes the concept of the area of the deflection basin, first proposed by Hoffman and Thompson (1981). As the results presented in this Report illustrate, this method simplifies considerably the effort required in interpreting nondestructive testing (NDT) data. A unique feature of this approach is that in addition to yielding the required backcalculated parameters, it also allows an evaluation of the degree to which the in-situ system behaves as idealized by theory. This assumes that the pavement consists of an elastic medium-thick plate, resting on a dense liquid (DL) or an elastic solid (ES) subgrade. Furthermore, the method provides an indication of possible equipment shortcomings when these arise in the field.

FUNDAMENTAL CONCEPTS

The backcalculation scheme used in this study employs two fundamental and theoretically valid concepts. These are:

1. A unique relationship exists between the deflection basin area, AREA, and the radius of relative stiffness, l , of the pavement-subgrade system (Ioannides, 1988); and
2. Deflections in rigid pavements, expressed in a dimensionless form, are solely a function of the governing load size ratio, (a/l) , where a is the radius of the applied load (Ioannides, 1986).

All three of these quantities (AREA, l , and a) are expressed in inches.

The area of the deflection basin is calculated as follows:

$$\text{AREA [in.]} = 6 [1 + 2 (D_1/D_0) + 2 (D_2/D_0) + (D_3/D_0)] \quad (1)$$

where D_0 , D_1 , D_2 and D_3 are the FWD deflections recorded at 0, 12 24 and 36 in. from the center of the loading plate, respectively.

Now, the radius of relative stiffness of the pavement-subgrade system is defined by:

$$\text{For the DL foundation: } l = l_k = \sqrt[4]{[Eh^3/(12(1-\mu^2)k)]} \quad (2a)$$

$$\text{For the ES foundation: } l = l_e = \sqrt[3]{[Eh^3(1-\mu_s^2)/(6(1-\mu^2)E_s)]} \quad (2b)$$

where:

- E: slab Young's modulus;
- E_s : soil Young's modulus;
- h: slab thickness;
- μ : slab Poisson ratio;
- μ_s : soil Poisson ratio; and

k: modulus of subgrade reaction.

Application of dimensional analysis indicates that a unique relationship between AREA and l exists and is valid for any chosen plate size and sensor arrangement. Figure 1 shows the AREA vs. l curves, for four different loading and support conditions, assuming four sensors at 12-in. spacing are employed.

Inspection of the interior loading formula presented by Westergaard (1939), shows that the maximum deflection in a two-layer, rigid pavement system may be rewritten in the following nondimensional form:

$$d_0 = D_0 D / (P l^2) - D_0 k l^2 / P \quad (3)$$

where P is the applied load, and D is the slab flexural stiffness, which is given by:

$$D = E h^3 / (12 (1-\mu^2)) \quad (4)$$

Similar expressions can be derived for the other three FWD deflections, i.e.:

$$d_i = D_i D / (P l^2) - D_i k l^2 / P \quad (i=0,3) \quad (5)$$

where d_i denotes the four nondimensional sensor deflections corresponding to the measured deflections, D_i . The nondimensional deflections are known functions of the ratio (a/l) only. In the case

of a constant plate load radius they are uniquely defined by l , alone. Figure 2 shows the variation with l of dimensionless deflections, d_i , for a circular load, radius $a = 5.9055$ in. ($= 300$ mm). The curves corresponding to d_0 are defined by the interior loading maximum deflection formulae presented by Westergaard (1939; Ioannides, et al., 1985) for the DL, and Losberg (1960) for the ES foundations, respectively. The remainder of the curves in Fig. 2 were derived more recently (Ioannides, 1988; Ioannides, et al., 1989).

OUTLINE OF THE BACKCALCULATION PROCEDURE

On the basis of the two fundamental concepts discussed above, the backcalculation procedure proceeds along the following lines:

- (1) Drop the weight, and record the applied load, P , as well as the resulting deflections, D_0 , D_1 , D_2 and D_3 .
- (2) Calculate the area of the deflection basin, AREA.
- (3) Enter Fig. 1 with this AREA-value, and pick up the corresponding radius of relative stiffness value, l .
- (4) Enter Fig. 2 with this l -value, and determine the corresponding dimensionless deflections, d_i .
- (5) Backcalculate the subgrade support values, as follows:

$$\text{For the DL foundation: } k = (d_i/D_i) (P/l^2) \quad (6a)$$

$$\text{For the ES foundation: } C = E_s / (1-\mu_s^2) = (d_i/D_i) (2P/l) \quad (6b)$$

For a chosen value of the subgrade Poisson's ratio, (say, $\mu_s = 0.4$ to 0.5), Eq. (6b) can be rewritten to yield the foundation modulus, E_s :

$$E_s = (1-\mu_s^2) (d_i/D_i) (2P/l) \quad (7)$$

- (5) Backcalculate the slab flexural stiffness, as follows:

$$D = E h^3 / (12 (1-\mu^2)) = (d_i/D_i) P l^2 \quad (8)$$

Thus, if the slab thickness, h , is known, the slab modulus can be calculated using:

$$E = (12(1-\mu^2)/h^3) (d_i/D_i) Pl^2 \quad (9)$$

Alternatively, if the slab modulus, E , is known, one can backcalculate thickness, h , from:

$$h = \sqrt[3]{\left((12(1-\mu^2)/E) (d_i/D_i) Pl^2 \right)} \quad (10)$$

For the slab Poisson ratio, μ , a value of 0.15 may be used.

Note that using these backcalculation equations (Eq. 6 through 10), four determinations of each pavement system parameter (k , E_s , h or E) are possible, each corresponding to one measured deflection, D_i . This provides a control on the accuracy of individual sensor readings, as well as a measure of in-situ material variability, and of the departure of the real system from the idealized conditions assumed in theory.

APPLICATION OF CLOSED-FORM BACKCALCULATION PROCEDURE

To illustrate the application of the procedure described above, a set of FWD data, collected from a PCC pavement section along Interstate 80 in Illinois, will be used to backcalculate the pavement parameters. The radius of the load plate was the standard $a = 5.9055$ in. = 300 mm, and the recorded load, P , was 7792 lbs. Sensors were located at 0, 12, 24 and 36 in. from the center of the plate. Recorded deflections, in inches, were as follows:

$$D_0 = 0.0030; D_1 = 0.0028; D_2 = 0.0024; D_3 = 0.0021.$$

Substituting these deflections in Eq. (1) yields:

$$\text{AREA} = 6 \left[1 + 2 (2.8/3.0) + 2 (2.4/3.0) + (2.1/3.0) \right] = 31.00 \text{ in.}$$

From Fig. 1, the corresponding radius of relative stiffness values are:

$$\text{DL: } l_k = 39 \text{ in.}; \quad \text{ES: } l_e = 28 \text{ in.}$$

Entering Fig. 2 with these l -values, one obtains the following nondimensional deflections:

$$\text{DL Foundation: } d_0 = 0.124; d_1 = 0.116; d_2 = 0.102; d_3 = 0.084.$$

$$\text{ES Foundation: } d_0 = 0.190; d_1 = 0.176; d_2 = 0.154; d_3 = 0.130.$$

Thus, Equations (6a) and (6b) give the following backcalculated subgrade support values (assuming $\mu_s = 0.45$ for the ES):

For the DL Foundation:

$$k = (0.124/0.0030) (7792 / 39^2) = 212 \text{ pci based on } D_0;$$

$$k = (0.116/0.0028) (7792 / 39^2) = 212 \text{ pci based on } D_1;$$

$$k = 218 \text{ pci based on } D_2; \text{ and } k = 205 \text{ pci based on } D_3.$$

The mean of these backcalculated k -values is 212 pci and their coefficient of variation (COV) is 2.15%.

For the ES Foundation:

$$E_s = (1-0.45^2) (0.190/0.0030) (2 \times 7792/28) = 28,111 \text{ psi based on } D_0;$$

$$E_s = (1-0.45^2) (0.176/0.0028) (2 \times 7792/28) = 27,900 \text{ psi based on } D_1;$$

$$E_s = 28,481 \text{ psi based on } D_2; \text{ and } E_s = 27,477 \text{ psi based on } D_3.$$

Thus, the average backcalculated value of the elastic solid foundation modulus is 27,992 psi, with a COV of 1.30%.

Assuming $\mu = 0.15$ and $E = 4,500,000$ psi, Eq. (10) is used to backcalculate the slab thickness, h . For the DL Foundation:

$$h = \sqrt[3]{ \left((12(1-0.15^2)/4,500,000) (0.124/0.0030) 7792 (39)^2 \right) } \\ = 10.85 \text{ in. based on } D_0.$$

Similarly, $h = 10.86$ in. based on D_1 ; $h = 10.95$ in. based on D_2 ; and h

- 10.73 in. based on D_3 . In this case, the mean slab thickness is found to be 10.85 in., and the corresponding COV 0.72%.

For the ES Foundation:

$$h = \sqrt[3]{\left\{ (12(1-0.15^2)/4,500,000) (0.190/0.0030) 7792 (28)^2 \right\}}$$

- 10.03 in. based on D_0 .

By comparison, $h = 10.00$ in. based on D_1 ; $h = 10.07$ in. based on D_2 ; and $h = 9.95$ in. based on D_3 . The backcalculated values of h for the elastic solid foundation have a mean of 10.01 in., and a COV of 0.44%.

Alternatively, if the thickness is known to be 10.0 inches, Eq. (9) is used with $\mu = 0.15$ to backcalculate the slab modulus. Thus, for the DL Foundation:

$$E = (12(1-0.15^2)/10.0^3) (0.124/0.0030) 7792 (39)^2$$

- 5,746,145 psi based on D_0 .

The other backcalculated E-values are: $E = 5,759,385$ psi based on D_1 ; $E = 5,908,335$ psi based on D_2 ; and $E = 5,560,786$ psi based on D_3 . Hence, an average value of $E = 5,743,662$ psi is determined (COV = 2.15%, identical to that for k-value).

For the ES Foundation:

$$E = (12(1-0.15^2)/10.0^3) (0.190/0.0030) 7792 (28)^2$$

- 4,538,323 psi based on D_0 .

The corresponding values for the other deflections are $E = 4,504,200$ psi based on D_1 ; $E = 4,598,037$ psi based on D_2 ; and $E = 4,435,954$ psi based on D_3 . The mean slab modulus is 4,519,128 psi and the COV is 1.30% (which is identical to that for E_s).

The results of the brief statistical analysis of the parameters backcalculated above provide some useful insights pertaining to the

testing procedure adopted, and the observed behavior of the in-situ pavement system. In all cases, a coefficient of variation substantially smaller than 10%, say, was obtained, indicating that no major blunders were involved in the individual sensor readings. If one of the sensors had malfunctioned, the backcalculated parameters based on that particular deflection reading would have been significantly different from the remainder, thus alerting the engineer to the probability of an error. In addition, Fig. 2 indicates that d_0 and d_1 are relatively insensitive to changes in the value of l , compared to d_2 and d_3 . Thus, it may be concluded that the latter are more reliable backcalculation tools. On the other hand, the actual measured deflections D_0 and D_1 are probably more accurate than D_2 and D_3 , owing to their larger magnitude and the equal sensitivity of all sensors, as used in conventional practice. Therefore, it may be desirable to use sensors of increased sensitivity for measuring deflections further away from the center of the applied load. Furthermore, care should be exercised in the field to achieve good seating of the loading plate, as well as of the sensors.

ADVANTAGES OF CLOSED-FORM BACKCALCULATION PROCEDURE USED

The major strengths of the method used in this study, compared to other currently available backcalculation schemes are as follows:

- (a) It is founded upon a rigorous, sound and fundamental theoretical basis, and is extremely powerful and versatile.
- (b) When the backcalculation is performed on a personal computer (computer program ILLI-BACK), execution time per deflection

basin is trivial (≈ 1 sec.). This permits the interpretation of a vast amount of NDT in a very reasonable time. In contrast, a typical backcalculation for a two-layer slab-on-grade system using BISDEF (Bush and Alexander, 1985) takes about 600 CPU sec. to complete (Van Cauwelaert, et al., 1988).

- (c) Each sensor reading provides an independent estimate of the backcalculated parameters. This allows the engineer to investigate the sources of variability in field measurements and materials. Either of the two major subgrade models, namely the dense liquid or the elastic solid foundation, may be employed, providing a rare opportunity for meaningful comparisons between the two. The departure of in-situ behavior from the theoretical assumptions is reflected in the backcalculation statistics obtained. This affords an estimate of the relative location of the actual pavement system behavior within the spectrum defined by the two extreme soil idealizations.
- (d) There is no need for the provision of seed moduli in this approach. These moduli greatly affect the accuracy of other backcalculation schemes (e.g. Mahoney, et al., 1988). If the slab thickness is known, however, the slab modulus can be estimated. Conversely, if the slab modulus is known, the slab thickness is backcalculated.
- (e) The method is general in nature, and is not based on a limited number of particular cases as are database approaches (e.g. Anderson, 1988; Tia and Eom, 1988). This permits very useful and theoretically valid inferences to be made for a given pavement system by examining data collected from a wide variety of other dissimilar systems.
- (f) Application of the procedure to actual field data from recent or on-going projects has confirmed that it yields very realistic, consistent and reliable results (e.g. Ioannides, et al., 1989). Calculations performed follow a definite and closed loop, all but eliminating the probability of calculation errors.
- (g) A number of interesting topics may be examined using this method. These include: the effect of number and spacing of sensors; correlation between backcalculated and intrinsic system properties, particularly with respect to the dynamic effect of the NDT procedure; examination of the effect of friction and bonding between layers, and comparison with results from an equivalent combined thickness approach; field determination of properties necessary in other aspects of pavement design, such as dowel concrete interaction, amount of load transferred by the critical dowel as well as by the entire dowel assembly, etc.

REFERENCES

- Anderson, M. (1988). "A Data Base Method for Backcalculation of Composite Pavement Layer Moduli," Presented at the First International Symposium on Nondestructive Testing of Pavements and Backcalculation of Moduli, ASTM, June 29-30, Baltimore, MD.
- Bush, A.J., and Alexander, D.R. (1985). "Pavement Evaluation Using Deflection Basin Measurements and Layered Theory," Transportation Research Record 1022, Transportation Research Board, National Research Council, Washington, D.C., pp. 16-29.
- Hoffman, M.S., and Thompson, M.R. (1981). "Mechanistic Interpretation of Nondestructive Pavement Testing Deflections," Civil Engineering Studies, Transportation Engineering Series No. 32, Illinois Cooperative Highway and Transportation Research Program Series No. 190, University of Illinois, at Urbana, IL.
- Ioannides, A.M. (1986). Discussion of "Response and Performance of Alternate Launch and Recovery Surfaces that Contain Layers of Stabilized Material," by R.R. Costigan and M.R. Thompson, Transportation Research Record 1095, Transportation Research Board, National Research Council, Washington, D.C., pp. 70-71.
- Ioannides, A.M. (1988). "Dimensional Analysis in NDT Rigid Pavement Evaluation, Submitted for publication, Journal of Transportation Engineering, ASCE, July.
- Ioannides, A.M., Thompson, M.R., and Barenberg, E.J. (1985). "Westergaard Solutions Reconsidered," Transportation Research Record 1043, Transportation Research Board, National Research Council, Washington, D.C., pp. 13-23.
- Ioannides, A.M., Barenberg, E.J., and Lary, J.A. (1989). "Interpretation of Falling Weight Deflectometer Results Using Principles of Dimensional Analysis," Submitted for publication, Fourth International Conference on Concrete Pavement Design and Rehabilitation, Purdue University, April 18-20.
- Losberg, A. (1960). "Structurally Reinforced Concrete Pavements," Doktorsavhandlingar Vid Chalmers Tekniska Högskola, Göteborg, Sweden.
- Mahoney, J.P., Coetzee, N.F., Stubstad, R.N., and Lee, S.W. (1988). "A Performance Comparison of Selected Backcalculation Computer Programs," Presented at the First International Symposium on Nondestructive Testing of Pavements and Backcalculation of Moduli, ASTM, June 29-30, Baltimore, MD.
- Tia, M., and Eom, K.S. (1988). "Development of DBCONPAS Computer Program for Estimating of Concrete Pavement Parameters from FWD Data," Presented at the First International Symposium on

Nondestructive Testing of Pavements and Backcalculation of Moduli,
Poster Session I, ASTM, June 29-30, Baltimore, MD.

Van Cauwelaert, F.J., Barker, W.J., White, T.D., and Alexander, D.R.
(1988). "A Competent Multilayer Solution and Backcalculation
Procedure for Personal Computers," Presented at the First
International Symposium on Nondestructive Testing of Pavements and
Backcalculation of Moduli, ASTM, June 29-30, Baltimore, MD.

Westergaard, H.M. (1939). "Stresses in Concrete Runways of Airports,"
Highway Research Board Proceedings, 19th Annual Meeting, pp. 197-
202; Discussion: pp. 202-205.

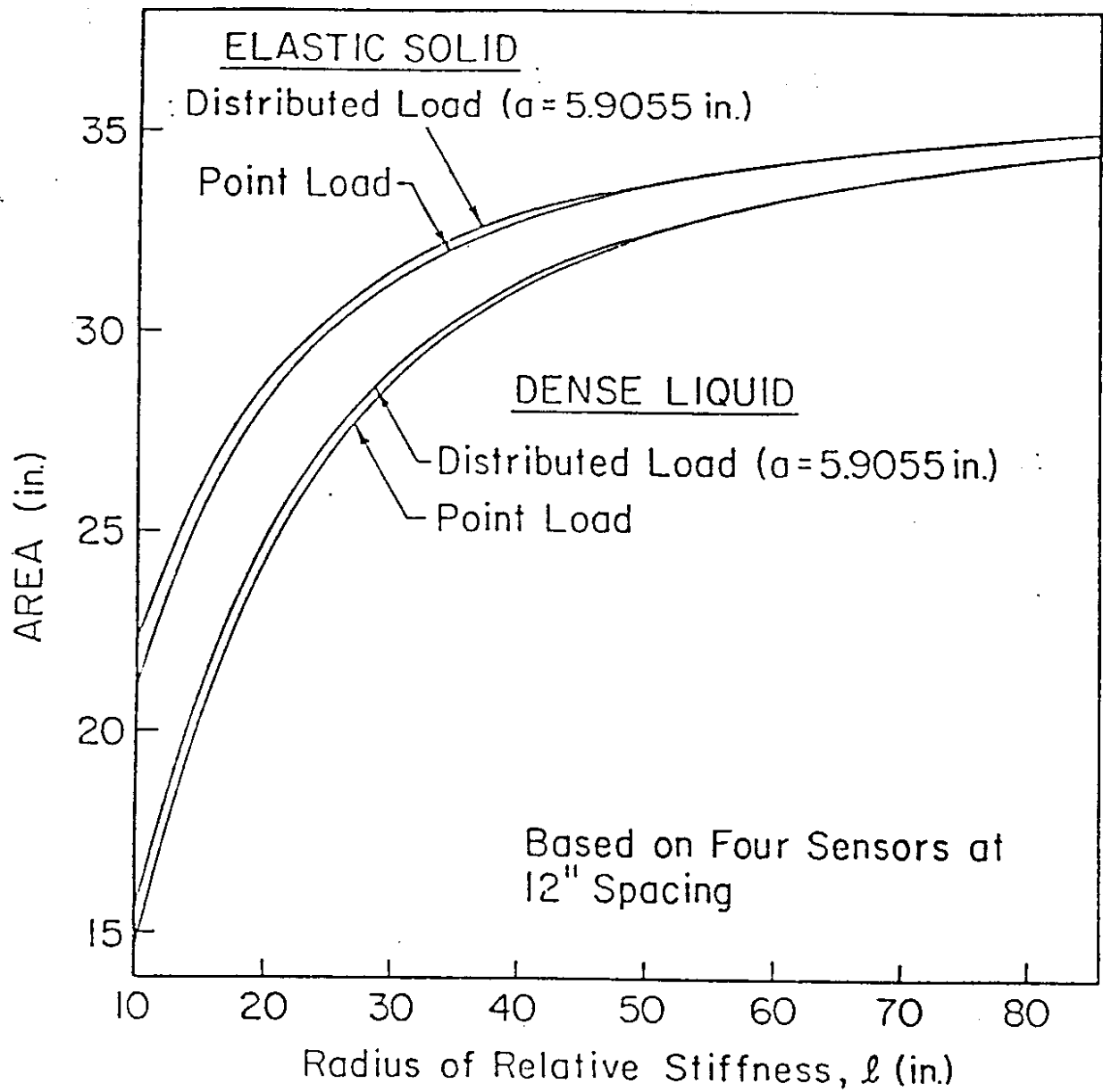


FIG. 1.- Variation of AREA with l (After Ioannides, 1988)

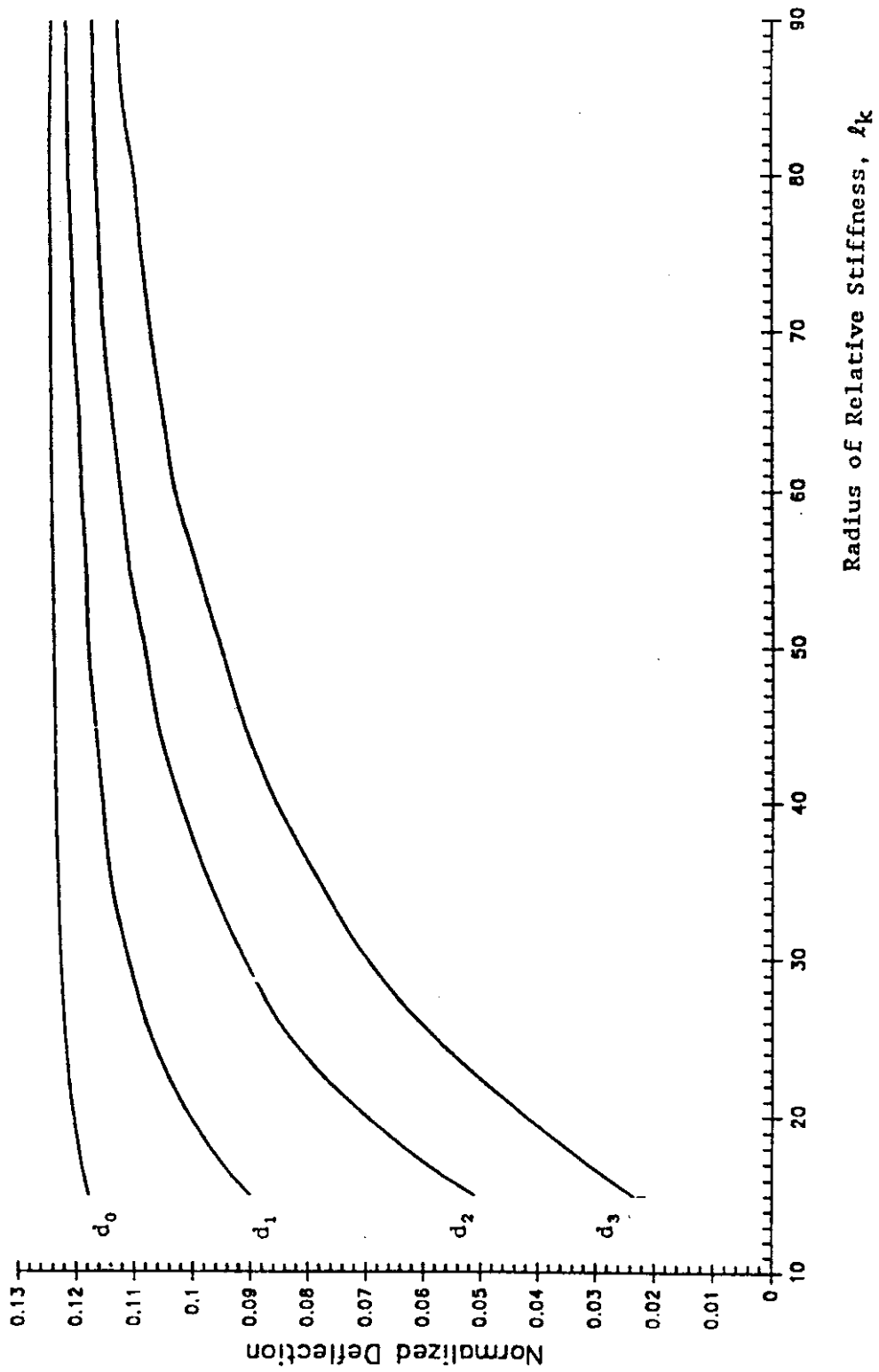


FIG. - Variation of Dimensionless Deflections with λ :
 (a) For Dense Liquid Foundation

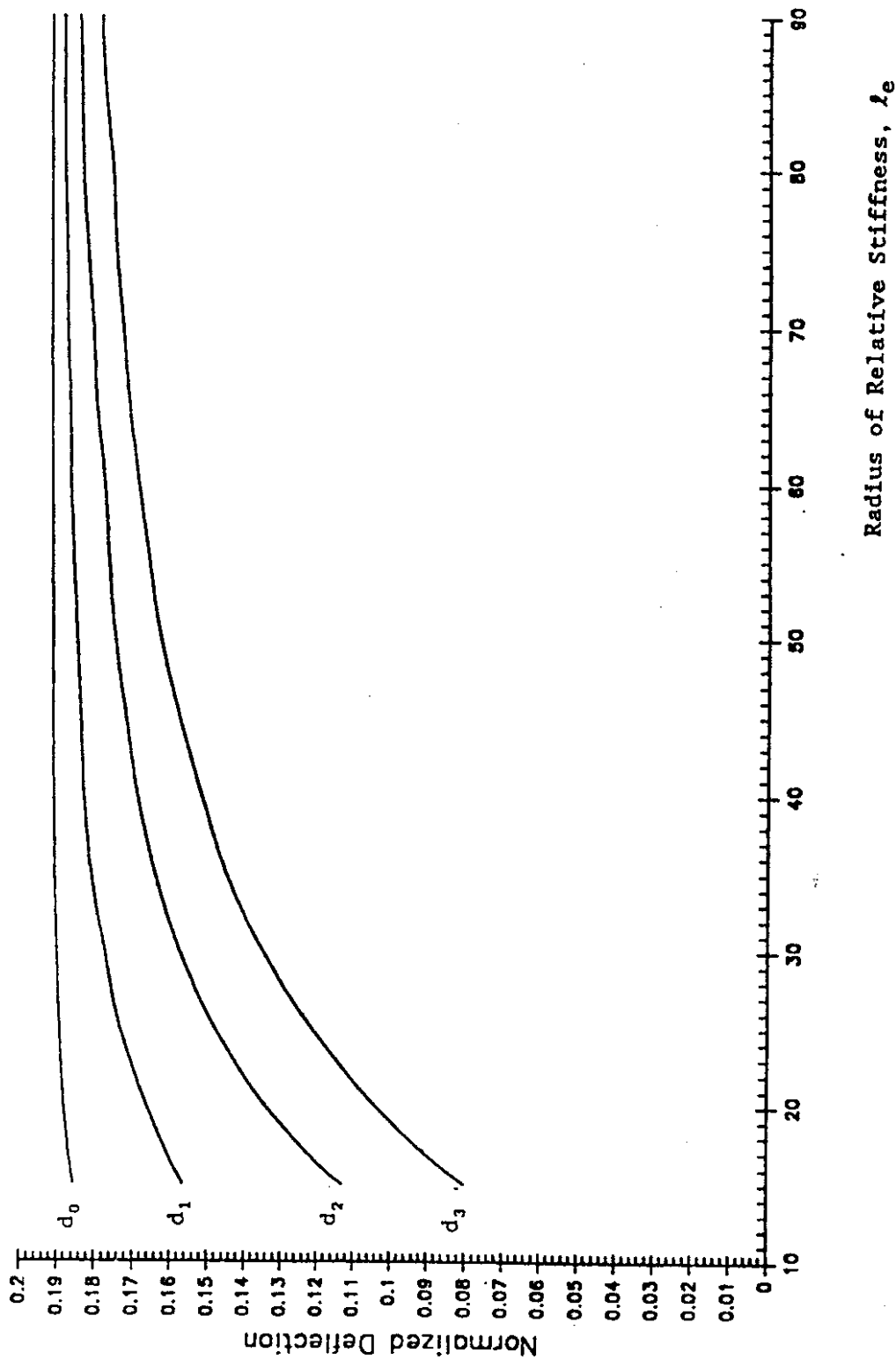


FIG. - Variation of Dimensionless Deflections with l_e :
 (b) For Elastic Solid Foundation
 (After Ioannides, et al., 1989)

APPENDIX E
BACKCALCULATED MATERIAL PROPERTIES
AND CONCRETE THICKNESSES

Table E-1. E-k for 9.0-Inch Design Thickness - SR 5.

Station	Load (lbs)	k (pci)	E (psi)	COV (%)
<u>Row 2 (outer lane) - Uncracked Slabs</u>				
3	15382	155	4,906,000	3.6
12	15494	236	5,840,000	5.0
17	15335	155	5,790,000	4.2
26	15414	317	6,210,000	4.4
40	15319	223	2,021,000	5.1
Mean	15389	217	4,953,000	4.5
St.Dev.	70	67	1,708,000	0.6
COV	0.45	30.96	34.48	
<u>Row 2 - Cracked Slabs</u>				
6	15462	231	5,206,000	5.4
9	15462	197	6,154,000	3.6
20	15478	354	3,702,000	8.7
23	15525	347	4,950,000	9.4
31	15366	301	5,400,000	7.0
34	15605	414	4,064,000	8.1
37	15478	392	4,799,000	6.4
Mean	15482	319	4,896,000	6.9
St.Dev.	72	81	823,000	2.0
COV	0.47	25.34	16.81	
<u>Row 5 (inner lane) - Uncracked Slabs</u>				
3	15176	95	5,054,000	0.9
6	15112	158	4,144,000	3.9
9	15017	83	5,963,000	0.9
12	15303	117	4,379,000	2.8
17	15255	110	4,829,000	3.2
20	15223	166	5,067,000	3.8
23	15255	208	4,944,000	5.2
26	15128	93	6,740,000	2.7
Mean	15184	129	5,140,000	2.7
St.Dev.	94	44	841,000	1.8
COV	0.62	34.14	16.37	

Table E-1. Continued.

Station	Load (lbs)	k (pci)	E (psi)	COV (%)
<u>Row 5 - Cracked Slabs</u>				
31	15223	139	6,366,000	0.9
34	15192	108	5,182,000	0.9
37	15207	113	9,125,000	0.9
40	15271	219	3,722,000	6.3
Mean	15223	145	6,099,000	2.3
St.Dev.	34	51	2,289,000	2.7
COV	0.23	35.46	37.53	

Table E-2. E-k for 9.06-Inch Average Thickness - SR 5.

Station	Load (lbs)	k (pci)	E (psi)	COV (%)
<u>Row 2 (outer lane) - Uncracked Slabs</u>				
3	15382	155	4,809,000	3.6
12	15494	236	5,741,000	5.0
17	15335	155	5,676,000	4.2
26	15414	317	6,087,000	4.4
40	15319	223	1,981,000	5.1
Mean	15389	217	4,859,000	4.5
St.Dev.	70	67	1,676,000	0.6
COV	0.45	30.96	34.50	
<u>Row 2 - Cracked Slabs</u>				
6	15462	231	5,102,000	5.4
9	15462	197	6,032,000	3.6
20	15478	354	3,629,000	8.7
23	15525	347	4,852,000	9.4
31	15366	301	5,293,000	7.0
34	15605	414	3,984,000	8.1
37	15478	392	4,704,000	6.4
Mean	15482	319	4,799,000	6.9
St.Dev.	72	81	806,000	2.0
COV	0.47	25.34	16.80	
<u>Row 5 (inner lane) - Uncracked Slabs</u>				
3	15176	95	4,951,000	0.9
6	15112	158	4,062,000	3.9
9	15017	83	5,845,000	0.9
12	15303	117	4,292,000	2.8
17	15255	110	4,734,000	3.2
20	15223	166	4,967,000	3.8
23	15255	208	4,846,000	5.2
26	15128	93	6,606,000	2.7
Mean	15184	129	5,038,000	2.9
St.Dev.	94	44	825,000	1.5
COV	0.62	34.14	16.37	

Table E-2. Continued.

Station	Load (lbs)	k (pci)	E (psi)	COV (%)
<u>Row 5 - Cracked Slabs</u>				
31	15223	139	6,238,000	0.9
34	15192	108	5,076,000	0.9
37	15207	113	8,978,000	0.9
40	15271	219	3,649,000	6.3
Mean	15223	145	5,985,000	2.2
St.Dev.	34	51	2,259,000	2.7
COV	0.23	35.46	37.74	

Table E-3. E-k for Actual Thickness, Uncracked Slabs Only - SR 5.

Station	Load (lbs)	Area (inches)	l-k (inches)	k (pci)	E (psi)	COV (%)	h (inches)
<u>Row 2 (outer lane)</u>							
3	15381	30.67	37.47	155	5,115,000	3.59	8.875
12	15493	30.25	35.20	236	5,167,000	4.99	9.375
17	15334	30.94	39.01	155	4,949,000	4.22	9.48
26	15413	29.87	33.23	316	5,228,000	4.37	9.53
Mean	15405	30.43	36.23	216	5,115,000	4.29	9.32
St.Dev.	67	0.47	2.54	77	120,000	0.57	0.30
COV	0.43	1.55	7.01	35.79	2.34		3.22
<u>Row 5 (inner lane)</u>							
3	15175	31.53	42.60	95	5,268,000	0.915	8.875
6	15111	30.36	35.75	158	4,708,000	3.854	8.625
9	15016	32.04	46.00	83	6,563,000	0.929	8.72
12	15302	30.95	39.07	117	3,874,000	2.770	9.37
17	15254	31.22	40.68	110	4,404,000	3.197	9.28
20	15223	30.60	37.09	166	5,067,000	3.832	9.00
23	15254	30.19	34.87	208	4,842,000	5.254	9.06
26	15127	32.05	46.04	93	5,730,000	2.705	9.50
Mean	15183	31.12	40.26	129	5,057,000	4.29	9.32
St.Dev.	94	0.72	4.36	44	824,000	0.57	0.30
COV	0.62	2.31	10.82	34.14	16.31		3.22

Table E-3. E-k for Actual Thickness, Uncracked Slabs Only - SR 5.

Station	Load (lbs)	Area (inches)	l-k (inches)	k (pci)	E (psi)	COV (%)	h (inches)
<u>Row 2 (outer lane)</u>							
3	15381	30.67	37.47	155	5,115,000	3.59	8.875
12	15493	30.25	35.20	236	5,167,000	4.99	9.375
17	15334	30.94	39.01	155	4,949,000	4.22	9.48
26	15413	29.87	33.23	316	5,228,000	4.37	9.53
Mean	15405	30.43	36.23	216	5,115,000	4.29	9.32
St.Dev.	67	0.47	2.54	77	120,000	0.57	0.30
COV	0.43	1.55	7.01	35.79	2.34		3.22
<u>Row 5 (inner lane)</u>							
3	15175	31.53	42.60	95	5,268,000	0.915	8.875
6	15111	30.36	35.75	158	4,708,000	3.854	8.625
9	15016	32.04	46.00	83	6,563,000	0.929	8.72
12	15302	30.95	39.07	117	3,874,000	2.770	9.37
17	15254	31.22	40.68	110	4,404,000	3.197	9.28
20	15223	30.60	37.09	166	5,067,000	3.832	9.00
23	15254	30.19	34.87	208	4,842,000	5.254	9.06
26	15127	32.05	46.04	93	5,730,000	2.705	9.50
Mean	15183	31.12	40.26	129	5,057,000	4.29	9.32
St.Dev.	94	0.72	4.36	44	824,000	0.57	0.30
COV	0.62	2.31	10.82	34.14	16.31		3.22

Table E-4. Thicknesses Calculated for a 6,088,000 psi Concrete Modulus
- SR 5.

Station	Load (lbs)	Thickness (inches)	COV (%)	Measured Thickness (inches)
<u>Row 2 (outer lane) - Uncracked Slabs</u>				
3	15382	8.37	1.20	8.875
12	15494	8.88	1.67	9.375
17	15335	8.85	1.42	9.48
26	15414	9.06	1.46	9.53
40	15319	6.23	1.70	9.00
Mean	15389	8.28	1.49	9.25
St.Dev.	70	1.17	0.20	0.30
COV	0.45	14.17		3.20
<u>Row 2 - Cracked Slabs</u>				
6	15462	8.54	1.81	8.375
9	15462	9.03	1.21	8.56
20	15478	7.62	2.94	9.00
23	15525	8.39	3.17	9.125
31	15366	8.64	2.35	8.875
34	15605	7.86	2.73	8.75
37	15478	8.31	2.18	8.25
Mean	15482	8.34	2.34	8.70
St.Dev.	72	0.48	0.68	0.32
COV	0.47	5.70		3.73
<u>Row 5 (inner lane) - Uncracked Slabs</u>				
3	15176	8.46	0.31	8.875
6	15112	7.92	1.29	8.625
9	15017	8.94	0.31	8.72
12	15303	8.06	0.93	9.37
17	15255	8.33	1.07	9.28
20	15223	8.46	1.28	9.00
23	15255	8.39	1.77	9.06
26	15128	9.31	0.91	9.50
Mean	15184	8.48	0.98	9.05
St.Dev.	94	0.45	0.50	0.31
COV	0.62	5.31		3.44

Table E-4. Continued.

Station	Load (lbs)	Thickness (inches)	COV (%)	Measured Thickness (inches)
<u>Row 5 - Cracked Slabs</u>				
31	15223	9.14	0.30	8.75
34	15192	8.53	0.31	8.44
37	15207	10.31	0.28	8.25
40	15271	7.64	2.10	?
Mean	15223	8.91	0.75	8.48
St.Dev.	34	1.12	0.90	0.25
COV	0.23	12.59		2.98

Table E-5. E-k for 7.8-Inch Design Thickness - SR 90.

Station	Load (lbs)	k (pci)	E (x 10 ⁶ psi)	COV (%)
<u>Row 1 (inner lane) - Uncracked Slabs</u>				
3	15843	208	6,908,000	5.7
6	15398	200	6,875,000	5.5
9	15430	203	6,869,000	4.5
12	15271	224	5,823,000	6.0
17	15398	278	4,272,000	7.7
20	15366	247	3,952,000	8.7
23	15366	271	4,223,000	7.4
26	15382	324	4,683,000	7.8
37	15414	263	3,554,000	6.8
40	15239	289	3,862,000	7.2
43	15207	227	6,727,000	4.8
Mean	15392	249	5,250,000	6.6
St.Dev.	167	40	1,391,000	1.4
COV	1.09	16.12	26.49	
<u>Row 1 - Cracked Slabs</u>				
31	15748	283	3,955,000	7.8
34	15509	280	4,795,000	7.4
Mean	15629	282	4,375,000	7.6
St.Dev.	169	2	594,000	0.3
COV	1.08	0.75	13.58	
<u>Row 4 (outer lane) - Uncracked Slabs</u>				
3	15239	141	7,683,000	2.9
18	15239	163	7,387,000	4.0
29	15335	320	4,716,000	8.0
38	15335	222	7,252,000	4.1
Mean	15287	212	6,760,000	4.8
St.Dev.	55	80	1,374,000	2.2
COV	0.36	37.83	20.33	

Table E-5. Continued.

Station	Load (lbs)	k (pci)	E ($\times 10^6$ psi)	COV (%)
<u>Row 4 - Cracked Slabs</u>				
6	14921	248	3,798,000	9.0
9	15271	215	5,626,000	6.0
12	15223	253	3,701,000	8.4
15	15192	231	4,401,000	8.0
23	15160	364	3,190,000	7.6
26	15192	309	3,649,000	7.9
32	15589	370	3,720,000	7.3
35	15144	315	3,896,000	6.9
43	15112	189	6,597,000	3.7
46	15144	283	3,288,000	6.9
49	15255	310	3,750,000	5.9
52	15160	283	3,652,000	6.7
55	15350	290	3,544,000	6.6
58	15112	273	3,682,000	6.4
61	15366	317	3,406,000	5.9
64	15319	216	3,214,000	6.1
Mean	15219	279	3,945,000	6.8
St. Dev.	146	52	912,000	1.2
COV	0.96	18.59	23.11	

Table E-6. E-k for 7.72-Inch Average Thickness - SR 90.

Station	Load (lbs)	k (pci)	E (x 10 ⁶ psi)	COV (%)
<u>Row 1 (inner lane) - Uncracked Slabs</u>				
3	15843	208	7,125,000	5.7
6	15398	200	7,090,000	5.5
9	15430	203	7,084,000	4.5
12	15271	224	6,006,000	6.0
17	15398	278	4,407,000	7.7
20	15366	247	4,076,000	8.7
23	15366	271	4,356,000	7.4
26	15382	324	4,830,000	7.8
37	15414	263	3,665,000	6.8
40	15239	289	3,984,000	7.2
43	15207	227	6,934,000	4.8
Mean	15392	249	5,414,000	6.6
St.Dev.	167	40	1,434,000	1.4
COV	1.09	16.12	26.48	
<u>Row 1 - Cracked Slabs</u>				
31	15748	283	4,079,000	7.8
34	15509	280	4,946,000	7.4
Mean	15629	282	4,512,000	7.6
St.Dev.	169	2	613,000	0.3
COV	1.08	0.75	13.59	
<u>Row 4 (outer lane) - Uncracked Slabs</u>				
3	15239	141	7,924,000	2.9
18	15239	163	7,619,000	4.0
29	15335	320	4,864,000	8.0
38	15335	222	7,480,000	4.1
Mean	15287	212	6,972,000	4.8
St.Dev.	55	80	1,417,000	2.2
COV	0.36	37.83	20.33	

Table E-6. Continued.

Station	Load (lbs)	k (pci)	E (x 10 ⁶ psi)	COV (%)
<u>Row 4 - Cracked Slabs</u>				
6	14921	248	3,917,000	9.0
9	15271	215	5,802,000	6.0
12	15223	253	3,817,000	8.4
15	15192	231	4,539,000	8.0
23	15160	364	3,290,000	7.6
26	15192	309	3,763,000	7.9
32	15589	370	3,837,000	7.3
35	15144	315	4,018,000	6.9
43	15112	189	6,804,000	3.7
46	15144	283	3,391,000	6.9
49	15255	310	3,868,000	5.9
52	15160	283	3,766,000	6.7
55	15350	290	3,655,000	6.6
58	15112	273	3,798,000	6.4
61	15366	317	3,513,000	5.9
64	15319	216	3,315,000	6.1
Mean	15219	279	4,068,000	6.8
St.Dev.	146	52	940,000	1.2
COV	0.96	18.59	23.11	

Table E-7. E-k for Actual Thickness, Uncracked Slabs Only - SR 90.

Station	Load (lbs)	Area (inches)	l-k (inches)	k (pci)	E (psi)	COV (%)	h (inches)
<u>Row 1 (inner lane)</u>							
3	15842	30.03	34.04	208	5,838,000	5.74	8.25
6	15397	30.09	34.34	200	6,082,000	5.49	8.12
9	15429	30.06	34.18	203	6,077,000	4.55	8.12
12	15270	29.62	32.01	224	5,189,000	6.00	8.10
17	15397	28.74	28.08	278	4,223,000	7.70	7.83
20	15366	28.81	28.36	247	4,028,000	8.65	7.75
23	15366	28.77	28.19	270	4,223,000	7.35	7.80
26	15382	28.64	27.66	324	4,542,000	7.82	7.88
37	15413	28.21	27.18	264	4,426,000	6.80	7.25
40	15238	28.51	27.11	289	4,414,000	7.25	7.46
43	15207	29.84	33.10	227	7,330,000	4.76	7.58
Mean	15392	29.21	30.39	249	5,125,000	6.56	7.83
St.Dev.	167	0.72	3.10	40	1,066,000	1.34	0.31
COV	1.08	2.45	10.20	16.11	20.80		3.96
<u>Row 4 (outer lane)</u>							
3	15238	31.00	39.35	136	7,583,000	2.25	7.96
18	15238	30.55	36.78	161	6,235,000	3.95	8.21
29	15334	28.67	27.79	320	5,138,000	8.02	7.58
38	15334	30.00	33.89	222	7,033,000	4.13	7.88
Mean	15286	30.06	34.45	210	6,497,000	4.58	7.91
St.Dev.	55	1.01	4.97	82	1,062,000	2.44	0.26
COV	0.36	3.36	14.43	39.04	16.34		3.28

Table E-8. Thicknesses Calculated for a 5,403,000 psi Concrete Modulus
- SR 90.

Station	Load (lbs)	Thickness (inches)	COV (%)	Measured Thickness (inches)
<u>Row 1 (inner lane) - Uncracked Slabs</u>				
3	15843	8.46	1.93	8.25
6	15398	8.45	1.84	8.12
9	15430	8.45	1.53	8.12
12	15271	7.99	2.00	8.10
17	15398	7.21	2.60	7.83
20	15366	7.02	2.92	7.75
23	15366	7.18	2.48	7.80
26	15382	7.43	2.64	7.88
37	15414	6.78	2.28	7.25
40	15239	6.97	2.44	7.46
43	15207	8.39	1.59	7.58
Mean	15392	7.67	2.20	7.83
St.Dev.	167	0.68	0.46	0.31
COV	1.09	8.92		3.96
<u>Row 1 - Cracked Slabs</u>				
31	15748	7.03	2.64	?
34	15509	7.49	2.48	?
Mean	15629	7.26	2.56	
St.Dev.	169	0.33	0.11	
COV	1.08	4.48		
<u>Row 4 (outer lane) - Uncracked Slabs</u>				
3	15239	8.77	0.96	7.96
18	15239	8.66	1.33	8.21
29	15335	7.45	2.71	7.58
38	15335	8.60	1.38	7.88
Mean	15287	8.37	1.60	7.91
St.Dev.	55	0.62	0.77	0.26
COV	0.36	7.38		3.28

Table E-8. Continued.

Station	Load (lbs)	Thickness (inches)	COV (%)	Measured Thickness (inches)
<u>Row 4 - Cracked Slabs</u>				
6	14921	6.93	3.04	7.75
9	15271	7.90	2.00	8.00
12	15223	6.87	2.83	7.92
15	15192	7.28	2.69	7.88
23	15160	6.54	2.54	7.54
26	15192	6.84	2.69	7.83
32	15589	6.88	2.45	7.50
35	15144	6.99	2.32	7.40
43	15112	8.34	1.25	7.55
46	15144	6.61	2.34	7.54
49	15255	6.90	1.98	7.25
52	15160	6.84	2.27	7.29
55	15350	6.77	2.22	7.38
58	15112	6.86	2.15	7.46
61	15366	6.69	1.97	7.56
64	15319	6.56	2.06	7.50
Mean	15219	6.99	2.30	7.58
St.Dev.	146	0.48	0.42	0.23
COV	0.96	6.92		2.99

APPENDIX F

CMS INPUT FILES, TEMPERATURE DIFFERENTIALS, AND THERMAL GRADIENTS

MATERIAL/LAYER DATA

LAYER TYPE THICK.

1 STABILIZED 9.00
2 A-1 7.00
3 A-2 128.00

STABILITY CHECK

STABILITY TEST = STABLE

PAVEMENT DATA

PAVEMENT NUMBER	LOCATION	DATE	TOTAL DEPTH (IN)	DEPTHX (IN)	DEPTHW (IN)	NORMAL NODE DEH (IN)	FREEZING TEMPERATURE (F)
I-5	Stat 1	Jul 1987	144.00	72.75	71.25	1.50	30.00

TERMINATION NODE DEPTH (IN)	TIME STEP (HR)	MAXIMUM CONVECTION COEFFICIENT (BTU/HR-FT ² -F)	LAYERS	NUMBER OF NORMAL NODES	NUMBER OF TERMINATION NODES
23.7500	0.1250	3.0000	3	49	3

PROPERTIES OF THE ASPHALT LAYERS

PROPERTIES OF THE STABILIZED LAYERS

LAYER = 1

THICKNESS (IN.) = 9.00
WATER CONTENT (%) = 3.00
THAWED FREEZING FROZEN
UNIT WEIGHT (PCF) 150.00 150.00 150.00
THERMAL CONDUCTIVITY (BTU/HR-FT-F) 1.25 1.29 1.33
HEAT CAPACITY (BTU/LB-F) 0.22 2.16 0.22

PROPERTIES OF COARSE-GRAINED LAYERS

LAYER = 2

THICKNESS (IN.) = 7.00
UNIT WEIGHT (PCF) = 125.00
HEAT CAPACITY (BTU/HR-FT-F) = 0.24
PERCENT FINES (%) = 8.00

LAYER = 3

THICKNESS (IN.) = 128.00
UNIT WEIGHT (PCF) = 112.50
HEAT CAPACITY (BTU/HR-FT-F) = 0.25
WATER CONTENT = 11.00

PROPERTIES OF FINE-GRAINED LAYERS

WATER TABLE DEPTH = 80.00 IN.

PAVEMENT TEMPERATURE PROFILE DATE = 7 /15 TIME(HR) = 1.00

NODE TEMPERATURE DEPTH (IN.)

NUMBER	(F)	
1	70.31	0.00
2	73.54	1.50
3	76.13	3.00
4	78.11	4.50
5	79.52	6.00
6	80.42	7.50
7	80.85	9.00

PAVEMENT TEMPERATURE PROFILE DATE = 7 /15 TIME(HR) = 2.00

NODE TEMPERATURE DEPTH (IN.)

NUMBER	(F)	
1	68.73	0.00
2	72.01	1.50
3	74.68	3.00
4	76.75	4.50
5	78.28	6.00
6	79.31	7.50
7	79.89	9.00

PAVEMENT TEMPERATURE PROFILE DATE = 7 /15 TIME(HR) = 3.00

NODE TEMPERATURE DEPTH (IN.)

NUMBER	(F)	
1	67.19	0.00
2	70.53	1.50
3	73.27	3.00
4	75.44	4.50
5	77.08	6.00
6	78.23	7.50
7	78.93	9.00

PAVEMENT TEMPERATURE PROFILE DATE = 7 /15 TIME(HR) = 4.00

NODE TEMPERATURE DEPTH (IN.)

NUMBER	(F)	
1	66.54	0.00
2	69.42	1.50
3	72.01	3.00
4	74.19	4.50
5	75.91	6.00
6	77.16	7.50
7	77.97	9.00

PAVEMENT TEMPERATURE PROFILE DATE = 7 /15 TIME(HR) = 5.00

NODE TEMPERATURE DEPTH (IN.)

NUMBER	(F)	
1	68.01	0.00
2	69.37	1.50
3	71.29	3.00
4	73.21	4.50
5	74.86	6.00
6	76.14	7.50
7	77.03	9.00

PAVEMENT TEMPERATURE PROFILE DATE = 7 /15 TIME(HR) = 6.00

NODE TEMPERATURE DEPTH (IN.)

NUMBER	(F)	
1	71.95	0.00
2	71.39	1.50
3	71.93	3.00
4	73.00	4.50
5	74.22	6.00
6	75.33	7.50
7	76.19	9.00

PAVEMENT TEMPERATURE PROFILE DATE = 7 /15 TIME(HR) = 7.00

NODE TEMPERATURE DEPTH (IN.)

NUMBER	(F)	
1	76.34	0.00
2	74.31	1.50
3	73.58	3.00
4	73.69	4.50
5	74.25	6.00
6	74.96	7.50
7	75.64	9.00

PAVEMENT TEMPERATURE PROFILE DATE = 7 /15 TIME(HR) = 8.00

NODE TEMPERATURE DEPTH (IN.)

NUMBER	(F)	
1	80.72	0.00
2	77.57	1.50
3	75.79	3.00
4	75.00	4.50
5	74.86	6.00
6	75.09	7.50
7	75.48	9.00

PAVEMENT TEMPERATURE PROFILE DATE = 7 /15 TIME(HR) = 9.00

NODE TEMPERATURE DEPTH (IN.)

NUMBER	(F)	
1	84.82	0.00
2	80.88	1.50
3	78.27	3.00
4	76.71	4.50
5	75.93	6.00
6	75.66	7.50
7	75.71	9.00

PAVEMENT TEMPERATURE PROFILE DATE = 7 /15 TIME(HR) = 10.00

NODE TEMPERATURE DEPTH (IN.)

NUMBER	(F)	
1	88.51	0.00
2	84.04	1.50
3	80.82	3.00
4	78.65	4.50
5	77.30	6.00

6	76.57	7.50
7	76.28	9.00

PAVEMENT TEMPERATURE PROFILE DATE = 7 /15 TIME(HR) = 11.00

NODE TEMPERATURE DEPTH (IN.)

NUMBER	(F)	
1	91.68	0.00
2	86.94	1.50
3	83.31	3.00
4	80.67	4.50
5	78.86	6.00
6	77.73	7.50
7	77.11	9.00

PAVEMENT TEMPERATURE PROFILE DATE = 7 /15 TIME(HR) = 12.00

NODE TEMPERATURE DEPTH (IN.)

NUMBER	(F)	
1	94.26	0.00
2	89.46	1.50
3	85.61	3.00
4	82.66	4.50
5	80.51	6.00
6	79.03	7.50
7	78.12	9.00

PAVEMENT TEMPERATURE PROFILE DATE = 7 /15 TIME(HR) = 13.00

NODE TEMPERATURE DEPTH (IN.)

NUMBER	(F)	
1	96.19	0.00
2	91.55	1.50
3	87.66	3.00
4	84.53	4.50
5	82.14	6.00
6	80.41	7.50
7	79.25	9.00

PAVEMENT TEMPERATURE PROFILE DATE = 7 /15 TIME(HR) = 14.00

NODE TEMPERATURE DEPTH (IN.)

NUMBER	(F)	
1	97.43	0.00
2	93.14	1.50
3	89.37	3.00
4	86.21	4.50
5	83.69	6.00
6	81.79	7.50
7	80.43	9.00

PAVEMENT TEMPERATURE PROFILE DATE = 7 /15 TIME(HR) = 15.00

NODE TEMPERATURE DEPTH (IN.)

NUMBER	(F)	
1	97.94	0.00
2	94.16	1.50
3	90.68	3.00

4	87.63	4.50
5	85.09	6.00
6	83.09	7.50
7	81.60	9.00

PAVEMENT TEMPERATURE PROFILE DATE = 7 /15 TIME(HR) = 16.00

NODE TEMPERATURE DEPTH (IN.)

NUMBER	(F)	
1	96.78	0.00
2	94.24	1.50
3	91.42	3.00
4	88.69	4.50
5	86.27	6.00
6	84.26	7.50
7	82.69	9.00

PAVEMENT TEMPERATURE PROFILE DATE = 7 /15 TIME(HR) = 17.00

NODE TEMPERATURE DEPTH (IN.)

NUMBER	(F)	
1	94.22	0.00
2	93.09	1.50
3	91.25	3.00
4	89.14	4.50
5	87.07	6.00
6	85.20	7.50
7	83.65	9.00

PAVEMENT TEMPERATURE PROFILE DATE = 7 /15 TIME(HR) = 18.00

NODE TEMPERATURE DEPTH (IN.)

NUMBER	(F)	
1	90.58	0.00
2	90.96	1.50
3	90.24	3.00
4	88.92	4.50
5	87.35	6.00
6	85.78	7.50
7	84.36	9.00

PAVEMENT TEMPERATURE PROFILE DATE = 7 /15 TIME(HR) = 19.00

NODE TEMPERATURE DEPTH (IN.)

NUMBER	(F)	
1	85.92	0.00
2	87.91	1.50
3	88.43	3.00
4	88.03	4.50
5	87.10	6.00
6	85.94	7.50
7	84.74	9.00

PAVEMENT TEMPERATURE PROFILE DATE = 7 /15 TIME(HR) = 20.00

NODE TEMPERATURE DEPTH (IN.)

NUMBER	(F)	
1	80.62	0.00

2	83.99	1.50
3	85.84	3.00
4	86.46	4.50
5	86.28	6.00
6	85.63	7.50
7	84.75	9.00

PAVEMENT TEMPERATURE PROFILE DATE = 7 /15 TIME(HR) = 21.00

NODE TEMPERATURE DEPTH (IN.)

NUMBER	(F)	
1	77.71	0.00
2	80.96	1.50
3	83.19	3.00
4	84.47	4.50
5	84.96	6.00
6	84.86	7.50
7	84.35	9.00

PAVEMENT TEMPERATURE PROFILE DATE = 7 /15 TIME(HR) = 22.00

NODE TEMPERATURE DEPTH (IN.)

NUMBER	(F)	
1	75.54	0.00
2	78.73	1.50
3	81.08	3.00
4	82.65	4.50
5	83.52	6.00
6	83.80	7.50
7	83.63	9.00

PAVEMENT TEMPERATURE PROFILE DATE = 7 /15 TIME(HR) = 23.00

NODE TEMPERATURE DEPTH (IN.)

NUMBER	(F)	
1	73.67	0.00
2	76.84	1.50
3	79.28	3.00
4	81.02	4.50
5	82.13	6.00
6	82.67	7.50
7	82.75	9.00

PAVEMENT TEMPERATURE PROFILE DATE = 7 /15 TIME(HR) = 24.00

NODE TEMPERATURE DEPTH (IN.)

NUMBER	(F)	
1	71.94	0.00
2	75.13	1.50
3	77.65	3.00
4	79.52	4.50
5	80.80	6.00
6	81.54	7.50
7	81.82	9.00

Table F-2. Temperature, Sunshine and Wind CMS Input File - SR 5.

ANNA WEEK	LOW		HIGH		MEAN		SUN	WIND
	AVERAGE	STNDEV NO	AVERAGE	STNDEV NO	AVERAGE	STNDEV NO		
1	36.96		52.04				50.0	9.9
2	37.80		53.27				50.0	9.9
3	38.63		54.51				50.0	9.9
4	39.46		55.76				50.0	9.9
5	40.36		57.04				53.0	9.6
6	41.50		58.66				53.0	9.6
7	42.77		60.31				53.0	9.6
8	44.01		61.97				53.0	9.6
9	45.24		63.63				53.0	9.6
10	46.40		64.88				56.0	09.0
11	47.5		66.00				56.0	09.0
12	48.70		67.10				56.0	09.0
13	49.8		68.20				56.0	09.0
14	50.80		69.40				54.0	08.8
15	51.60		70.80				54.0	08.8
16	52.30		72.30				54.0	08.8
17	53.10		73.70				54.0	08.8
18	53.80		75.10				64.0	08.3
19	53.80		74.80				64.0	08.3
20	53.80		74.50				64.0	08.3
21	53.70		74.20				64.0	08.3
22	53.70		73.90				64.0	08.3
23	53.30		73.10				63.0	07.9
24	52.50		72.00				63.0	07.9
25	51.80		70.80				63.0	07.9
26	51.00		69.70				63.0	07.9
27	50.20		68.40				59.0	08.1
28	48.90		66.20				59.0	08.1
29	47.70		64.10				59.0	08.1
30	46.40		61.90				59.0	08.1
31	45.10		59.70				59.0	08.1
32	42.80		57.70				44.0	08.6
33	40.20		55.60				44.0	08.6
34	37.70		53.60				44.0	08.6
35	35.20		51.60				44.0	08.6
36	38.50		49.90				30.0	09.2
37	37.70		48.70				30.0	09.2
38	36.90		47.60				30.0	09.2
39	36.20		46.40				30.0	09.2
40	35.40		45.30				20.0	9.8
41	43.90		44.90				20.0	9.8
42	34.30		44.40				20.0	9.8
43	33.70		44.00				20.0	9.8
44	33.20		43.50				20.0	09.8
45	30.70		44.20				24.0	09.9
46	31.20		45.40				24.0	09.9
47	31.60		46.50				24.0	09.9
48	32.10		47.70				24.0	09.9
49	36.00		48.70				38.0	9.7

50	36.20	49.50	38.0	9.7
51	36.30	50.20	38.0	9.7
52	36.50	51.00	38.0	9.7
53	36.60	51.40	38.0	9.7

Table F-3. Radiation Data CMS Input File - SR 5.

6	17	4.1395	19.8605	3781.2655
6	18	4.1365	19.8635	3783.2470
6	19	4.1346	19.8654	3784.5680
6	20	4.1327	19.8673	3781.9780
6	21	4.1317	19.8683	3782.6379
6	22	4.1317	19.8683	3782.6379
6	23	4.1317	19.8683	3782.6379
6	24	4.1327	19.8673	3781.9780
6	25	4.1346	19.8654	3780.6584
6	26	4.1375	19.8625	3778.6789
6	27	4.1404	19.8596	3776.6994
6	28	4.1433	19.8567	3774.7200
6	29	4.1482	19.8518	3771.4210
6	30	4.1530	19.8470	3768.1219
7	1	4.1588	19.8412	3764.1632
7	2	4.1655	19.8345	3759.5446
7	3	4.1723	19.8277	3754.9262
7	4	4.1800	19.8200	3749.6479
7	5	4.1876	19.8124	3744.3698
7	6	4.1972	19.8028	3737.7721
7	7	4.2057	19.7943	3731.8342
7	8	4.2162	19.7838	3724.5768
7	9	4.2266	19.7734	3717.3194
7	10	4.2379	19.7621	3709.4021
7	11	4.2492	19.7508	3701.4848
7	12	4.2614	19.7386	3692.9076
7	13	4.2745	19.7255	3683.6704
7	14	4.2885	19.7115	3673.7732
7	15	4.3024	19.6976	3663.8756
7	16	4.3163	19.6837	3653.9776
7	17	4.3319	19.6681	3642.7594
7	18	4.3466	19.6534	3632.2005
7	19	4.3630	19.6370	3620.3210
7	20	4.3794	19.6206	3612.1723
7	21	4.3957	19.6043	3600.2787
7	22	4.4137	19.5863	3587.0625
7	23	4.4308	19.5692	3574.5058
7	24	4.4504	19.5496	3559.9649
7	25	4.4673	19.5327	3547.4054
7	26	4.4868	19.5132	3532.8610
7	27	4.5061	19.4939	3518.3145
7	28	4.5254	19.4746	3503.7660
7	29	4.5454	19.4546	3488.5538
7	30	4.5663	19.4337	3472.6776
7	31	4.5870	19.4130	3456.7985

MATERIAL/LAYER DATA

LAYER TYPE THICK.

1 STABILIZED 7.80
2 A-1 5.20
3 A-3 130.00

STABILITY CHECK

STABILITY TEST = STABLE

PAVEMENT DATA

PAVEMENT NUMBER	LOCATION	DATE	TOTAL DEPTH (IN)	DEPTHX (IN)	DEPTHW (IN)	NORMAL NODE TEMPERATURE (F)	FREEZING
I-90	Stat 1	July 1987	143.00	72.15	70.85	1.30	30.00

TERMINATION NODE DEPTH (IN)	TIME STEP (HR)	MAXIMUM CONVECTION COEFFICIENT (BTU/HR-FT ² -F)	LAYERS	NUMBER OF NORMAL NODES	NUMBER OF TERMINATION NODES
23.6167	0.1000	3.0000	3	56	3

PROPERTIES OF THE ASPHALT LAYERS

PROPERTIES OF THE STABILIZED LAYERS

LAYER = 1

THICKNESS (IN.) = 7.80
WATER CONTENT (%) = 3.00

	THAWED	FREEZING	FROZEN
UNIT WEIGHT (PCF)	150.00	150.00	150.00
THERMAL CONDUCTIVITY (BTU/HR-FT-F)	1.25	1.29	1.33
HEAT CAPACITY (BTU/LB-F)	0.22	2.16	0.22

PROPERTIES OF COARSE-GRAINED LAYERS

LAYER = 2

THICKNESS (IN.) = 5.20
UNIT WEIGHT (PCF) = 125.00
HEAT CAPACITY (BTU/HR-FT-F) = 0.24
PERCENT FINES (%) = 8.00

LAYER = 3

THICKNESS (IN.) = 130.00
UNIT WEIGHT (PCF) = 112.50
HEAT CAPACITY (BTU/HR-FT-F) = 0.25

PROPERTIES OF FINE-GRAINED LAYERS

WATER TABLE DEPTH = 80.00 IN.

PAVEMENT TEMPERATURE PROFILE DATE = 7/15 TIME(HR) = F-10

NODE TEMPERATURE DEPTH (IN.)

NUMBER	(F)	
1	63.14	0.00
2	66.88	1.30
3	69.98	2.60
4	72.47	3.90
5	74.39	5.20
6	75.79	6.50
7	76.70	7.80

PAVEMENT TEMPERATURE PROFILE DATE = 7 /15 TIME(HR) = 2.00

NODE TEMPERATURE DEPTH (IN.)

NUMBER	(F)	
1	61.04	0.00
2	64.85	1.30
3	68.05	2.60
4	70.66	3.90
5	72.71	5.20
6	74.25	6.50
7	75.31	7.80

PAVEMENT TEMPERATURE PROFILE DATE = 7 /15 TIME(HR) = 3.00

NODE TEMPERATURE DEPTH (IN.)

NUMBER	(F)	
1	58.97	0.00
2	62.87	1.30
3	66.17	2.60
4	68.88	3.90
5	71.06	5.20
6	72.73	6.50
7	73.93	7.80

PAVEMENT TEMPERATURE PROFILE DATE = 7 /15 TIME(HR) = 4.00

NODE TEMPERATURE DEPTH (IN.)

NUMBER	(F)	
1	58.17	0.00
2	61.49	1.30
3	64.54	2.60
4	67.22	3.90
5	69.46	5.20
6	71.23	6.50
7	72.55	7.80

PAVEMENT TEMPERATURE PROFILE DATE = 7 /15 TIME(HR) = 5.00

NODE TEMPERATURE DEPTH (IN.)

NUMBER	(F)	
1	60.05	0.00
2	61.63	1.30
3	63.79	2.60
4	66.05	3.90
5	68.12	5.20
6	69.87	6.50
7	71.24	7.80

PAVEMENT TEMPERATURE PROFILE DATE = 7 /15 TIME(HR) = 6.00

NODE TEMPERATURE DEPTH (IN.)

NUMBER	(F)	
1	64.69	0.00
2	64.27	1.30
3	64.89	2.60
4	66.09	3.90
5	67.52	5.20
6	68.93	6.50
7	70.18	7.80

PAVEMENT TEMPERATURE PROFILE DATE = 7 /15 TIME(HR) = 7.00

NODE TEMPERATURE DEPTH (IN.)

NUMBER	(F)	
1	69.86	0.00
2	67.91	1.30
3	67.18	2.60
4	67.27	3.90
5	67.88	5.20
6	68.75	6.50
7	69.68	7.80

PAVEMENT TEMPERATURE PROFILE DATE = 7 /15 TIME(HR) = 8.00

NODE TEMPERATURE DEPTH (IN.)

NUMBER	(F)	
1	75.03	0.00
2	71.92	1.30
3	70.08	2.60
4	69.20	3.90
5	69.01	5.20
6	69.26	6.50
7	69.79	7.80

PAVEMENT TEMPERATURE PROFILE DATE = 7 /15 TIME(HR) = 9.00

NODE TEMPERATURE DEPTH (IN.)

NUMBER	(F)	
1	79.90	0.00
2	75.97	1.30
3	73.27	2.60
4	71.58	3.90
5	70.67	5.20
6	70.35	6.50
7	70.43	7.80

PAVEMENT TEMPERATURE PROFILE DATE = 7 /15 TIME(HR) = 10.00

NODE TEMPERATURE DEPTH (IN.)

NUMBER	(F)	
1	84.32	0.00
2	79.84	1.30
3	76.52	2.60
4	74.18	3.90
5	72.68	5.20
6	71.83	6.50

7 71.50 7.80

PAVEMENT TEMPERATURE PROFILE DATE = 7 /15 TIME(HR) = 11.00

NODE TEMPERATURE DEPTH (IN.)

NUMBER	(F)	
1	88.17	0.00
2	83.40	1.30
3	79.66	2.60
4	76.85	3.90
5	74.87	5.20
6	73.58	6.50
7	72.87	7.80

PAVEMENT TEMPERATURE PROFILE DATE = 7 /15 TIME(HR) = 12.00

NODE TEMPERATURE DEPTH (IN.)

NUMBER	(F)	
1	91.36	0.00
2	86.52	1.30
3	82.56	2.60
4	79.45	3.90
5	77.12	5.20
6	75.48	6.50
7	74.44	7.80

PAVEMENT TEMPERATURE PROFILE DATE = 7 /15 TIME(HR) = 13.00

NODE TEMPERATURE DEPTH (IN.)

NUMBER	(F)	
1	93.83	0.00
2	89.13	1.30
3	85.13	2.60
4	81.87	3.90
5	79.31	5.20
6	77.41	6.50
7	76.10	7.80

PAVEMENT TEMPERATURE PROFILE DATE = 7 /15 TIME(HR) = 14.00

NODE TEMPERATURE DEPTH (IN.)

NUMBER	(F)	
1	95.52	0.00
2	91.14	1.30
3	87.29	2.60
4	84.01	3.90
5	81.35	5.20
6	79.28	6.50
7	77.77	7.80

PAVEMENT TEMPERATURE PROFILE DATE = 7 /15 TIME(HR) = 15.00

NODE TEMPERATURE DEPTH (IN.)

NUMBER	(F)	
1	96.39	0.00
2	92.51	1.30
3	88.95	2.60
4	85.81	3.90

5	83.16	5.20
6	81.01	6.50
7	79.38	7.80

PAVEMENT TEMPERATURE PROFILE DATE = 7 /15 TIME(HR) = 16.00

NODE TEMPERATURE DEPTH (IN.)

NUMBER	(F)	
1	94.91	0.00
2	92.48	1.30
3	89.76	2.60
4	87.07	3.90
5	84.62	5.20
6	82.53	6.50
7	80.84	7.80

PAVEMENT TEMPERATURE PROFILE DATE = 7 /15 TIME(HR) = 17.00

NODE TEMPERATURE DEPTH (IN.)

NUMBER	(F)	
1	91.86	0.00
2	90.94	1.30
3	89.34	2.60
4	87.42	3.90
5	85.45	5.20
6	83.62	6.50
7	82.03	7.80

PAVEMENT TEMPERATURE PROFILE DATE = 7 /15 TIME(HR) = 18.00

NODE TEMPERATURE DEPTH (IN.)

NUMBER	(F)	
1	87.55	0.00
2	88.22	1.30
3	87.86	2.60
4	86.86	3.90
5	85.55	5.20
6	84.13	6.50
7	82.76	7.80

PAVEMENT TEMPERATURE PROFILE DATE = 7 /15 TIME(HR) = 19.00

NODE TEMPERATURE DEPTH (IN.)

NUMBER	(F)	
1	82.05	0.00
2	84.40	1.30
3	85.38	2.60
4	85.43	3.90
5	84.89	5.20
6	84.01	6.50
7	82.98	7.80

PAVEMENT TEMPERATURE PROFILE DATE = 7 /15 TIME(HR) = 20.00

NODE TEMPERATURE DEPTH (IN.)

NUMBER	(F)	
1	75.79	0.00
2	79.56	1.30

3	81.93	2.60
4	83.13	3.90
5	83.46	5.20
6	83.23	6.50
7	82.64	7.80

PAVEMENT TEMPERATURE PROFILE DATE = 7 /15 TIME(HR) = 21.00

NODE TEMPERATURE DEPTH (IN.)

NUMBER	(F)	
1	72.24	0.00
2	75.89	1.30
3	78.59	2.60
4	80.41	3.90
5	81.44	5.20
6	81.83	6.50
7	81.71	7.80

PAVEMENT TEMPERATURE PROFILE DATE = 7 /15 TIME(HR) = 22.00

NODE TEMPERATURE DEPTH (IN.)

NUMBER	(F)	
1	69.51	0.00
2	73.12	1.30
3	75.95	2.60
4	78.02	3.90
5	79.41	5.20
6	80.18	6.50
7	80.44	7.80

PAVEMENT TEMPERATURE PROFILE DATE = 7 /15 TIME(HR) = 23.00

NODE TEMPERATURE DEPTH (IN.)

NUMBER	(F)	
1	67.10	0.00
2	70.72	1.30
3	73.64	2.60
4	75.88	3.90
5	77.49	5.20
6	78.53	6.50
7	79.06	7.80

PAVEMENT TEMPERATURE PROFILE DATE = 7 /15 TIME(HR) = 24.00

NODE TEMPERATURE DEPTH (IN.)

NUMBER	(F)	
1	64.84	0.00
2	68.51	1.30
3	71.52	2.60
4	73.90	3.90
5	75.68	5.20
6	76.92	6.50
7	77.66	7.80

Table F-5. Temperature, Sunshine and Wind CMS Input File - SR 90.

ANNA WEEK	LOW		HIGH		MEAN		SUN	WIND
	AVERAGE	STNDEV NO	AVERAGE	STNDEV NO	AVERAGE	STNDEV NO		
1	29.40		47.20				53.0	9.6
2	30.90		49.70				53.0	9.6
3	32.33		52.10				53.0	9.6
4	33.80		54.60				53.0	9.6
5	35.20		57.00				60.0	9.8
6	37.00		59.20				60.0	9.8
7	38.70		61.40				60.0	9.8
8	40.50		63.70				60.0	9.8
9	42.30		65.90				60.0	9.8
10	43.90		67.60				63.0	08.9
11	45.40		69.20				63.0	08.9
12	46.80		70.90				63.0	08.9
13	48.30		72.50				63.0	08.9
14	49.80		74.30				65.0	08.9
15	51.10		76.80				65.0	08.9
16	52.40		79.30				65.0	08.9
17	53.80		81.80				65.0	08.9
18	55.10		84.30				80.0	08.3
19	54.90		83.80				80.0	08.3
20	54.60		83.20				80.0	08.3
21	54.40		82.70				80.0	08.3
22	54.10		82.10				80.0	08.3
23	53.10		80.70				77.0	08.1
24	51.40		78.60				77.0	08.1
25	49.80		76.40				77.0	08.1
26	48.10		74.30				77.0	08.1
27	46.40		72.00				70.0	08.1
28	44.20		68.70				70.0	08.1
29	42.10		65.30				70.0	08.1
30	40.00		61.90				70.0	08.1
31	37.80		58.60				70.0	08.1
32	35.90		54.90				53.0	08.0
33	34.00		51.30				53.0	08.0
34	32.10		47.60				53.0	08.0
35	30.30		43.90				28.0	08.3
36	28.70		41.00				28.0	08.3
37	27.50		39.20				28.0	08.3
38	26.30		37.30				28.0	08.3
39	25.00		35.50				28.0	08.3
40	23.90		33.80				21.0	8.7
41	22.90		33.20				21.0	8.7
42	21.90		32.50				21.0	8.7
43	20.90		31.90				21.0	8.7
44	19.90		31.30				21.0	08.7
45	20.50		32.40				26.0	08.7
46	21.80		34.20				26.0	08.7
47	23.10		35.90				26.0	08.7
48	24.40		37.70				26.0	09.2
49	25.60		39.50				38.0	9.2

50	26.40	41.30	38.0	9.2
51	27.30	43.10	38.0	9.2
52	28.20	44.90	38.0	9.2
53	28.70	45.90	38.0	9.2

Table F-6. Radiation Data CMS Input File - SR 90.

6	17	4.1324	19.8676	3781.0169
6	18	4.1294	19.8706	3783.0056
6	19	4.1275	19.8725	3784.3314
6	20	4.1255	19.8745	3781.7464
6	21	4.1245	19.8755	3782.4087
6	22	4.1245	19.8755	3782.4087
6	23	4.1245	19.8755	3782.4087
6	24	4.1255	19.8745	3781.7464
6	25	4.1275	19.8725	3780.4220
6	26	4.1304	19.8696	3778.4353
6	27	4.1333	19.8667	3776.4487
6	28	4.1362	19.8638	3774.4621
6	29	4.1411	19.8589	3771.1511
6	30	4.1460	19.8540	3767.8402
7	1	4.1518	19.8482	3763.8671
7	2	4.1586	19.8414	3759.2319
7	3	4.1653	19.8347	3754.5969
7	4	4.1730	19.8270	3749.2997
7	5	4.1807	19.8193	3744.0027
7	6	4.1903	19.8097	3737.3814
7	7	4.1989	19.8011	3731.4224
7	8	4.2094	19.7906	3724.1393
7	9	4.2199	19.7801	3716.8562
7	10	4.2313	19.7687	3708.9110
7	11	4.2426	19.7574	3700.9659
7	12	4.2549	19.7451	3692.3587
7	13	4.2680	19.7320	3683.0893
7	14	4.2821	19.7179	3673.1577
7	15	4.2960	19.7040	3663.2260
7	16	4.3100	19.6900	3653.2940
7	17	4.3257	19.6743	3642.0374
7	18	4.3404	19.6596	3631.4425
7	19	4.3569	19.6431	3619.5228
7	20	4.3734	19.6266	3611.3331
7	21	4.3897	19.6103	3599.3997
7	22	4.4078	19.5922	3586.1394
7	23	4.4249	19.5751	3573.5411
7	24	4.4447	19.5553	3558.9523
7	25	4.4616	19.5384	3546.3517
7	26	4.4811	19.5189	3531.7600
7	27	4.5006	19.4994	3517.1666
7	28	4.5199	19.4801	3502.5713
7	29	4.5401	19.4599	3487.3106
7	30	4.5610	19.4390	3471.3841
7	31	4.5818	19.4182	3455.4551

Table F.7. Thermal Stresses, Calculated from Westergaard, SR 5

	Jan	Feb	Mar	Apr	May	Jun	Jul	Aug	Sep	Oct	Nov	Dec
1 am	-38.24	-41.44	-55.26	-71.30	-83.25	-85.03	-93.94	-85.83	-72.02	-55.26	-37.61	-34.22
2 am	-42.96	-45.81	-59.63	-76.20	-88.15	-90.56	-99.47	-91.00	-76.47	-59.98	-41.36	-37.43
3 am	-47.60	-50.18	-63.73	-80.93	-92.87	-95.72	-104.64	-95.81	-80.66	-64.35	-44.92	-40.64
4 am	-46.70	-49.11	-61.77	-78.70	-90.29	-93.14	-101.87	-93.50	-78.79	-63.10	-44.30	-40.62
5 am	-42.16	-44.39	-55.88	-71.93	-77.10	-69.25	-80.39	-86.19	-72.82	-58.02	-40.82	-36.81
6 am	-36.54	-38.59	-48.84	-51.25	-39.40	-30.04	-37.79	-51.70	-63.55	-51.52	-36.45	-32.71
7 am	-30.48	-32.35	-26.47	-12.57	1.78	9.80	6.24	-7.40	-27.90	-40.55	-31.82	-28.43
8 am	-18.63	-9.98	8.91	26.20	39.84	45.99	46.70	35.12	12.66	-10.34	-21.12	-23.80
9 am	3.21	18.00	42.78	60.43	72.64	76.83	81.20	72.28	49.73	21.30	0.89	-8.02
10 am	24.15	42.87	71.04	88.33	98.93	101.78	109.00	102.41	80.30	48.75	21.93	9.18
11 am	41.00	62.21	92.25	109.09	118.63	120.77	129.86	124.87	103.30	69.97	38.68	23.35
12	52.76	74.96	106.06	122.64	131.73	133.60	143.85	139.58	118.01	83.87	49.73	33.16
1 pm	58.91	81.02	112.30	128.97	138.15	140.47	150.98	146.71	124.60	90.56	54.81	37.86
2 pm	59.36	80.13	111.05	128.43	138.15	141.54	151.52	146.44	123.09	89.75	53.66	37.23
3 pm	54.10	72.46	102.41	121.04	132.00	136.99	145.64	138.77	113.64	81.73	46.26	31.37
4 pm	37.88	52.68	80.22	99.91	112.57	119.16	125.58	116.67	90.47	60.79	28.88	16.58
5 pm	15.42	23.00	47.15	67.92	82.44	91.09	94.21	82.62	55.62	29.06	6.06	3.12
6 pm	3.48	2.41	6.77	28.43	45.28	56.33	55.44	40.55	12.21	-1.78	-5.08	-4.10
7 pm	-4.81	-8.38	-13.64	-14.53	2.32	16.13	10.52	-8.74	-22.55	-16.40	-12.12	-9.54
8 pm	-11.59	-16.04	-25.40	-34.67	-36.72	-28.61	-36.81	-41.27	-38.24	-25.76	-17.47	-14.17
9 pm	-17.74	-22.28	-33.60	-46.44	-54.10	-51.43	-59.18	-57.13	-48.04	-32.98	-22.02	-18.27
10 pm	-23.26	-27.81	-40.29	-54.72	-64.71	-64.26	-72.10	-67.56	-55.35	-39.13	-26.03	-22.19
11 pm	-28.52	-32.80	-46.08	-61.32	-72.37	-73.26	-80.93	-75.40	-61.23	-44.65	-29.86	-25.76
12 pm	-33.51	-37.61	-51.43	-67.02	-78.52	-80.30	-88.06	-81.91	-66.31	-49.73	-33.42	-29.32

C = 0.699
 $\frac{b}{l} = 4.941$
 l = 36.428"

b = 180"
 h = 9.0"
 k = 180 pci

E = 5.1 x 10⁶ psi
 $\Sigma_t = 5.0 \times 10^{-6}$ in/in°F

(-) compression at slab bottom
 (+) tension at slab bottom

Table F.8. Thermal Stresses, Calculated from Westergaard, SR 90

	Jan	Feb	Mar	Apr	May	Jun	Jul	Aug	Sep	Oct	Nov	Dec
1 am	-51.26	-47.24	-63.25	-112.72	-128.20	-136.34	-155.50	-143.57	-123.27	-87.50	-40.25	-53.67
2 am	-61.01	-49.54	-88.99	-119.72	-135.08	-144.37	-163.64	-151.83	-130.61	-93.11	-42.66	-57.34
3 am	-69.95	-51.37	-94.38	-126.60	-141.74	-152.06	-171.55	-159.85	-137.61	-98.62	-50.57	-61.69
4 am	-72.24	-54.01	-90.36	-121.55	-136.34	-146.09	-164.90	-154.35	-133.25	-95.87	-50.46	-61.24
5 am	-70.18	-50.57	-80.84	-109.63	-115.59	-108.02	-128.32	-140.59	-122.13	-88.18	-48.96	-57.34
6 am	-63.30	-46.44	-69.72	-78.21	-61.69	-49.88	-62.96	-86.92	-105.73	-79.12	-46.79	-51.60
7 am	-57.45	-41.86	-38.19	-23.39	-4.47	7.22	2.06	-21.21	-52.52	-62.50	-44.49	-46.44
8 am	-44.49	-33.37	9.75	29.70	47.13	57.68	60.09	40.02	6.31	-19.15	-35.55	-40.94
9 am	-18.46	-18.46	54.12	75.45	90.48	100.11	108.60	92.20	58.48	24.77	-28.32	-21.33
10 am	5.50	16.97	90.25	111.69	124.88	133.94	147.01	133.82	100.80	61.81	-17.89	-0.34
11 am	10.55	51.83	116.97	138.30	150.11	159.05	175.45	164.78	131.99	89.33	2.64	16.51
12	17.09	81.30	133.71	155.27	166.62	176.02	194.03	184.74	149.65	106.88	15.60	19.15
1 pm	28.67	92.88	140.70	162.73	174.19	184.85	203.31	194.26	160.66	114.10	30.39	19.95
2 pm	31.99	92.77	138.18	161.34	173.73	186.00	203.54	193.68	158.48	111.23	36.81	19.04
3 pm	29.47	83.25	126.48	151.25	165.13	179.81	195.06	183.36	145.86	96.10	35.89	16.17
4 pm	20.87	56.08	94.49	119.03	134.86	150.45	161.34	147.35	109.86	66.62	17.20	9.75
5 pm	13.19	17.20	40.96	73.16	91.51	107.91	112.72	95.64	59.60	21.44	-5.17	1.95
6 pm	6.31	-8.03	-4.47	18.35	39.79	57.22	54.93	33.48	-3.90	-21.56	-20.41	-7.45
7 pm	0.69	-20.87	-30.50	-39.45	-19.26	0.00	-10.66	-37.61	-51.95	-40.02	-22.13	-14.68
8 pm	-9.29	-30.16	-43.80	-65.13	-70.29	-62.38	-78.55	-82.68	-72.93	-51.49	-24.77	-23.39
9 pm	-14.91	-37.73	-55.39	-79.47	-91.51	-92.66	-108.60	-104.01	-86.46	-60.20	-27.18	-31.99
10 pm	-24.77	-44.49	-63.99	-90.02	-140.24	-109.05	-125.34	-118.46	-96.78	-67.66	-29.47	-39.45
11 pm	-33.26	-48.05	-71.78	-98.85	-113.87	-120.64	-137.15	-130.04	-105.73	-74.19	-31.76	-43.46
12 pm	-43.89	-47.36	-79.01	-106.64	-122.01	-130.27	-147.01	-140.36	-113.87	-80.50	-34.40	-47.70

C = 0.936
 $\frac{1}{l} = 6.149$
 l = 29.272"

b = 180"
 h = 7.8"
 k = 270 pci

E = 4.9 x 10⁶ psi
 $\Sigma_t = 5.0 \times 10^{-6}$ in/in°F

(-) compression at slab bottom
 (+) tension at slab bottom

APPENDIX G
ECONOMIC TABLES

2% Interest Tables

Year Y	SCA P-F	SPW F-P	UCA A-F	USF F-A	UCR P-A	UPW A-P
1	1.020	.9804	1.000	1.000	1.020	0.980
2	1.040	.9612	2.020	.4951	.5151	1.942
3	1.061	.9423	3.060	.3268	.3468	2.884
4	1.082	.9238	4.122	.2426	.2626	3.808
5	1.104	.9057	5.204	.1922	.2122	4.713
6	1.126	.8880	6.308	.1585	.1785	5.601
7	1.149	.8706	7.434	.1345	.1545	6.472
8	1.172	.8535	8.583	.1165	.1365	7.325
9	1.195	.8368	9.755	.1025	.1225	8.162
10	1.219	.8203	10.95	.0913	.1113	8.983
11	1.243	.8043	12.17	.0822	.1022	9.787
12	1.268	.7885	13.41	.0746	.0946	10.58
13	1.294	.7730	14.68	.0681	.0881	11.35
14	1.319	.7579	15.97	.0626	.0826	12.11
15	1.346	.7430	17.29	.0578	.0778	12.85
16	1.373	.7284	18.64	.0537	.0737	13.58
17	1.400	.7142	20.01	.0500	.0700	14.29
18	1.428	.7002	21.41	.0467	.0667	14.99
19	1.457	.6864	22.84	.0438	.0638	15.68
20	1.486	.6730	24.30	.0412	.0612	16.35
21	1.516	.6600	25.78	.0388	.0588	17.01
22	1.546	.6468	27.30	.0366	.0566	17.66
23	1.577	.6342	28.85	.0347	.0547	18.29
24	1.608	.6217	30.42	.0329	.0529	18.91
25	1.641	.6100	32.03	.0312	.0512	19.52
30	1.811	.5521	40.57	.0247	.0447	22.40
35	2.000	.5000	49.99	.0200	.0400	25.00
40	2.208	.4529	60.40	.0166	.0366	27.36
45	2.438	.4102	71.89	.0139	.0339	29.49
50	2.692	.3715	84.58	.0118	.0318	31.42
60	3.281	.3048	114.1	.0088	.0288	34.76
70	4.000	.2500	150.0	.0067	.0267	37.50
80	4.875	.2051	193.8	.0052	.0252	39.75
90	5.943	.1683	247.2	.0041	.0241	41.59
100	7.245	.1380	312.2	.0032	.0232	43.10

4% Interest Tables

Year Y	SCA P-F	SPW F-P	UCA A-F	USF F-A	UCR P-A	UPW A-P
1	1.040	.9615	1.000	1.000	1.040	0.962
2	1.082	.9246	2.040	.4902	.5302	1.886
3	1.125	.8890	3.122	.3204	.3604	2.775
4	1.170	.8548	4.246	.2355	.2755	3.630
5	1.217	.8219	5.416	.1846	.2246	4.452
6	1.265	.7903	6.633	.1508	.1908	5.242
7	1.316	.7599	7.898	.1266	.1666	6.002
8	1.369	.7307	9.214	.1085	.1485	6.733
9	1.423	.7026	10.58	.0945	.1345	7.435
10	1.480	.6756	12.01	.0833	.1233	8.111
11	1.539	.6496	13.49	.0742	.1142	8.760
12	1.601	.6246	15.03	.0666	.1066	9.385
13	1.665	.6006	16.63	.0601	.1001	9.986
14	1.732	.5775	18.29	.0547	.0947	10.56
15	1.801	.5553	20.02	.0499	.0899	11.12
16	1.873	.5339	21.83	.0452	.0858	11.65
17	1.946	.5134	23.70	.0422	.0822	12.17
18	2.026	.4936	25.65	.0390	.0790	12.66
19	2.107	.4746	27.67	.0361	.0761	13.13
20	2.191	.4564	29.78	.0336	.0736	13.59
21	2.279	.4388	31.97	.0313	.0713	14.03
22	2.370	.4220	34.25	.0292	.0692	14.45
23	2.465	.4057	36.67	.0273	.0673	14.86
24	2.563	.3901	39.08	.0256	.0656	15.26
25	2.666	.3751	41.65	.0240	.0640	15.62
30	3.243	.3083	56.09	.0178	.0578	17.29
35	3.946	.2534	73.65	.0136	.0536	18.67
40	4.801	.2083	95.03	.0105	.0505	19.79
45	5.841	.1712	121.0	.0083	.0483	20.72
50	7.107	.1407	152.7	.0066	.0466	21.48
60	10.52	.0951	238.0	.0042	.0442	22.62
70	15.57	.0642	364.3	.0028	.0428	23.40
80	23.05	.0434	551.2	.0018	.0418	23.92
90	34.12	.0293	828.0	.0012	.0412	24.27
100	50.51	.0198	1238.	.0008	.0409	24.51

6% Interest Tables

Year Y	SCA P-F	SPW F-P	UCA A-F	USF F-A	UCR P-A	UPW A-P
1	1.060	.9434	1.000	1.000	1.060	0.943
2	1.124	.8900	2.060	.4854	.5454	1.833
3	1.191	.8400	3.184	.3141	.3741	2.673
4	1.262	.7921	4.375	.2286	.2886	3.465
5	1.338	.7473	5.637	.1774	.2374	4.212
6	1.419	.7050	6.975	.1434	.2034	4.917
7	1.504	.6651	8.394	.1191	.1791	5.582
8	1.594	.6274	9.897	.1010	.1610	6.210
9	1.689	.5919	11.49	.0870	.1470	6.802
10	1.791	.5584	13.18	.0759	.1359	7.360
11	1.898	.5268	14.97	.0668	.1268	7.887
12	2.012	.4970	16.87	.0593	.1193	8.384
13	2.133	.4688	18.88	.0530	.1130	8.853
14	2.261	.4423	21.02	.0476	.1076	9.295
15	2.397	.4173	23.28	.0430	.1030	9.712
16	2.540	.3936	25.67	.0390	.0990	10.11
17	2.693	.3714	28.21	.0354	.0954	10.48
18	2.854	.3503	30.91	.0324	.0924	10.83
19	3.026	.3305	33.76	.0296	.0896	11.16
20	3.207	.3118	36.79	.0272	.0872	11.47
21	3.400	.2942	39.99	.0250	.0850	11.76
22	3.604	.2775	43.40	.0231	.0831	12.04
23	3.820	.2618	47.00	.0213	.0813	12.30
24	4.049	.2470	50.82	.0197	.0797	12.55
25	4.292	.2330	54.87	.0182	.0782	12.78
30	5.743	.1741	79.06	.0127	.0727	13.77
35	7.686	.1301	111.4	.0090	.0690	14.50
40	10.29	.0972	154.8	.0065	.0665	15.05
45	13.77	.0727	212.7	.0047	.0647	15.46
50	18.42	.0543	290.3	.0034	.0634	15.76
60	32.99	.0303	533.1	.0019	.0619	16.16
70	59.08	.0169	967.9	.0010	.0610	16.39
80	105.8	.0095	1747.	.0006	.0606	16.51
90	189.5	.0053	3141.	.0003	.0603	16.58
100	339.3	.0029	5638.	.0002	.0602	16.62

8% Interest Tables

Year Y	SCA P-F	SPW F-P	UCA A-F	USF F-A	UCR P-A	UPW A-P
1	1.080	.9259	1.000	1.000	1.080	0.926
2	1.166	.8573	2.080	.4808	.5608	1.783
3	1.260	.7938	3.246	.3080	.3880	2.577
4	1.360	.7350	4.506	.2219	.3019	3.312
5	1.469	.6806	5.867	.1705	.2505	3.993
6	1.587	.6302	7.336	.1363	.2163	4.623
7	1.714	.5835	8.923	.1121	.1921	5.206
8	1.851	.5403	10.64	.0940	.1740	5.747
9	1.999	.5002	12.49	.0801	.1601	6.247
10	2.159	.4632	14.49	.0690	.1490	6.710
11	2.332	.4289	16.65	.0601	.1401	7.139
12	2.518	.3971	18.98	.0527	.1327	7.536
13	2.720	.3677	21.50	.0466	.1265	7.904
14	2.937	.3405	24.22	.0413	.1213	8.244
15	3.172	.3152	27.15	.0368	.1168	8.559
16	3.426	.2919	30.32	.0330	.1130	8.851
17	3.700	.2703	33.75	.0396	.1096	9.122
18	3.996	.2502	37.45	.0267	.1067	9.372
19	4.316	.2317	41.45	.0241	.1041	9.604
20	4.661	.2145	45.76	.0219	.1019	9.818
21	5.034	.1987	50.42	.0198	.0998	10.02
22	5.437	.1839	55.46	.0180	.0980	10.20
23	5.871	.1703	60.89	.0164	.0964	10.37
24	6.341	.1577	66.77	.0150	.0950	10.53
25	6.848	.1460	73.11	.0137	.0937	10.68
30	10.06	.0994	113.3	.0088	.0088	11.26
35	14.79	.0676	172.3	.0058	.0058	11.66
40	21.73	.0460	259.1	.0039	.0039	11.93
45	31.92	.0313	386.5	.0025	.0025	12.11
50	46.90	.0213	573.7	.0017	.0017	12.23
60	101.3	.0099	1253.	.0008	.0008	12.38
70	218.6	.0046	2720.	.0004	.0004	12.44
80	472.0	.0021	5887.	.0002	.0002	12.47
90	1019.	.0005	12724.	.0001	.0001	12.49
100	2200.	.0005	27485.	.0000	.0000	12.49

APPENDIX H
COST CALCULATIONS

1. AREA AND EXCAVATION CALCULATIONS

1.1 Location assumes a total of 4 lanes (in one direction) in the vicinity of NE 175th in Seattle (SR 5). This example is typical of the kinds of costs associated with urban Interstate PCC pavement rehabilitation. Actual job costs will, undoubtedly differ. One of the largest uncertainties is the duration of construction for each rehabilitation approach.

1.2 Mainline:

$$(4 \text{ lanes})(5 \text{ mi})(12 \text{ ft/ln})(5280 \text{ ft/mi})(1 \text{ yd}^2/9 \text{ ft}^2) \\ = 140,800 \text{ yd}^2$$

1.3 Shoulders (includes the width of both shoulders):

$$(11 \text{ ft} + 5 \text{ ft})(5 \text{ mi})(5280 \text{ ft/mi})(1 \text{ yd}^2/9 \text{ ft}^2) \\ = 46,933 \text{ yd}^2$$

2. REMOVE AND REPLACE

2.1 General Cost Calculations

2.1.1 Cost to Remove AC Shoulders

$$(\$3.37/\text{yd}^2)(46,933 \text{ yd}^2) \\ = \$158,165$$

2.1.2 Cost for New AC Shoulders (surfacing, 4.2 inches, density = $145 \frac{\text{lb}}{\text{ft}^3}$)

$$(\$27.79/\text{ton})(10,718.4 \text{ tons}) \\ = \$297,864$$

2.1.3 Cost for Tack Coat for New AC Shoulders

$$(\$214.17/\text{ton})(9.57 \text{ tons})(2 \text{ tack coats}) \\ = \$4,101$$

2.1.4 Cost of Shoulder Excavation for ATB (4.2 inches)

$$(\$6.71/\text{yd}^3)(5,476 \text{ yd}^3) \\ = \$36,741$$

2.1.5 Cost of ATB (Shoulder, 4.2 inches, density = $140 \frac{\text{lb}}{\text{ft}^3}$)

$$(\$24.96/\text{ton})(10,349 \text{ tons}) \\ = \$258,306$$

2.1.6 Cost for Shoulder Excavation (PCC Shoulder)

2.1.6.1 10 inch section (assumes 4.2 inch ATB as subbase)

$$\begin{aligned} &= (\$6.71/\text{yd}^3)(46,933 \text{ yd}^2)(0.28 \text{ yd}) \\ &= \$88,178 \end{aligned}$$

2.1.6.2 12 inch section (assumes 4.2 inch ATB as subbase)

$$\begin{aligned} &= (\$6.71/\text{yd}^3)(46,933 \text{ yd}^2)(0.33 \text{ yd}) \\ &= \$103,924 \end{aligned}$$

2.1.6.3 15 inch section (assumes 4.2 inch ATB as subbase)

$$\begin{aligned} &= (\$6.71/\text{yd}^3)(46,933 \text{ yd}^2)(0.42 \text{ yd}) \\ &= \$132,267 \end{aligned}$$

2.1.7 Cost for New Concrete Shoulders

2.1.7.1 10 inch section

$$\begin{aligned} &= (\$21.00/\text{yd}^2)(46,933 \text{ yd}^2) \\ &= \$985,600 \end{aligned}$$

2.1.7.2 12 inch section¹

$$\begin{aligned} &= (\$22.24/\text{yd}^2)(46,933 \text{ yd}^2) \\ &= \$1,043,797 \end{aligned}$$

2.1.7.3 15 inch section¹

$$\begin{aligned} &= (\$29.70/\text{yd}^2)(46,933 \text{ yd}^2) \\ &= \$1,393,920 \end{aligned}$$

2.1.8 Cost to Remove Existing PCC Pavement

$$\begin{aligned} &(\$7.20/\text{yd}^2)(140,800 \text{ yd}^2) \\ &= \$1,013,760 \end{aligned}$$

2.1.9 Cost for Roadway Excavation (PCCP Mainline)

2.1.9.1 10 inch section (excavate 1 inch)

$$\begin{aligned} &(\$6.71/\text{yd}^3)(140,800 \text{ yd}^2)(0.028 \text{ yd}) \\ &= \$26,244 \end{aligned}$$

¹Costs were taken from R.S. Means Company, Inc., "Building Construction Cost Data," 46th Annual Edition, 1988.

2.1.9.2 12 inch section (excavate 3 inches)

$$(\$6.71/\text{yd}^3)(140,800 \text{ yd}^2)(0.083 \text{ yd}) \\ = \$78,731$$

2.1.9.3 15 inch section (excavate 6 inches)

$$(\$6.71/\text{yd}^3)(140,800 \text{ yd}^2)(0.167 \text{ yd}) \\ = \$157,461$$

2.1.10 Cost of Mainline Excavation for ATB (4.2 inches)

$$(\$6.71/\text{yd}^3)(16,427 \text{ yd}^3) \\ = \$110,225$$

2.1.11 Cost of Mainline ATB (4.2 inches)⁴

$$(\$24.96/\text{ton})(31,046 \text{ tons}) \\ = \$774,918$$

2.1.12 Cost to Place PCC Pavement (14 day cure)

2.1.12.1 10 inch section

$$(\$21.00/\text{yd}^2)(140,800 \text{ yd}^2) \\ = \$2,956,800$$

2.1.12.2 12 inch section¹

$$(\$22.24/\text{yd}^2)(140,800 \text{ yd}^2) \\ = \$3,131,392$$

2.1.12.3 15 inch section¹

$$(\$29.70/\text{yd}^2)(140,800 \text{ yd}^2) \\ = \$4,181,760$$

2.1.13 Traffic Control Costs for PCC Pavements

2.1.13.1 Labor for Traffic Control (estimate 3 flaggers)

$$(\$19.75/\text{hr})(90 \text{ days})(24 \text{ hr/day})(3) \\ = \$127,980$$

2.1.13.2 Plastic Drums

$$(\$62.00 \text{ each})(10 \text{ drums}) \\ = \$620$$

2.1.13.3 Sequential Arrow Sign

$$(\$6.52/\text{hour})(90 \text{ days})(24 \text{ hr/day}) \\ = \$14,083$$

2.1.13.4 Temporary Concrete Barrier

$$(\$9.81/\text{LF})(5280 + 170 \text{ ft taper}) \\ = \$53,465$$

2.1.13.5 Total Traffic Costs

$$\$127,980 + \$620 + \$14,083 + \$53,465 \\ = \$196,148$$

2.2 If concrete is not to be recycled, then the costs associated with disposal include the following:

2.2.1 Determination of Hauling and Dumping Costs

2.2.1.1 Density of blasted rock² (analogous to broken PCC)

$$113 \text{ lb/ft}^3$$

2.2.1.2 Volume of PCC to be excavated

$$(140,800 \text{ yd}^2)(9 \text{ ft}^2/\text{yd}^2)(0.75 \text{ ft}) \\ = 950,400 \text{ ft}^3$$

2.2.1.3 Weight of Concrete Rubble

$$950,400 \text{ ft}^3(113 \text{ lb/ft}^3) \\ = 107,395,200 \text{ lbs}$$

2.2.1.4 Volume of PCC to be hauled

$$\text{Load factor of blasted rock}^2 = 0.67 \\ \frac{950,400 \text{ ft}^3}{0.67} = 1,418,507 \text{ ft}^3$$

2.2.1.5 Dump trucks (12 yd³) hauled 20 miles (round trip)¹

$$(\$14.41/\text{yd}^3)(1,418,507 \text{ ft}^3)/(27 \text{ ft}^3) \\ = \$757,063$$

²S.W. Nunnally, "Construction Methods and Management," Prentice-Hall, Inc., 1980.

2.2.1.6 Disposal at Cedar Hills³ (\$48.69/ton)

$$(\$48.69)(107,395,200 \text{ lb})/(2000 \text{ lb}) \\ = \$2,614,536$$

2.2.1.7 Total Disposal Costs

$$\$757,063 + \$2,614,536 \\ = \underline{\underline{\$3,371,600}}$$

3. ASPHALT CONCRETE OVERLAY

3.1 General Cost Calculations

3.1.1 Cost of Planing AC Pavement (milling of overlay after 10.0 or 12.5 years)

$$(\$3.37/\text{yd}^2)(140,800 \text{ yd}^2) \\ = \$474,496$$

3.1.2 Cost of Planing AC Shoulders (milling of overlay after 10.0 or 12.5 years)

$$(\$3.37/\text{yd}^2)(46,933 \text{ yd}^2) \\ = \$158,164$$

3.1.3 Cost for Tack Coat for AC Shoulders

$$(\$214.17/\text{ton})(9.57 \text{ ton})(2 \text{ tack coats}) \\ = \$4,100$$

3.1.4 Cost for AC Shoulders (4.2 inch overlay)⁴

$$(\$27.79/\text{ton})(10,718 \text{ tons}) \\ = \$297,864$$

3.1.5 Cost for Tack Coat for AC Pavement

$$(\$214.17/\text{ton})(28 \text{ ton})(2 \text{ tack coats}) \\ = \$11,994$$

3.1.6 Cost for AC Pavement (4.2 inch overlay)⁴

$$(\$27.79/\text{ton})(32,155 \text{ tons}) \\ = \$893,593$$

³Costs based on phone call to the King County Solid Waste Division, February 21, 1988

⁴ACP density = 145 lbs/ft³; ATB density = 140 lbs/ft³

3.1.7 Cost for AC Pavement (6.0 inch overlay)

$$\begin{aligned} &(\$27.79/\text{ton})(45,936 \text{ tons}) \\ &= \$1,276,561 \end{aligned}$$

3.1.8 Cost for Crack Sealing

$$\begin{aligned} &(\$5,280.00/\text{lane-mile})(4 \text{ lanes})(5 \text{ miles}) \\ &= \$105,600 \end{aligned}$$

3.1.9 Cost for Various Interlayers

3.1.9.1 Cost for Fabric Interlayer

$$\begin{aligned} &= (\$1.00/\text{yd}^2)(140,800 \text{ yd}^2) \\ &= \$140,800 \end{aligned}$$

3.1.9.2 Cost for Asphalt-Rubber Interlayer

$$\begin{aligned} &= (\$2.00/\text{yd}^2)(140,800 \text{ yd}^2) \\ &= \$281,600 \end{aligned}$$

3.1.9.3 Cost for Crack and Seat Operation

$$\begin{aligned} &= (\$1.00/\text{yd}^2)(140,800 \text{ yd}^2) \\ &= \$140,800 \end{aligned}$$

3.2 Determination of Construction Duration

3.2.1 Production Rate = 250 ton/hour

3.2.2 Number of Production Hours Worked per Day = 5.5 hours

3.2.3 Weight/yd²

$$\begin{aligned} &\text{Overlay thickness}(3')(3')(145 \text{ lbs}/\text{ft}^3) \\ &= (1,305 \text{ lb}/\text{yd}^2)(\text{foot overlay}) \end{aligned}$$

3.2.4 Production per Day

3.2.4.1 4.2 inch overlay

$$\begin{aligned} &\frac{(250 \text{ ton}/\text{hr})(2000 \text{ lb}/\text{ton})}{(1305 \text{ lb}/\text{yd}^2)(0.35 \text{ ft})} \\ &= 1,095 \text{ yd}^2/\text{hour} \end{aligned}$$

3.2.4.2 6.0 inch overlay

$$\frac{(250 \text{ ton/hr})(2000 \text{ lb/ton})}{(1305 \text{ lb/yd}^2)(0.50 \text{ ft})}$$
$$= 766 \text{ yd}^2/\text{hour}$$

3.2.5 Placement per Day

3.2.5.1 4.2 inch overlay

$$(1095 \text{ yd}^2/\text{hr})(5.5 \text{ hr/day})$$
$$= 6,022 \text{ yd}^2/\text{day}$$
$$= 0.86 \text{ ln-mi/day}$$

3.2.5.2 6.0 inch overlay

$$(766 \text{ yd}^2/\text{hr})(5.5 \text{ hr/day})$$
$$= 4,215 \text{ yd}^2/\text{day}$$
$$= 0.60 \text{ ln-mi/day}$$

3.2.6 Construction Period

3.2.6.1 4.2 inch overlay

$$\frac{(5 \text{ miles})(4 \text{ lanes})}{(0.86 \text{ ln-mi/day})} = 23 \text{ days}$$

3.2.6.2 6.0 inch overlay

$$\frac{(5 \text{ miles})(4 \text{ lanes})}{(0.60 \text{ ln-mi/day})} = 33 \text{ days}$$

To allow for surface preparation, shoulder paving, etc., double the construction period required

3.2.7 Cost of Traffic Control for AC Overlay

(Assume 8 hrs/day — nighttime construction restriction of 10 p.m. to 6 a.m. for traffic control)

3.2.7.1 Traffic Control Labor (2 flaggers)

$$(\$19.75/\text{hr})(2)(\text{construction period})$$
$$= (\$40)(\text{construction period})$$

3.2.7.2 Sequential Arrow Sign (2 signs)

$$(\$6.52/\text{hr})(2)(\text{construction period}) \\ = (\$13)(\text{construction period})$$

3.2.7.3 Plastic Drums

$$(\$62.00 \text{ each})(10 \text{ drums}) \\ = \$620$$

3.2.7.4 Total Traffic Costs (368 hours)

4.2 inch Overlay (368 hours)

$$(\$40 + \$13)(\text{construction period (hours)}) + \$620 \\ = \$20,124$$

6.0 inch Overlay (528 hours)

$$(\$40 + \$13)(\text{construction period (hours)}) + \$620 \\ = \$28,604$$

4. UNBONDED PORTLAND CEMENT CONCRETE OVERLAY

4.1 General Cost Calculations

4.1.1 Cost for Bond Breaker (1 inch of ACP)

$$(\$27.79/\text{ton})(7,656 \text{ tons})^4 \\ = \$212,760$$

4.1.2 Cost for AC Shoulders (4.2 inch overlay)

$$(\$27.79/\text{ton})(10,718 \text{ tons}) \\ = \$297,864$$

4.1.3 Cost for PCC Shoulders (10 inch)

4.1.3.1 PCC

$$(\$21.00/\text{yd}^2)(46,933 \text{ yd}^2) \\ = \$985,600$$

4.1.3.2 Levelup ACP (1 inch)

$$(\$27.79/\text{ton})(2552 \text{ tons}) \\ = \$70,920$$

4.1.4 Crack Sealing (estimate)

\$105,600

4.1.5 Cost to Place PCC Pavement (14 day cure) (total of approximately 40,000 yd³ of PCC)

10 inch section

$$\begin{aligned} &(\$21.00/\text{yd}^2)(140,800 \text{ yd}^2) \\ &= \$2,956,800 \end{aligned}$$

4.1.6 Cost of Tie Bars (2', #4, @ 3 ft centers)

$$\begin{aligned} &(\$0.54 \text{ lb})(7040 \text{ joints})(0.668 \text{ lb/ft})(2')(1/3) \\ &= \$1,693 \end{aligned}$$

4.1.7 Cost for Traffic Control

4.1.7.1 Labor for Traffic Control (estimate: 3 flaggers)

$$\begin{aligned} &(\$24.96/\text{hr})(24 \text{ hr/day})(60 \text{ days})(3) \\ &= \$107,827 \end{aligned}$$

4.1.7.2 Plastic Drums

$$\begin{aligned} &(\$62.13 \text{ each})(10 \text{ drums}) \\ &= \$621 \end{aligned}$$

4.1.7.3 Sequential Arrow Sign

$$\begin{aligned} &(\$6.52/\text{hr})(24 \text{ hr/day})(60 \text{ days}) \\ &= \$9,389 \end{aligned}$$

4.1.7.4 Temporary Concrete Barrier

$$\begin{aligned} &(\$9.81/\text{LF})(5,280 + 170 \text{ ft. taper}) \\ &= \$43,565 \end{aligned}$$

4.1.7.5 Total Traffic Costs

$$\begin{aligned} &= \$107,827 + \$621 + \$9,389 + \$53,465 \\ &= \$171,302 \end{aligned}$$

5. CALCULATION OF TOTAL CONSTRUCTION COSTS

5.1 Initial Construction Costs for Remove and Replace with PCC

5.1.1 Tied Concrete Shoulders with ATB

Cost for (removing existing AC shoulders + shoulder excavation (for slab and ATB) + shoulder ATB + concrete shoulders + removing existing mainline PCCP + mainline

excavation + excavation for mainline ATB + mainline ATB + new PCCP + Traffic) + Mobilization (6%) + Tax (7.8%) + Engineering/Contingencies (17%)

10 inch section	\$8,826,590
12 inch section	\$9,229,038
15 inch section	\$11,244,554

5.1.2 Asphalt Concrete Shoulders and Mainline ATB

Cost for (removing AC shoulders + tack coat + AC shoulder (4.2 inches) + removing existing mainline PCCP + mainline excavation + excavation for mainline ATB + mainline ATB + new PCCP + Traffic) + Mobilization (6%) + Tax (7.8%) + Engineering/Contingencies (17%)

10 inch section	\$7,404,611
12 inch section	\$7,707,840
15 inch section	\$9,217,371

5.2 Initial Construction Costs for AC Overlay

5.2.1 General Equation

Cost for (shoulder tack coat + AC shoulders + mainline tack coat + AC pavement + crack sealing + interlayer + traffic) + Mobilization (6%) + Tax (7.8%) + Contingencies (17%)

No Interlayer	
4.2" overlay	\$1,782,503
6.0" overlay	\$2,305,844
Fabric or Crack and Seal	
4.2" overlay	\$1,970,743
6.0" overlay	\$2,494,084
Rubber Interlayer	
4.2" overlay	\$2,158,984
6.0" overlay	\$2,682,325

5.3 Initial Construction Costs for 10" Unbonded PCC Overlay

5.3.1 General Equation

Cost for (bond breaker + shoulders + crack sealing + PCC unbonded overlay + tie bars + traffic) + Mobilization (6%) + Tax (7.8%) + Contingencies (17%)

with AC Shoulders	\$5,008,187
with PCC Shoulders	\$6,022,461

5.4 Other Considerations

Disposal of Concrete Rubble

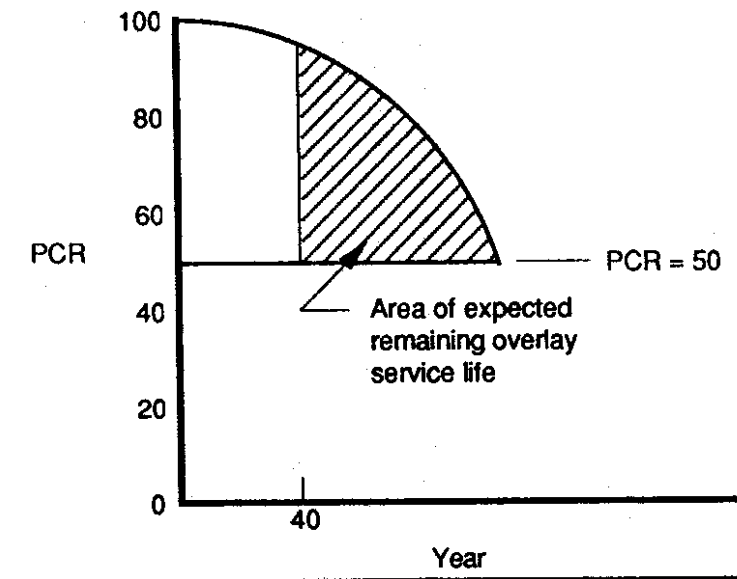
If the removed concrete rubble will not be used for recycling, then an additional cost of \$168,580/lane-mile should be added to the above figures.

The costs associated with preparing the concrete rubble for use in a recycled concrete mix was not estimated for this report.

6. DETERMINATION OF SALVAGE VALUE FOR AC OVERLAY

The calculation of the salvage value will determine the cost credited to the remaining life of the overlay beyond the analysis period of 40 years.

The salvage value will apply only to the option of an ACP overlay occurring every 12.5 years. (For the AC overlays with a performance period of 10.0 years, there is no salvage for the 40 year analysis period used in this example.) A total of four overlays are possible, totalling a service life of 50 years, which is 10 years beyond the analysis period. Therefore, the salvage value will be the cost associated with the remaining 10 years of service life and the total construction cost.



Standard Equation:	$PCR = 100 - 0.32(\text{Age})^2$
Total Area Beneath the Curve:	$(100 - PCR) - 0.107(\text{Age})^3$
Total Area	$= (100 - 50)(12.5) - 0.107(12.5)^3$
	$= 416.7$
Area _{to 2.5 years}	$= (100 - 50)(2.5) - 0.107(2.5)^3$
(or 37.5 years to 40.0 years)	$= 123.3$
Area _{remaining}	$= 416.7 - 123.3$
	$= 293.4$
Salvage Value	$= \text{Construction Cost} \times \frac{(293.4)}{(416.7)}$

<u>No Interlayer</u>	
4.2" overlay	\$1,850,616
6.0" overlay	\$2,219,102
<u>Fabric or Crack and Seat</u>	
4.2" overlay	\$1,983,157
6.0" overlay	\$2,351,643
<u>Rubber Interlayer</u>	
4.2" overlay	\$2,115,698
6.0" overlay	\$2,484,184

7. REHABILITATION COSTS — AC OVERLAYS

7.1 General Assumption

Construction costs for future overlays were assumed to be equal to the construction cost of the initial overlay plus milling costs. Salvage value applies only to overlay applied at year 37.5 (refer to previous paragraph 6).

<u>Overlay</u>	<u>Thickness</u>	<u>Construction</u>	<u>Salvage</u>
No interlayer	4.2	\$2,628,329	\$1,850,616
	6.0	\$3,151,670	\$2,219,102
Fabric/C & S	4.2	\$2,816,569	\$1,983,157
	6.0	\$3,339,910	\$2,351,643
Rubber	4.2	\$3,004,810	\$2,115,698
	6.0	\$3,528,151	\$2,484,184

7.2 Present Worth of Future Overlay Construction Costs (Overlay every 12.5 years)

7.2.1 No Interlayer or Pretreatment

7.2.1.1 4.2 inch AC Overlay

Overlay in 12.5 years
 $\$2,628,329 \times (1.04)^{-12.5} = \$1,609,767$

Overlay in 25.0 years
 $\$2,628,329 \times (1.04)^{-25.0} = \$985,930$

Overlay in 37.5 years
 $\$2,628,329 \times (1.04)^{-37.5} = \$603,851$

Total Overlay Costs \$3,199,548

PW Salvage Value
 $\$1,850,616 \times (1.04)^{-40.0} = -385,463$

Total Rehabilitation Cost \$2,814,085

7.2.1.2 6.0 inch AC Overlay

Overlay in 12.5 years	
$\$3,151,670 \times (1.04)^{-12.5} =$	\$1,930,296
Overlay in 25.0 years	
$\$3,151,670 \times (1.04)^{-25.0} =$	\$1,182,244
Overlay in 37.5 years	
$\$3,151,670 \times (1.04)^{-37.5} =$	\$724,087
Total Overlay Costs	\$3,836,627
PW Salvage Value	
$\$2,219,102 \times (1.04)^{-40.0} =$	-462,215
<u>Total Rehabilitation Cost</u>	<u>\$3,374,412</u>

7.2.2 Fabric Interlayer or Crack and Seal

7.2.2.1 4.2 inch AC Overlay

Overlay in 12.5 years	
$\$2,816,569 \times (1.04)^{-12.5} =$	\$1,725,058
Overlay in 25.0 years	
$\$2,816,569 \times (1.04)^{-25.0} =$	\$1,056,542
Overlay in 37.5 years	
$\$2,816,569 \times (1.04)^{-37.5} =$	\$647,098
Total Overlay Costs	\$3,428,698
PW Salvage Value	
$\$1,983,157 \times (1.04)^{-40.0} =$	-413,070
<u>Total Rehabilitation Cost</u>	<u>\$3,015,628</u>

7.2.2.2 6.0 inch AC Overlay

Overlay in 12.5 years	
$\$3,339,910 \times (1.04)^{-12.5} =$	\$2,045,587
Overlay in 25.0 years	
$\$3,339,910 \times (1.04)^{-25.0} =$	\$1,252,856
Overlay in 37.5 years	
$\$3,339,910 \times (1.04)^{-37.5} =$	\$767,334
Total Overlay Costs	\$4,065,777
PW Salvage Value	
$\$2,351,643 \times (1.04)^{-40.0} =$	-489,821
<u>Total Rehabilitation Cost</u>	<u>\$3,575,956</u>

7.2.3 Asphalt Rubber Interlayer

7.2.3.1 4.2 inch AC Overlay

Overlay in 12.5 years
 $\$3,004,810 \times (1.04)^{-12.5} = \$1,840,349$

Overlay in 25.0 years
 $\$3,004,810 \times (1.04)^{-25.0} = \$1,127,155$

Overlay in 37.5 years
 $\$3,004,810 \times (1.04)^{-37.5} = \$690,346$

Total Overlay Costs 3,657,850

PW Salvage Value
 $\$2,115,698 \times (1.04)^{-40.0} = -440,677$

Total Rehabilitation Cost \$3,217,173

7.2.3.2 6.0 inch AC Overlay

Overlay in 12.5 years
 $\$3,528,151 \times (1.04)^{-12.5} = \$2,160,879$

Overlay in 25.0 years
 $\$3,528,151 \times (1.04)^{-25.0} = \$1,323,469$

Overlay in 37.5 years
 $\$3,528,151 \times (1.04)^{-37.5} = \$810,582$

Total Overlay Costs 4,294,930

PW Salvage Value
 $\$2,484,184 \times (1.04)^{-40.0} = -517,428$

Total Rehabilitation Cost \$3,777,502

7.3 Present Worth of Future Overlay Construction Costs (Overlay every 10.0 years)

7.3.1 No Interlayer or Pretreatment

7.3.1.1 4.2 inch AC Overlay

Overlay in 10.0 years
 $\$2,628,329 \times (1.04)^{-10.0} = \$1,775,605$

Overlay in 20.0 years
 $\$2,628,329 \times (1.04)^{-20.0} = \$1,199,535$

Overlay in 30.0 years
 $\$2,628,329 \times (1.04)^{-30.0} = \$810,363$

Total Rehabilitation Cost \$3,785,503

7.3.1.2 6.0 inch AC Overlay

Overlay in 10.0 years
 $\$3,151,670 \times (1.04)^{-10.0} = \$2,129,155$

Overlay in 20.0 years
 $\$3,151,670 \times (1.04)^{-20.0} = \$1,438,381$

Overlay in 30.0 years
 $\$3,151,670 \times (1.04)^{-30.0} = \$971,719$

Total Rehabilitation Cost \$4,539,255

7.3.2 Fabric Interlayer or Crack and Seal

7.3.2.1 4.2 inch AC Overlay

Overlay in 10.0 years
 $\$2,816,569 \times (1.04)^{-10.0} = \$1,902,773$

Overlay in 20.0 years
 $\$2,816,569 \times (1.04)^{-20.0} = \$1,285,445$

Overlay in 30.0 years
 $\$2,816,569 \times (1.04)^{-30.0} = \$868,401$

Total Rehabilitation Cost \$4,056,619

7.3.2.2 6.0 inch AC Overlay

Overlay in 10.0 years
 $\$3,339,910 \times (1.04)^{-10.0} = \$2,256,324$

Overlay in 20.0 years
 $\$3,339,910 \times (1.04)^{-20.0} = \$1,524,291$

Overlay in 30.0 years
 $\$3,339,910 \times (1.04)^{-30.0} = \$1,029,757$

Total Rehabilitation Cost \$4,810,372

7.3.3 Asphalt Rubber Interlayer

7.3.3.1 4.2 inch AC Overlay

$$\begin{aligned} \text{Overlay in 10.0 years} \\ \$3,004,810 \times (1.04)^{-10.0} = \$2,029,942 \end{aligned}$$

$$\begin{aligned} \text{Overlay in 20.0 years} \\ \$3,004,810 \times (1.04)^{-20.0} = \$1,371,356 \end{aligned}$$

$$\begin{aligned} \text{Overlay in 30.0 years} \\ \$3,004,810 \times (1.04)^{-30.0} = \$926,439 \end{aligned}$$

$$\text{Total Rehabilitation Cost} \quad \underline{\$4,327,737}$$

7.3.3.2 6.0 inch AC Overlay

$$\begin{aligned} \text{Overlay in 10.0 years} \\ \$3,528,151 \times (1.04)^{-10.0} = \$2,383,492 \end{aligned}$$

$$\begin{aligned} \text{Overlay in 20.0 years} \\ \$3,528,151 \times (1.04)^{-20.0} = \$1,610,202 \end{aligned}$$

$$\begin{aligned} \text{Overlay in 30.0 years} \\ \$3,528,151 \times (1.04)^{-30.0} = \$1,087,795 \end{aligned}$$

$$\text{Total Rehabilitation Cost} \quad \underline{\$5,081,489}$$

8. DETERMINATION OF FUTURE TRAFFIC LEVELS

NE 175th (Seattle) — One Way

$$(\text{ADT})_{10.0} = (133,500/2)(1 + 0.0274)^{10.0} = 87,468$$

$$(\text{ADT})_{12.5} = (133,500/2)(1 + 0.0274)^{12.5} = 93,583$$

$$(\text{ADT})_{20.0} = (133,500/2)(1 + 0.0274)^{20.0} = 114,615$$

$$(\text{ADT})_{25.0} = (133,500/2)(1 + 0.0274)^{25.0} = 131,202$$

$$(\text{ADT})_{30.0} = (133,500/2)(1 + 0.0274)^{30.0} = 150,189$$

$$(\text{ADT})_{37.5} = (133,500/2)(1 + 0.0274)^{37.5} = 183,944$$

$$(\text{ADT})_{40.0} = (133,500/2)(1 + 0.0274)^{40.0} = 196,804$$

9. DETERMINATION OF USER AND OPERATING COSTS

9.1 General Assumptions

No stopping of vehicles (progression is at a reduced speed through the construction area)

10 percent of ADT occurs during construction period, for AC overlays, from 11:30 p.m. to 4:30 a.m.

75% of ADT occurs during construction period, for PCC overlay and remove and replace, from 6:00 a.m. to 6:00 p.m.

Initial ADT one way = $133,500/2 = 66,750$

Initial speed = 50 mph. Speed through construction zone = 20 mph (or speed on parallel route)

Construction Periods = 46 days (4.2" AC overlay)
66 days (6.0" AC overlay)
60 days (PCC overlay)
90 days (R&R PCC)

9.2 User and Operating Costs Associated with Remove and Replace and PCC Overlay

9.2.1 Texas A&M Method

$$\begin{aligned} & [(\$77.47/1000)(66,750)(0.75) + (\$515.56 - \$270.09)/1000 \text{ mi}] \\ & (5 \text{ mi})(66,750)(0.75)](90 \text{ days}) \\ & = \$5,879,030 \end{aligned}$$

9.2.2 Caltrans Method

$$\begin{aligned} & (\$6.25/\text{veh-h})(5 \text{ mi}/20 \text{ mph} - 5 \text{ mi}/50 \text{ mph})(66,750)(0.75)(90 \text{ days}) \\ & = \$4,224,023 \end{aligned}$$

9.3 Initial User and Operating Costs Associated with an AC Overlay, Overlay is Milled and New AC Placed Every 12.5 Years

9.3.1 Texas A&M Method

$$\begin{aligned} & [(\$77.47/1000)(66,750)(0.10) + (\$515.56 - \$270.09)/1000 \text{ mi}](5 \text{ mi})(66,750)(0.10)](\text{days}) \\ & = \$400,645 \text{ (4.2" overlay)} \\ & = \$574,838 \text{ (6.0" overlay)} \end{aligned}$$

9.3.2 Caltrans Method

$$\begin{aligned} & [(\$6.25/\text{veh-h})(5 \text{ mi}/20 \text{ mph} - 5 \text{ mi}/50 \text{ mph})(66,750)(0.10)](\text{days}) \\ & = \$287,859 \text{ (4.2" overlay)} \\ & = \$413,016 \text{ (6.0" overlay)} \end{aligned}$$

9.4 Future User and Operating Costs for AC Overlay, Overlay is Milled and New AC Placed Every 12.5 Years

9.4.1 Texas A&M Method

$$\begin{aligned} (\text{Year})_{12.5} & = [(\$77.47/1000)(93,583)(0.10) + (\$515.56 - \$270.09)/(1000 \text{ mi}) \\ & \quad (5 \text{ mi})(93,583)(0.10)](\text{days}) \\ & = \$528,352 \text{ (4.2" overlay)} \\ & = \$758,070 \text{ (6.0" overlay)} \\ (\text{Year})_{25.0} & = [(\$77.47/1000)(131,202)(0.10) + (\$515.56 - \$270.09)/(1000 \text{ mi}) \\ & \quad (5 \text{ mi})(131,202)(0.10)](\text{days}) \\ & = \$740,242 \text{ (4.2" overlay)} \\ & = \$1,062,803 \text{ (6.0" overlay)} \\ (\text{Year})_{37.5} & = [(\$77.47/1000)(183,944)(0.10) + (\$515.56 - \$270.09)/(1000 \text{ mi}) \\ & \quad (5 \text{ mi})(183,944)(0.10)](\text{days}) \\ & = \$1,038,513 \text{ (4.2" overlay)} \\ & = \$1,490,040 \text{ (6.0" overlay)} \end{aligned}$$

9.4.2 Caltrans Method

$$\begin{aligned} (\text{Year})_{12.5} & = [(\$6.25/\text{veh-h})(5 \text{ mi}/20 \text{ mph} - 5 \text{ mi}/50 \text{ mph})(93,583)(0.10)](\text{days}) \\ & = \$403,577 \text{ (4.2" overlay)} \\ & = \$579,045 \text{ (6.0" overlay)} \\ (\text{Year})_{25.0} & = [(\$6.25/\text{veh-h})(5 \text{ mi}/20 \text{ mph} - 5 \text{ mi}/50 \text{ mph})(131,202)(0.10)](\text{days}) \\ & = \$565,809 \text{ (4.2" overlay)} \\ & = \$811,812 \text{ (6.0" overlay)} \end{aligned}$$

$$\begin{aligned}
(\text{Year})_{37.5} &= [(\$6.25/\text{veh-h})(5 \text{ mi}/20 \text{ mph} - 5 \text{ mi}/50 \text{ mph})(183,944)(0.10)](\text{days}) \\
&= \$793,257 \text{ (4.2" overlay)} \\
&= \$1,138,151 \text{ (6.0" overlay)}
\end{aligned}$$

9.5 Initial User and Operating Costs Associated with an AC Overlay, Overlay is Milled and New AC Placed Every 10.0 years

9.5.1 Texas A&M Method

$$\begin{aligned}
& [(\$77.47/1000)(66,750)(0.10) + (\$515.56 - \$270.09)/(1000 \text{ mi})(5 \text{ mi})(66,750)(0.10)](\text{days}) \\
&= \$400,645 \text{ (4.2" overlay)} \\
&= \$574,838 \text{ (6.0" overlay)}
\end{aligned}$$

9.5.2 Caltrans Method

$$\begin{aligned}
& [(\$6.25/\text{veh-h})(5 \text{ mi}/20 \text{ mph} - 5 \text{ mi}/50 \text{ mph})(66,750)(0.10)](\text{days}) \\
&= \$287,859 \text{ (4.2" overlay)} \\
&= \$413,015 \text{ (6.0" overlay)}
\end{aligned}$$

9.6 Future User and Operating Costs for AC Overlay, Overlay is Milled and New AC Placed Every 10.0 years

9.6.1 Texas A&M Method

$$\begin{aligned}
(\text{Year})_{10.0} &= [(\$77.47/1000)(87,468)(0.10) + (\$515.56 - \$270.09)/(1000 \text{ mi}) \\
& \quad (5 \text{ mi})(87,468)(0.10)](\text{days}) \\
&= \$524,998 \text{ (4.2" overlay)} \\
&= \$753,258 \text{ (6.0" overlay)}
\end{aligned}$$

$$\begin{aligned}
(\text{Year})_{20.0} &= [(\$77.47/1000)(114,615)(0.10) + (\$515.56 - \$270.09)/(1000 \text{ mi}) \\
& \quad (5 \text{ mi})(114,615)(0.10)](\text{days}) \\
&= \$687,939 \text{ (4.2" overlay)} \\
&= \$987,043 \text{ (6.0" overlay)}
\end{aligned}$$

$$\begin{aligned}
(\text{Year})_{30.0} &= [(\$77.47/1000)(150,189)(0.10) + (\$515.56 - \$270.09)/(1000 \text{ mi}) \\
& \quad (5 \text{ mi})(150,189)(0.10)](\text{days}) \\
&= \$901,460 \text{ (4.2" overlay)} \\
&= \$1,293,399 \text{ (6.0" overlay)}
\end{aligned}$$

9.6.2 Caltrans Method

$$\begin{aligned}(\text{Year})_{10.0} &= [(\$6.25/\text{veh-h})(5 \text{ mi}/20 \text{ mph} - 5 \text{ mi}/50 \text{ mph})(87,468)(0.10)](\text{days}) \\ &= \$377,206 \text{ (4.2" overlay)} \\ &= \$541,209 \text{ (6.0" overlay)}\end{aligned}$$

$$\begin{aligned}(\text{Year})_{20.0} &= [(\$6.25/\text{veh-h})(5 \text{ mi}/20 \text{ mph} - 5 \text{ mi}/50 \text{ mph})(114,615)(0.10)](\text{days}) \\ &= \$494,277 \text{ (4.2" overlay)} \\ &= \$709,180 \text{ (6.0" overlay)}\end{aligned}$$

$$\begin{aligned}(\text{Year})_{30.0} &= [(\$6.25/\text{veh-h})(5 \text{ mi}/20 \text{ mph} - 5 \text{ mi}/50 \text{ mph})(150,189)(0.10)](\text{days}) \\ &= \$647,690 \text{ (4.2" overlay)} \\ &= \$929,294 \text{ (6.0" overlay)}\end{aligned}$$

9.7 User and Operating Costs Associated with PCC Overlay

9.7.1 Texas A & M Method

$$\begin{aligned}& [(\$77.47/1000)(66,750)(0.75) + (\$515.56 - \$270.09)/(1000 \text{ mi}) \\ & (5 \text{ mi})(66,750)(0.75)](60 \text{ days}) \\ &= \$3,919,353\end{aligned}$$

9.7.2 Caltrans Method

$$\begin{aligned}& [(\$6.25/\text{veh-h})(5 \text{ mi}/20 \text{ mph} - 5 \text{ mi}/50 \text{ mph})(66,750)(0.75)](60 \text{ days}) \\ &= \$2,816,016\end{aligned}$$

9.8 Present Worth Analysis for User Costs

9.8.1 AC Overlay, Overlay is Milled and New AC Placed Every 12.5 Years

Texas A&M Method

$$\begin{aligned}\text{PW} &= \$400,645 + \$528,352(0.6125) + \$740,742(0.3751) + \\ & \$1,038,513(0.2297) \\ &= \$1,240,659 \text{ (4.2" overlay)}\end{aligned}$$

$$\begin{aligned}\text{PW} &= \$574,838 + \$758,070(0.6125) + \$1,062,803(0.3751) + \\ & \$1,490,040(0.2297) \\ &= \$1,780,075 \text{ (6.0" overlay)}\end{aligned}$$

Caltrans Method

$$\text{PW} = \$287,859 + \$403,577(0.6125) + \$565,809(0.3751) + \$793,257(0.2297)$$

$$= \$929,496 \text{ (4.2" overlay)}$$

$$\text{PW} = \$413,016 + \$579,045(0.6125) + \$811,812(0.3751) + \$1,138,151(0.2297)$$

$$= \$1,333,625 \text{ (6.0" overlay)}$$

9.8.2 AC Overlay, Overlay is Milled and New AC Placed Every 10.0 years

Texas A&M Method

$$\text{PW} = \$400,645 + \$524,998(0.6756) + \$687,939(0.4564) + \$901,460(0.3083)$$

$$= \$1,347,229 \text{ (4.2" overlay)}$$

$$\text{PW} = \$574,838 + \$753,258(0.6756) + \$987,043(0.4564) + \$1,293,399(0.3083)$$

$$= \$1,932,980 \text{ (6.0" overlay)}$$

Caltrans Method

$$\text{PW} = \$287,859 + \$377,206(0.6756) + \$494,277(0.4564) + \$647,690(0.3083)$$

$$= \$967,970 \text{ (4.2" overlay)}$$

$$\text{PW} = \$413,015 + \$541,209(0.6756) + \$709,180(0.4564) + \$929,294(0.3083)$$

$$= \$1,388,827 \text{ (6.0" overlay)}$$

APPENDIX I

**REVIEW OF CALTRANS PCC PAVEMENT DESIGN,
PERFORMANCE, AND REHABILITATION**

APPENDIX I
**REVIEW OF CALTRANS PCC PAVEMENT DESIGN,
PERFORMANCE, AND REHABILITATION**

I.1 TRIP TO CALTRANS

Newton C. Jackson (WSDOT) and Joe P. Mahoney (TRAC/UW) visited the California Department of Transportation (Caltrans) from July 5 to 10, 1988. Their primary purpose was to review Caltrans PCC pavement rehabilitation practices. A secondary purpose was to better understand Caltrans' PCC pavement design practices, including the use of "drainable" designs. Further, during the visit they visited two experimental pavement projects.

This appendix will summarize some of the more significant information received and collected.

The visit included two separate visits to the Caltrans Transportation Laboratory in Sacramento (July 5 and July 8, 1988). Additionally, following receipt of site specific project information, the researchers travelled about 1,700 miles on the Caltrans route system during the visit. Figure I-1 shows the routes/mileage reviewed on the trip.

Personnel visited at the Caltrans Transportation Laboratory included

- | | |
|----------------|-----------------|
| • Ray Forsyth | • Joe Hannon |
| • Bob Doty | • Bill Nokes |
| • Gordon Wells | • Jim Woodstrom |

These individuals made the visit a success by providing both their time and extensive information.

Briefly, Caltrans has a centerline route system of about 15,000 miles and 49,000 lane miles (about twice as many centerline miles as WSDOT and three times as many lane miles). About one-third of the Caltrans lane miles are rigid pavements. Further, 27 percent of the lane miles are on the Interstate system.

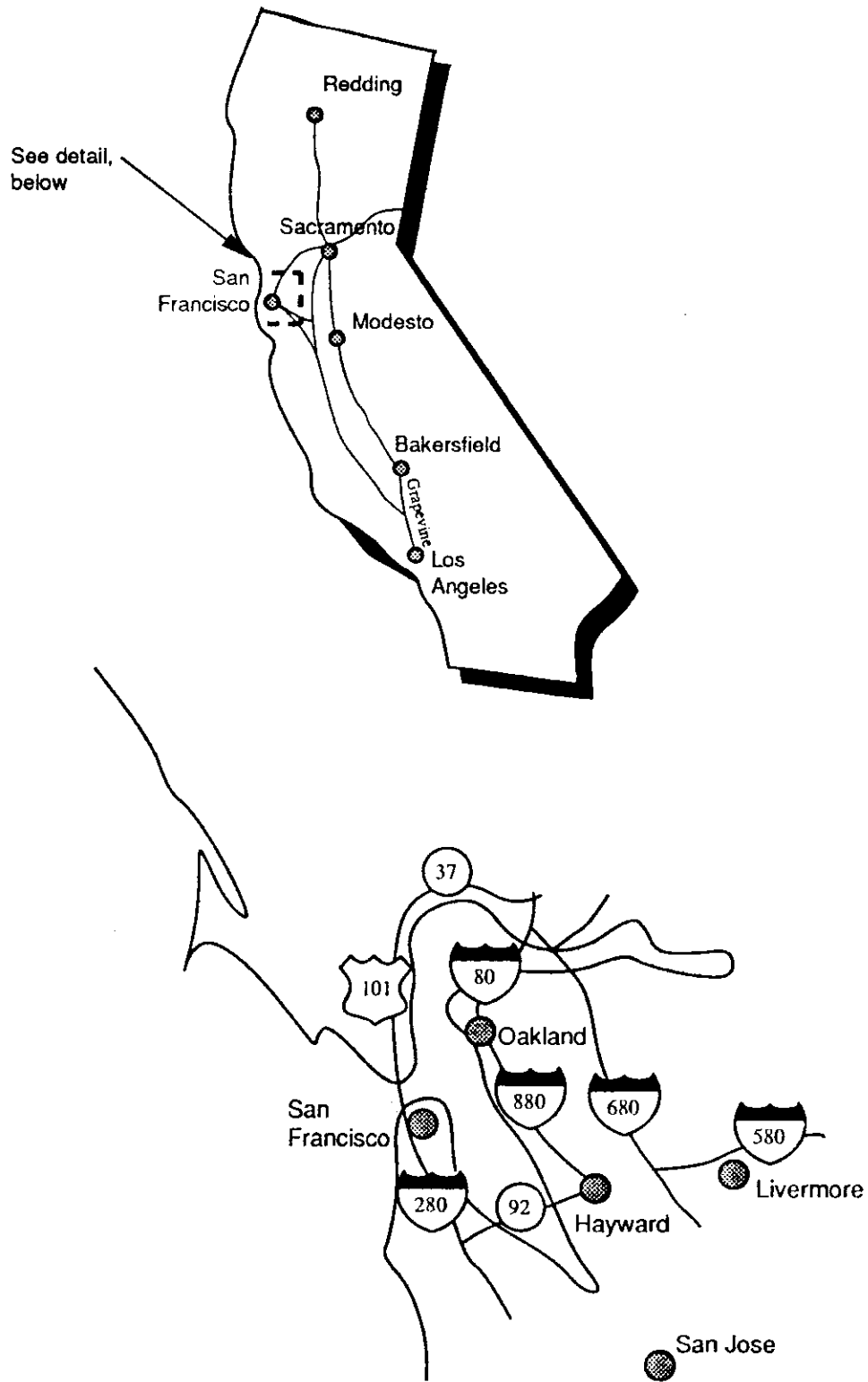


Figure I.1. Route of Travel – Visual Surveys

This appendix will be organized by the following major sections:

- New pavement design/construction
 - Portland cement concrete (PCC)
 - Asphalt concrete (AC)
- PCC rehabilitation
 - PCC distress types
 - Retrofit edge drains
 - Crack and seat with AC overlay
 - Other treatments
- I-5 experimental sections

I.2 NEW PAVEMENT DESIGN/CONSTRUCTION

Chapter 600, "Design of the Pavement Structural Section," from the Caltrans Highway Design Manual [I.1], is the primary reference used in this section (Section I.2).

I.2.1 General Design Considerations

Some of the general design considerations are listed from Ref. I.1:

I.2.1.1 Design Period

Caltrans uses a 20-year period for determining the "projected one-way truck traffic" for all Interstate routes and all PCC pavements on other routes. It uses a 10-year design period for non-Interstate AC pavements. ("The service life before major maintenance or rehabilitation is required may actually be considerably longer or shorter than the design period.")

I.2.1.2 ESAL Constants

The ESAL Constants used in the structural design of outside lanes (heaviest truck traffic) are as follows:

<u>Vehicle Type</u>	<u>ESAL Constants</u>	
	<u>10 Year Design</u>	<u>20 Year Design</u>
2-axle trucks	690	1,380
3-axle trucks	1,840	3,680
4-axle trucks	2,940	5,880
5-axle or more	6,890	13,780

The above constants are multiplied by the Average Daily Trucks to obtain ESALs.

Thus, an approximate estimate of ESALs per truck would be as follows:

<u>Vehicle Type</u>	<u>ESAL Constant ÷ 20 yr ÷ 365 d/yr</u>
2-axle trucks	$1,380 \div 20 \div 365 \cong 0.19$ ESALs/truck
3-axle trucks	$3,680 \div 20 \div 365 \cong 0.50$ ESALs/truck
4-axle trucks	$5,880 \div 20 \div 365 \cong 0.81$ ESALs/truck
5-axle or more	$13,780 \div 20 \div 365 \cong 1.89$ ESALs/truck

Thus, on a per axle basis, the following results:

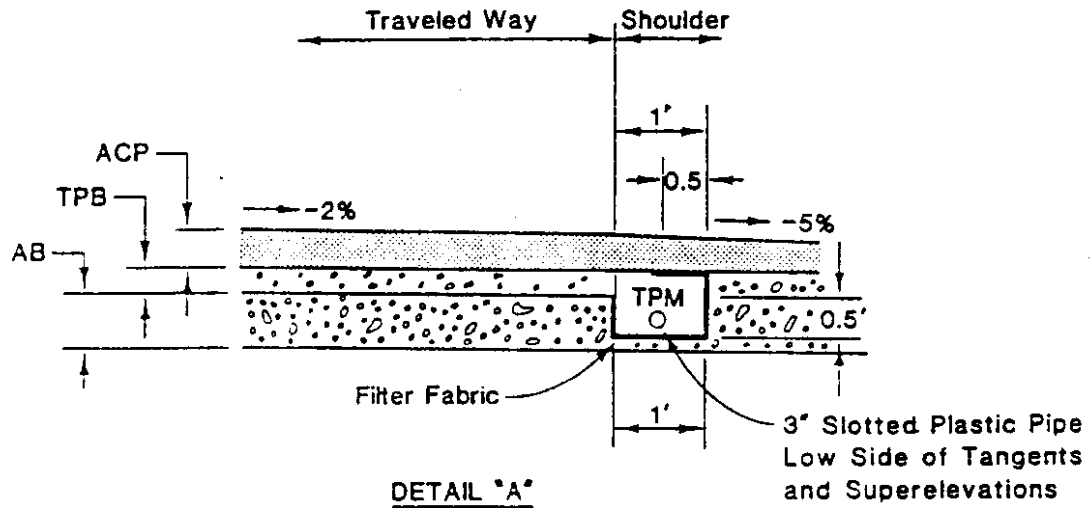
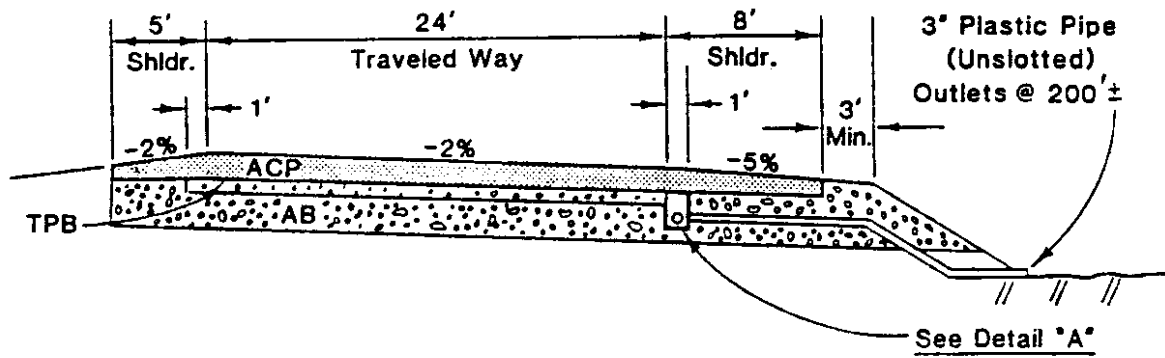
<u>Vehicle Type</u>	<u>ESAL/Axle</u>
2-axle trucks	0.10
3-axle trucks	0.17
4-axle trucks	0.20
5-axle or more (use 6)	0.32

The above figures tend to support WSDOT's general rule-of-thumb of allocating 0.25 ESALs per axle for estimating prior traffic ESALs.

I.2.1.3 Drainage of the Structural Section

I.2.1.3.a Flexible Pavement Structural Section Drainage. The structural section drainage is provided to handle surface water inflow (thus, it is a separate drainage system from that provided to accommodate groundwater inflow). The structural drainage layer can be either 0.25 ft of asphalt treated permeable base (ATPB) or 0.35 ft of cement treated permeable base (CTPB) and is placed immediately below the AC surfacing/pavement to intercept surface water. The permeability of the ATPB is estimated to be 15,000 ft/day, and that of the CTPB is 4,000 ft/day. The layer thicknesses (0.25 ft or 0.35 ft) are based primarily on constructability and construction tolerances. Further, the drainage layer drains to a 3-in. diameter slotted plastic pipe placed longitudinally, with outlet pipes placed every 200 ft. Refer to Figure I.2 for additional details.

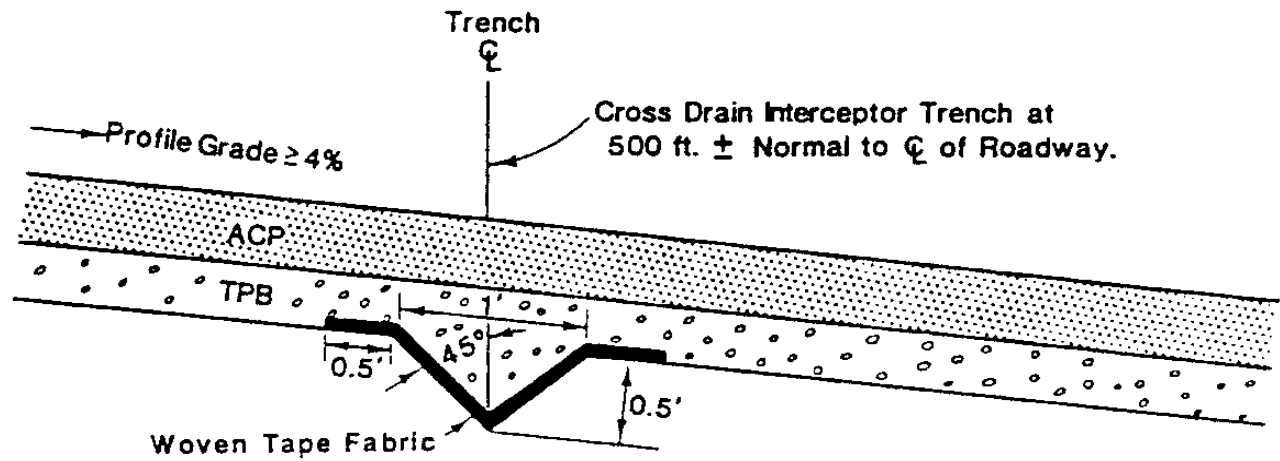
I.2.1.3.b Rigid Pavement Structural Section Drainage. Caltrans design policy states that "treated permeable bases shall be given first consideration in the design of structural sections for concrete pavements." This concept is illustrated in Figure I.3.



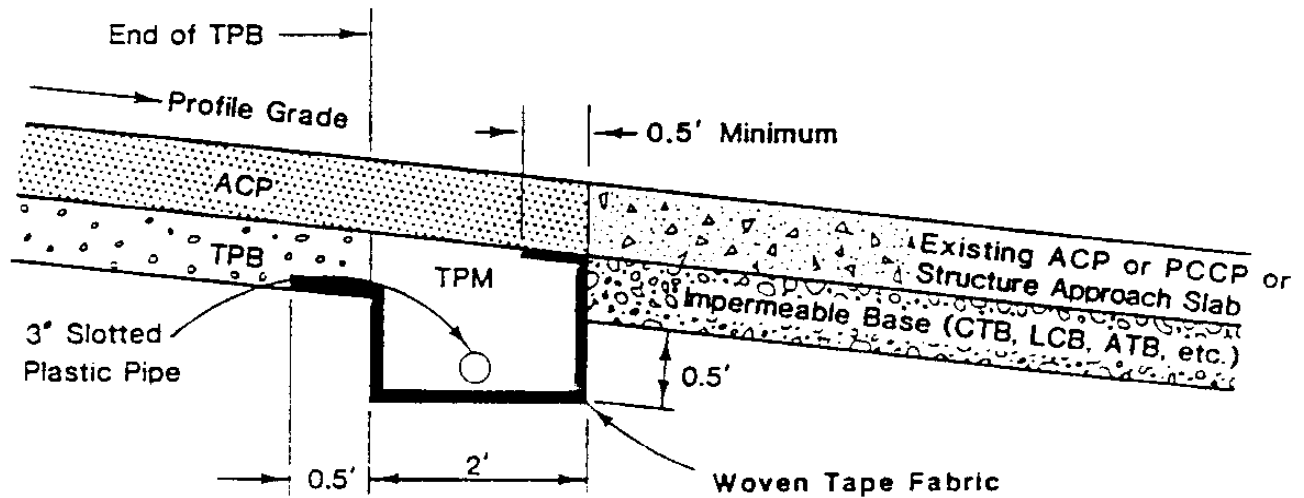
Note: Section shown is half-section of a divided highway.
 An edge drain collector and outlet system should be
 provided on both sides of 2-way crowned sections.

Figure I.2. Caltrans Flexible Pavement with Treated Permeable Base [from Ref I.1]

Cross Drain Interceptor Trench with AC Pavement (Longitudinal Section)

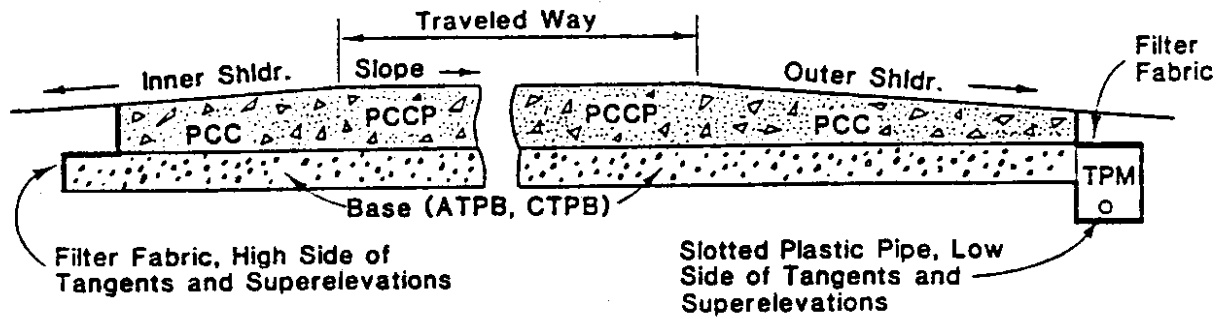


Intermediate Cross Drain

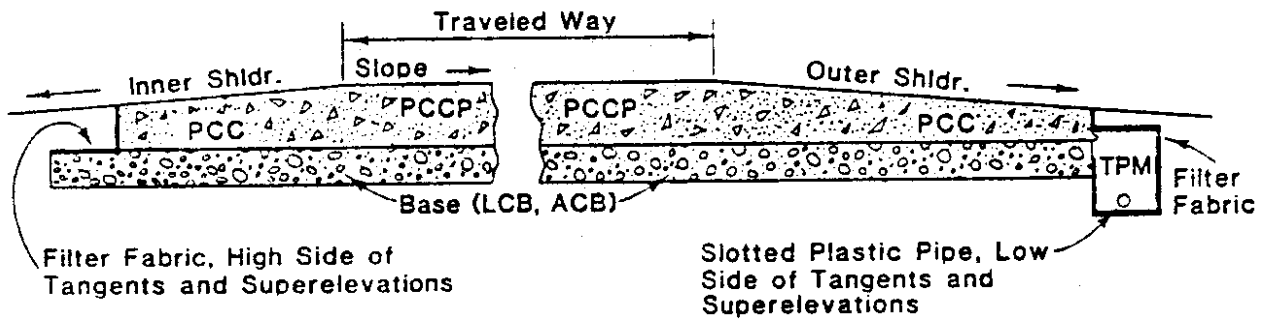


Terminal Cross Drain

Figure I.2....Continued

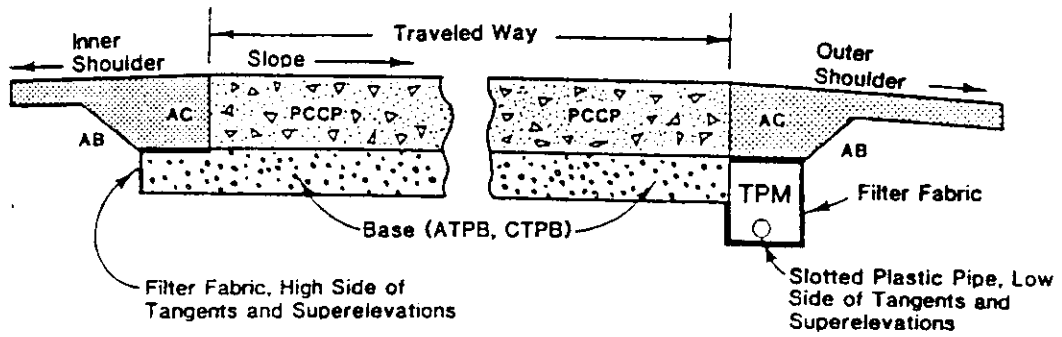


Concrete Shoulders - Permeable Base

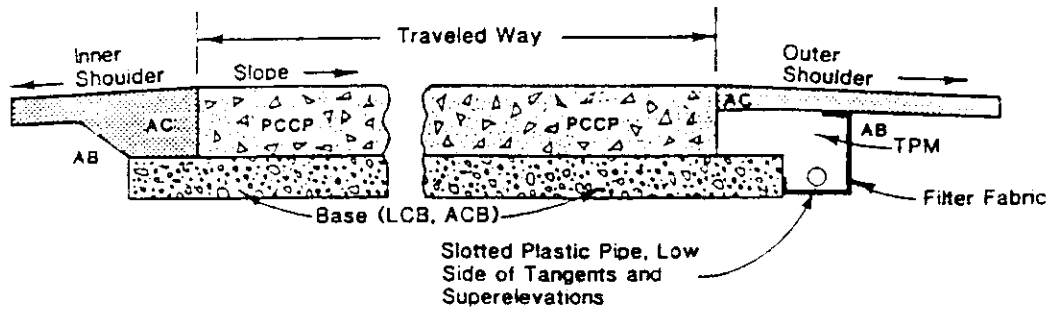


Concrete Shoulders - Dense Base

Figure I.3. Caltrans Rigid Pavement with Treated Permeable Base and Dense Base [from I.1]



Asphalt Concrete Shoulders - Permeable Base



Asphalt Concrete Shoulders - Dense Base

Figure I.3....Continued

I.2.2 PCC Pavement Structural Section Design

I.2.2.1 General Structural Design (from Ref. I.1)

"Generally, the use of portland cement concrete pavement (PCCP) has been confined to moderate to high traffic volume freeways. A rational design method for the design of PCCP was adopted in 1967 with the hope that it would better relate the PCCP thickness to traffic loading and that it might result in the use of PCCP on a wider variety of facilities and ultimately in some long term cost and service benefits. It was found, however, that the rational design method did not reflect field conditions accurately and it was not sensitive to wide variations in truck traffic. The 1967 design method was replaced in 1982 by a series of standard structural sections that are still current and which are based primarily on experience and research. A major change in that cement treated base (CTB), the traditional standard for PCCP (from 1950 to late 1970's), is no longer considered to be appropriate for PCCP because of its susceptibility to erosion."

Additional information provided by Caltrans personnel at the Transportation Laboratory was particularly helpful in understanding how the PCC/CTB combination became so widely used on the Caltrans route system.

F. Hveem recognized that PCC faulting was a major contributor to PCC distress and recommended that CTB be used to combat this problem (in the late 1930s-early 1940s). The first CTB was placed on the California route system in 1937 (AC surfacing, however). The early CTBs were good performers, except for shrinkage cracks in the AC surfacings. During the 1950s, the cement content of the CTBs was reduced to address the shrinkage cracking problem (in both AC and PCC surfaces). Another problem that impacted CTB performance was the "trimming pass," which disturbed the surface of the CTB upon which the PCC slabs were placed.

The primary distress of PCC pavements constructed during the 1950s and 1960s is faulting. The amount of time between initial construction to rehabilitation is greatly influenced by rainfall (i.e., pavement has shorter life in northern California, longer life in southern California).

Table I.1 shows the standard structural section thicknesses for new construction. These sections are a function of the Traffic Index (TI). The relationship between TI and ESALs is as follows:

Table I.1. Caltrans PCC Pavement Thickness Guidelines [from Ref I.1]

Basement Soil R-value 10-40 ⁽¹⁾							
TI	PCCP	Base (ATPB)	Subbase (AS)	Base (CTPB)	Subbase (AS)	Base ⁽³⁾ (LCB,ACB)	Subbase (AS)
6-7	0.50	0.25	0.55	0.35	0.40	0.35	0.40
7.5-8	0.60	0.25	0.55	0.35	0.40	0.35	0.40
8.5-10	0.70	0.25	0.65	0.35	0.50	0.35	0.50
10.5-12	0.75	0.25	0.80	0.35	0.70	0.40	0.60
12 +	0.85	0.25	1.05	0.35	0.95	0.50	0.70

Basement Soil R-value > 40							
TI	PCCP	Base ⁽⁴⁾ (ATPB)	Subbase (AS)	Base ⁽⁴⁾ (CTPB)	Subbase (AS)	Base ⁽³⁾ (LCB,ACB)	Subbase (AS)
6-7	0.50	0.35 ⁽²⁾	--	0.35 ⁽²⁾	--	0.35 ⁽²⁾	--
7.5-8	0.60	0.35 ⁽²⁾	--	0.35 ⁽²⁾	--	0.35 ⁽²⁾	--
8.5-10	0.70	0.25	0.35	0.40	--	0.40	--
10.5-12	0.75	0.25	0.35	0.40	--	0.40	--
12 +	0.85	0.25	0.35	0.50	--	0.50	--

NOTES :

- (1) With an expansive basement soil (Plasticity Index > 12) and/or basement soil R-value < 10 a flexible structural section, (ACP) should be specified unless the R-value of the basement soil is raised above 10 by treatment, to a minimum depth of 6 inches, with an approved stabilizing agent such as lime.
- (2) The base layer may be eliminated if the natural compacted subgrade is free draining ($k > 100$ feet/day) and is not confined by a cut slope or other side constraints.
- (3) CTB with a 0.10 foot DGAC cap may be used only under special conditions with the approval of the Office of Project Planning and Design.
- (4) The standard thickness is 0.25' for ATPB and 0.35' for CTPB. Greater than the standard thicknesses are shown to eliminate the need for very thin ASB layer which would be impractical to construct.

- LCB = Lean Concrete Base
- ACB = Asphalt Concrete Base
- ATPB = Asphalt Treated Permeable Base
- CTPB = Cement Treated Permeable Base
- AS = Aggregate Subbase

$$TI = 9.0 \left(\frac{ESAL}{10^6} \right)^{0.119}$$

The above equation rewritten to solve for ESALs is thus

$$ESAL = (10^6) \left(10^{\frac{\text{Log TI} - \text{Log}(9)}{0.119}} \right)$$

and the associated TI and ESAL equivalents (for values shown in Table I.1) are

<u>TI</u>	<u>ESAL</u>
6	33,000
7	121,000
7.5	216,000
8	372,000
8.5	619,000
10	2,424,000
10.5	3,652,000
12	11,218,000

As an illustration of a recently designed PCC pavement, the Century Freeway in Los Angeles will have 0.85-ft PCC slabs on 0.35 ft asphalt treated permeable base (ATPB) on a lean concrete base. (A lean concrete base is a concrete mixture of aggregate mixed with about one-half the portland cement content of a "conventional" PCC mix.) This structure will have edge drains and PCC shoulders, and the joints will be sealed with silicone joint sealant.

I.2.2.2 Joints

PCC pavement contraction joints are skewed counterclockwise 2 ft in 12 ft (the same as WSDOT). The repetitive joint spacing is 12, 15, 13, and 14 ft, for an average of 13.5 ft. Neither dowel bars nor tiebars are used in the PCC pavement joints. In the past, Caltrans rarely used joint sealers in new PCC construction, but it is increasingly encouraging their use.

Before the currently used joint spacing, Caltrans used a skewed spacing (2 ft in 12 ft) of 13, 19, 18, and 12 ft, for an average of 15.5 ft. The windshield survey N. Jackson and J. Mahoney conducted of Caltrans Interstate PCC pavements revealed that

many (if not most) of the 19- and 18-ft slabs have mid-panel transverse cracks (generally in pavements about 20 years old).

I.2.3 AC Pavement Structural Section Design (from Ref. I.1)

"Design of the flexible pavement structural section is based on a relationship between the gravel equivalent (GE) of the structural section materials, the Traffic Index (TI), and the R-value (R) of the underlying material."

I.3 PCC REHABILITATION

I.3.1 General Design Criteria/Alternatives

Like most state DOTs, Caltrans continually evaluates and updates its policy on pavement rehabilitation. The Caltrans original rehabilitation policy was developed in 1961 and recognized that PCC faulting was a primary distress. Some of the general design criteria/rehabilitation alternatives Caltrans uses are as follows [from Ref. I.1 — Highway Design Manual].

- (a) Rehabilitation strategies should provide corrective measures that will extend the service life of an existing pavement structure at least 10 years.
- (b) A list of some of the PCC pavement rehabilitation strategies that have been used is as follows:
 - (i) retrofit edge drains,
 - (ii) cement-pozzolan grout subsealing,
 - (iii) replacement of cracked slabs,
 - (iv) lane replacement,
 - (v) diamond grinding (to correct faulted slabs),
 - (vi) cracking and seating of slabs in conjunction with AC overlays,
 - (vii) thin-bonded PCC overlays, and
 - (viii) AC overlays.

I.3.2 PCC Pavement Distress Types

The following primary distress descriptions are from Ref. I.1:

I.3.2.1 Faulting

"Also called step-faulting, this is a phenomenon that is common on California's plain-jointed PCCP. This occurs primarily at transverse joints and at 'working transverse cracks,' as a result of slab pumping action that occurs with the passage of each heavy truck axle when the structural section is saturated. Pumping may continue for several weeks after a rainstorm.

"A badly faulted pavement generally exhibits a history of shoulder distress adjacent to the edge of the traveled way, due primarily to the pumping of aggregate base fines from under the AC shoulder. Faulting, and the accompanying loss of full base support of the slab, generally precedes and is considered to be a major contributing factor to slab cracking and eventual breakup."

I.3.2.2 Slab Cracking

"Pavement cracks generally result from heavy wheel loading combined with lack of uniform base support. Cracking also results from weak subgrades, expansive soils and differential settlement. The degrees of cracking are described below.

- (a) "First-stage cracking. Non-intersecting transverse, longitudinal or diagonal cracks in a slab which divide the slab into two or three large pieces. This does not include corner breaks.
- (b) "Second-stage cracking. Transverse, longitudinal or diagonal cracks which develop in a slab within two feet of planned or unplanned cracks or joints. Second stage cracking divides the slab into smaller pieces than first-stage cracking. The cracks are basically parallel and do not intersect. PMS will rate corner breaks as second-stage cracking.
- (c) "Third-stage cracking. Cracking of the slab into three or more pieces with interconnected cracks developing between cracks or joints."

I.3.3 Retrofit Edge Drains

I.3.3.1 Description/Criteria for Use (from Ref. I.1)

"This strategy is a preventive measure that is generally applied to relatively 'new' concrete pavement (up to 10 years of service) which is generally in very good condition but is beginning to show signs of pumping with little or no faulting."

Edge drains are installed continuously at the outside edge of the outside (thick) lanes. Caltrans uses the following criteria for determining project eligibility for retrofitting with drains:

- (a) pavement age is ≤ 10 years;
- (b) mean first stage cracking is ≤ 10 percent;
- (c) mean third stage cracking is ≤ 1 percent;
- (d) treated base is in good condition (i.e., CTB is still a cemented mass, not deteriorated to uncemented aggregate base); and

- (e) cumulative one-way ESAL is $\leq 13,000,000$ on four lane roads and ESAL $\leq 20,000,000$ on roads with six lanes or more.

Additionally from Ref. I.1:

"It is anticipated that the rapid removal of the infiltrated surface water through edge drains will result in a significant extension of the service lives of existing pavement that is still in good condition. Hopefully, instead of requiring extensive rehabilitation at a pavement age of 20 to 25 years, rehabilitation might be deferred an additional 5 to 10 years."

Caltrans started retrofitting PCC pavements during the late 1970s.

I.3.3.2 Performance of Edge Drains — Caltrans' Comments

Caltrans personnel at the Transportation Laboratory in Sacramento (July 8, 1988, meeting) offered the following comments:

- (a) Outflow rates of retrofitted edge drains have not been measured. These rates are difficult to measure, since surface infiltration outflow is short-lived.
- (b) Some retrofitted edge drains have been removed and examined. Plugged drains appear to be related to
 - (i) advanced third stage cracking (drains can plug quickly in this situation),
 - (ii) pavements with a grade that nearly equals 0 percent, and
 - (iii) poor outlet opportunities (e.g., curb and gutter sections).Of the drains examined,
 - (i) 50 percent were performing adequately,
 - (ii) 25 percent were performing marginally, and
 - (iii) 25 percent were plugged.
- (c) For pavements retrofitted with edge drains outside of the criteria stated in Paragraph I.3.3.1, pavement damage increased and the drains often contributed to corner cracking.

I.3.3.3 Performance of Edge Drains — Visual Survey

The visual (windshield) surveys conducted by N. Jackson and J. Mahoney on a wide variety of PCC pavements (mostly Interstate — refer to Figure I.1 for routes traveled) revealed that sections with retrofitted edge drains were generally performing poorly. More specifically, "fines" from the CTB underlying the PCC slabs were being pumped through the edge drains. Clearly, as discussed in Paragraph I.3.3.1, Caltrans had criteria to limit the use of retrofitted edge drains at that time (July 1988), which should minimize this poor performance.

I.3.4 Crack and Seat with AC Overlay

I.3.4.1 Description/Criteria for Use (from Ref. I.1)

"This strategy is used where concrete pavement has an unacceptable ride and is in an intermediate to advanced stage of structural deterioration. Generally, this means there is extensive third stage cracking (over 10%) of individual concrete slabs and it appears to be futile to try to 'keep up' by utilizing individual slab replacement and grinding. Slab replacement is not appropriate under this strategy, unless there is complete disintegration of a slab or segment.

"In this case, the combination strategy used is to crack and seat the PCCP slabs, install edge drains, and place a 0.35 ft fabric reinforced DGAC (dense graded asphalt concrete) overlay. The DGAC overlay should consist of first placing a 0.10 ft leveling course of DGAC, followed by pavement reinforcing fabric interlayer, a 0.10 ft lift of DGAC and a final 0.15 ft of DGAC. If the criteria for OGAC (open graded asphalt concrete) has been satisfied, place 0.10 ft DGAC leveling course followed by a pavement reinforcing fabric interlayer, a 0.15 ft lift of DGAC and a final lift of 0.10 ft lift of OGAC.

"On four-lane divided freeways, both lanes in each direction are cracked and seated whereas on facilities with 3 or more lanes in each direction, if no significant distress or signs of deterioration exists in the median lane(s), they need not be cracked and seated before the overlay and fabric are placed.

"The AC overlay includes a reinforcing fabric interlayer that extends at least 2 ft outside the edge of PCCP into the shoulder area. The fabric interlayer retards infiltration of surface water and reflection cracking. It is assumed to be equivalent to 0.10 ft of AC in its effectiveness to prevent reflective cracking. This reduction of 0.10 ft in required thickness of AC can result in a significant savings, especially on multilane facilities. Where the slab deterioration is primarily limited to the outer lane or lanes on multilane facilities, an economic analysis should be made to compare the cost of lane replacement with the cost of overlaying all lanes and shoulders.

"In utilizing the cracking and seating procedure, which Caltrans considers to be one of the highest forms of recycling, the goal is to break the slabs into appropriate 4 ft by 6 ft segments to serve as a stable base for the overlay. Prior to placement of the AC overlay, the slab segments are rolled to assure that the segments are firmly seated onto the underlying base. The cracking, seating and rolling not only stabilizes the slab segments to minimize any differential vertical movement but it also reduces the magnitude of thermal movement and strains that are transmitted into the overlay and reinforcing fabric interlayer. This minimizes the reflective cracking tendency that has been observed on asphalt concrete overlays over PCCP.

"The installation of edge drains, when combined with the fabric interlayer, minimizes the potential for entry and entrapment of water and pumping action of the PCCP segments under the AC overlay.

"The cracking, seating, installation of edge drains, and on AC overlay with a fabric interlayer combination strategy is anticipated to last a minimum of 10 years without required significant pavement maintenance."

A sketch of a crack and seat with an AC overlay is shown as Figure I.4, and the cracking pattern used by Caltrans is shown in Figure I.5. Caltrans began using this rehabilitation technique in 1982.

I.3.4.2 Performance of Crack and Seat with AC Overlay — Caltrans Comments

Caltrans Transportation Laboratory personnel offered the following comments:

- (a) No known crack and seat with AC overlay (CSO) projects have rutted or experienced significant reflection cracking.
- (b) Originally, Caltrans used a 4-ft by 4-ft crack spacing, but this scheme resulted in spalling of the cracks under traffic (prior to AC overlay). This problem resulted in the current practice of roughly a 6-ft by 4-ft crack pattern. Thus, the 6-ft dimension results in a longitudinal crack down the middle of the slab and at roughly the 1/3 points transversely.
- (c) A CSO has been used in the Los Angeles area on a freeway (3 to 4 lanes in each direction) with an ADT \cong 280,000 and percentage of trucks \cong 15-20 percent (thus, results in an outside lane ESALs per year of about 5,000,000).

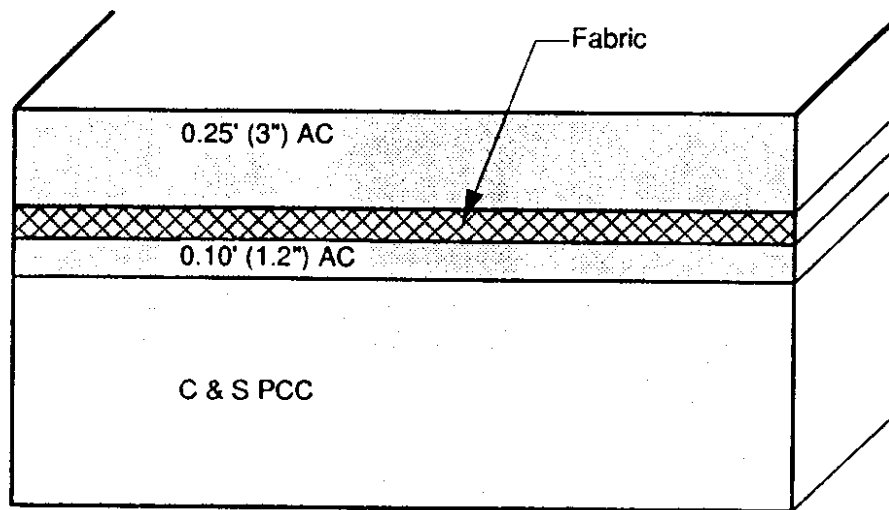


Figure I.4. Sketch of Crack and Seat PCC Slab with AC Overlay

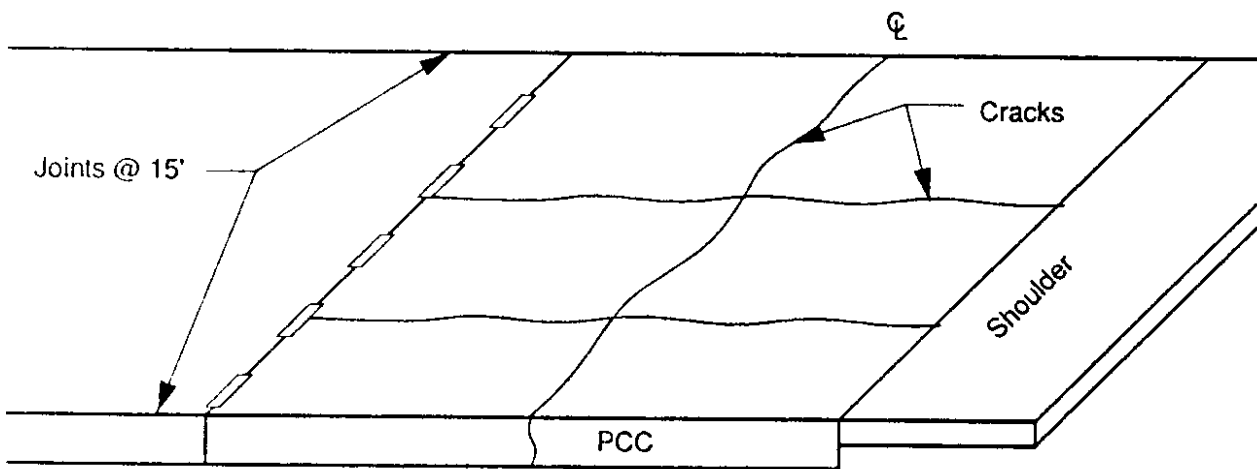


Figure I.5. Caltrans Crack and Seat Crack Pattern

- (d) In situations where cracking and seating cannot be done (because of noise or seismic constraints), Caltrans adds an extra 0.10 ft to the AC overlay (0.45 ft in lieu of 0.35 ft). This approach has been used mostly in Caltrans District 4 (San Francisco Bay area).
- (e) Caltrans personnel feel that CSOs will fail by reflection cracking. Further, it is quite likely the CSOs could achieve a 15-year service life in rural areas. The expected service life is lower for urban areas, in part because of nighttime construction.
- (f) The question was posed, "How does Caltrans keep its AC overlays from rutting?" The response was that Caltrans AC mixtures are "dry" (with a lower asphalt content, about 5.0-5.5 percent by dry weight of aggregate). Additionally, the penetration of asphalt cement typically used is in the 55 to 60 range (unaged, as delivered). The gradation band for the aggregate conforms to the 0.45 power curve (traditional dense graded asphalt concrete).
- (g) Caltrans has no plans (as of July 1988) to increase the thickness of the AC overlay for the CSO system. Personnel stated that the fabric is an important element in the system.
- (h) During a follow-up telephone conversation with Transportation Laboratory personnel (April 1991), it was stated that reflection cracks are coming through some of the CSO's. Generally, these cracks are from the original transverse joints, not the induced cracks done just prior to overlay.

I.3.4.3 Performance of Crack and Seat with AC Overlay — Visual Survey

The visual (windshield) surveys conducted by N. Jackson and J. Mahoney can be summarized as follows:

- (a) Of the CSO projects reviewed (the oldest of which was 6 years old), none displayed rutting of the AC overlays.
- (b) A summary of specific CSO projects that were visited is shown as Table I.2. From the summarized information, a few, general comments are appropriate:
- (i) The CSO projects are performing well (however, the oldest project is only 6 years old).

Table I.2. Summary of Crack and Seat with AC Overlay Projects — Observations During July 1988

Route No.	Mileposts	Nearest City (County)	Total AC Overlay Thickness (feet)*	ADT (1987)	Age (years)	Observations (July 1988)
I-680	22.7-24.3	Martinez (Contra Costa)	0.35 and 0.20	70,000	~4	Minor cracking. Poor appearance AC mix.
I-680	21.6-22.7	Martinez (Contra Cost)	0.35	83,000	~3	No cracking
I-680	12.7-15.2	Walnut Creek (Contra Costa)	0.40	123,000	~3	Friction course surfacing. No Cracking
I-580	1.5-6.9	Altamont Pass (Alameda)	0.35	68,000	~4	0.10' OGAC/fabric/0.15' DGAC. No cracks
I-680	15.2-17.7	Pleasant Hill (Contra Costa)	0.28	193,000	~4	0.08' OGAC/fabric/0.20' DGAC. A few cracks including longitudinal joint. Very minor cracks in the wheelpath
SR 99	31.2-32.4	Bakersfield (Kern)	0.35	38,000	~4	No cracks
I-5	23.0-27.1	Dunnigan (Yolo)	0.40	20,000	~4	No cracks
I-5	3.8-14.0	Anderson (Shasta)	0.35	24,000	~6	No cracks
I-80	6.6-0.2	Albany (Contra Costa)	0.35	160,000	~6	No cracks
I-80	0.0-5.8	Davis (Yolo)	0.40	80,000	~4	No cracks

* All projects had 6 ft x 4 ft cracking pattern on the PCC slabs

- (ii) The CSO projects that had AC overlays of less than 0.35 ft are showing early cracking (4-year old projects).
- (iii) The ADT levels (two-way) for the projects listed in Table I.1 range from 20,000 to almost 200,000. Thus, the projects are being subjected to relatively "heavy" traffic.

I.3.5 Other Rehabilitation/Reconstruction Treatments

I.3.5.1 Remove and Replace PCC Pavement

Caltrans personnel at the Transportation Laboratory stated that the only places reconstruction of PCC pavement is considered are those locations where overhead clearances are a constraint to other rehabilitation techniques. Caltrans maintains at least a 14.5-ft clearance.

I.3.5.2 Full Depth PCC Partial Slab Replacement

This rehabilitation technique can include slab replacement, subsealing (as of July 1988 a subsealing moratorium was in effect), grinding, and installation of edge drains. The slab replacement results in removal of the deteriorated slab (or partial removal) by saw cutting and overexcavation into the base and possibly subgrade. The new PCC is thicker (generally 1.0 to 1.2 ft) than the original slab and not doweled to the existing PCC. The performance of this system based on visual surveys conducted in July 1988 (mostly on I-5 between Sacramento and Redding, California) showed that the performance is poor. Projects that were relatively new in appearance were highly distressed (by cracking mostly). Often, the PCC full depth patches were essentially shattered.

I.4 I-5 EXPERIMENT — TRACY, CALIFORNIA

A section of I-5 near Tracy, California, was constructed to evaluate several experimental design features. This experiment is quite unique and provides insight of value to WSDOT. Therefore, a brief description of the experimental sections and their performance (as of July 1988) is provided below.

I.4.1 Experiment Site Information

- (a) Annual rainfall: 10 to 15 inches per year
- (b) Annual air temperature range: 20°F to 115°F
- (c) ADT (1987) \cong 11,000 (about 16,000,000 ESALs since construction)
- (d) Located about 60 miles east of San Francisco
- (e) All sections constructed May-June 1971 (17 years of performance when reviewed in 1988). Further, replicate sections constructed in north and southbound lanes.

I.4.2 Experimental Section Description and Performance

I.4.2.1 Control Section (10,556 ft length) "The Standard"

- (a) 0.70-ft (8.4-in.) slabs
- (b) 0.45-ft (5.4-in.) Class A CTB (CTB plant-mixed and slipformed — thus no trimming required during construction)
- (c) Construction joint spacing (sawed): skewed at 13, 19, 18, and 12 ft. Joints not sealed during construction
- (d) Performance — Northbound
 - (i) Minor faulting
 - (ii) Minor pumping
 - (iii) One corner break
- (e) Performance — Southbound
 - (i) Pumping
 - (ii) Joints faulted (more than northbound)
 - (iii) Mid-panel cracks
 - (iv) Corner breaks — some patched
 - (v) Ride OK, overall condition good

I.4.2.2 Section 1A (5,028 ft length), Section 1B (11,052 ft), Section 1C (11,319 ft) "Continuously Reinforced"

- (a) 0.70-ft (8.4-in.) slabs
- (b) 0.45-ft (5.4-in.) CTB
- (c) Continuously reinforced with steel amounting to 0.56 percent of the cross-sectional area of PCC pavement

- (d) Section 1A: longitudinal bars only (No. 5s)
Section 1B: longitudinal bars (No. 5s) and transverse bars (No. 4s)
Section 1C: welded wire fabric (D-19 longitudinal and D-6 transverse)
- (e) Performance — Northbound
- (i) Section 1A
- No observable distress
 - Ride "unusual"
- (ii) Section 1B
- Transverse crack spacing about 2 to 2.5 ft (typical). Numerous transverse cracks spaced as close as 1 ft.
 - No distress noted
 - Ride good
- (iii) Section 1C
- Same comments as for Section 1B (NB) except that the ride was "unusual"
 - Some patching at the WWF overlaps (occurred during original construction)
- (f) Performance — Southbound
- (i) Section 1A
- Punchouts
 - No faulting of cracks
 - No pumping
 - Transverse crack spacing longer than for Sections 1B (SB) and 1C (SB)
- (ii) Section 1B
- No observable distress

(iii) Section 1C

- One punchout
- Large patch
- Transverse crack spacing typically 1 to 2 ft apart (some as close as 6 in.)

I.4.2.3 Section 2 (2,900 ft length) "Shorter Joint Spacing"

- (a) 0.70-ft (8.4-in.) slabs
- (b) 0.45-ft (5.4-in.) CTB
- (c) Joint spacing: 8, 11, 7, 5 ft (average spacing 7.75 ft) skewed 2 ft in 12 ft.
Joints unsealed.
- (d) Performance — Northbound
- Small amount of pumping
 - One mid-panel crack in an 11-ft slab
 - Longitudinal joint at shoulder depressed
 - Overall appearance and ride was very good
- (e) Performance — Southbound
- Some third stage cracking
 - Numerous corner breaks
 - Pumping
 - Some longitudinal cracks between the more closely spaced transverse joints
 - Faulting (varied — more severe on steeper grades)
 - Patching — extensive in some areas

I.4.2.4 Section 3 (2,900 ft length) "Higher Strength"

- (a) 0.70-ft (8.4-in.) slabs
- (b) 0.45-ft (5.4-in.) CTB

- (c) PCC mix of 7.5 sacks/yd³ (versus 5.5 sacks/yd³ for the other sections)
 - (i) Control Section PCC compressive strength (28-day) = 3,850 psi
 - (ii) Section 3 PCC compressive strength (28-day) = 4,500 psi
- (d) Joint spacing same as Control Section
- (e) Performance — Northbound
 - Pumping — more than Section 2
 - Transverse crack in most of the 18- and 19-ft long slabs
 - Corner breaks
 - Faulting — more than Section 2
- (f) Performance — Southbound
 - Pumping
 - Faulting
 - Corner breaks
 - Patching

I.4.2.5 Section 4 (2,800 ft length) "Thicker Slabs"

- (a) 0.95-ft (11.4-in.) slabs
- (b) 0.45-ft (5.4-in.) CTB
- (c) Joint spacing: 13, 19, 18, and 12 ft (same as Control Section) — joints not sealed during construction
- (d) Performance — Northbound
 - No transverse cracks in the longer slabs (18, 19 ft)
 - Minor faulting
 - Overall: very good condition
- (e) Performance — Southbound
 - Minor amount of pumping
 - Some of the longer slabs (18, 19 ft) have transverse mid-panel cracks
 - No patching (many of SB sections do)
 - Overall: much better condition than southbound Sections 2, 3 or 5

I.4.2.6 Section 5 (2,903 ft length) "Lean Concrete Base"

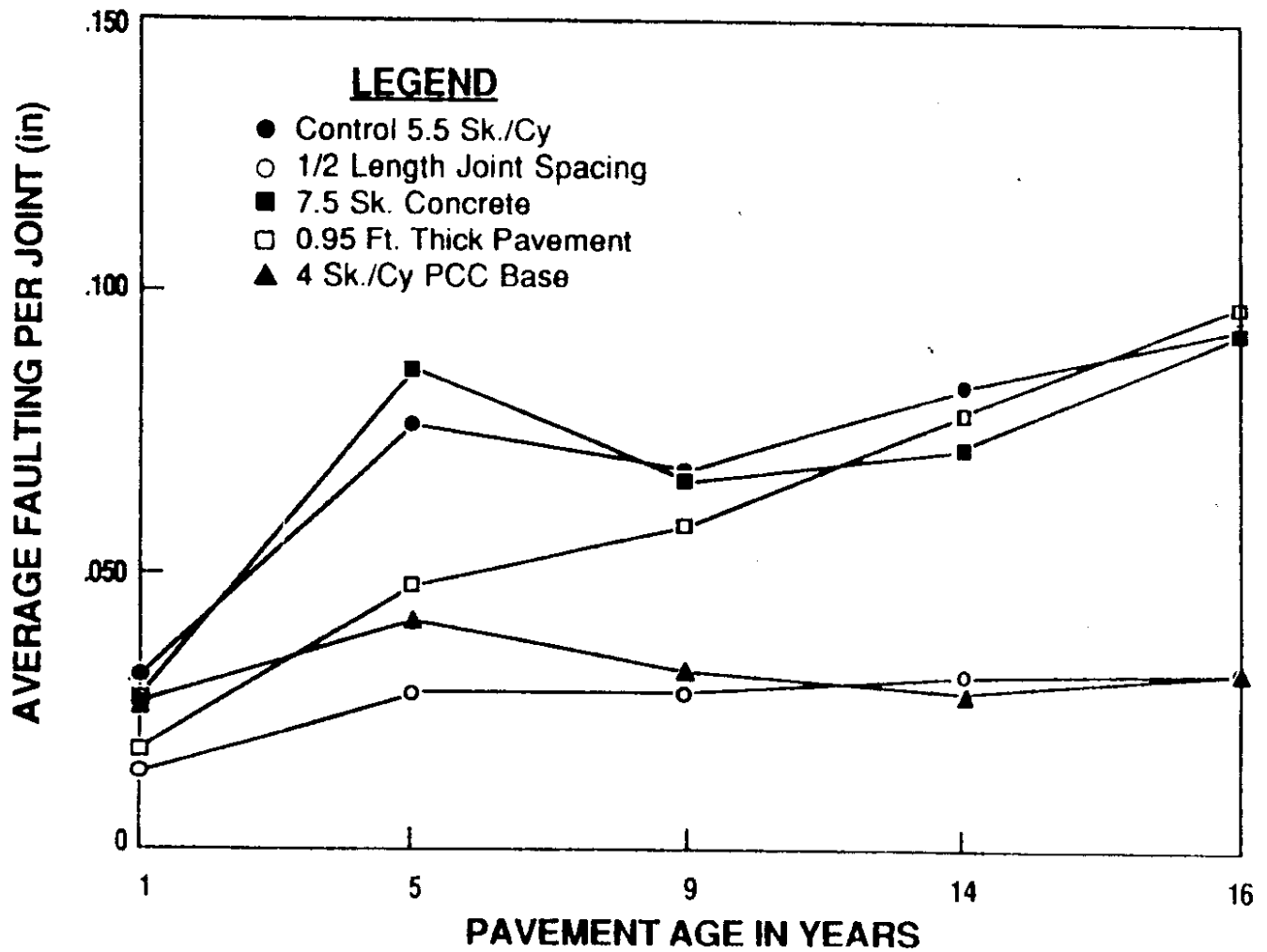
- (a) 0.70-ft (8.4-in.) slabs
- (b) 0.45-ft (5.4-in.) 4 sack lean concrete base (transverse joints cut in LCB every 30 ft)
- (c) Joint spacing: 13, 19, 18 and 12 ft (same as Control Section)
- (d) Performance — Northbound
 - Pumping
 - Small corner breaks on approach slabs
 - Mid-panel transverse cracks in longer slabs (18, 19 ft)
 - Minor faulting
- (e) Performance — Southbound
 - More pumping than Section 4 SB
 - Some corner breaks
 - Mid-panel transverse cracks — some in the shorter slabs (12, 13 ft)
 - This section performing better than the Control Section (SB)

I.4.2.7 Concluding Observations

- (a) There was a major difference in the performance of the northbound (better) and southbound (poorer) sections. The southbound section seemed to be a bit lower in elevation. The irrigation on both sides of I-5 and the silty soil may have contributed to the observed differences.
- (b) At 17 years old, these sections should now provide Caltrans excellent information; however, none of the drainage features Caltrans currently uses were incorporated into these sections.
- (c) The length of the sections is an excellent design feature.
- (d) Specific faulting data are shown as Figures I.6 and I.7 [from Ref. I.2].
- (e) During a follow-up telephone conversation with Transportation Laboratory personnel (April 1991), it was stated that the CRCP pavements (Sections 1A, 1B, 1C) were performing the best. The next best was the lean concrete base pavements (Section 5). The poorest performing pavements are the

PAVEMENT JOINT FAULTING

10-SJ-5
E. TRACY (NB)
PAVED 1971

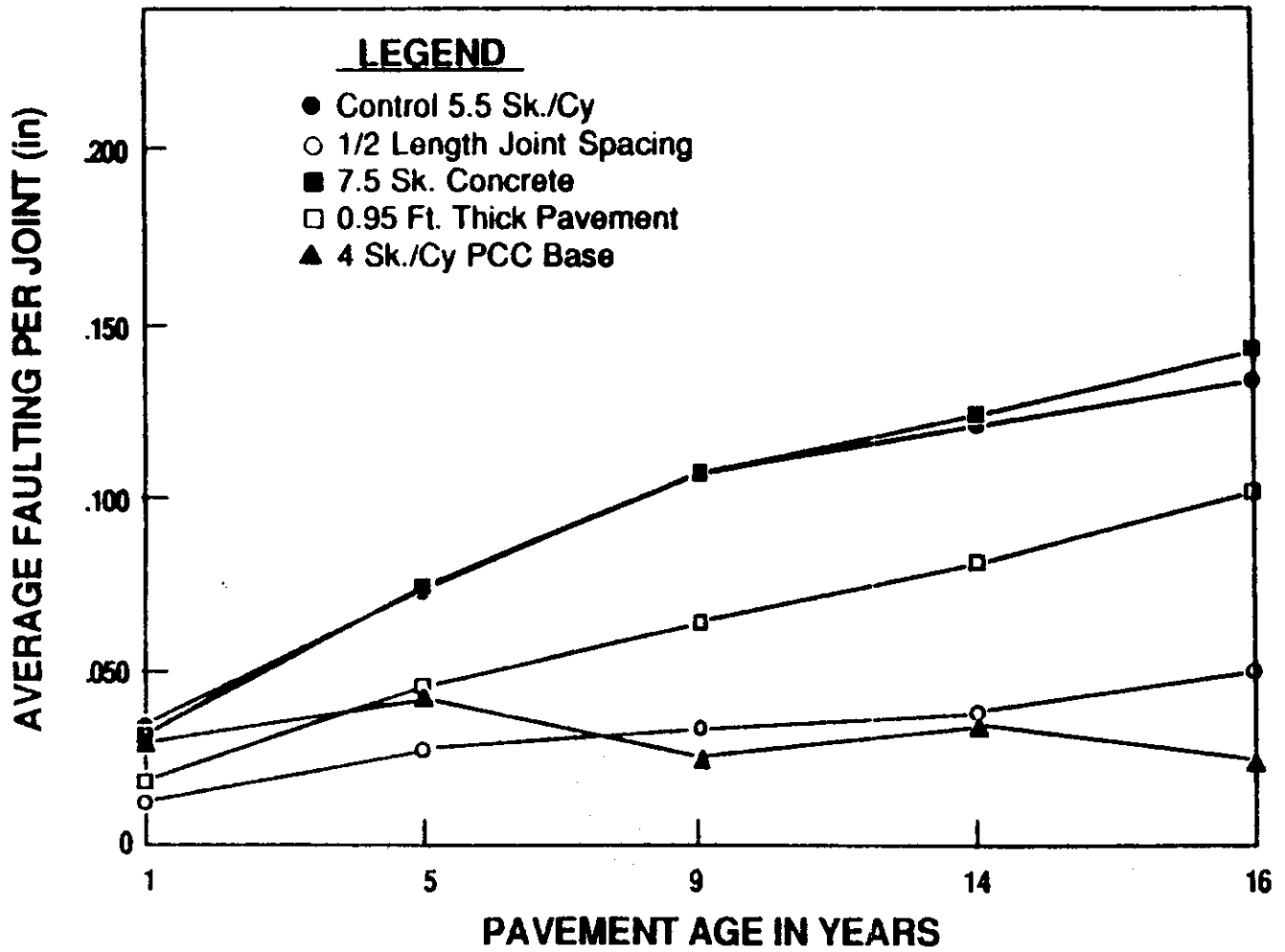


FAULTING TREND LINE

Figure I.6. Caltrans Faulting Measurements (I-5 -- Tracy Experimental Sections - Northbound)

PAVEMENT JOINT FAULTING

10-SJ-5
E. TRACY (SB)
PAVED 1971



FAULTING TREND LINE

Figure I.7. Caltrans Faulting Measurements (1-5 -- Tracy Experimental Sections - Southbound)

Standard Control Section and the higher PCC strength (Section 3). Further, the thicker slabs (Section 4) have significant faulting.

I.5 REFERENCES

- I.1 Caltrans Highway Design Manual, "Chapter 600 — Design of the Pavement Structural Section," May 2, 1988.
- I.2 Neal, B.F., "Evaluation of Design Changes and Experimental PCC Construction Features," Report No. FHWA/CA/TL-85/07, California Department of Transportation, Sacramento, California, July 1987.